



Provided by the author(s) and University of Galway in accordance with publisher policies. Please cite the published version when available.

Title	Development of a gene-eluting stent for the treatment of in-stent restenosis
Author(s)	Ganly, Sandra Maria
Publication Date	2016-05-12
Item record	<a href="http://hdl.handle.net/10379/5783">http://hdl.handle.net/10379/5783</a>

Downloaded 2024-05-04T16:34:25Z

Some rights reserved. For more information, please see the item record link above.





**Development of a Gene-eluting stent for the  
treatment of In-stent restenosis**

A thesis submitted to the National University of Ireland,  
Galway for the Degree of Doctor of Philosophy

By

**Sandra Ganly**

Discipline of Biomedical Engineering

National University of Ireland, Galway

**Thesis Supervisors:** Professor Peter E. McHugh  
and Professor Timothy O'Brien

**Submitted:** October 2015

## **ABSTRACT**

In-stent restenosis (ISR) results from stent-induced arterial injury, characterized by a complex cascade of cellular and biochemical events. The removal of endothelium during an angioplasty procedure causes the underlying medial layer to change phenotype, thus inducing the formation of neointimal hyperplasia (NIH) in certain patient populations. It is proposed that promoting re-endothelialisation at a very early stage post-stenting could stimulate the exposed smooth muscle cell layer to return to a quiescent, non-proliferative state, thus preventing NIH formation.

Drug-eluting stents (DES) have revolutionized the field of stenting and the treatment of ISR specifically. However, off-label use in contra-indicated patients, the incidence of late stent thrombosis (LST), and the necessity for the long-term administration of anti-platelet therapy hampers DES technology, and as a result, ISR continues to be a significant clinical complication for high-risk cardiovascular patients. Gene therapy approaches have recently emerged as a potential therapeutic strategy for the treatment of a variety of cardiovascular diseases. In the case of ISR, taking a gene therapy approach to stenting, which aims to repair and regenerate endothelium while preventing NIH formation, could be an attractive alternative to DES.

The work presented in this thesis focused on the development of a Gene-eluting stent (GES) platform to safely and efficiently deliver a therapeutic gene to the vasculature to prevent the incidence of ISR post-stenting. This research is multi-disciplinary by nature, merging engineering, scientific and clinical principles and perspectives, to develop a proof-of-concept GES.

A coronary stent, coated with a non-viral vector containing a therapeutic gene (eNOS), was successfully implanted in a hypercholesterolemic rabbit model. Successful transduction of the cells at the site of injury was achieved. Although, the hyperplasia mass of the in-stent lesions was not reduced, the re-establishment of a functioning endothelium was a significant result. Restoring the original, non-thrombogenic properties of this intimal layer is particularly noteworthy, as it is the thrombogenic nature of an exposed medial layer (caused by stent-induced arterial injury) that warrants the long-term administration of anti-platelet therapy, to prevent late stent thrombotic events, currently associated with DES.

## DECLARATION

This thesis contains no material which has been accepted for a degree or diploma by the University or any other institution, except by way of background information and duly acknowledged in the thesis. To the best of my knowledge and belief no material previously published or written by another person except where due acknowledgement is made in the text of the thesis, nor does the thesis contain any material that infringes copyright.

Part of the work contained within this thesis (Chapters 4, 5 and 6) was supported by Science Foundation Ireland grant nos. 08/CE/B1436 and 09/SRC/B1794 and Enterprise Ireland/ ERDF grant no. CFTD/07/105 LIPOSTENT.

### Publications

**Ganly S**, Hynes SO, Sharif F, Aied A, Barron V, McCullagh K, McMahon J, McHugh P, Crowley J, Wang W, O'Brien T, Greiser U. **Liposomal surface coatings of metal stents for efficient non-viral gene delivery to the injured vasculature.** *J Control Release.* 2013 Apr 28;167(2):109-19. doi: 10.1016/j.jconrel.2013.01.036. Epub 2013 Feb 10. PubMed PMID: 23403396. (Chapter 5)

Sharif F, Hynes SO, McCullagh KJ, **Ganly S**, Greiser U, McHugh P, Crowley J, Barry F, O'Brien T. **Gene-eluting stents: non-viral, liposome-based gene delivery of eNOS to the blood vessel wall in vivo results in enhanced endothelialisation but does not reduce restenosis in a hypercholesterolemic model.** *Gene Ther.* 2012. Mar;19(3):321-8. doi: 10.1038/gt.2011.92. Epub 2011 Jun 30. PubMed PMID: 21716298. (Chapter 6)

## DEDICATION

Do mo mháthair iontach,  
Ní bheidh a leithéid arís ann  
Le grá agus buíochas go deo,  
D'iníon croí-briste



*“Educating the mind, without educating the heart, is no  
education at all”*

**Aristotle - Greek Philosopher, Scientist & Physician  
384 BC-322 BC**

## ACKNOWLEDGEMENTS

I would like to take this opportunity to extend a sincere thank you to my joint supervisors, Professor Peter McHugh and Professor Timothy O'Brien for their support, guidance and direction. I have learned so much and consider myself very privileged to have been able to work in such an exciting, inter-disciplinary research area.

To all the members of the Biomechanics group, the REMEDI Gene Therapy group and the Enterprise Ireland Commercialisation Team: Dr Faisal Sharif, Dr Karl McCullagh and Mr Jim Crowley.

Dr Valerie Barron - thank you for making that first telephone interview. I will always be grateful for that initial step. Dr Udo Greiser, thank you for taking over the role as my academic PhD mentor at a critical point of the journey. I am very grateful for all you have taught me, especially the finer details of German efficiency and plasmid preps!

I wish to extend a very, sincere thank you to Dr Sean Hynes. Your selfless nature and willingness to always help others is an inspiration to us all. Thank you for giving me the opportunity to work on the grant and for always being so considerate. It was a pleasure to work for you. I hope we will work together again in the future.

Dr Pat Morgan - I will always be indebted to you for your gentle encouragement and firm belief in me. I hope I made a good attempt to rise to your high expectations.

Dr Jill McMahon, my mentor and dear friend. Thank you for guiding my very tentative introduction to molecular biology. Cloning, plasmid preparation and over-feeding my cells is a far cry from my life of stress-strain curves and fickian diffusion! You've educated me on so many levels, both personally and professionally. Your friendship means so very much to me.

Aideen, Tina and Denise - my 10 am breaks were often the only light during long days of experimental disaster. Thank you for all the advice and support over the years. I will always cherish our friendship and look forward to many more gatherings in the House!

A sincere thank you to my band of life-long, loyal and wonderful friends, who bore the brunt of my complaining and venting. Apologies to anyone I let-down, cancelled or postponed on, over the last few years, due to a chronic case of PhD-itis. I can officially say now that you can count me in for any social occasion as I'll have no prior engagement with an experiment or thesis chapter!

-

A special thank you to my cousin Linda- an inspirational lady and a very talented scientist! Here's a little night-time reading for you - Enjoy! Also to Auntie Stephi – thank you for always believing in me.

A special thank you to my extraordinary sisters. Marissa- your journey is just beginning. Enjoy and just remember to always be your fabulous self. Thanks for always adding a little humour to any given situation (you can stop taking me off now!). I am very lucky to have a sister like you to rely on and I wish you every success as you embark on your career. Carol – you have always been my source of comfort and advice. Your endless help and support has been instrumental in actually making it over the finish line. No one could ask for a better sister or friend. I'm so blessed to have both in you.

To my parents Marie and Tony. I will never be able to thank you enough for all the support (emotional and financial) through-out my 25 year educational process! I bet you didn't think it would take me this long when I started in St. Mary's in 1983! It's most definitely finished now. Thank you from the bottom of my heart. Anything I've achieved is because I received the desire, talent and nurturing from you both. Thanks for believing in me. I hope that I've made you proud. I love you both very much.

To my beautiful children - Donnacha, Orlaith Cáit and Tadhg. You are, and will continue to be, my greatest teachers. I am so humbled and thankful for the privilege of being your mother. You will never know how much your little faces have been my saving grace. Be the best you can be and enjoy every moment! Always remember how much I love you.

And last, but certainly by no means least, to my husband Mark. Thank you for always supporting and gently encouraging me to continue even when I was determined to give up. You always did have a way of bringing me onside! Our children top the list of my proudest achievements but you will always be the best (and easiest) decision I ever made. Thank you for always walking beside me and reminding me to dream big! I love you with all my heart, Let the dance continue.....

# TABLE OF FIGURES

## CHAPTER 1

FIGURE 1.1: DEVELOPMENT OF ATHEROSCLEROSIS. ....	21
FIGURE 1.2: GROSS STRUCTURE OF THE BLOOD VESSEL WALL. ....	22
FIGURE 1.3: PATHOGENESIS OF ATHEROSCLEROSIS .....	26
FIGURE 1.4: STENT-INDUCED INJURY CASCADE OF MOLECULAR AND CELLULAR EVENTS ..	30
FIGURE 1.5: SUB-CELLULAR SEQUENCE OF EVENTS FOLLOWING ARTERIAL INJURY .....	32
FIGURE 1.6: HISTOMORPHOMETRY IMAGES. ....	33
FIGURE 1.7: RESTENOTIC LESION. ....	34
FIGURE 1.8: CURRENT ISR TREATMENT STRATEGIES .....	39
FIGURE 1.9: INORGANIC COATED STENTS .....	42
FIGURE 1.10: STENT COATINGS.....	45
FIGURE 1.11: ISR PATHOPHYSIOLOGY AT BOTH A TISSUE AND SUB-CELLULAR LEVEL. ....	47
FIGURE 1.12: CURRENT PHARMACOLOGICAL AGENTS – ISR AT A TISSUE LEVEL.....	50
FIGURE 1.13: CURRENT PHARMACOLOGICAL AGENTS – ISR AT A SUB-CELLULAR LEVEL ..	52
FIGURE 1.14: SIROLIMUS.....	53
FIGURE 1.15: PACLITAXEL.....	55
FIGURE 1.16: COMPOSITION OF A GENE-ELUTING STENT .....	63
FIGURE 1.17: GENE THERAPY CATEGORIES - NON-VIRAL AND VIRAL VECTORS. ....	66
FIGURE 1.18: LIPOSOMES.....	67
FIGURE 1.19: ADENOVIRUS.....	69
FIGURE 1.20: ADENO-ASSOCIATED VIRUS.....	70
FIGURE 1.21: RETROVIRUS .....	70
FIGURE 1.22: LENTI-VIRUS.....	71
FIGURE 1.23: DEFINITIONS OF ATMPs. ....	75
FIGURE 1.24: ADVANCED THERAPY MEDICINAL PRODUCTS.....	76
FIGURE 1.25: GENE THERAPY CLINICAL TRIALS (1989-2012) .....	80
FIGURE 1.26: ORGANISATION OF THE THESIS.....	84

## CHAPTER 2

FIGURE 2.1 PLURONIC F127 MORPHOLOGY .....	95
FIGURE 2.2 PLURONIC F127 – CELLULAR UPTAKE.....	97
FIGURE 2.3 CHEMICAL STRUCTURE OF PLASMID DNA.....	99
FIGURE 2.4 CHEMICAL AND MOLECULAR STRUCTURE OF PLURONIC F127 .....	100
FIGURE 2.5 HERA INCUBATOR – CELL CULTURE.....	106
FIGURE 2.6 CROWNCELL™ EXPERIMENTAL SET-UP .....	107
FIGURE 2.7 IMAGES OF CELL-LINED SILICONE TUBE EXPERIMENTAL SET-UP .....	109
FIGURE 2.8 ELUTION KINETIC EXPERIMENTAL SET-UP .....	109

FIGURE 2.9 HITACHI TRANSMISSION ELECTRON MICROSCOPE .....	111
FIGURE 2.10 FT-IR 8300.....	112
FIGURE 2.11 PLURONIC F127 – DSC THERMOGRAM .....	115
FIGURE 2.12 PF127 POLYPLEX DSC THERMOGRAMS .....	116
FIGURE 2.13 FTIR ABSORBANCE SPECTRAL DATA .....	118
FIGURE 2.14 FTIR SPECTRAL ANALYSIS.....	119
FIGURE 2.15 ZETA-SIZER CHARGE ANALYSIS .....	120
FIGURE 2.16 DLS SIZE DISTRIBUTION HISTOGRAMS .....	122
FIGURE 2.17 POLYPLEX ELUTION KINETIC PROFILES .....	124
FIGURE 2.18 IN VITRO (2D) TRANSFECTION EFFICIENCY – LUCIFERASE EXPRESSION .....	126
FIGURE 2.19 IN VITRO (3D) TRANSFECTION EFFICIENCY – EGFP EXPRESSION .....	127
<b>CHAPTER 3</b>	
FIGURE 3.1 VECTOR STENT COATING.....	152
FIGURE 3.2 IN VITRO (3D) SYSTEM PROTOCOL .....	158
FIGURE 3.3 SCHEMATIC OF 3D TRANSFECTION EFFICIENCY SYSTEM. ....	159
FIGURE 3.4 ADENOVIRUS TRANSDUCTION OPTIMISATION .....	163
FIGURE 3.5 CELLULAR VIABILITY ASSESSMENT – ALAMAR BLUE™ .....	164
FIGURE 3.6 CUMULATIVE DNA RELEASE ELUTION CURVES .....	165
FIGURE 3.7 IN VITRO (2D) TRANSFECTION EFFICIENCY RESULTS .....	166
FIGURE 3.8 NON VIRAL VS VIRAL GENE EXPRESSION – (2D) IN VITRO SYSTEM .....	167
FIGURE 3.9 IN VITRO (3D) TRANSFECTION EFFICIENCY RESULTS .....	169
FIGURE 3.10: NON VIRAL VS VIRAL GENE EXPRESSION – (3D) IN VITRO SYSTEM .....	170
FIGURE 3.11 EX VIVO (3D) TRANSFECTION EFFICIENCY RESULTS .....	171
FIGURE 3.12 NON VIRAL VS VIRAL GENE EXPRESSION – (3D) EX VIVO SYSTEM .....	172
FIGURE 3.13 COMPARISON ACROSS ASSESSMENT SYSTEMS.....	173
<b>CHAPTER 4</b>	
FIGURE 4.1 OVERVIEW OF ISO 10993 STANDARD.....	191
FIGURE 4.2 CHEMICAL STRUCTURE OF LIPSOSOME CONSTITUENTS.....	197
FIGURE 4.3 ISO 10993- PART 5 .....	202
FIGURE 4.4 CELL VIABILITY ASSAY .....	206
FIGURE 4.5 PHASE CONTRAST IMAGES .....	209
FIGURE 4.6 AFM SURFACE ROUGHNESS PLOTS .....	210
FIGURE 4.7 BIOPHYSICAL CHARACTERISATION .....	211
FIGURE 4.8 ZETA CHARGE ANALYSIS .....	212
FIGURE 4.9 SEM MICROGRAPHS .....	214
<b>CHAPTER 5</b>	
FIGURE 5.1 MICROPIPETTE LIPOPLEX DEPOSITION.....	233

FIGURE 5.2 AEROSOLISATION PROCESS .....	234
FIGURE 5.3 GE C-ARM FOR FLUOROSCOPIC GUIDANCE .....	236
FIGURE 5.4 RABBIT COMMON ILIAC ARTERY STENTING .....	237
FIGURE 5.5 STENT PRE-DEPLOYMENT IN SITU .....	238
FIGURE 5.6 LIPOPLEX TRANSGENE EXPRESSION – 28 AND 42 DAYS .....	241
FIGURE 5.7 COMPARATIVE ANALYSIS OF TRANSGENE EXPRESSION – 28 AND 42 DAYS ...	242
FIGURE 5.8 LIPOCOUPON TRANSGENE EXPRESSION ANALYSIS – 28 DAYS .....	243
FIGURE 5.9 AEROSOL DELIVERY QUANTIFICATION .....	244
FIGURE 5.10 IN VITRO VS IN VIVO GENE EXPRESSION .....	246

## CHAPTER 6

FIGURE 6.1 PLASMID MAP - PWPTENOS .....	263
FIGURE 6.2 LACZ EXPRESSION OF BMS AND PC COATED STENTS – 28 DAYS .....	271
FIGURE 6.3 NUCLEAR VS CYTOPLASMIC LACZ EXPRESSION – 28 DAYS .....	273
FIGURE 6.4 LACZ EXPRESSION IN THE NEOINTIMA .....	275
FIGURE 6.5 ENOS TRANSGENE EXPRESSION – 21 DAYS .....	276
FIGURE 6.6 QUANTIFIED ENDOTHELISATION – 14 AND 28 DAYS .....	278
FIGURE 6.7 SEM IMAGES OF EXCISED VESSELS .....	280

## LIST OF TABLES

TABLE 1.1	COMMERCIALY AVAILABLE DES	56
TABLE 1.2	STATUS OF ATMPs IN PHASE III CLINICAL TRIALS	81
TABLE 2.1	DSC EXPERIMENTAL DATA	117
TABLE 3.1	STANDARD CURVE SERIAL DILUTIONS FOR PICOGREEN™ ASSAY	153
TABLE 4.1	BIOPHYSICAL DATA – LIPOPLEXES	211
TABLE 5.1	GENE DELIVERY COMPARISON (LIPOPLEXES)	252
TABLE 6.1	ANIMAL AND STENTS, WITH VECTOR COMBINATIONS	265
TABLE 6.2	HISTOMORPHOMETRIC DATA – 28 DAYS	282
TABLE 6.3	HEAD-TO-HEAD COMPARISON OF MEDIAN LEVEL GENE EXPRESSION	283

## LIST OF ABBREVIATIONS

<b>α-SMA</b>	Alpha Smooth Muscle Actin	<b>HDL</b>	High density lipoprotein
<b>AAV</b>	Adeno-associated virus	<b>HEK</b>	Human Embryonic Kidney Cells
<b>Adv</b>	Adenovirus	<b>HPRT</b>	Hypoxanthine phosphoribosyltransferase
<b>Ad-GFP</b>	Adenovirus-GFP	<b>HUVEC</b>	Human Umbilical Vein Endothelial Cells
<b>Ad-βgal</b>	Adenovirus- β-gal	<b>ICAM-1</b>	Intracellular Adhesion Molecule 1
<b>Ad-LacZ</b>	Adenovirus-LacZ	<b>IEL</b>	Internal elastic lamina
<b>AFM</b>	Atomic Electron Spectroscopy	<b>IL-6</b>	Interleukin-6
<b>AFUs</b>	Arbitrary Fluorescent Units	<b>iNOS</b>	inducible Nitric Oxide Synthase
<b>ANOVA</b>	Analysis of variance	<b>ISR</b>	In-stent Restenosis
<b>AR</b>	As received	<b>KCl</b>	Potassium chloride

<b>ATCC</b>	American type culture collection	<b>LacZ</b>	Beta Galactosidase
<b>ATM</b>	Atmospheres	<b>LCST</b>	Lower Critical Solution Temp
<b>β-gal</b>	Beta Galactosidase	<b>LDL</b>	Low-Density Protein
<b>BMS</b>	Bare Metal Stent	<b>Lipo-eNOS</b>	Lipoplex with eNOS gene
<b>Bp</b>	Base pair	<b>Lipo-Null</b>	Lipoplex with no gene
<b>BSA</b>	Bovine Serum Albumin	<b>Lipo-βGal</b>	Lipoplex with βGal gene
<b>CASMC</b>	Coronary Artery Smooth Muscle Cells	<b>Luc</b>	Luciferase
<b>cDNA</b>	Complementary DNA	<b>MACE</b>	Major Adverse Cardiac Event
<b>Chol</b>	Cholesterol	<b>MgCl<sub>2</sub></b>	Magnesium Chloride
<b>CMV</b>	Cytomegalovirus	<b>MOI</b>	Multiplicity of infection
<b>CS</b>	Coverslip	<b>MI</b>	Myocardial Infarction
<b>CVD</b>	Cardiovascular Disease	<b>MTT</b>	2-(4, 5-dimethyltriazol-2-yl)-2, 5-diphenyl tetrazolium bromide
<b>DAPI</b>	4',6-diamidino-2-phenylindole	<b>NaCl</b>	Sodium Chloride
<b>DDAB</b>	Dimethyldioctadecylammonium bromide salt	<b>NaOH</b>	Sodium Hydroxide
<b>DES</b>	Drug Eluting Stents	<b>ND</b>	Not Detected
<b>dH<sub>2</sub>O</b>	Distilled Water	<b>NF -κβ</b>	Nuclear factor Kappa Beta
<b>DMEM</b>	Dulbecco's modified eagles medium	<b>NLS</b>	Nuclear Localising Signal
<b>DMF</b>	Dimethylformamide	<b>NP-40</b>	Nonidet P-40
<b>DMTA</b>	Dynamic Mechanical Thermal Analysis	<b>NZW</b>	New Zealand White
<b>DNA</b>	Deoxyribose Nucleic Acid	<b>O<sub>2</sub></b>	Superoxide
<b>DOPE</b>	1,2-dioleoylphosphatidylcholine	<b>OH</b>	Hydroxyl
<b>DOTMA</b>	(N-[1-(2,3-dioleoyloxy)propyl]-n,n,n-trimethylammonium chloride	<b>PBS</b>	Phosphate Buffered Solution
<b>DSC</b>	Differential Scanning Calorimetry	<b>PC</b>	Phosphorylcholine
<b>dsDNA</b>	Double Stranded DNA	<b>pDNA</b>	plasmid DNA
<b>EC</b>	Endothelial Cell	<b>PLGA</b>	Poly-Lactic Glycolic Acid
<b>ECM</b>	Extracellular matrix	<b>POPC</b>	1,-Palmitoyl-2 Oleoyl-sn Glycerol-3
<b>EDTA</b>	Ethylenediaminetetraacetic Acid	<b>PTCA</b>	Percutaneous Transluminal Coronary
<b>EEL</b>	External Elastic Lamina	<b>PU</b>	Polyurethane
<b>ELISA</b>	Enzyme-Linked Immunosorbent Assay	<b>Rms</b>	Root Mean Square
<b>eGFP</b>	Enhanced Green Fluorescent Protein	<b>RPM</b>	Revolutions Per Minute
<b>eNOS</b>	Endothelial Nitric Oxide Synthase	<b>RT-PCR</b>	RT Polymerase Chain Reaction
<b>FBS</b>	Foetal Bovine Serum	<b>SDS</b>	Sodium dodecyl sulfate
<b>FTIR</b>	Fourier Transform InfraRed	<b>SEM</b>	Scanning Electron Microscopy
<b>GAPDH</b>	Glyceraldehyde Phosphate Dehydrogenase	<b>SMC</b>	Smooth Muscle Cells
<b>GES</b>	Gene Eluting Stents	<b>SS</b>	Stainless Steel
<b>H&amp;E</b>	Haematoxylin and Eosin	<b>SSC</b>	Stainless Steel Coupon
<b>HBSS</b>	Hank's Balanced Salt Solution	<b>TE</b>	Tris EDTA
<b>hCASMC</b>	Human Coronary Smooth Muscle	<b>VCAM-1</b>	Vascular Cell Adhesion Molecule 1
<b>VEGF</b>	Vascular Endothelial Growth Factor	<b>vWF</b>	von Willebrand Facto
<b>VERO</b>	African Green Monkey Kidney Epithelial	<b>X-gal</b>	5-bromo-4-chloro-3-indolyl-β-D galactopyranoside

## TABLE OF CONTENTS

ABSTRACT.....	i
DECLARATION.....	ii
DEDICATION.....	iii
ACKNOWLEDGEMENTS.....	iv, v
LIST OF FIGURES.....	vi, vii, viii
LIST OF TABLES.....	viii
LIST OF ABBREVIATIONS.....	viii, ix
1. Chapter - Introduction .....	18
1.1 Overview.....	19
1.2 Introduction to Cardiovascular Disease .....	20
1.2.1 The Blood Vessel Wall and the Role of Endothelium .....	21
1.2.2 Atherosclerosis.....	24
1.2.3 Treatment of atherosclerosis.....	26
1.3 Restenosis- The healing response .....	27
1.3.1 In-stent Restenosis.....	29
1.4 Current Treatment Strategies for ISR.....	35
1.4.1 Percutaneous transluminal coronary angioplasty (PTCA) .....	36
1.4.2 Cutting balloon angioplasty (CBA) .....	37
1.4.3 Directional coronary atherectomy (DCA) .....	37
1.4.4 High speed rotational atherectomy (HSRA or rotablation) ....	38
1.4.5 Excimer laser coronary angioplasty .....	38
1.4.6 Intravascular brachytherapy .....	38
1.5 Stents and stent coatings .....	39
1.5.1 Inorganic coatings .....	40
1.5.2 Polymeric coatings .....	42
1.6 Drug-eluting stents.....	43
1.6.1 Sirolimus.....	53

1.6.2 Paclitaxel .....	54
1.6.3 Commercially available DES .....	55
1.6.4 DES - Primary complications .....	57
1.7 Gene Therapy .....	60
1.7.1 Cardiovascular Gene Therapy .....	61
1.7.2 Gene Delivery Systems for the vasculature .....	61
1.7.3 Gene-eluting stents (GES) .....	62
1.8 Regulatory affairs .....	75
1.8.1 Medical device regulation.....	77
1.8.2 Regulatory route in Europe for GES.....	78
1.8.3 Gene Therapy Clinical Trials .....	79
1.9 Research Summary.....	82
1.9.1 Phase I: Exploratory proof-of-principle study.....	84
1.9.2 Phase II: Selection Process Study.....	87
1.10 Specific study aims .....	89
2. Evaluation of non-viral Pluronic®F127 (PF127) as a potential coating/vector for delivery of a reporter gene <i>in vitro</i> .....	91
2.1 Introduction.....	92
2.1.1 Non-viral vectors .....	93
2.1.2 Pluronics.....	93
2.1.3 Pluronic - medical applications .....	96
2.1.4 Pluronic - gene therapy applications .....	98
2.1.5 Pluronic® F127 .....	100
2.1.6 Experimental Rationale.....	101
2.1.7 Experimental Objectives .....	102
2.2 Materials and Methods .....	103
2.2.1 Preparation of PF127 .....	103
2.2.2 Plasmids .....	104
2.2.3 Synthesis of DNA loaded PF127 formulations .....	104
2.2.4 Stent preparation .....	105

2.2.5 Cell culture .....	105
2.2.6 <i>In vitro</i> transfection.....	106
2.2.7 Elution kinetic profiling .....	109
2.2.8 Differential Scanning Calorimetry (DSC) .....	110
2.2.9 Transmission Electron Microscopy (TEM).....	111
2.2.10 FTIR Spectroscopy .....	111
2.2.11 Dynamic Light Scattering (DLS) .....	112
2.2.12 Zeta Potential – Surface Charge Analysis.....	113
2.2.13 Statistical Analysis .....	113
2.3 Results .....	113
2.3.1 Physical characterisation – DSC .....	113
2.3.2 Chemical characterisation – FTIR.....	117
2.3.3 Charge Analysis – Zeta Potential.....	119
2.3.4 Morphological characterisation – DLS, TEM.....	121
2.3.5 Elution kinetics .....	123
2.3.6 Transfection efficiency – 2D and 3D .....	125
2.4 Discussion .....	127
2.5 Conclusion .....	135
3. Comparison of viral and non-viral vectors delivery from stent substrates <i>in vitro</i> and <i>ex vivo</i> .....	138
3.1 Introduction.....	139
3.1.1 <i>In vitro</i> versus <i>in vivo</i> performance.....	141
3.1.2 Advanced <i>in vitro</i> systems .....	142
3.1.3 Elution kinetics .....	144
3.1.4 Experimental Rationale .....	145
3.1.5 Experimental Objectives .....	147
3.2 Materials and Methods .....	147
3.2.1 Cell culture .....	147
3.2.2 Vector Preparation.....	148
3.2.3 Viral vector optimisation study.....	149

3.2.4	Viral vector cellular response.....	150
3.2.5	Stent coating procedure .....	151
3.2.6	Elution kinetics .....	153
3.2.7	<i>In vitro</i> – 2D transfection efficiency .....	156
3.2.8	<i>In vitro</i> – 3D transfection efficiency .....	156
3.2.9	Carotid artery explant protocol .....	159
3.2.10	Statistical Analysis .....	161
3.3	Results .....	161
3.3.1	Adenoviral optimisation.....	161
3.3.2	Adenoviral vector cytotoxicity .....	163
3.3.3	Comparison of elution profiles .....	164
3.3.4	<i>In vitro</i> transfection efficiency – 2D .....	165
3.3.5	<i>In vitro</i> transfection efficiency – 3D .....	167
3.3.6	<i>Ex vivo</i> transfection efficiency.....	170
3.4	Discussion .....	173
3.5	Conclusion .....	182
4.	<i>In vitro</i> characterisation study of candidate non-viral lipoplexes from a coronary artery stent substrate .....	187
4.1	Introduction.....	188
4.1.1	Lipoplexes.....	189
4.1.2	Medical device evaluation - ISO 10993.....	190
4.1.3	Experimental Rationale .....	193
4.1.4	Experimental objectives.....	194
4.2	Materials and methods .....	195
4.2.1	Plasmids .....	195
4.2.2	Candidate liposomes.....	195
4.2.3	Coupon preparation .....	197
4.2.4	Construction of lipoplexes .....	198
4.2.5	Preparation of Lipo-coupons.....	198
4.2.6	Long-term storage of Lipo-coupons.....	198

4.2.7 Lipoplex release studies from coupons .....	199
4.2.8 <i>In vitro</i> cell seeding and culture .....	199
4.2.9 <i>In vitro</i> transfection.....	200
4.2.10 Assessment of cellular response.....	201
4.2.11 Biophysical characterisation .....	203
4.2.12 Statistical Analysis .....	205
4.3 Results .....	205
4.3.1 Cytotoxicity evaluation .....	205
4.3.2 <i>In vitro</i> transfection efficiency .....	207
4.3.3 Biophysical characterisation of lipoplexes.....	209
4.4 Discussion .....	214
4.5 Conclusion .....	218
5. A comparison of liposomal gene delivery <i>in vivo</i> , from bare metal and PC coated, coronary stents in a normocholesterolemic rabbit model 220	
5.1 Introduction.....	221
5.1.1 Stent-based gene delivery to the vasculature .....	224
5.1.2 PC Stents: Gene delivery .....	225
5.1.3 Stent coating methodology.....	226
5.1.4 Deployment pressure and implantation site .....	229
5.1.5 Experimental rationale.....	231
5.2 Materials and methods .....	232
5.2.1 Plasmids .....	232
5.2.2 “Lipocoupon” and Lipostent preparation .....	232
5.2.3 Aerosolised Stents.....	233
5.2.4 Animals.....	235
5.2.5 Animal model .....	235
5.2.6 <i>In vivo</i> catheter procedures .....	237
5.2.7 Histochemical analysis of gene expression.....	239
5.2.8 Image analysis of Lipo-βgal transduced vessels.....	239

5.2.9 Statistical Analysis .....	239
5.3 Results .....	240
5.3.1 <i>In vivo</i> Lipostent efficacy evaluation.....	240
5.3.2 Transgene expression - <i>in vivo</i> .....	241
5.3.3 Subcutaneous Lipocoupon mediated transgene delivery <i>in vivo</i> .....	243
5.3.4 Alternative coating methodology: Aerosolisation .....	243
5.4 Discussion .....	245
5.4.1 <i>In vivo</i> Lipostent evaluation .....	245
5.4.2 Time course comparison with other vectors .....	247
5.4.3 Impact of coating methodologies on transfection capabilities .....	249
5.4.4 <i>In vivo</i> time course of candidate Lipostents .....	251
5.4.5 Implantation of subcutaneous candidate Lipocoupons .....	252
5.5 Conclusion .....	255
6. Liposome-mediated delivery of a therapeutic gene, eNOS, to the vasculature of a hypercholesterolemic rabbit model.....	257
6.1 Introduction.....	258
6.1.1 Endothelial Nitric Oxide Synthase (eNOS) .....	259
6.1.3 Experimental rationale.....	261
6.2 Materials and methods .....	262
6.2.1 Plasmids .....	262
6.2.2 Cloning of human eNOS .....	262
6.2.3 Lipostent preparation .....	264
6.2.4 Animals.....	264
6.2.6 Histochemical analysis of gene expression.....	265
6.2.7 Transgene positive cell identification .....	266
6.2.8 eNOS detection in transduced vessels.....	266
6.2.9 Image analysis of Lipo- $\beta$ Gal transduced vessels.....	267
6.2.10 Endothelialisation Detection.....	268

6.2.11 Tissue SEM .....	268
6.2.12 Histological endothelial assessment .....	269
6.2.13 Morphometric analysis .....	269
6.2.14 Statistical Analysis .....	270
6.3 Results .....	270
6.3.1 Lipo-βgal stents <i>in vivo</i> time course.....	270
6.3.2 Target cell population .....	273
6.3.3 Detection of eNOS expression .....	275
6.3.4 Endothelium regeneration .....	277
6.3.5 Histomorphometry.....	281
6.4 Discussion .....	282
6.5 Conclusion .....	287
7. Conclusions and Future Direction .....	289
7.1 Study Conclusions.....	289
7.2 Future Direction .....	290

# **1. Chapter - Introduction**

## 1.1 Overview

Gene therapy approaches have recently emerged as a potential therapeutic strategy for the treatment of a variety of cardiovascular diseases. Given the increasing prevalence of cardiovascular disease in modern society and the limited treatments available, there is an opportunity for research to be conducted into potential therapeutic interventions, which do not solely target symptom alleviation but aim to restore lost function, relieve pain and prevent disease. Tailor-made targeted gene therapy strategies may offer treatment where none has existed before or improve existing pharmacological treatments.

In the case of In-stent restenosis (ISR), taking a gene therapy approach, which aims to repair and regenerate the injured endothelium of the vessel wall while preventing the formation of Neointimal Hyperplasia (NIH), is a an attractive alternative to pharmacological approaches. This proposed dual gene therapy approach offers the potential to significantly improve outcomes in patients with a propensity to ISR, provide treatment of contra-indicated patients, as well as avoiding the side-effects that are associated with Drug-eluting stents (DES) currently commercially available.

The work presented in this thesis involves the development of a Gene-eluting stent (GES) platform to safely and efficiently deliver a therapeutic gene to the vasculature to prevent the incidence of ISR post-stenting. The work presented focuses on the proof-of-concept required to develop a GES. This research is multi-disciplinary by nature, merging engineering, scientific and clinical principles and perspectives to develop a proposed platform for the delivery of a biologic to the vasculature.

As the development of such a platform requires the input from a variety of subjects, several areas of research are discussed in this introductory chapter. These include: cardiovascular disease,

atherosclerosis, differentiation between restenosis and ISR, as well as the pathophysiology, biological cascade and time course of the cellular events associated with ISR. The current strategies commercially available for the treatment of ISR and the current state-of-the-art gene therapies utilised for the treatment of cardiovascular disease are also discussed. The specific objectives of this study are outlined at the end of this introductory chapter.

## **1.2 Introduction to Cardiovascular Disease**

Cardiovascular disease (CVD) is a family of disorders including coronary and peripheral artery disease, cerebro-vascular disease, congenital heart disease, rheumatic heart disease and deep vein thrombosis. In recent years, CVD has reached epidemic proportions. In 2010, Lloyd-Jones and colleagues estimated that the combined direct and indirect costs of CVD for 2010 would amount to \$503.2 billion, with over 800,000 deaths in the United States alone (Lloyd-Jones *et al.*, 2010). More recently in 2014, The Centre for Economics and Business Research (CEBR) quantified the economic burden of CVD by using existing prevalence data (from 6 selected European countries: France, Germany, Italy, Spain, Sweden and the UK) as a basis for estimating the combined direct (healthcare) and indirect (lost productivity from morbidity and mortality rates) costs (Sidney *et al.*, 2013). Across the six countries examined, the report predicted that mortality from CVD will rise from 1,118,457 in 2014 to 1,215,088 in 2020. The report also projected increased CVD healthcare costs to €122.6 billion by 2020. It is projected that by 2030, CVD will be responsible for almost 23.6 million deaths globally (Roger *et al.*, 2011). CVD, as a result of atherosclerosis, is the primary cause of mortality in the western world. While atherosclerosis is a systemic disease, focal manifestations lead to obstructive lesion formation in critical areas of the vasculature. Currently, these obstructive atherosclerotic lesions are treated by the implantation of stents to re-open the lumen of the vessel and restore blood flow.

Figure 1.1 below graphically illustrates how the development of atherosclerosis narrows the arterial lumen, restricting blood flow, exacerbating the accumulation of sediment and leading to the formation of atherosclerotic plaque.

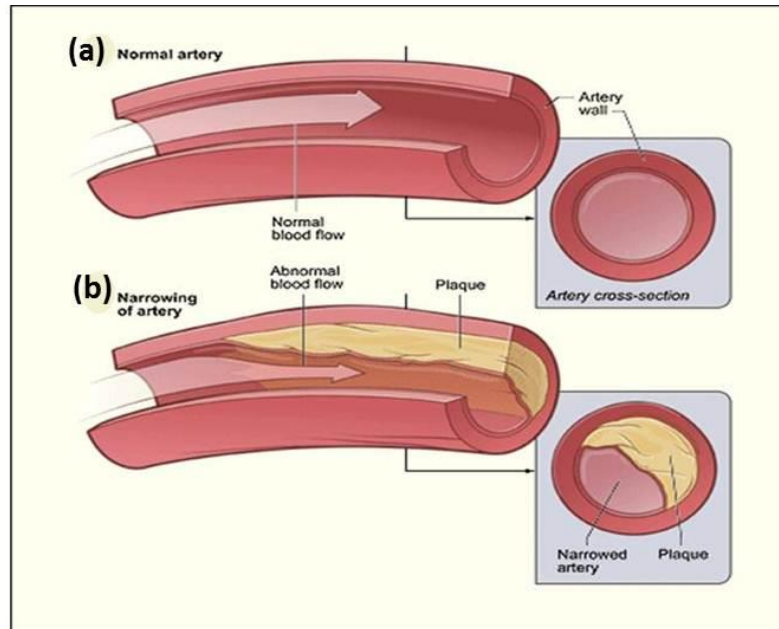


**Figure 1.1:** Development of Atherosclerosis (a) Illustrates normal blood flow and cross section of a healthy vessel. (b) Illustrates accumulation of plaque and a narrowed cross section. Source: National Heart, Blood and Lung Institute. <http://www.nhlbi.nih.gov/>.

Atherosclerosis can be predicted by a number of risk factors including obesity, hypertension, diabetes mellitus, smoking, elevated LDL (low-density lipoprotein), reduced HDL (high-density lipoprotein) levels and increased triglyceride levels in the blood in addition to a multitude of genetic factors (McGill *et al.*, 2000), (Novelli *et al.*, 2003), (Stassen, Vainas, & Bruggeman, 2008), (Kullo & Cooper, 2010), (Teramoto *et al.*, 2013), (Mancia, Facchetti, Parati, & Zanchetti, 2012) and (Fesinmeyer *et al.*, 2013).

### 1.2.1 The Blood Vessel Wall and the Role of Endothelium

The clinical definition of restenosis is given as “*loss of greater or equal to 50% of the gain produced at angioplasty or a > 50% stenosis at follow-up angiography*” (Bennett, 2001). To truly understand the pathogenesis of restenosis (understanding the origin and development of

the disease), knowledge of the structure and biology of the normal artery, in addition to its indigenous cell types, is required. Normal, un-diseased arteries possess a well-developed, tri-laminar structure: tunica adventitia, tunica media and tunica intima as illustrated in Figure 1.2.

Each layer is constitutively different and has a function to perform. The outermost layer (Tunica Adventitia) is predominantly composed of collagen and elastic fibres in a connective tissue and its primary function is to provide a limiting barrier, protecting the vessel from overexpansion. This adventitial layer is serviced by a network of minute blood vessels and nerves, collectively referred to as the *vasa vasorum*. The middle layer (tunica media) is composed of two elastic membranes (internal and external) within which there is a layer of quiescent vascular smooth muscle cells (VSMCs). The innermost layer (tunica intima) is composed of basement membrane which anchors a monolayer of endothelial cells (ECs), more commonly referred to as the endothelium (Pfister & Campbell, 1996), (Irving & Walker, 1999) and (Jones, le Noble, & Eichmann, 2006).

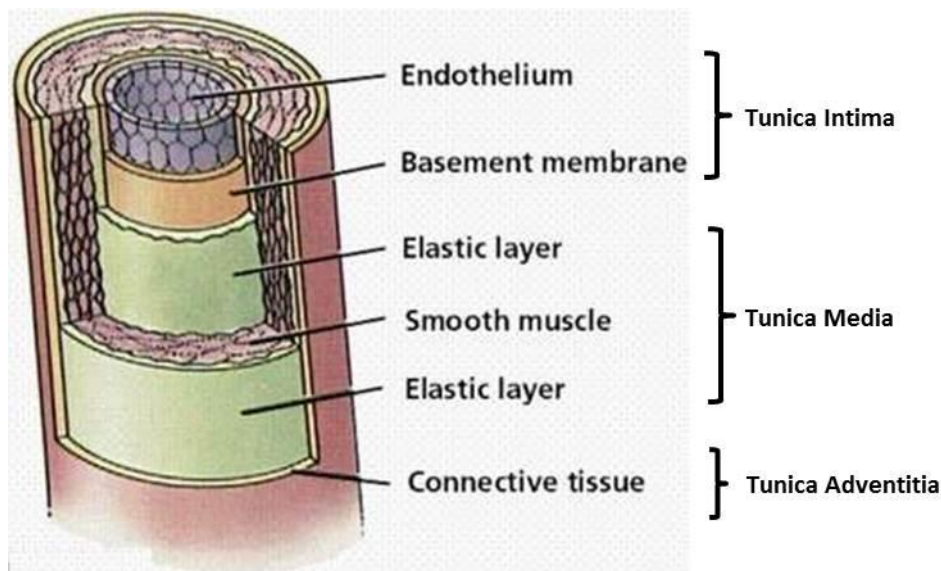


**Figure 1.2:** Schematic illustrating the gross structure of the blood vessel wall with three distinctive layers from the innermost to the outermost: Tunica Intima, Tunica Media and Tunica Adventitia (adapted from McGraw-Hill, 2003).

The VSMCs of the tunica media are highly specialised cells. VSMCs afford the blood vessel wall its ability to involuntarily contract and relax (Frid, Shekhonin, Koteliansky, & Glukhova, 1992), (Trion & van der Laarse, 2004), (Clarke *et al.*, 2008), (E. T. Lee, Lu, Bennett, & Keen, 2001) and (T. Matsumoto & Nagayama, 2012). These spindle-shaped, mono-nucleated, contractile cells remain in a quiescent, non-proliferative state in a healthy vessel. When this layer is exposed to biological or physiological stressors *in vivo*, the cells lose their dormancy, exiting G<sub>0</sub> of the cell cycle and progressing to the G<sub>1</sub> (migration) and the G<sub>2</sub>/S (proliferation) transition stages.

This results in cell migration and accelerated proliferation (Frid *et al.*, 1992), (Riessen *et al.*, 1999), (Laeremans, Rensen, Ottenheijm, Smits, & Blankesteyjn, 2010) and (K. B. Lee, Song, Paik, & Shin, 2011), both of which are characteristic features of atherosclerosis and restenosis in hypertensive patients and animals (Warrenburg, Schwartz, Henderson, Crits-Christoph, & Nuzzo, 1986), (Falcetti *et al.*, 2010; T. Matsumoto & Nagayama, 2012; Zeng, Yang, & Xu, 2004).

Endothelial cells are mesodermal in origin and possess the ability to continually migrate, proliferate and replicate (M. K. Wong & Gotlieb, 1986), (Herman, Newcomb, Coughlin, & Jacobson, 1987), (Lipton, Bensch, & Karasek, 1991), (Peetla & Labhasetwar, 2008) and (Brunt, Hall, Ward, & Melo, 2007). The interactions between ECs and SMCs are fundamental in a diverse range of cardiovascular processes from arteriogenesis and collateral blood vessel development to atherosclerosis and restenosis (S. Hojo *et al.*, 2003), (D. J. Brown *et al.*, 2005), (Milliat *et al.*, 2006) and (M. Wang *et al.*, 2012). The ECs of the arterial intima constitute the crucial contact surface with blood. It is the only surface, either natural or synthetic, that can maintain blood in a liquid state during protracted contact.

### 1.2.2 Atherosclerosis

Atherosclerosis is now well established as a slowly progressive, inflammatory disease of the artery (Libby, 2002), (Crowther, 2005), (Steinberg, 2006), (Libby, 2008a), and (Weber & Noels, 2011). Understanding the underlying pathophysiology of the disease is fundamental to improving treatment strategies. Atherosclerosis was once considered to be a lipid-storage disease but now it is recognized as a sub-acute, inflammatory condition of the vessel wall, characterised by the infiltration of inflammatory cells such as macrophages and T-cells (B. G. Brown, Zhao, Sacco, & Albers, 1993), (Falk & Fernandez-Ortiz, 1995), (Qiao *et al.*, 1997) and (Libby, 2008b). It is a highly complex disease state which commences initially with endothelial dysfunction caused by subtle injury to the vessel wall either by physical or inflammatory stresses. These can include hypertension, diabetes mellitus, elevated LDL levels or evidence of caffeine and/or nicotine in the blood plasma (Novelli *et al.*, 2003) and (Muntner, He, Astor, Folsom, & Coresh, 2005). These factors, independently or in combination, have the ability to induce endothelium damage, a precursor to the development of atherosclerotic plaque and ultimately the formation of coronary "lesions". The most common classification of atherosclerotic plaque found in the majority of coronary lesions is a necrotic core fibroatheroma or NCFA (Schroeder & Gao, 1995), (S. M. Schwartz, Virmani, & Rosenfeld, 2000) and (Giral *et al.*, 2007). This important pathological process of atherosclerotic lesion formation, specifically the formation of a NCFA, is described below and schematically illustrated in Figure 1.3.

Atherosclerosis is usually associated with the following risk factors: hypertension, smoking, high cholesterol, diabetes or hemodynamic stresses which all known to cause endothelium injury. This resultant damage can induce the activation of a number of cellular pathways, ultimately leading to the recruitment of inflammatory cells. The

inflammatory cells migrate to the sites of endothelium injury and transform into lipid-laden foam cells. These foam cells aggregate and subsequently absorb a variety of materials, including cell debris, cholesterol crystals and calcium deposits. This material accumulation by these inflammatory cell-derived foam cells forms the lipid core of an atherosclerotic plaque. As a consequence, the presence of this lipid core releases cytokines to indicate to the proliferative smooth muscle cells in the medial layer of the injured vessel wall to form collagen in the sub-intimal layer (Fuster, Badimon, Badimon, & Chesebro, 1992), (Uno & Nicholls, 2010), (Nguyen & Levy, 2010) and (Hishikawa, Iihara, Yamada, Ishibashi-Ueda, & Miyamoto, 2010). It is the collagen synthesis which forms the primary component of a fibrous cap which shields the atherosclerotic plaque from the circulatory blood. In combination, the lipid core and the fibrous cap form a NCFA. The thickness of the fibrous cap determines the stability of the plaque (Giral *et al.*, 2007). If this fibrous cap ruptures or the lesion is otherwise eroded, the plaque ultimately ruptures. This plaque rupture can cause acute arterial thrombosis resulting in unstable angina, myocardial infarction, cerebral stroke and sudden cardiovascular death (Nguyen & Levy, 2010).

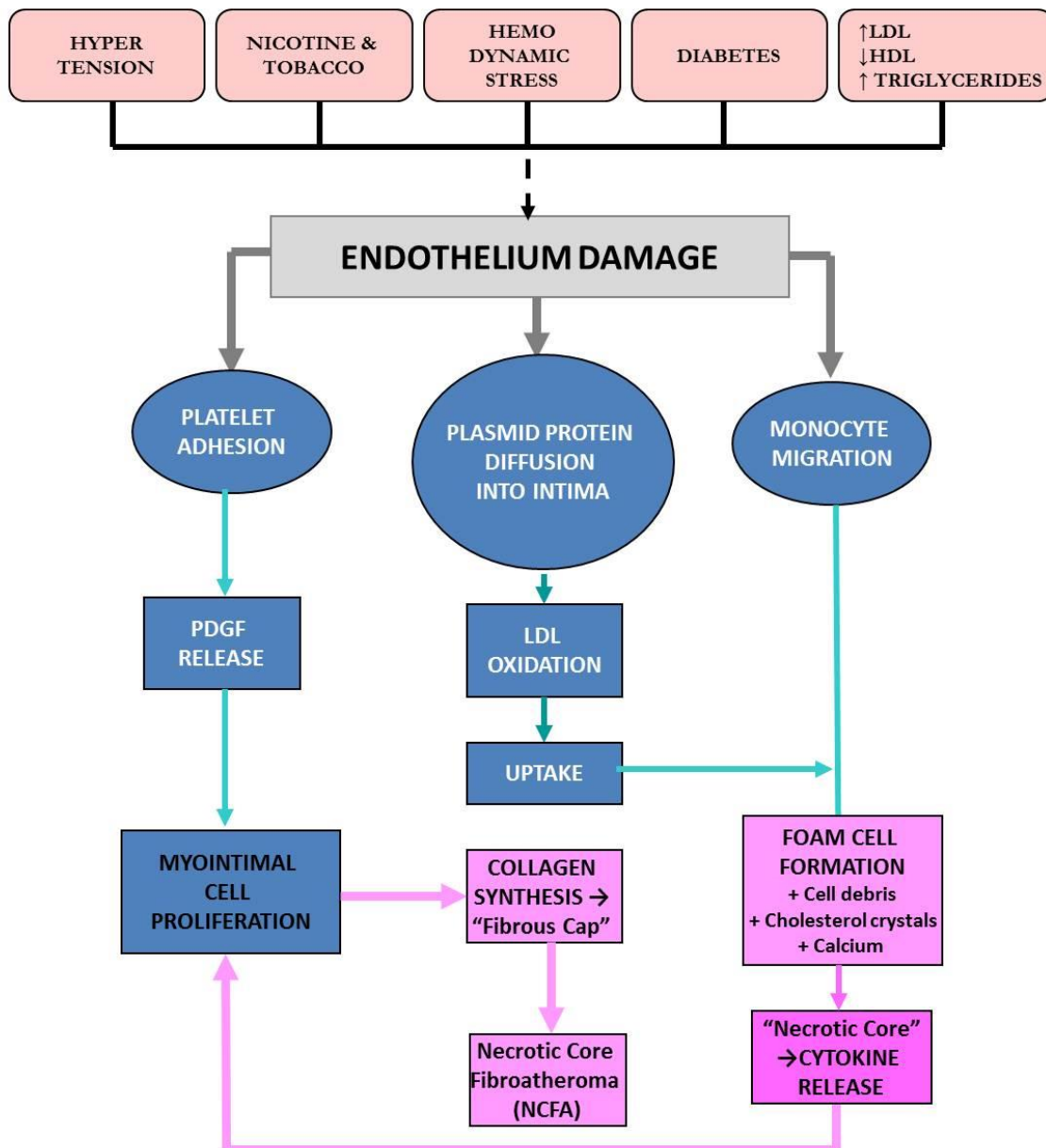


**Figure 1.3:** Pathogenesis of atherosclerosis in the formation of Necrotic Core Fibroatheroma (NCFA) reaction to injury hypothesis. Following endothelium damage, that could be induced by a number of factors, several pathways are induced including platelet adhesion, plasmid protein diffusion and monocyte migration. This indirectly results in LDL oxidation and uptake, foam cell formation. The foam cell absorbs particulate such as cell debris and cholesterol crystals to form a lipid-laden “necrotic core”. This pathological artefact, incites SMCs to migrate to the intimal layer, induce collagen synthesis to provide a matrix for the development of a fibrous cap, ultimately producing a NCFA (adapted from Kahn *et al.*,2007).

### 1.2.3 Treatment of atherosclerosis

The treatment of atherosclerosis has evolved from coronary artery by-pass grafting (CABG) in the 1960’s to serial improvements in percutaneous coronary intervention (Abraham *et al.*, 2010), which

revolutionized the treatment of coronary artery disease when it was introduced in 1977 (Gruntzig, 1979). The term percutaneous transluminal coronary angioplasty (PTCA) is a term that is often used interchangeably with PCI throughout the literature although they are not identical procedures. PCI can be a term applied generically for all procedures relating to coronary intervention. However, PTCA refers specifically to catheter-related interventions that are delivered percutaneously. For the purposes of this thesis, the term PTCA will be used. PTCA has advanced significantly over the past few decades from plain old balloon angioplasty (POBA) procedures used to force open atherosclerotic lesions to the implantation of bare metal stents (BMS) deployed from a balloon catheter to act as permanent scaffolds or “splints”. This theoretical concept of “splinting” was first proposed in 1964 (Dotter & Judkins, 1964), however it was more than 20 years after this that the first human coronary artery stent was actually implanted (Puel *et al.*, 1987). The stents acted as luminal scaffolds that were permanently implanted to keep diseased vessels patent, restoring blood flow (Jeremias *et al.*, 1997) and (Froeschl, Olsen, Ma, & O'Brien, 2004). Coronary stents have the ability to produce favourable acute results after angioplasty, radically improving the safety and long-term clinical outcomes compared to angioplasty alone (Serruys *et al.*, 1994). The most recent advancement involves the addition of a drug to the metal stent scaffold, generating the drug-eluting stent. Before the advent of DES, restenosis remained a significant problem, with 15-20% of patients affected post stent-implantation (Erbel *et al.*, 1998) and (Bettmann *et al.*, 1998).

### **1.3 Restenosis- The healing response**

The term restenosis can be defined in several ways. From a clinical or diagnostic perspective, the more quantitative definition (as referred to in section 1.2.1) is the “*loss of greater or equal to 50% of the gain produced at angioplasty or a > 50% stenosis at follow-up angiography*” (Bennett,

2001). However, from a biological point of view, it is defined as “*the arterial healing response after injury incurred during transluminal coronary revascularization*” (S. M. Schwartz & Reidy, 1987). Both definitions are accurate. However, from the perspective of attempting to prevent the condition with a therapeutic agent the biological definition is the appropriate one to employ.

Restenosis is classed as an iatrogenic disorder (one which is caused by a medical intervention or treatment), and it remains the ‘Achilles’ heel’ of interventional cardiology worldwide, despite the technological advances made (Nageh, Duncan, & Thomas, 2004). Balloon-induced restenosis presents a very different histology to ISR (Moreno *et al.*, 1999), (Mach, 2000) and (Nakatani *et al.*, 2003). During balloon angioplasty there is a relatively short, acute moment of injury (Nageh *et al.*, 2004) and the luminal diameter reduction is primarily caused by adventitial constriction with elastic recoil, negative arterial remodelling and in some cases thrombus formation, with SMC proliferation and ECM formation contributing to the luminal narrowing to a lesser extent (M. K. Hong, Mehran, Mintz, & Leon, 1997), (S. M. Schwartz, 1983), (Schiele *et al.*, 1999), (Van Belle *et al.*, 1999) and (Nageh *et al.*, 2004).

Conversely, with stenting, reduction in the luminal diameter arises primarily from the formation of neointimal hyperplasia post stent-implantation (Virmani *et al.*, 2002), (Nageh *et al.*, 2004) (Funakoshi & Egashira, 2007). The stent placement, in this case, negates the remodelling and recoil. This exaggerated hyperplastic response results from multiple pathophysiologies, including thrombus inflammation as well as intimal and medial dissection (Kornowski *et al.*, 1998), (R. S. Schwartz & Henry, 2002) and (Kibos, Campeanu, & Tintoiu, 2007). The extent of vessel damage during stent deployment and the ensuing inflammatory reaction plays a pivotal role in how the biological cascade of events associated with ISR

occurs. It is well documented that inflammation is an important contributory factor to the development of NIH or Neointimal Hyperplasia (Meuwissen *et al.*, 2002), (Bhatt, 2004), (Drachman & Simon, 2005), (Kremneva, Semukhin, & Kuznetsov, 2006), (Kozinski, Sukiennik, Rychter, Kubica, & Sinkiewicz, 2007) and (Inoue *et al.*, 2011). Increased levels of the inflammatory cytokine interleukin-6 (IL-6) have been found in patients post-stenting and it is proposed that these elevated levels are related to the development of ISR (Y. Hojo & Shimada, 1998), (Y. Hojo, Ikeda, Takahashi, & Shimada, 2002) and (Tepliakov & Rybal'chenko, 2008). A number of variables are known to increase the risk of ISR, including diabetes or patients with a previous history of restenosis (Abizaid *et al.*, 1998; Marso, Mak, & Topol, 1999), (Abizaid *et al.*, 2001), (Trisal, Paulson, Hans, & Mittal, 2002) and (Radke *et al.*, 2006).

### **1.3.1 In-stent Restenosis**

#### **1.3.1.1 Pathophysiology**

All forms of percutaneous coronary intervention confer injury to the vessel. The arterial response to that injury is the basis for the long-term outcome (Doornekamp, Borst, Haudenschild, & Post, 1996), (J. J. Li, 2009) (Costa & Moussa, 2006). However, the process of ISR parallels wound healing responses very closely (Virmani *et al.*, 2002), (Scott, 2006) and (Tahir *et al.*, 2011). Stenting causes localised vessel wall injury, principally, proximal to the stent strut/vessel wall interface (Gunn *et al.*, 1997), (Kibos *et al.*, 2007) and (Shin, Garcia-Garcia, & Serruys, 2010). This stent-induced injury causes a variety of thrombogenic, vasoactive and mitogenic factors to be released to the bloodstream, thus inducing a complex cascade of molecular and cellular events (Kibos *et al.*, 2007). This complex biological cascade, schematically outlined in Figure 1.4, is a multi-faceted problem and involves a multitude of biological events. Once injury has been inflicted on the vessel wall, two events occur almost simultaneously: early thrombus deposition and an acute inflammatory response. These events stimulate

the release of cytokines and growth factors thus attracting SMCs to migrate through the vessel wall and from the circulating bloodstream to the site of injury. Because of the absence of an endothelium, the injured underlying SMCs are caused to undergo a change of phenotype, leaving their non-proliferative quiescent state, entering into the cell cycle mechanism and thus inducing the proliferation of these cells sub-intimally. Extra-cellular matrix (ECM) synthesis and granular tissue development mediated by distinctive molecular pathways (Thery *et al.*, 2005) also occurs and collectively these processes contribute to the formation of an in-stent restenotic lesion.

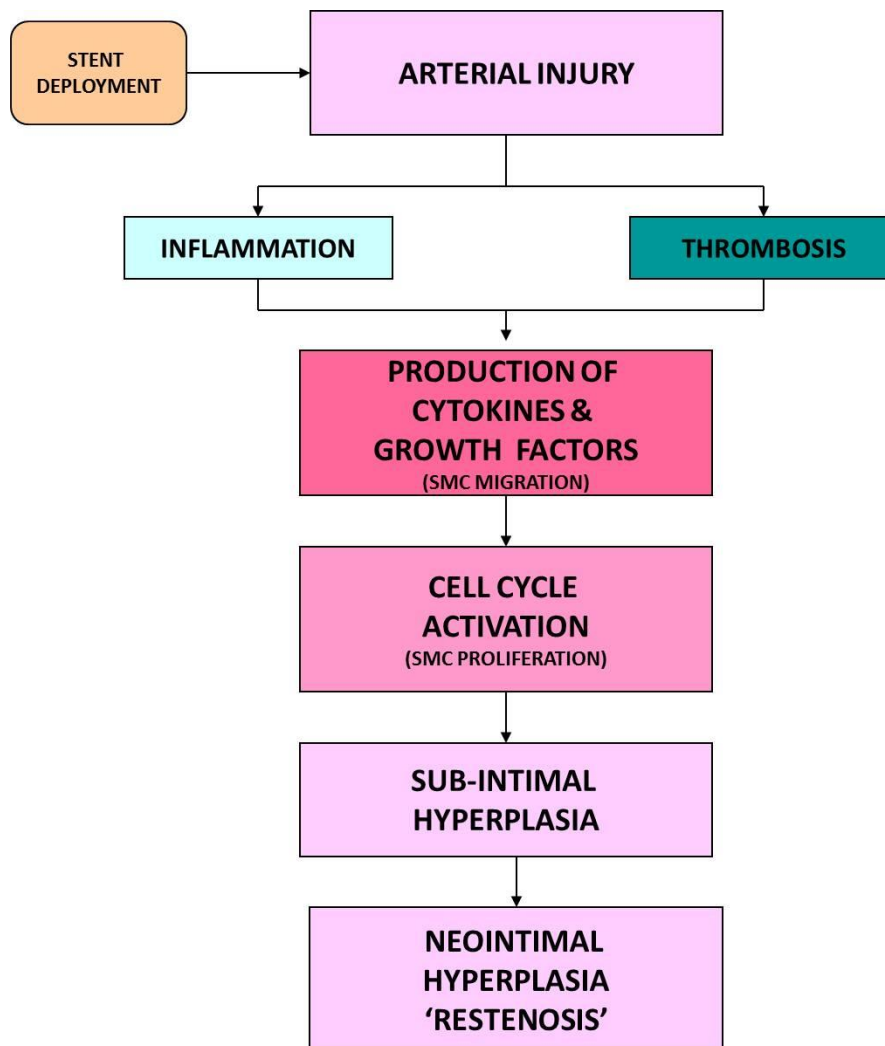


**Figure 1.4:** Stent-induced injury cascade of molecular and cellular events which include the release of a variety of thrombogenic, vasoactive and mitogenic factors that are systematically released into the bloodstream (adapted from Cath Lab Digest, 2003).

### **1.3.1.2 Biological cascade of events**

The inflammatory response is the primary acute response post-stenting, as the body attempts to limit the extent of injury sustained during the procedure (Yeh, Anderson, Pasceri, & Willerson, 2001), (Schillinger *et al.*, 2002), (Dibra *et al.*, 2005) and (Wilson, 2012). Inflammation is a wound healing response; however it is an exaggerated inflammatory response which contributes to restenosis (Kornowski *et al.*, 1998), (Rauchhaus *et al.*, 2002), (Farb, Weber, Kolodgie, Burke, & Virmani, 2002) and (Babapulle & Eisenberg, 2002). The severity of injury directly affects the degree of inflammation (Virmani *et al.*, 2002). The molecular and cellular overview of this biological cascade was discussed in Figure 1.4.

However, this cascade of events is further expanded in Figure 1.5, to track, at both a cellular and sub-cellular level, the detail and the sequence of events following injury to the blood vessel wall during stent deployment and/or balloon angioplasty. As previously discussed, inflammation is the primary trigger for cell recruitment at the site of injury. Neutrophils are the principal mediators of this response initially, whereas monocytes and macrophages are the predominant inflammatory cells during the chronic stage of the inflammatory process (Yeh *et al.*, 2001).

Inflammation causes altered gene expression in circulating blood cells, in the inherent inflammatory system and especially in the endothelium (K. Kirkpatrick *et al.*, 2002), (Swerlick & Lawley, 1993), (Poher & Cotran, 1990) and (Niculescu & Rus, 1990). The presence of inflammatory cells in conjunction with the elevation of chemokines and cytokines, such as interleukin-6 (IL-6), locally activate the cell signalling pathways of influential growth factors and mitogens (bFGF, PDGF, VEGF and MAPKs) which in turn simultaneously stimulate both the proliferation of SMCs and the formation of ECM. These two biological events ultimately result in the synthesis of NIH *in vivo*.

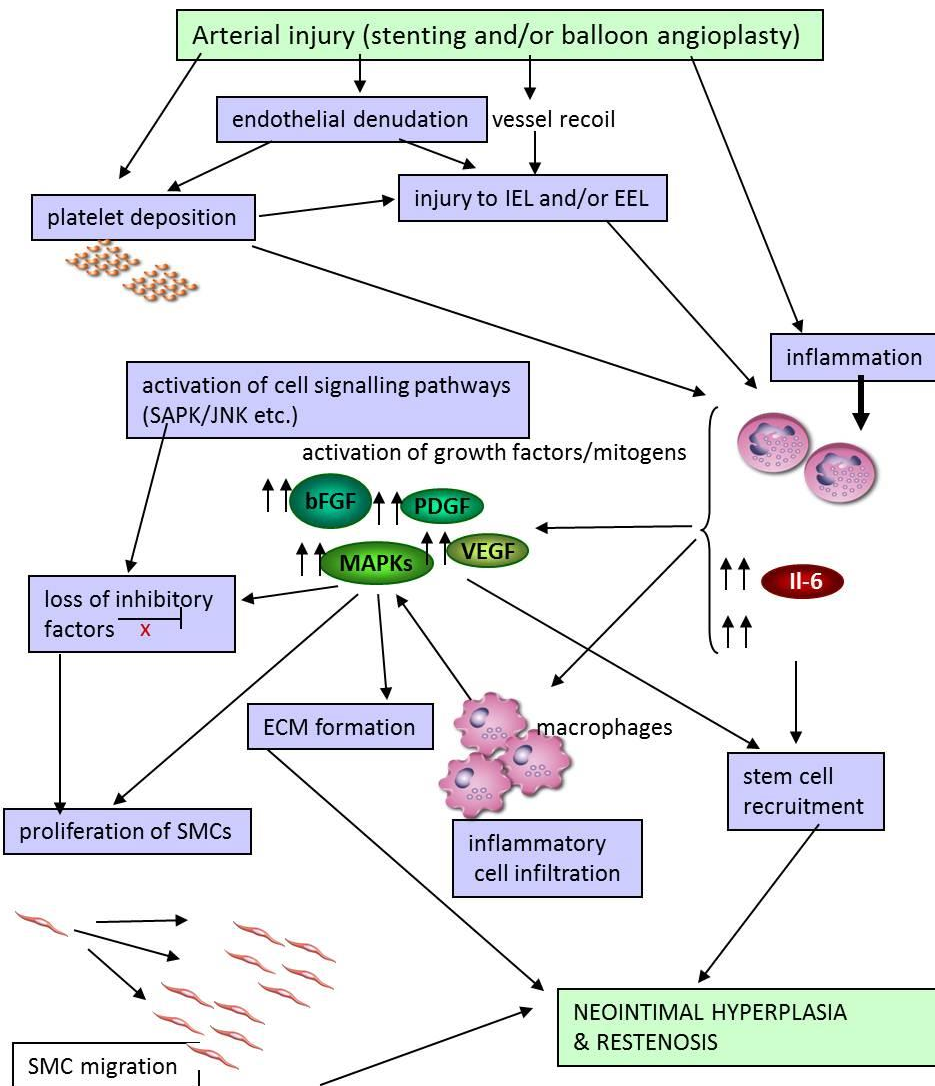


**Figure 1.5:** Sub-cellular sequence of events following injury to the arterial wall during stent deployment and/or balloon angioplasty, leading to the development of neointimal hyperplasia and restenosis of the vessel. IEL = internal elastic lamina, EEL = external elastic lamina, SAP/JNK = Stress-activated protein kinase/c-Jun NH2-terminal kinases, bFGF = basic fibroblast growth factor, PDGF = platelet derived growth factor, VEGF = vascular endothelial growth factor, MAPKs = mitogen activated protein kinases, ECM = extra-cellular matrix. Adapted from figures in Mitra & Agrawal (2006). *Journal of Clinical Pathology* (59:232 -239). Acknowledgements to <http://www.aic-belgium.net> for free call images.

The formation of NIH around the struts of a stent can be clearly observed during histomorphometric analysis. Figure 1.6 depicts the morphometric presentation of a stented arterial lumen with both a bare metal and drug-eluting stent at 28 days post-procedure.

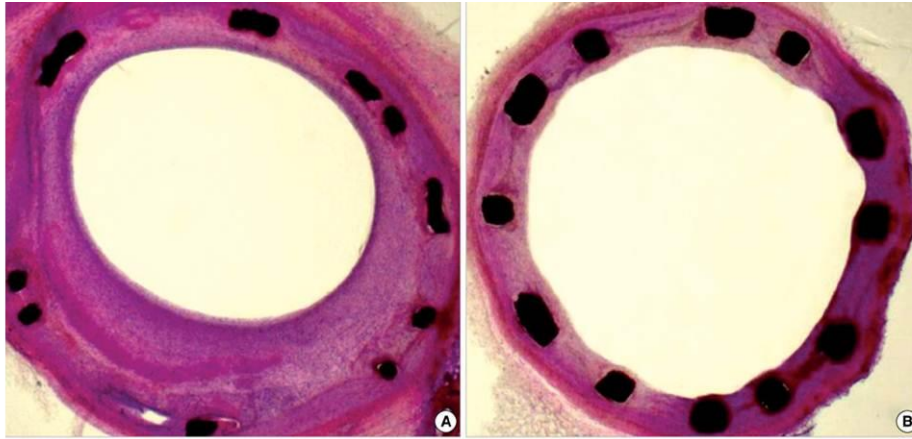


**Figure 1.6:** Histomorphometry image (20 x magnifications) of stented porcine coronary arteries 28 days post-implantation A) bare metal stent B) Drug-eluting stent (Cho *et al.*, 2010).

### **1.3.1.3 Time course of ISR**

In 2000, Germing and colleagues investigated the pathological implications of stent implantation in humans . Their primary findings related to the mechanisms of neointimal hyperplasia formation, in parallel with endothelial regeneration activity. The authors discovered that the latter occurred in a clear three-phase progression, and the neointimal formation occurred in a two-part manner amounting to five stages overall (Germing *et al.*, 2002), (R. S. Schwartz & Henry, 2002) as illustrated in Figure 1.7.

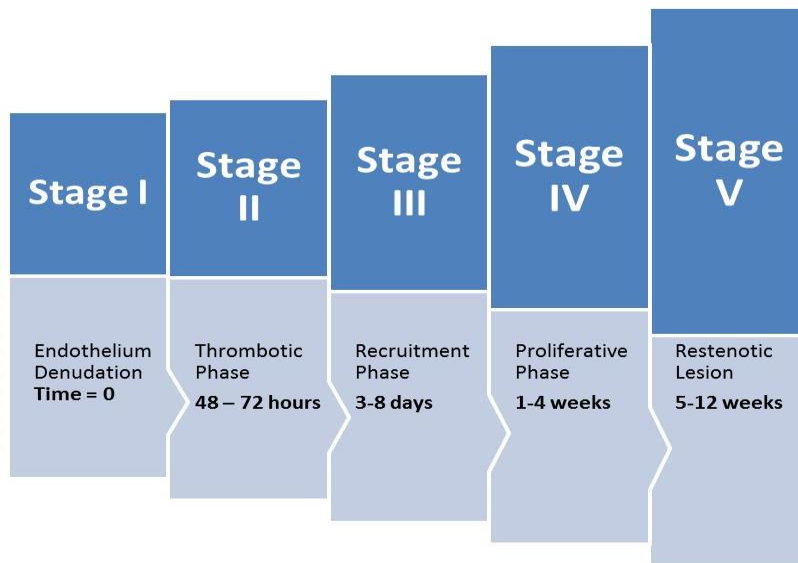


**Figure 1.7:** Timeline of the development (Stages I - V) of a restenotic lesion.

**Stage I - Time Zero:** At the time of arterial injury, the endothelium is denuded, exposing the SMC medial layer. As an initial wound healing response, activated platelets adhere and aggregate followed by fibrinogen deposition around the platelet site. The platelet thrombus becomes fibrin-rich (Nagaoka *et al.*, 2000) and (Majno, 1998).

**Stage II - Thrombotic phase (48-72 hours):** This stage consists of rapid thrombus formation. Fibrin also interacts with red blood cells to form a fibrin/erythrocyte complex which then adheres to the platelet mass. Leukocytes are recruited to the injury site, predominantly neutrophils with a small population of macrophages. Acute inflammatory cytokines (MCP-1, IL-6, IL-8) are also released in this stage (R. S. Schwartz & Henry, 2002).

**Stage III- Recruitment phase (3-8 days):** The thrombus mass forms an outer layer composed of endothelial-like cells, this is followed by an intense monocyte infiltration from the circulating bloodstream; these predominantly evolve into macrophages as they migrate into to the sub-endothelial mural thrombus (R. S. Schwartz & Henry, 2002). Lymphocytes also demarginate from the bloodstream and congregate at the luminal site of the thrombus. The removal of the endothelium exposes the SMCs and

causes them to change phenotype. They lose their quiescence and begin to proliferate. SMCs also begin to migrate into the mural thrombus. The infiltrate also releases a large number of growth factors at this stage (FGF, PDGF, IGF, TGF- $\beta$ , and VEGF) (Maiellaro & Taylor, 2007) and (R. S. Schwartz & Henry, 2002).

**Stage IV-** Proliferative phase (1-4 weeks): Actin-positive cells colonise the residual thrombus from the lumen inward. Smooth muscle cells progressively proliferate toward the injured medial layer, resorbing the thrombus until it diminishes and is replaced by neointimal cells (Maiellaro & Taylor, 2007) and (R. S. Schwartz & Henry, 2002).

**Stage V-** Restenotic Lesion (5-12 weeks): For the remaining weeks, proliferative activity continues along with continued accumulation of extracellular matrix within the lesion (Riessen *et al.*, 1999; Riessen *et al.*, 1994) and (Kawano *et al.*, 2004).

## **1.4 Current Treatment Strategies for ISR**

ISR is a major clinical problem and poses a therapeutic dilemma with a high risk of recurrence (Alfonso *et al.*, 1999), (Fujii *et al.*, 2004), (Fujii, Masutani, & Ohyanagi, 2008; Habara *et al.*, 2008), (Obata *et al.*, 2013) and (Ozawa *et al.*, 2012). A substantial amount of work has been performed on stent design and delivery to prevent restenosis, however a number of other strategies have been implemented in an attempt to eliminate this clinical problem, including surgical intervention and also systemic and local drug delivery.

Puel and Sigwart implanted the first BMS in 1987 to permanently keep a vessel open where a lesion previously obstructed it, thus preventing blood flow (Sigwart, Puel, Mirkovitch, Joffre, & Kappenberger, 1987). The

development of stents to treat focal stenoses in the coronary circulation represented a paradigm shift in the management of these lesions. Since the mid 1990's, multi-disciplinary teams of engineers, material scientists and chemists, have explored every facet of stent design and material selection. These improvements have resulted in metallic stents becoming more flexible, deliverable, radio-opaque and most importantly more biocompatible as the metallic surface, unmodified or untreated, is essentially thrombogenic in nature, increasing the incidence of ISR. The first-generation coronary stents were composed of medical grade stainless steel (316L) or Tantalum (Ta); these materials are still in use. However, current stent technologies predominantly use Cobalt Chromium (CoCr) and Nitinol. Even so, these metals alone still pose a problem of thrombogenicity when exposed to the aggressive environmental conditions *in vivo*, resulting in the increased incidence of ISR.

The following section will describe how the treatment of ISR has evolved from a solely mechanical intervention (balloon angioplasty) to the administration of more invasive and high-risk procedures to treat the obstructive lesions.

#### **1.4.1 Percutaneous transluminal coronary angioplasty (PTCA)**

As with the treatment of atherosclerosis described in section 1.2.3, the treatment of ISR with conventional PTCA is still the prevalent. The benefits of the re-dilatation technique are deemed to be two-fold: the balloon deployment compresses the luminal tissue as well as further expanding the stent *in situ* (Kuntz *et al.*, 1992), (Prpic *et al.*, 2002), (Mehran *et al.*, 2001) and (Radke, Kaiser, Frost, & Sigwart, 2003). However, the success rates are inconsistent, with rates of angiographic and clinical restenosis varying from 30 to 80% (Moussa *et al.*, 1997) and (Dauerman *et al.*, 1998). However, taking this into consideration, PTCA is still the treatment of choice in high risk patients (with diabetes, etc.) that may be

contra-indicated for other options, as corroborated by Li and colleagues in a recent study (J. Li *et al.*, 2015).

#### **1.4.2 Cutting balloon angioplasty (CBA)**

This strategy involves the use of a balloon with multiple microsurgical blades (atherotomes) bonded longitudinally to its surface. The 'cutting' balloon is placed *in situ* and the blades incise the restenotic tissue up to the stent strut position. Albeiro and colleagues performed a randomized study comparing cutting balloon and conventional PTCA techniques in a large cohort of patients with ISR (Albeiro *et al.*, 2004). They reported that the recurrent restenosis rates (29.8% vs. 31.4%) and the incidence of major adverse cardiac events (MACE) (16.4% vs. 15.4%), such as total lesion revascularisation (TLR), myocardial infarction, emergent CABG or death, were similar in both groups. The Global trial, a multi-centred randomized trial, also determined that CBA did not report superior results to PTCA in terms of restenosis but did recommend that the more controlled technique (i.e. PTCA) at lower deployment pressure could be beneficial for complex, diffuse restenotic lesions (Mauri *et al.*, 2002).

#### **1.4.3 Directional coronary atherectomy (DCA)**

Directional coronary atherectomy is another example of a surgical intervention strategy to combat ISR. It was first performed in human coronary arteries in 1988 (Simpson *et al.*, 1988). This is primarily a 'debulking' methodology which removes obstructive restenotic tissue in large segments from between the stent struts via a catheter-based excision technique. Despite reports of relatively low levels (~25%) of target lesion revascularization (TLR) at 1 year in an initial study, the CAVEAT trial demonstrated increased morbidity rates rendering the strategy of limited use (Harrington *et al.*, 1999). TLR is defined as any percutaneous intervention required for a lesion after a stent has been introduced.

#### **1.4.4 High speed rotational atherectomy (HSRA or rotablation)**

A more aggressive form of atherectomy is high speed rotational atherectomy, and as the name suggests it is performed at a significantly high rpm (150,000 rpm). McKenna and colleagues first demonstrated that this type of rotablation could be used *in vivo* to mechanically debulk the restenotic lesion prior to PTCA, in 1998 (McKenna *et al.*, 1998). Although it was performed successfully in an animal model, this method was not successfully replicated in humans. Both the ARTIST (vom Dahl *et al.*, 2002) and ROSTER trials (Sharma *et al.*, 2004) illustrated that there was no significant long term benefits to using the techniques, and the restenosis rates and TLR were similar to PTCA alone in patients with ISR.

#### **1.4.5 Excimer laser coronary angioplasty**

ISR has also been treated with lasers to remove the restenotic tissue (Nageh & Meier, 2005). This mechanical intervention has been successfully used to safely and effectively ablate the neointima (Mehran *et al.*, 1997). This was a popular methodology to remove restenotic tissue in the early 1990's and was considered to be very innovative and effective (Cook *et al.*, 1991). However, a randomised trial comparing the excimer laser to HSRA found no significance difference between TLR rates at 12 months (Mehran *et al.*, 2001).

#### **1.4.6 Intravascular brachytherapy**

The FDA approved the use of brachytherapy for the treatment of vascular lesions in November 2000. This is another minimally invasive angioplasty technique where a small dose of radiation is delivered locally to the obstructive lesion. Although very effective in disintegrating lesions, there are still major concerns of the effect of ionizing radiation on the structure of the vessels in which it is delivered (Waksman *et al.*, 2001).

In conclusion, the treatment of ISR using the aforementioned strategies, and graphically depicted in Figure 1.8, have not been hugely successful. However, research and development efforts have continued to focus on advancing the stent platform's capabilities and sophistication. The greatest advance in making the BMS platform more biocompatible for instance was the introduction of stent surface coatings.

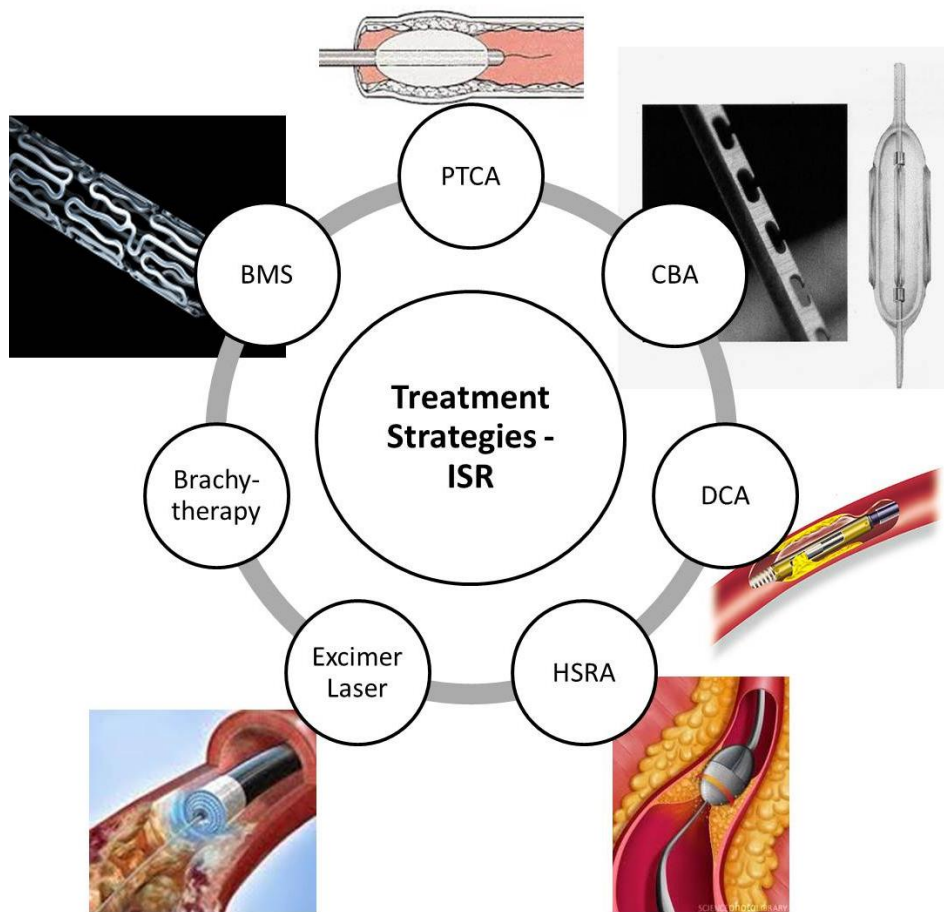


**Figure 1.8:** Images of current ISR treatment strategies. PTCA graphic: Canobbio *et al*, 1990; CBA graphic: Bendok *et al*, 2003, DCA graphic: <http://biomed.brown.edu/courses.html>. HSRA graphic: [www.bostonscientific.com](http://www.bostonscientific.com), Excimer Laser graphic: Diagnostic interventional cardiology, Spectranectics corp, Brachytherapy graphic: Vassieux *et al.*, 2011 and BMS graphic: Abbott Vascular Multi-link cobalt chromium [www.abbott.com](http://www.abbott.com).

## 1.5 Stents and stent coatings

The treatment of the surface of metallic stents with coatings became an area of great interest in the late 1990's. Surface coatings for coronary stents were initially used to afford the implanted device more

biocompatibility without compromising the mechanical integrity of the underlying metallic substrate, thus improving its long term performance *in vivo*. Candidate materials for stent coatings can be broadly categorised as inorganic or polymeric (synthetic or biological) (Hofma, van Beusekom, Serruys, & van Der Giessen, 2001). In addition to biocompatibility, there are some other essential characteristics that required consideration when selecting a polymer stent coating, in order to perform adequately *in vivo* (P. B. Wong *et al.*, 2012) , namely: (1) inertness (2) conformability, (3) mechanical loading capacity, (4) sterilisability, (5) flake resistance and (6) uniform spreadability (Bar, van der Veen, Benzina, Habets, & Koole, 2000) and (Mani, Feldman, Patel, & Agrawal, 2007).

### **1.5.1 Inorganic coatings**

A number of inorganic substances have been investigated for their potential use on a stent platform, including, gold, diamond-like carbon (amorphous hydrogenated DLC), silicon carbide (SiC) and zinc (Zn). These coatings, although they have attractive properties such as those mentioned above are not capable of holding therapeutic agents.

#### **1.5.1.1 Gold**

Gold was one of the first inorganic coatings to be investigated as a stent platform primarily because of its inertness and its advantage of radiopacity under fluoroscopic procedures. Preclinical studies have shown that gold-coated stents yielded fewer macroscopic and histopathologic changes in the aorta than stainless steel stents and those coated with silver, copper, Teflon<sup>®</sup> or silicone. And some groups reported reduced thrombogenicity and a decrease in neointimal formation in these preclinical studies (Tanigawa, Sawada, & Kobayashi, 1995), (Alt *et al.*, 2000), (Kastrati *et al.*, 2001) and (Menown, Lowe, & Penn, 2005). Conversely, Park and colleagues found that there was a tendency toward greater restenosis levels in their pig model (Park *et al.*, 2003). In addition,

Kastrati and co-workers implanted gold-coated stainless steel stents randomized against a cohort of uncoated stents in a human trial and, although radiopacity was increased, the incidence of restenosis was also significantly higher than the control untreated stents (Kastrati *et al.*, 2000). Vom Dahl and colleagues corroborated this finding at a 6-month follow-up in a randomised, multi-centre, prospective trial (vom Dahl *et al.*, 2002).

#### **1.5.1.2 Diamond-Like Carbon (DLC)**

DLC coatings are used because of their low co-efficient of friction and their smoothness (Laube, Kleinen, Bradenahl, & Meissner, 2007) and they exhibit relatively low levels of cytotoxicity (Thomson, Law, Rushton, & Franks, 1991) and (Zakrzewska *et al.*, 2015). The mechanism of action for DLC involves decreasing thrombogenicity via decreased platelet activation. Numerous *in vitro* studies have been performed to assess the biocompatibility aspect of DLC coated stents (Gutensohn *et al.*, 2000), (Allen, Myer, & Rushton, 2001), (Allen, Law, & Rushton, 1994), (T. Das, Ghosh, Bhattacharyya, & Maiti, 2007), (Hinuber *et al.*, 2010) and (Q. Li *et al.*, 2011). However, despite promising *in vitro* results, a randomized trial (n=329) comparing a DLC coated stent (CarboStent™) with a non-coated stainless steel counter-part, showed no difference in MACE or Binary restenosis, defined as  $\geq 50\%$  stenosis reduction, offering no significant advantage over a BMS (Sick *et al.*, 2004).

#### **1.5.1.3 Silicon Carbide (SiC)**

SiC has been previously shown to be capable of altering the electro-chemical properties of the stent surface (Heublein, Ozbek, & Pethig, 1998), (Monnink *et al.*, 1999). The semi-conductor properties of this material confer anti-thrombogenic properties to the stent surface thus making it an attractive option (Kalnins, Erglis, Dinne, Kumsars, & Jegere, 2002), (Hamm, Hugenholtz, & Investigators, 2003). Monnink and colleagues extensively assessed the biocompatibility of the SiC coating (Monnink *et al.*, 1999).

However, its brittleness does not make it suitable for a stent coating and as it delaminates or “flakes off” *in vivo* (Kalnins *et al.*, 2002). Figure 1.9 below illustrates examples of the aforementioned inorganic coated stents.



**Figure 1.9:** Examples of different types of inorganic coated stents: a) Gold-coated stent b) MOMO DLC coated stent, Japan Stent Technology and c) PRO-Kinetic Coronary stent with PROBIO® coating, Biotronik AG, Switzerland, with its characteristic iridescent blue-green colour.

### 1.5.2 Polymeric coatings

Bertrand and colleagues investigated at length the concept of encapsulating a metallic stent with a biocompatible polymer layer in 1998 (Bertrand *et al.*, 1998). This group extensively explored the addition of 5 different polymers to the surface of a stent to improve biocompatibility. However, polymer coatings subsequently evolved to become vehicles/carriers for the delivery of therapeutics, and drugs in particular. By careful selection, polymers could be modified and/or a number of polymers could be multi-layered, on stent surfaces to produce delivery systems that could effectively control the release of drugs into the circulation by local delivery, hence the introduction of the concept of “controlled release technologies” or CRT.

In 2001, Hofma published a comprehensive review which investigated the developments in stent coatings (Hofma *et al.*, 2001). This immediately preceded the launch of the first DES in 2003 (Johnston and Johnston Cypher™ DES) and so the focus of the review was predominantly on the use of polymer coatings as vehicles for drug delivery to the vasculature. Pharmacological agents can be absorbed into or adsorbed onto polymeric coatings.

### **1.5.2.1 Biomimetic polymers**

One of the most important advances in polymer technologies for the use on the surface of a metallic stent was the emergence of “biomimetic” polymers. This is a category of polymers which are designed to mimic a natural biological membrane. This confers a “stealth” property to the exposed layer of the metallic surface of the stent, enabling it to trick the body’s inflammatory system into believing that the stent is a naturally occurring phospholipid bilayer thus obscuring its thrombogenic surface.

### **1.5.2.2 Biomimetic polymer case study – Phosphorylcholine (PC)**

Phosphorylcholine (PC) is a naturally occurring, zwitterionic (neutrally charged), phospholipid and its synthetic derivatives are designed to mimic the membrane (phospholipid bilayer) of an erythrocyte. PC is a copolymer of methylacrylate and methacryloylphosphorylcholine (Whelan, van Beusekom, & van der Giessen, 1997) and is a proprietary formulation that is not commercially available. In 2000, Whelan and colleagues first tested the biocompatibility of PC coated stents in a porcine model (Whelan *et al.*, 2000).

The biological mimicry of the PC polar head groups confers anti-thrombogenic properties onto the substrate material (Zwaal & Hemker, 1982). The synthetic derivative of PC that is utilised as a stent coating was first developed by a UK company, Biocompatibles Ltd, and they quickly developed the PC coated *BiodivYsio*<sup>™</sup> stent. Biocompatibles was later acquired by Abbott Vascular who subsequently licensed the PC technology to Medtronic Inc. for use in the delivery system and stents.

## **1.6 Drug-eluting stents**

In the early 1990’s, bare metal stents (Palmaz-Schwartz, Gianturco-Roubin and Wallstents) were still presenting with a high incidence of thrombotic complications (Serruys *et al.*, 1991), (Agrawal, Macander,

Cannon, & Roubin, 1991) and (Garratt, Holmes, & Roubin, 1991) and still evoked a significant ISR. These adverse complications were marginally improved when stent surfaces were coated with non-thrombogenic substances (section 1.5), however the incidence of clinical ISR (i.e. requiring target lesion or vessel revascularisation and or the incidence of a major adverse cardiac event) was still unacceptably high  $\sim 42.5\%$  (Rinfret *et al.*, 2002). One group of investigators studied PCI databases between May 1999 and September 2003, concluding that more than a third were presenting with an acute Myocardial Infarction (MI) or unstable angina requiring hospitalisation (M. S. Chen *et al.*, 2006), warranting the clinical need for drug-eluting stents. It was at this point that stent coatings were investigated for their use as potential carriers or “vehicles” of therapeutic agents leading to significant advances in the treatment of ISR. Investigators explored the possibility of adding a drug to or mixing a drug with a stent coating substrate so that the drug could be delivered locally to the site of vascular injury, circumventing the significant problem of systemic administration of a drug to the patient.

A drug-eluting stent is defined as a “*device that presents or releases one or more bioactive agents to tissue at and near implant*” (Waksman, 2002). Drugs can be embedded and released from within “matrix” or surrounded by and released through “reservoir” polymer carriers (R. S. Schwartz *et al.*, 2002). Figure 1.10 graphically illustrates how the drug molecules are adhered to the stent coating (Fig 1.10 c) or dispersed through the polymer coating (Figure 1.10 d). This polymer loading directly affects how the drug is released into to the blood vessels, cells, plaques, or tissues either adjacent to the stent or distally (R. S. Schwartz *et al.*, 2002). The drug molecules can either elute “off” or “from” the stent’s surface adluminally into the vessel wall or luminally in to the bloodstream. Drugs will either act by “killing” (cytotoxic) or “freezing” (cytostatic) the migratory SMCs that are actively recruited during the inflammatory response.

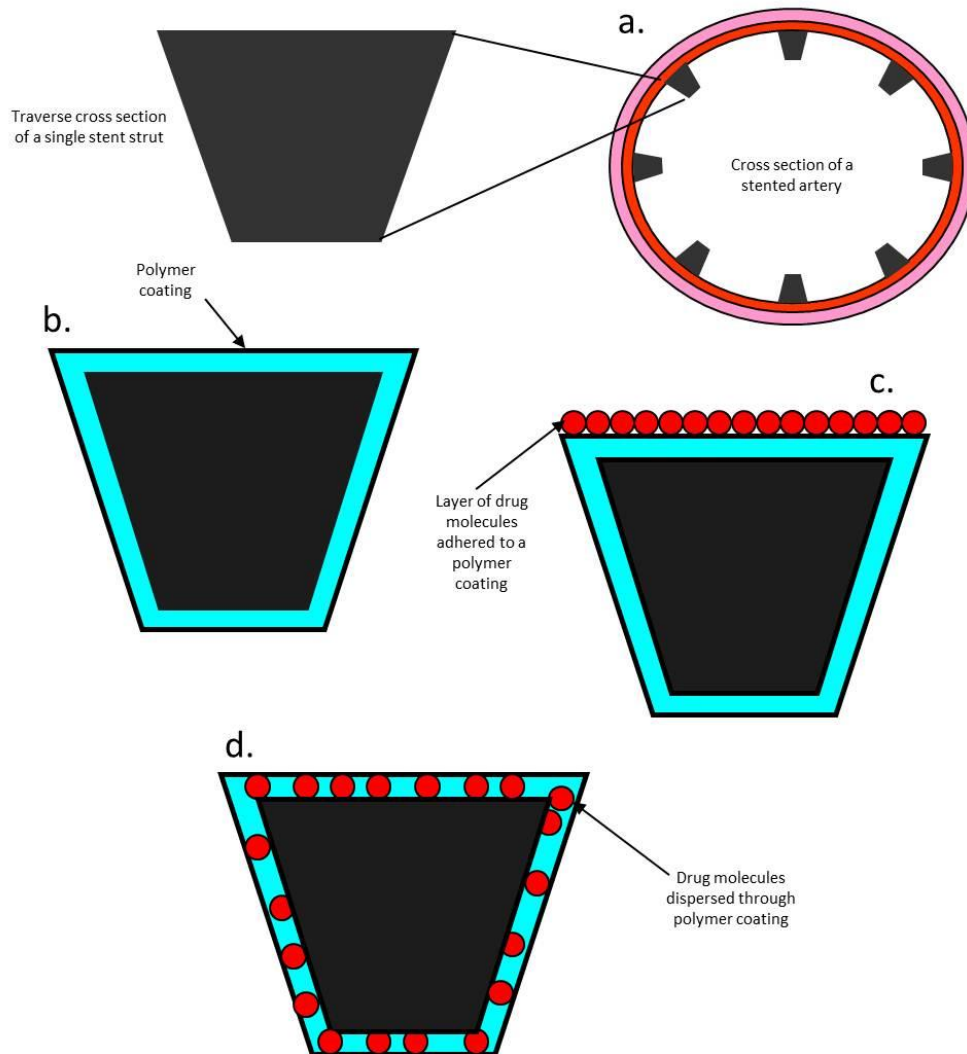


**Figure 1.10:** Graphical illustration of stent coatings: (a) cross section of an implanted metallic stent with individual stent struts flush against the vessel wall (b) single stent strut coated with a polymer (c) drug molecules adhered to the stent coating and (d) drug molecules dispersed through the stent coating.

By the mid 2000's, the use of DES to treat the clinical problem of ISR was becoming the standard of care and several research groups published on how well DES were addressing all the limitations of BMS and postulated how they would completely replace BMS and eliminate ISR (Leon, Bakhai, & Cardiovascular Research Foundation, 2003), Hill, Dundar, Bakhai, Dickson, and Walley (2004), (Heye, Vanbeckevoort, Blockmans, Nevelsteen, & Maleux, 2005) and (Htay & Liu, 2005). The pathophysiology of ISR was previously described in section 1.3.1.1, and the understanding of ISR

pathophysiology was critical to the clinical burden-of-proof that stent manufacturers had to adhere to in order to commercialise DES. They had to explicitly demonstrate 1) the mechanism of action of how their drug worked (anti-proliferative, anti-inflammatory, pro-endothelial etc.), 2) where the drug interrupted the cell cycle and 3) what aspect of arterial injury did it claim to address (endothelium dysfunction, thrombus formation, inflammation or growth factor mitigation). To this end, ISR Pathophysiology targets could be broadly described at a tissue level or a sub-cellular level and the candidate drugs could be similarly categorised. Figure 1.11 illustrates the cascade of events which occurs during the pathophysiology of ISR. The figure graphically depicts these primary processes of ISR pathophysiology (tissue level) and the cell cycle phases (sub-cellular level).

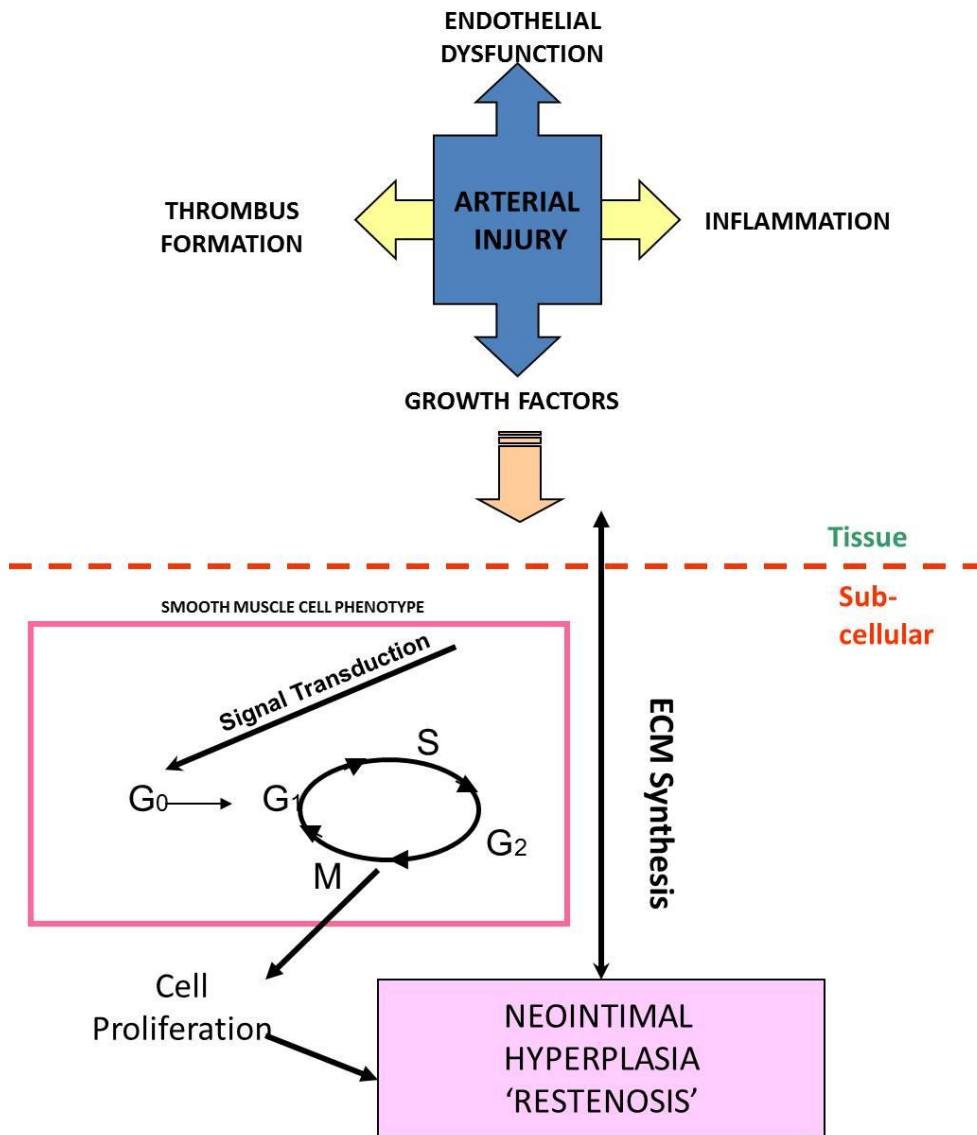


**Figure 1.11:** The leading processes in ISR pathophysiology at both a tissue and sub-cellular level.

At a tissue level, arterial injury induces endothelial which in turn recruits inflammatory factors to stimulate both thrombus formation and ECM synthesis. These molecular events result in the release of substantial amounts of growth factors into the local circulation. Subsequently, at a sub-cellular level, the removal (or damage) of the endothelial layer causes the underlying SMCs to change phenotype. This results in proliferative SMCs infiltrating the ECM matrix, resulting in the formation of a restenotic lesion *in vivo*. Therefore, DES manufacturers at that time (mid 2000s), used their knowledge of the natural cascade of biological events that occur post-

stent implantation to their advantage by selecting candidate drugs that could specifically target these processes at both a tissue and sub-cellular level. Each DES employs a pharmacological agent, usually one that has demonstrated previous efficacy in another application, to induce a specific response, as the biology of vascular cells and the cell cycle provide multiple potential targets for the prevention of neointimal hyperplastic lesion formation (Dibra *et al.*, 2005), (Luscher *et al.*, 2007), (Silva *et al.*, 2009) and (Jabara *et al.*, 2009). Pharmacological agents have been commonly selected from the following categories: anti-inflammatory, immunosuppressive, anti-migratory, anti-proliferative or pro-healing on a multitude of stent platforms to prevent ISR (Hiatt, Ikeno, Yeung, & Carter, 2002), (Carter, 2002) and (Salu, Bosmans, Bult, & Vrints, 2004).

DES, in general, target the primary contributory processes, as illustrated in figure 1.11, to the formation of neointimal hyperplasia which are at a tissue level (P. B. Wong *et al.*, 2012): (1) Endothelial Dysfunction; (White, 2001); (2) Thrombus Formation; (3) Inflammation and (4) Release of Growth Factors and Chemokines and/or at the sub-cellular level targeting the 5 basic phases of the cell cycle: mitosis (M), Gap phase 1 (P. B. Wong *et al.*, 2012); Dormancy or Quiescence (G0); Synthesis (S); and Gap phase 2 (G2). Therefore, to modulate any of the aforementioned processes to prevent the manifestation of a focal lesion within a stented vessel, specific drugs are required.

Prior to the current sub-cellular targeted DES on the market, coated stents were first utilised to deliver existing anti-inflammatory agents (Corticosteroids, Tranilast, Batimastat), anti-thrombotic agents (Hirundin/Iloprost, Heparin, NO, IIb/IIa inhibitors) or pro-endothelial (oestrogen, VEGF, CD34 antibody) agents to the site of vascular injury at a tissue level.

Figure 1.12 expands on the previous figure by illustrating the drugs that have been used to date to target the primary processes at a tissue level. The earliest studies, conducted in the mid-nineties, showed that anti-thrombotic stents presented with acute or sub-acute thrombosis in 18% of cases (Steinhubl, Tan, Foody, & Topol, 1999). However the clinical data generated from these studies, for the aforementioned anti-thrombotic drugs, was subjective and weak statistically (Dobesh, Stacy, Ansara, & Enders, 2004). Certain anti-inflammatory drugs (corticosteroids) contributed to reducing the extent of NIH formation but overall drugs at a tissue level could not prevent NIH formation significantly (Virmani *et al.*, 2002), (X. Liu, De Scheerder, & Desmet, 2004) and (S. J. Hong *et al.*, 2006).

However, in this early development stage it was also noted by several investigators that the regeneration of the endothelium could negate the migration and proliferation of the underlying SMC layer. In 2002, an Estrogen-eluting stent exhibited reduced NIH formation in comparison to a bare metal stent control (New *et al.*, 2002). Similarly, Aoki and colleagues illustrated that a CD34 antibody tethered stent was safe and feasible by virtue of the fact that only one MACE event was noted over a 6 month period in a first-in-man (Klionsky *et al.*) study (Aoki, Ong, *et al.*, 2005). However, it was the incorporation of both immunosuppressive and anti-proliferative drugs, which specifically targeted the cell cycle at a sub-cellular level, onto the stent substrate, that provided clinical data demonstrating significant impact on the formation of NIH *in vivo*.

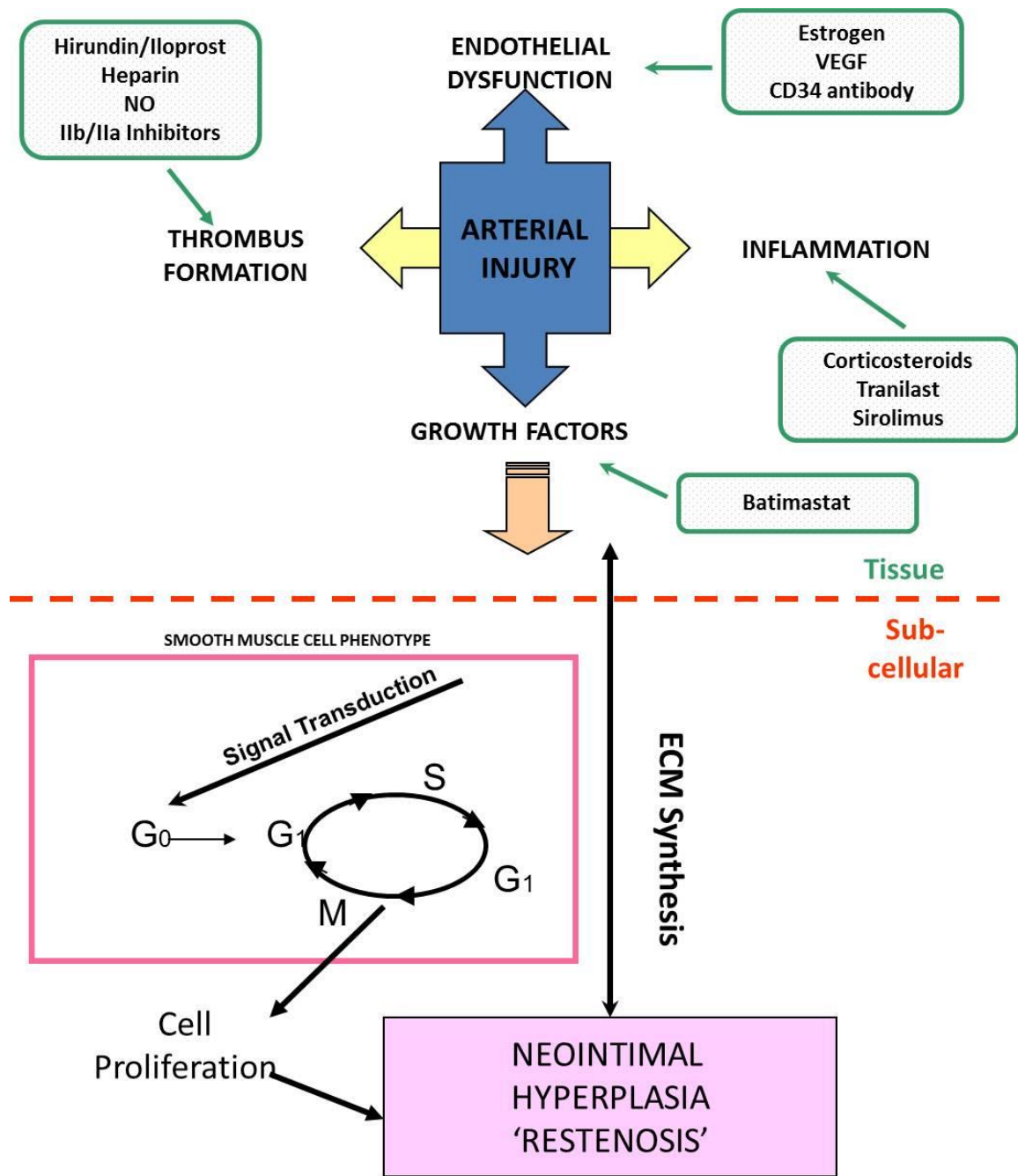


**Figure 1.12:** Current pharmacological agents (drugs) used to specifically target pathophysiological events at a tissue level to combat ISR. These include anti-thrombotic drugs (Hirundin/Iloprost, Heparin, NO, IIb/IIa inhibitors) to inhibit thrombus formation; pro-endothelial drugs (Estrogen, VEGF, CD34 antibody) to restore endothelium function and anti-inflammatory drugs (Corticosteroids, Tranilast, Sirolimus) to mitigate the inflammatory process.

Beyond the tissue level, the next step in the evolution of the pharmacological component of the stent platform involved refining the selection of pharmacological agents to specifically target the disease at a sub-cellular level to prevent SMC proliferation and ultimately the formation of neointimal hyperplasia. These sub-cellular agents, both cytotoxic and cytostatic drugs, were first introduced commercially in 2002, and were able to reduce the rate of restenosis to approximately 10% by using technology to apply these specific anti-proliferative agents locally to the site of arterial injury. Figure 1.13 illustrates the pharmacological agents that are targeted at a sub-cellular level and where specifically in the cell cycle they are targeted to prevent the proliferation of SMCs. The specific drugs indicated on the figure are discussed below.

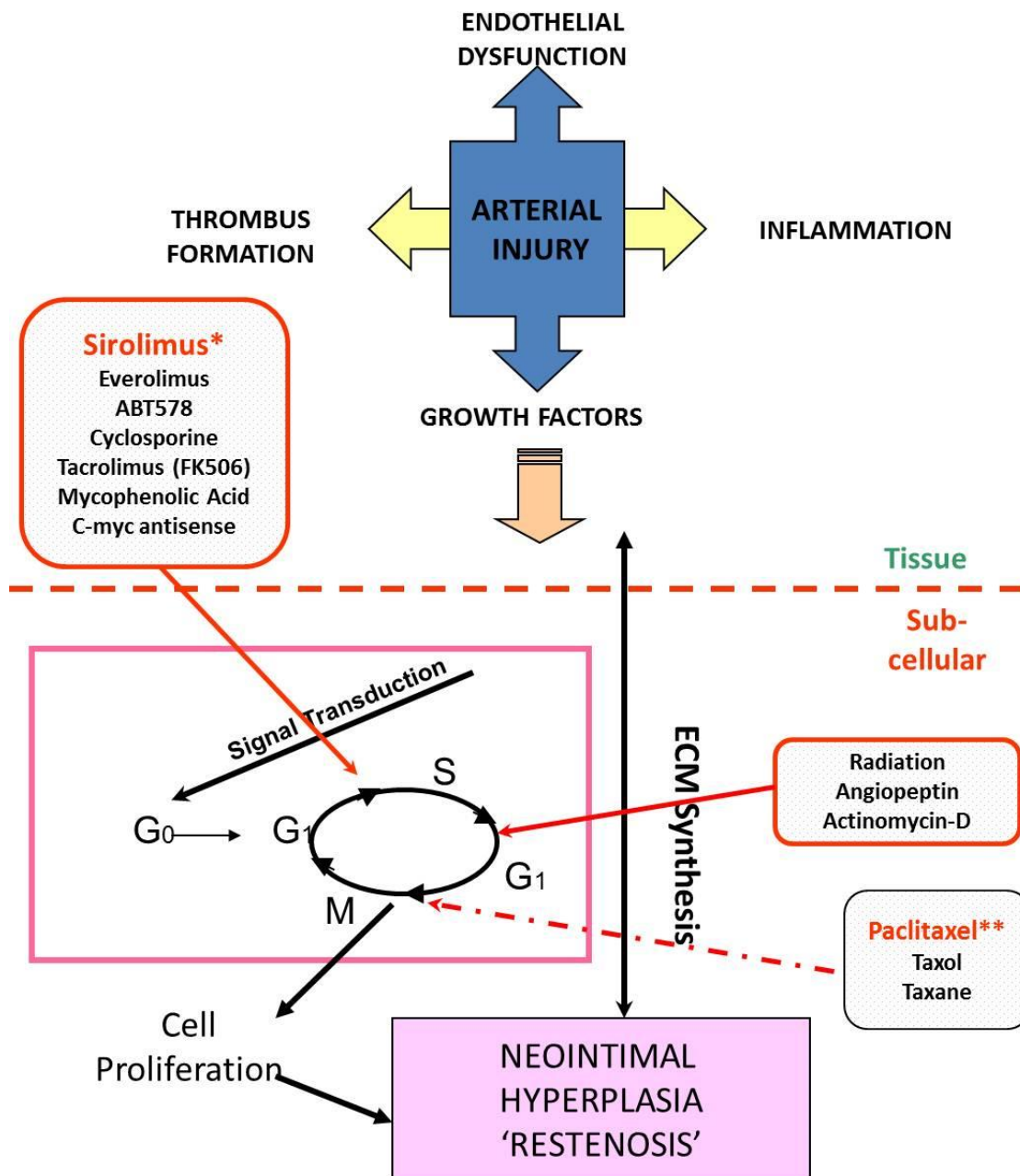


**Figure 1.13:** Current pharmacological agents (drugs) employed at a sub-cellular level and the point of interruption on the cell cycle to combat ISR. \* indicates the leading drug used to inhibit ISR at G<sub>1</sub>/S phase of the cell cycle and \*\* represents the leading drug at the G<sub>1</sub>/M phase of the cell cycle, commercially available on a stent platform.

Several commercially available drugs are utilised to specifically target the G<sub>1</sub>/S phase of the cycle. These agents include rapamycin analogues such as Sirolimus, Everolimus, Tacrolimus and ABT 578. Other cytostatic agents such as cyclosporine and C-myc antisense also act by interrupting the cell cycle at an early phase (P. B. Wong *et al.*, 2012) and

eliciting a cellular necrosis and inflammation. Other strategies target the cell cycle at a later stage, suppressing DNA synthesis (Abid *et al.*, 2005), and are categorised as being cytotoxic. Paclitaxel, and its derivatives Taxol and Taxane, are the most widely used late-stage pharmacological agents to prevent SMC proliferation during the restenosis process. Of all the drugs indicated on Figure 1.13, there are two which currently dominate the commercial DES landscape (Sirolimus and Paclitaxel) and these are discussed in greater detail below.

### 1.6.1 Sirolimus

Sirolimus is a naturally occurring macrolide antibiotic, derived from a fungal source, *Streptomyces hygroscopicus* discovered in 1975 from a soil sample collected from *Rapa Nui* (Easter Island) (Myckatyn *et al.*, 2002). The drug was initially developed as an anti-fungal (Rapamycin) but was found to also have potent immunosuppressive effects (Froeschl *et al.*, 2004). The FDA approved its use for the prevention of renal allograft rejection in 1999. Figure 1.14 below depicts the chemical structure, formula and molecular weight of Sirolimus.

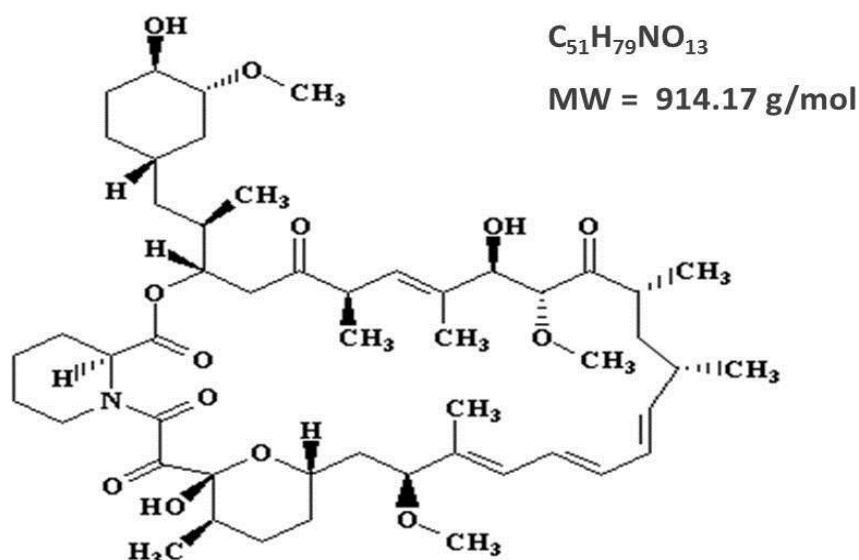


**Figure 1.14:** Sirolimus - Chemical structure, chemical formula and molecular weight.  
Source: [www.fermentelutionkinetic.co.il](http://www.fermentelutionkinetic.co.il).

It is lipophilic in nature with low aqueous solubility and a molecular weight of 914.2. These properties ensure minimal loss to the circulating blood (Zohlhofer *et al.*, 2001). Its mechanism of action is distinct from other immunosuppressive agents in that it acts solely by inhibiting DNA synthesis. As already illustrated in Figure 1.13, Sirolimus acts on the G<sub>1</sub>/S phase of the cell cycle, and binds to specific cytosolic proteins, first complexing with the upregulated FKBP12 protein and then with mTOR (mammalian target of rapamycin), a specific cell-cycle regulatory protein. This complex formation augments the level of cyclin dependent kinase p21 while also inhibiting retinoblastoma protein phosphorylation (Marx, Jayaraman, Go, & Marks, 1995), (Poon *et al.*, 1996) and (Burke *et al.*, 1999). Therefore, the net effect of Sirolimus is a cytostatic cell-cycle arrest in late G1 phase (Javier *et al.*, 1997), (Sehgal, 1998), (Burton, Yacoub, & Barton, 1998) and (Gallo *et al.*, 1999). The other drugs from Rapamycin analogues utilised in DES include Everolimus (Abbott Xience™ V; Boston Scientific Promus™) and Zotarolimus (Medtronic Endeavour™), and like Sirolimus, these compounds act as mTOR inhibitors.

### **1.6.2 Paclitaxel**

Paclitaxel was the second drug to be delivered from a stent platform. Paclitaxel was discovered in 1967 as a result of a US National Cancer Institute funded screening programme when two scientists, Wall and Wani, isolated the drug from the bark of the Pacific Yew Tree otherwise known as *taxus brevifolia* (Wani, Taylor, Wall, Coggon, & McPhail, 1971). This is where it derived its current family name Taxol. It was commercially developed by Bristol-Myers-Squibb who changed its generic name to “paclitaxel”. It was originally used in the treatment of ovarian cancer (Rowinsky & Donehower, 1995) as it possesses potent anti-neoplastic properties. Figure 1.15 graphically depicts the compound’s chemical formulation.

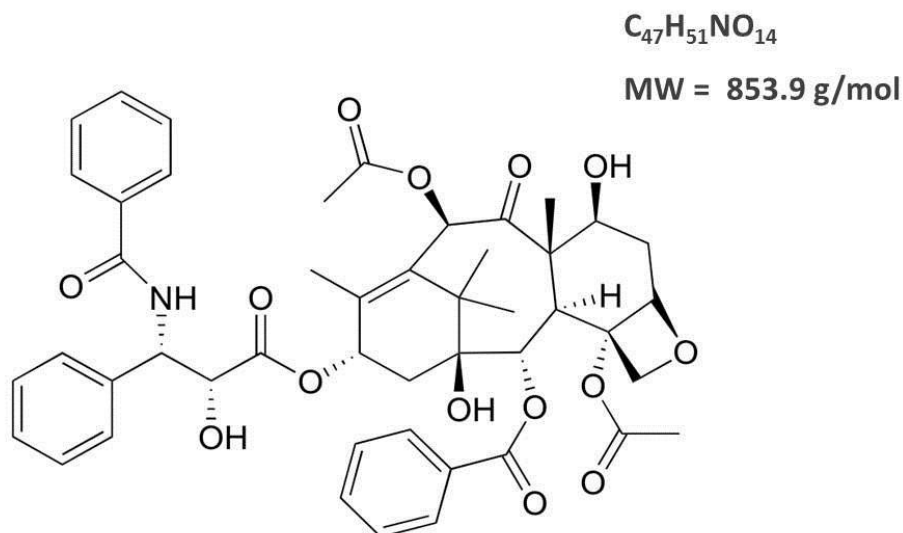


**Figure 1.15:** Paclitaxel - Chemical structure, chemical formula and molecular weight.  
Source: <http://chemwiki.ucdavis.edu>.

As previously described in Figure 1.13, Paclitaxel interrupts the cell cycle between the G1 and M phases. Its mechanism of action is cytotoxic as it induces cell death by arresting microtubule function (Honda, Meguro, Takizawa, & Isoyama, 2005). This compound interrupts the G1/S transition phase preventing cell division (Bornfeldt, 2003). Like Sirolimus, Paclitaxel is lipophilic and insoluble in water, and therefore, well-suited for stent-based delivery (Froeschl *et al.*, 2004).

### 1.6.3 Commercially available DES

Currently only four DES have been approved by the FDA for US Markets (CYPHER<sup>®</sup>, TAXUS<sup>®</sup>, Endeavor<sup>®</sup> and Xience™ V/Promus), one for the European market (Endeavor Resolute) and one currently on trial has the status of an investigational device exemption (IDE). These DES have different stent platforms, balloon catheters, drugs and coating materials, as tabulated in Table 1.1, however, they all share similar principles in their drug/carrier design and drug pharmacokinetic profiles that result in clinical efficacy. Cordis Corporation, a subsidiary of Johnson and Johnson (J&J), commercialised the first CE marked DES in 2002 and received FDA approval for their Cypher™ stent (Drug: Sirolimus), in April 2003. This was quickly

followed by Boston Scientific's entry to the market with its Paclitaxel-eluting stent, Taxus™, in March 2004. DESs are now used routinely in angioplasty procedures (Brilakis *et al.*, 2010). The DES platform succeeded in quickly reducing the incidence of restenosis from 20-30% to single digit levels and began to overtake the BMS, almost doubling the total market size to over \$5 billion US dollars.

Manufacturer	Trade Name (Market Share % - Approval Status)	Drug	Stent Material	Polymer Coating
Cordis Corp (J&J)	Cypher™ (11% - WW approval)	Sirolimus	316L SS	Parylene C PEVA PBMA (Top-coat)
Boston Scientific	Taxus® Liberté (22% - WW approval)	Paclitaxel	316L SS	SIBS (Translute™)
Medtronic	Endeavour™ (13%- CE marked)	Zotarolimus	CoCr	Phosphorycholine
Abbott/BSCI	Endeavour Resolute™	Zotarolimus	CoCr	BioLinx
	Xience™ V/Promus (30%- WW approval)	Everolimus	CoCr Multilink Vision™	Acrylate Primer PVDF-HFP
Abbott	Zomaxx (IDE)	Zotarolimus	CoCr	Phosphorycholine

**Table 1.1:** Illustrates the leading commercially available DES detailing their respective constituents: Stent material, stent coating and drug.

Boston Scientific is currently the market leader with a combined strategy of providing two commercially available DES platforms: Promus™, with the Everolimus drug (derivative of Sirolimus) licensed from Abbott Laboratories alongside its own Paclitaxel-eluting stent, Taxus™, to afford the medical device company 46% of the market share. Table 1.1 consolidates the current market leaders in the DES space. The research and development activity in DES platforms over the last 15 years has been significant. There are currently in excess of 70 companies investigating and advancing developments in the elements and factors that constitute a DES including stent design and material selection, choice of polymer coatings and matrices, drug candidates and their respective elution kinetics.

The optimal anti-restenotic agent for localised stent delivery to the vasculature should have potent anti-proliferative properties with the capability to regenerate the endothelium. Drug release to the vasculature is dependent on several factors: the concentration and solubility of the candidate drug, its molecular weight, the surface area and chemistry of the polymer coating and if there are diffusion barriers present. There is now steep competition to formulate the next generation iterations of DES to achieve a share of the DES market share and R&D teams need to address most, if not all, of the aforementioned factors in order to be the next generation DES. The next section will discuss the primary complications associated with the use of DES.

#### **1.6.4 DES - Primary complications**

There are several problems associated with the use of DES. Some of these issues have been elucidated by animal models and others have their origins in adverse events (Froeschl *et al.*, 2004), (van der Hoeven, Schlij, & van der Wall, 2005) and (Teirstein, 2010). In the first instance, the drugs utilised in currently commercially available DES have been used in previous applications and have not been specifically developed for the prevention of ISR. They are generally broad in their targeting, many of them capable of multiple modes of actions (e.g. anti-proliferative and anti-inflammatory). Secondly, there has also been the suggestion by a variety of investigators (Waksman *et al.*, 2002), (Froeschl *et al.*, 2004), (Kipshidze *et al.*, 2003), (New *et al.*, 2002), (Hassan *et al.*, 2010) and (Kimura *et al.*, 2010) that other potential problems, such as drug-loading capacity, release kinetics, biocompatibility, mal-apposition (incorrect positioning within the vessel) and aneurysm needed further evaluation in the context of DES placement in the vasculature. However, the dependence on long-term administration of anti-platelet agents and the late development of thrombosis and aneurysms still remain the leading causes of concern of the continued use of DES.

In 2006, Yang and colleagues were one of the first groups to critically appraise the performance of DES (J. Yang *et al.*, 2006) . They analysed clinical trial and registry data for DES and concluded that although these stents demonstrated reduced angiographic and clinical restenosis, this did not follow through with “hard” clinical outcomes and prompted the concern that DES were actually predisposing patients to late stent thrombosis (LST) and stent induced myocardial infarction (STEMI). (Skyttberg, Linder, & Carlsson, 2006) and (Daemen *et al.*, 2007).

#### **1.6.4.1 Long-term administration of anti-platelet therapy**

As previously mentioned, the anti-mitotic drugs eluted by DES prevent the formation of neointima at the price of delayed re-endothelialisation and this has the knock-on effect of requiring the long term administration of dual anti-platelet therapy, usually Aspirin™ and Clopidogrel™. The clinical importance of delayed re-endothelialisation was highlighted following a report by McFadden and co-workers in which they discovered that four patients developed LST after the discontinuation of anti-platelet treatment at eleven months post a single Sirolimus or Paclitaxel stent deployment (McFadden *et al.*, 2004). LST following cessation of anti-platelet therapy was also documented by Farb and colleagues (Farb, Burke, Kolodgie, & Virmani, 2003). Sibbing and co-workers also reported the incidence of LST 42 months post Sirolimus eluting stent implantation (Sibbing, Laugwitz, Bott-Flugel, & Pache, 2009). Thus, while DES reduce the risk of restenosis, they are clearly associated with delayed re-endothelialisation (Joner *et al.*, 2006; Virmani, Farb, Guagliumi, & Kolodgie, 2004).

#### **1.6.4.2 Late stent thrombosis**

In October 2003, the FDA issued a report on the incidence of sub-acute thrombosis associated with the Cypher™ stent. After further investigation it transpired that the incidence of thrombosis was no greater

in DES than in BMS. However, LST that occurs 1-2 years or more after implantation, was deemed a complication of DES, and this highlighted the absolute necessity for long-term administration of anti-platelet therapies. Unlike restenosis, LST is a rare complication of coronary stenting but has catastrophic consequences when it does occur, as documented in several studies (Babapulle, Joseph, Belisle, Brophy, & Eisenberg, 2004), (McFadden *et al.*, 2004), (Iakovou *et al.*, 2005), (Ge *et al.*, 2005) and (Ong *et al.*, 2005). More recently Nishiguchi and colleagues confirmed, using coronary angiography and OCT techniques on one LST patient, that 99% of the vessel was occluded and established the evidence of intracoronary thrombi in a vessel treated with a cypher DES 25 months previously. The investigators confirmed that the patient had discontinued the use of anti-platelet therapy (Nishiyama, Shizuta, Doi, Morimoto, & Kimura, 2010).

The exposed medial layer, post PTCA procedures, is thrombogenic in nature and therefore thrombi are predisposed to forming prior to re-endothelialisation, which normally occurs at 14 days when conventional BMS implantation is performed. For BMS, thrombus formation is reduced with the short term administration of an anti-platelet therapy for a month. However with DES, the cell-cycle inhibitory nature of the agents causes re-endothelialisation to be further delayed and thus a longer time-frame of anti-platelet therapy is required.

In the SCORE Trial, 0% ISR was reported in the DES versus the bare metal control stent however the trial was prematurely concluded because of the relatively high incidence of late stent thrombosis (Kataoka *et al.*, 2002). Kremastinos and co-workers observed a rise in acute coronary syndromes in DES following the early cessation of dual anti-platelet therapy within 6 months of procedure sparking the phenomenon of “Stent Wars” (Kremastinos, 2007). This event initiated a plethora of studies and meta-analyses to provide evidence that DES were “safe” and reduced

restenosis, thus reducing the necessity for revascularization; however these studies also confirmed that there was an increase in the incidence of myocardial infarction (MI)-induced death (Berger *et al.*, 2010).

#### **1.6.4.3 DES Complications - Conclusions**

The “negative” results uncovered in the clinical trial studies summarised above clearly illustrate that DES do not completely eliminate ISR, especially complex ISR in coronary applications and do not perform at all in the more complicated environment of the peripheral vasculature where DES are used “off-label” by treating physicians. This is when DES are implanted in the peripheral vasculature but not as per the guidelines developed and approved by the FDA. This is very problematic area and in 2012, The National Institute for Health and Clinical Excellence's (NICE) guideline on "Lower limb peripheral arterial disease: Diagnosis and management" recommended the use of bare metal stents where stenting is indicated for intermittent claudication (pain experienced when walking or exercising) because of a lack of evidence of superior clinical outcomes with DES. In addition, the comprehensive documentation of the leading adverse effects of LST demonstrated that there is scope for further development to make DES more tailored in their targeting. Potential means of overcoming obstacles that DES have met, and have caused, has highlighted the need for innovative therapies and thus there is ample scope for next generation of stenting, using, for example, Gene-eluting stents.

## **1.7 Gene Therapy**

Gene therapy is a relatively new and emerging technology. Essentially it is a techniques that uses gene to treat or prevent disease by either “*replacing a mutated gene with a healthy gene, inactivating a mutated gene or introducing an entirely new gene*” (Morgan & Anderson, 1993). All diseases are due to malfunctions in cellular processes. These

cellular processes are regulated by proteins, which are ultimately the target for gene therapy. However, the delivery of DNA to the nucleus of target cells is a huge undertaking, given the numbers of barriers that must be circumvented to achieve this end. Hence there is a need for the use of molecular constructs, more commonly referred to as vectors, to deliver the therapeutic gene.

### **1.7.1 Cardiovascular Gene Therapy**

Cardiovascular gene therapy has made substantial advances over the last decade and a number of target cardiovascular diseases have been identified. In the area of stent-based gene therapy the following diseases have been the subject of investigation: restenosis, thrombosis, vascular graft disease and chronic vascular occlusion. In the context of this thesis, restenosis is the only disease that is discussed in relation to gene therapy treatments from stent platforms.

In order to understand the underlying principles of delivering gene therapy to the vasculature from the stent platform, it is important to evaluate the studies conducted on delivering therapeutic genes using both balloon catheters and stents. In the first instance, balloon catheters were used to deliver genes locally to the vessel wall. Gene delivery methods then evolved from using the balloon to utilising the stents themselves. This enabled a more pro-longed contact with the vessel wall, thus inducing a more controlled release of the gene at the site of vascular injury.

### **1.7.2 Gene Delivery Systems for the vasculature**

#### ***1.7.2.1 Balloon delivery***

A variety of molecular therapies have been delivered to the vasculature via balloon-only delivery but have generally failed to produce efficacious results. Varenne and Sinnaeve reported delivery of VEGF, Oligonucleotides (ODNs) and Adenovirus via pressure driven porous balloons (Varenne & Sinnaeve, 2000). It was clear from these early gene

therapy attempts that a more sustained delivery to the vasculature was required in order to be an efficacious therapy.

### **1.7.2.2 Stent delivery**

Stents provide potential as an ideal platform for delivery of a molecular agent, such as a gene vector, to the vasculature. Stent platforms, in broad terms, enable sustained delivery of a gene, as well as providing an opportunity to modify the stent design and stent coatings to modulate release kinetics *in vivo*. A technique that was utilised initially for endovascular graft coatings to encourage a “pro-healing” approach for grafting procedures, i.e. coating the graft with genetically engineered endothelial cells (Zilla *et al.*, 1987), prompted the use of this technique in vascular stents (Aoki, Abizaid, Ong, Tsuchida, & Serruys, 2005).

### **1.7.3 Gene-eluting stents (GES)**

The ideal GES platform should be safe and non-immunogenic, capable of efficient gene delivery to target cells/tissue, simple to construct and manufacture and be capable of inducing long-term, cell-specific controllable gene expression. Vascular site-specific, stent-based, gene therapy requires three components to be successful:

- (1) Delivery Vehicle: polymer coating (with optimal release kinetic properties) on an appropriate stent delivery system
- (2) Gene Vector: (viral or non-viral) which can be adhered to or absorbed into the polymer coating
- (3) Gene : an appropriate therapeutic gene, that can be encapsulated by the vector

These components are outlined in Figure 1.16. As with any convergence product, the development of a GES presents technical challenges, which need to be overcome in order to be successfully

translated to the clinic. Many of these technical challenges will be identified and investigated throughout the course of this study.

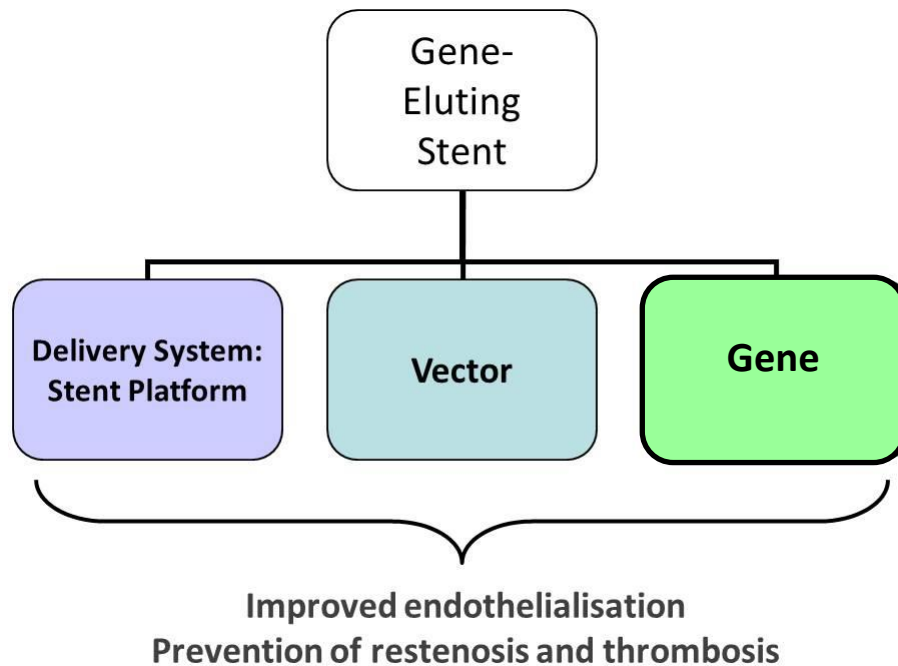


**Figure 1.16:** Composition of a Gene-eluting stent. Adapted from a slide courtesy of Dr. Sean Hynes, European Gene and Somatic Cell Therapy conference, Germany November 2009.

The development of a safe and efficacious GES requires investigation of one, or all, of the components independently or in combination. This requires in-depth research and development to be performed in the following areas: stent material and stent coatings, vector carriers (viral or non-viral), and the selection of an appropriate therapeutic gene to deliver to the vasculature.

Historically, systemic delivery of gene therapy agents has raised significant safety concerns. Serious adverse events associated with some viral gene therapy clinical trials, which occurred in the early 2000s (Hilts, 2000), (Hacein-Bey-Abina, von Kalle, *et al.*, 2003) and (Raper *et al.*, 2003) inevitably had a negative impact on the progress in this research area. However, localised gene delivery from a stent platform, as proposed in this study, will address and alleviate such safety implications.

The goal of gene therapy in restenosis is to produce a transient and localised specific effect on a particular cell, inhibiting SMC proliferation as well as ECM formation. It is critically important to select a gene that will induce the clinically relevant therapeutic effect for this disease state and also to have it release in a time frame that coincides with the natural time course of biological events that occur during the wound healing phase. An optimal therapeutic approach would involve a strategy which inhibits intimal hyperplasia while promoting re-endothelialisation and suppressing stent- or vector-related inflammatory side effects.

#### **1.7.3.1 Delivery vehicle: GES stent coatings**

In DES, the stent coating is of prime importance. It must be biocompatible, durable and flexible but also capable of carrying a candidate drug and controlling its release kinetics *in vivo*. The majority of polymers utilised on stents for DES (as described in section 1.5.2) are capable of holding small hydrophobic drugs (Sirolimus and Paclitaxel at approximately 1000 Daltons) very easily. However, using these polymers in next generation stents may not always be a viable option, as therapeutic biological molecules such as proteins, peptides, cells, or DNA, tend to be large, sometimes exceeding 50,000 Daltons. The capacity to absorb this amount of biological agent onto currently available polymers used in DES would need to be further investigated before deciding if they could be used for GES applications. Furthermore, the coating would have to be able to adhere to the stent substrate surface effectively and have sufficient gene vector encapsulation capacity to generate an appropriate level of transduction to elicit a therapeutic effect *in vivo* (Sharif, Daly, Crowley, & O'Brien, 2004).

It has been hypothesised that polymeric delivery may enhance gene transfer by first protecting DNA from degradation and then maintaining the

vector at effective concentrations, extending the opportunity for nuclear internalisation (i.e. the uptake of the DNA into the cell nucleus) (Pannier & Shea, 2004). Polymers used in gene therapy applications can be derived from natural or synthetic sources and processed into a variety of forms or microstructures (e.g. nanospheres, microspheres) with the gene vector encapsulated. This polymer processing substantially affects both the structural and morphological properties of the polymers and the microstructures produced can have a significant effect on cellular uptake and ultimately on gene expression. Nanospheres are particles with diameters ranging from 50-700nm (Desai, Labhasetwar, Walter, Levy, & Amidon, 1997), consistent with the size of viral and non-viral vectors, which can be readily endocytosed by the cell membrane. Microspheres, range in diameter from 2 - 100µm, cannot be internalised but are retained within the tissue to release DNA at the cellular membrane interface (Mathiowitz *et al.*, 1997), (Ochiya *et al.*, 1999). The interaction of DNA with the polymeric vehicle, and to what size diameter the complex forms, ultimately determines the cellular uptake.

#### **1.7.3.2 Gene vector**

Gene vectors have several roles to perform:

- Encapsulate and protect the DNA,
- Facilitate uptake by the cellular membrane, e.g. endocytosis,
- Enable appropriate release from intracellular compartments and
- Allow optimal release across the nuclear membrane to ensure transgene expression (Barthel, Remy, Loeffler, & Behr, 1993), (Loeffler & Behr, 1993) and (Gao & Huang, 1995).

An “ideal” vector is characterised by its high cell transfection efficiency, cell specificity (ability to target specific cells), low toxicity, unlimited insert size, prolonged expression, and lack of immunogenicity (Sharif *et al.*, 2004). Vectors are predominantly categorised as either viral or non-viral vectors. Figure 1.17 illustrates the vectors that belong to each

category. Non-viral vectors are composed of naked plasmids, liposomes and polymers; whereas the most commonly used viruses in gene therapy applications are adenovirus, adeno-associated virus, retrovirus and lentivirus.

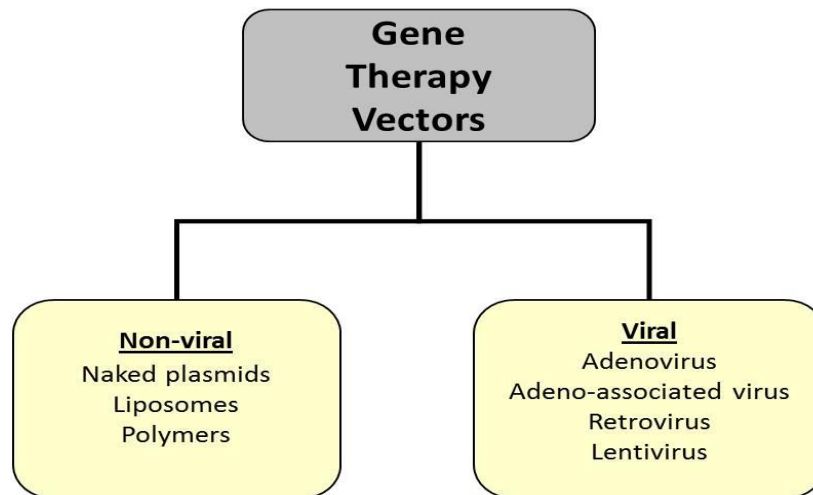


**Figure 1.17:** Gene therapy categories - Non-viral and viral vectors.

#### 1.7.3.2.1 Non-viral

A plasmid is defined as a circular, double-stranded unit of DNA (pDNA) that replicates within a cell independently of the chromosomal DNA and is most often found in bacteria (Masai, Kaziro, & Arai, 1983) and (Frerix, Geilenkirchen, Muller, Kula, & Hubbuch, 2007). Non-viral gene delivery systems are composed of this type of plasmid DNA, and are often conjugated to lipids and/or polymers. Although they are much less efficient than their viral counterparts, in terms of delivering genes into cells, non-viral vector systems are less immunogenic and toxic and do not run the risk of insertional mutagenesis, i.e. where a genetic mutation is caused by inserting new genetic material into a normal gene (Romano, Marino, Pentimalli, Adamo, & Giordano, 2009), (Kustikova *et al.*, 2009) and (Romano, 2012). However, making non-viral vectors more sophisticated will help overcome their current shortcomings and evolve them into delivery systems that will transfect tissue efficiently without biosafety concerns.

- **Naked Plasmids**

Naked DNA is the simplest gene delivery vector, consisting of a DNA molecule containing the recombinant gene and adjoining DNA sequence that permits its replication as a plasmid in bacterial hosts (G. M. Huang *et al.*, 2002) and (Walther *et al.*, 2003).

- **Liposomes**

In 1987, Felgner and colleagues were the first group to successfully encapsulate DNA into a cationic lipid (DOTMA) - producing nanoscale particles capable of cellular endocytosis and subsequent expression (Felgner *et al.*, 1987). The concept of forming electrostatic interactions between the partially negative DNA backbone and positively charged cationic head groups of the lipids as a method of liposome-mediated DNA transfer in eukaryotic cells was explored by Nicolau and Sene in 1982 (Nicolau & Sene, 1982). Their first attempt was unsuccessful. However, DOGS (Dioctadecylamido-glycylspermine) was synthesised and investigated by Behr *et al* in 1989 (Behr, Demeneix, Loeffler, & Perez-Mutul, 1989), and DC-Chol (3 $\beta$ -[N-(N',N'-dimethylaminoethyl) carbamoyl] cholesterol) was investigated as a potential lipid vector to transfect mammalian cells by Gao (Gao & Huang, 1991). Figure 1.18 graphically depicts the morphology of a liposomal particle with its characteristic lipid bilayer.

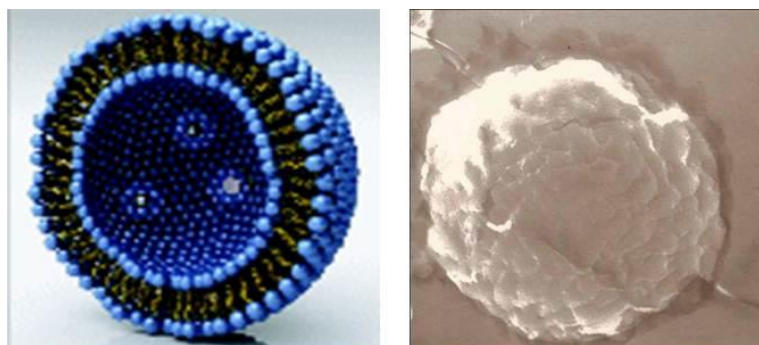


**Figure 1.18:** Liposome - Structural schematic and live image.

Source: [www.universityofcalifornia.com/techtransfer/edu](http://www.universityofcalifornia.com/techtransfer/edu); [www.readisorb.com](http://www.readisorb.com).

- **Polymers**

Several cationic polymers, synthetic and biological, have been utilised as non-viral vectors to encapsulate DNA and deliver it for uptake to the cellular membrane. Polymers such as PEI (polyethyleneimine) (Haensler & Szoka, 1993), (Boussif *et al.*, 1995), Chitosan (Erbacher, Zou, Bettinger, Steffan, & Remy, 1998), (Su & Wang, 2006), Dextran (Nimesh, Kumar, & Chandra, 2006), (Delgado *et al.*, 2012) and Polyamidine (Tang, Ji, & Wang, 2011) have all been successfully used to deliver exogenous genes to cells *in vitro* and *in vivo*.

#### 1.7.3.2.2 Viral

Viruses have evolved to become highly efficient at nucleic acid delivery to specific cell types (Gunzburg & Salmons, 1995). Although a number of viruses have been developed for gene therapy applications (Morgan & Anderson, 1993), research has primarily focused on four viruses, namely adenovirus, adeno-associated virus, retrovirus and lentivirus, although other viruses such as Herpes Simplex Virus (HSV) type-1 (Latchman, 2001), (Toda, 2005) and Vaccinia virus (Lattime, Lee, Eisenlohr, & Mastrangelo, 1996), (Mastrangelo, Maguire, & Lattime, 2000), (Gomella *et al.*, 2001) have also been investigated. Gene therapy approaches using viral vectors have been applied to combat the clinical problem of ISR (Sinnaeve, Varenne, Collen, & Janssens, 1999), (Klugherz *et al.*, 2002), (Robertson, McDonald, Oldroyd, Nicklin, & Baker, 2012) and (Lompre *et al.*, 2013).

- **Adenovirus**

Of all the vector systems, the adenoviral vector is the most widely used for gene delivery in pre-clinical and clinical models (D'Souza *et al.*, 2004). The main advantage of an adenoviral vector is its capability to transfect non-dividing cells efficiently, resulting in a high level of transient gene expression (Verma & Somia, 1997). With adenovirus, there is no risk of insertional mutagenesis, as it does not have the ability to integrate into the host cell's genome (Prince, 1998). It can be produced at high titres and

has a relatively large packing capacity (Morgan & Anderson, 1993), (Verma & Somia, 1997). However, adenovirus induces a severe inflammatory response and may result in innate and adaptive immune response which precludes re-administration (Muruve, 2004). Figure 1.19 below illustrates the morphological features of an adenoviral particle.

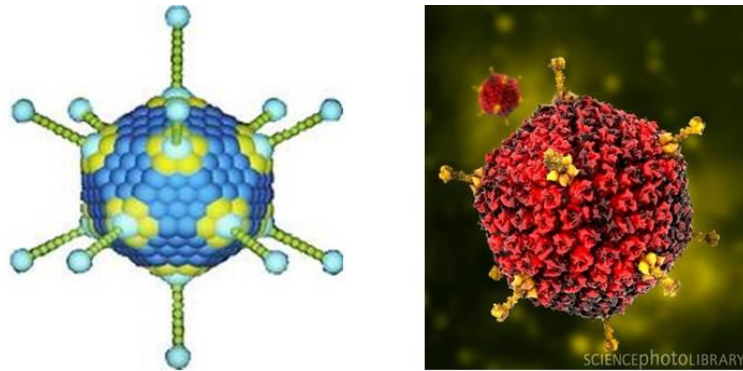


**Figure 1.19:** Adenovirus - Structural schematic and live image.  
Source: [www.sciencephoto.com](http://www.sciencephoto.com); [www.bio.davidson.com](http://www.bio.davidson.com).

- **Adeno-associated Virus (AAV)**

This viral vector functions mid-way between its adenoviral and retroviral counterparts. AAV has emerged as a potential candidate for vascular gene therapy for a number of reasons. It is a non-pathogenic virus, capable of condensing into high titres and transducing a wide range of both non-dividing and dividing (albeit at relatively lower rates than non-dividing) cell types. AAV vectors can also integrate into the host cell's genome affording the vector long-term expression profiles *in vivo*. However, the major drawback of host cell genome integration is that it increases the risk of insertional mutagenesis. Deliberate mutagenesis can be a desirable aspect for certain gene therapy applications, however for this study, mutagenesis in highly proliferating SMCs is not a benefit. Figure 1.20 illustrates the morphology and structure of an adeno-associated viral particle (AAV serotype 2).

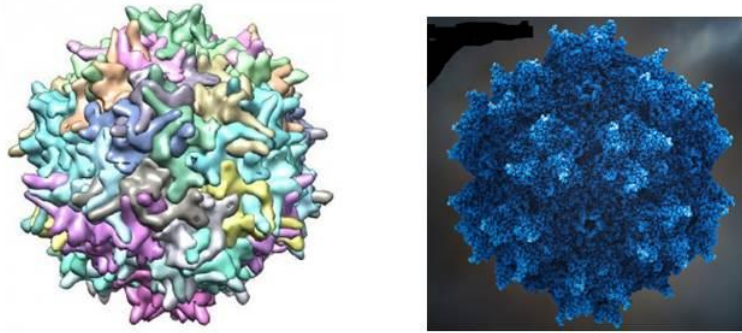


**Figure 1.20:** Adeno-associated virus - Structural schematic and live image (AAV serotype2).  
Source: [www.virology.wisc.edu](http://www.virology.wisc.edu)

- **Retrovirus**

Recombinant retroviruses are RNA viruses that are capable of integrating into the host's genome, resulting in long-term gene expression. However, this characteristic also heightens the risk of insertional mutagenesis which can lead to unforeseen and potentially severe clinical consequences (Hacein-Bey-Abina, von Kalle, *et al.*, 2003). Retroviruses were among the first viruses used for *in vivo* vascular gene transfer (E. G. Nabel, Plautz, & Nabel, 1990) despite the fact that they exhibit low efficiency due to the fact that they must divide in order to express (Miller, 1990) and they are difficult to attain in high titres. They are considered not to be appropriate vectors for delivery to the vasculature as both ECs and SMC have low mitotic rates (Gordon *et al.*, 1997). Figure 1.21 below illustrates the morphology of a retroviral particle.

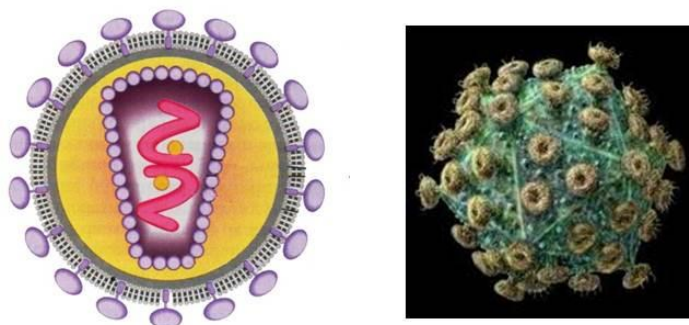


**Figure 1.21:** Retrovirus - Structural schematic and live image. Source: [www.itqb.unl.pt](http://www.itqb.unl.pt).

- **Lentivirus**

Lentiviruses are the most recently discovered subset of the retrovirus family and include HIV-1 and HIV-2. Like other retroviruses, lentiviruses integrate into the host genome. They differ from other members in their ability to transduce both dividing cells and non-dividing cells including neurones, retinal cells, hepatocytes, skeletal muscle and airway epithelial cells (Naldini *et al.*, 1996). Their drawbacks are currently dominated by the public perception of using a HIV-based vector, insertional mutagenesis and the fact that they are not as well characterised as the other viral vectors. The shape and distribution of the appendages on this viral particle are significantly different to those of other viral particles, with a distinctive multi-head cluster on each appendage. Figure 1.22 illustrates the structural characteristics of this type of viral particle.

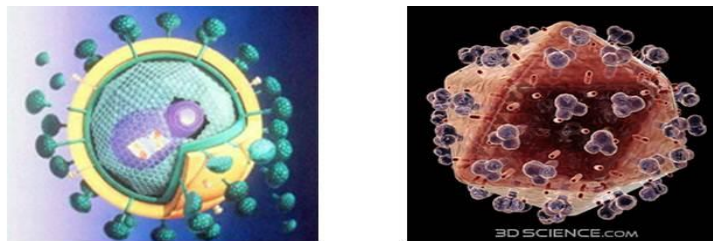


**Figure 1.22:** Lenti-virus - Structural schematic and live image. Source: [www.3Dscience.com](http://www.3Dscience.com)

#### 1.7.3.2.3 Conclusions

Since 1989, numerous gene therapy clinical trials have been completed for a multiple pathologies including cancer, inherited monogenic disease, neurological disorders and cardiovascular disease. As of June 2012, there were 1843 gene therapy clinical trials on-going across 31 countries (Ginn, Alexander, Edelstein, Abedi, & Wixon, 2013). However, the majority of trials have shown poor therapeutic effects or clinically relevant responses. Some of these shortcomings can be attributed to poor delivery devices, lack of stable gene expression and immunogenicity concerns (Pagliaro *et al.*, 2003), (Palmer, Chen, & Kerr, 2003), (Kerr, 2003), 2003, (Powell *et al.*, 2010) and (Ginn *et al.*, 2013).

According to the American Society of Gene and Cell Therapy (ASGCT), Cardiovascular disease is the third most popular gene therapy application for acquired diseases (after Cancer and Neurodegenerative diseases). Cardiovascular gene therapy currently accounting for 8.4% of active gene therapy clinical trials (Ginn *et al.*, 2013). There will be a continued opportunity to develop gene therapy strategies to treat a range of cardiovascular diseases, like ISR, in the future. These strategies will be predominantly determined by the choice of gene product and the ability to deliver it effectively to the vasculature, over a sustained period of time.

### **1.7.3.3 Gene**

The third, and most important, component of a GES is the gene itself. Humans have approximately 50,000 different genes. A gene is the basic physical and functional unit of heredity, which can be defined as a section of the DNA strand that carries the instructions for a specific function (e.g. production of protein). A gene has two parts:

- a protein-coding sequence which contains the structural blueprints for the protein and
- a promoter which controls when, where, and to what degree a gene is switched on or “expressed”.

Gene expression is the process by which information from a gene is used in the synthesis of a functional gene product. Over-expression causes the over-production of a gene product which will have a specific biological effect, and under-expression causes the reduced production of a gene product. The choice of an effective, therapeutic gene is a very important decision in developing a GES. The over-expression, i.e. switching on a gene so it over-produces a functional product (a protein for example), of several gene products has demonstrated their ability to reduce restenosis in both pre-clinical and clinical models (Varenne & Sinnaeve, 2000). These strategies will be discussed in detail in the section below and, like their

pharmaceutical counter-parts, therapeutic gene products can intercept and modulate early stages of the cell cycle (cytostatic) or later stages (cytotoxic).

#### 1.7.3.3.1 Cytostatic gene therapy

Cytostatic strategies are aimed at the inhibition of key components of the cell cycle to inhibit cell proliferation without cell death. Yang and co-workers demonstrated that the over-expression of a constitutively active mutant form of Retinoblastoma (Rb) and p21 (CKI protein) resulted in the cytostatic inhibition of VSMC proliferation *in vitro* and *in vivo* (N. S. Yang, Sun, & McCabe, 1996). Adenovirus-mediated over-expression of human p21 also blocks the cell cycle cytostatically, resulting in significant neointimal hyperplasia development in a rat model (Chang *et al.*, 1995), (R. Y. Chen *et al.*, 2003). Scheinman and colleagues demonstrated a similar result with the over-expression of p53 (Scheinman *et al.*, 1999). The proto-oncogene *ras* is a key transducer in several growth–signalling pathways and several studies have used this gene product to significantly reduce neointimal formation (Maillard *et al.*, 1997), (Indolfi, Coppola, Torella, Arcucci, & Chiariello, 1999) and (Ueno, Kanellakis, Agrotis, & Bobik, 2000).

#### 1.7.3.3.2 Cytotoxic gene therapy

Cytotoxic approaches have also been successfully employed to deliver gene products. These approaches intercept at a later stage of the cell cycle and inhibit DNA synthesis; this action results in the death of both transduced and adjacent cells (bystander effect). Both Ohno and co-workers and Guzman and co-workers successfully used a Herpes simplex virus thymidine kinase (HSV-tk) to inhibit VSMCs cytotoxically post arterial injury (Uchio *et al.*, 1994), (Guzman *et al.*, 1994).

#### *1.7.3.3.3 Conclusions*

The above examples all involve delivering a gene product (cytostatic or cytotoxic) to the vessel wall to arrest SMC proliferation. However, as already discussed in section 1.6 in relation to DES, preventing SMC proliferation alone is not an adequate solution to the clinical manifestation of ISR. SMCs proliferate because their quiescent state (i.e. non-dividing state) is interrupted when the overlying endothelial layer is removed or damaged. Thus it is scientifically sound to suggest that by restoring the endothelium as quickly as possible, this will modulate the exposed underlying SMC medial layer back into its natural quiescent phenotype. This will have a dual benefit in reducing neointimal hyperplasia formation and preventing thrombus formation, because the non-thrombogenic nature of the inner lumen will be restored.

In the context of GES development, the pro-healing strategy of delivering a therapeutic gene which encourages re-endothelialisation is an opportunity for targeting the recruitment of endogenous progenitor cells, which have the ability to differentiate into mature ECs, as opposed to, “killing” cells with cytotoxic and/or cytostatic approaches.

Section 1.7 has presented the individual components of a prospective GES platform. The technological aspects of these components will need to be explored and scientifically validated in the development of a GES. However, in parallel, it is vitally important to consider the regulatory requirements that are essential in the development of any commercial treatment for patients. The following section explores this topic in detail.

## 1.8 Regulatory affairs

Significant and rapid developments in the fields of biology, biotechnology, engineering and medicine have led to the development of new treatments and highly innovative medicinal products, including medicinal products containing viable cells and bio-molecules (Donawa, 2008). These emerging Advanced Therapy Medicinal Products (ATMPs) hold a promising potential for the treatment of various diseases where there is a previously unmet medical need. ATMPs are defined as innovative, medicinal products whose therapeutic, prophylactic or diagnostic effects relate to the action of recombinant nucleic acids for gene therapy applications or cells or tissue, in the instance of cell therapy (Committee for Advanced *et al.*, 2010).

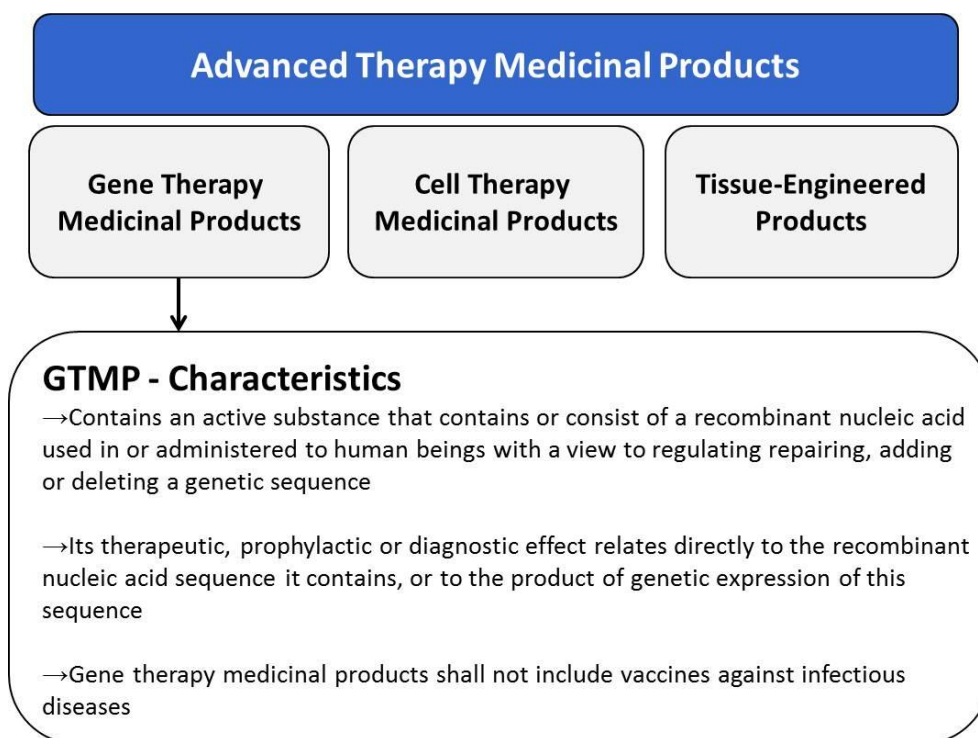


**Figure 1.23:** Definitions of ATMPs in accordance with the European pharmaceutical legislation (adapted from Schneider, 2010; Regulations (EC) No 1394/2007 and Commission Directive 2009/120/EC).

ATMPs can be divided into three categories: Gene therapy medicinal products (GTMP), cell therapy medicinal products (CTMP) and

tissue-engineered products (TEP). A GES would fall under the GTMP category. Figure 1.23 captures this further categorisation of the ATMPs and summarises the specific characteristics of a GTMP.

ATMPs “bridge the gap” from both a legislative and scientific perspective, linking traditional medical devices (Medical Device Directive 93/42/ECC) and medicinal products (Directive 2001/83/EC). Figure 1.24 graphically depicts where ATMPs are positioned from both a scientific and regulatory viewpoint. The commercialisation pathway of any ATMP is currently governed by an independent committee (CAT = Committee for Advanced Therapies) responsible for cell therapy, gene therapy and tissue-engineered products.

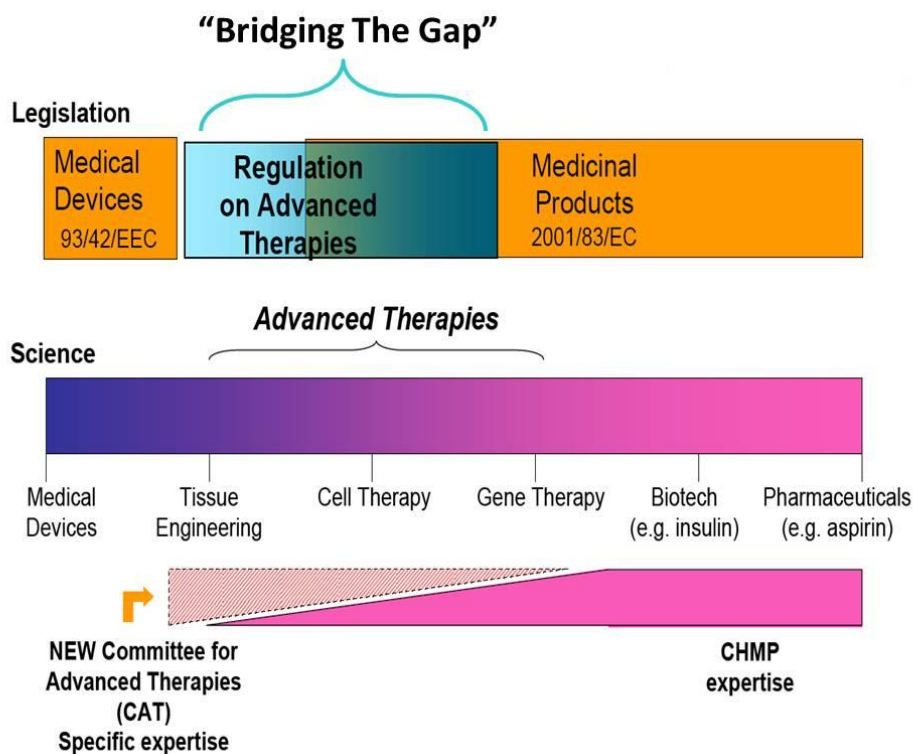


**Figure 1.24:** Advanced Therapy Medicinal Products – positioned between Medical Devices (93/42/EEC) and Medicinal Products (2001/83/EC.) Adapted from the European Medicines Agency (2008).

As this study focuses on the development of a GES, with a focus on developing a platform that could be potentially commercialised, the regulatory route to market will be governed by either European CE marking or US FDA criteria. Medical device regulation employs a three-pronged approach to the development of products: safety, efficacy and performance. This work presented within this thesis addresses all three elements and to ensure that due diligence is observed. To this end, the aforementioned medical device regulation pathways, in Europe and the US, will be further described in the next section.

### **1.8.1 Medical device regulation**

The regulatory route demonstrating the safety and efficacy for a new medical device has always been a lengthy, difficult, and expensive process from concept to commercialisation. The approval process varies significantly in accordance with the clinical and regulatory environments in the United States and Europe, respectively. There are inherent differences in the criteria for approval and the process for obtaining approval, with the introduction of new devices into clinical practice occurring more swiftly in Europe than in the United States (Kaplan *et al.*, 2004).

In the US, medical devices are classified according to their perceived risk using a 3-tiered system (Class I, II, or III). Similarly in Europe, the Medical Device Directive (MDD) also employs a tiered system (Class I, IIa, IIb, and III). In both systems a DES is deemed to be a Class III device (i.e. an implantable with an active pharmacological agent) with a high risk perception, requiring a comprehensive clinical trial plan and always requiring a pre-market approval (PMA). The European CE Mark process requires demonstration of safety only, and not efficacy. The process is mediated by non-governmental Notified Bodies (NBs) within each member state. The United States, in contrast, factors a 1-4 year delay in introducing a high-risk Class III medical device as they require significant safety and

efficacy data to support an application and the process is regulated by a centralised governmental agency: Centre for Devices and Radiological Health/Food and Drug Administration (CDRH/FDA).

The introduction of DES to the market aptly illustrated the aforementioned time-lag in regulatory approval systems, with the DES platform becoming available in Europe a year before its US counter-part. As previously discussed in section 1.6.3, the Cypher™ stent arrived in Europe in 2002 and was approved by the FDA for the US market in 2003 following the completion of a pivotal trial to assure efficacy (Serruys *et al.*, 2006).

### **1.8.2 Regulatory route in Europe for GES**

The next generation of stenting will involve the production and commercialisation of a GES, a combined biologic device, which consists of an active biological agent (gene vector) on an existing medical device platform. This evolves the medical device to fall under the gene therapy sub-category (Part IV of Annex 1 to Directive 2001/83/EC) of ATMPs, and therefore it will be subject to a very stringent and rigorous regulatory approval pathway. Because of the complicated nature of all ATMPs (GTMP, CTMP and TEP), the development of a specialised regulatory pathway is still in its initial stages and innovators of such medicinal products will be faced with many unprecedented challenges during this period.

As illustrated in Figure 1.24, in the European jurisdiction, a dedicated committee, the Committee for Advanced Therapies (CAT) is currently revising Annex I to the Medicinal Products Directive 2001/83/EC to reflect the needs of an ATMP route to market. This multi-disciplinary, scientific committee of experts has representatives from all EU member states in addition to the European Economic Area (EEA) and the European Free Trade Association (EFTA). The committee also heralds representatives from patient associations (EGAN: European Genetic Alliance's Network and

EURORDIS: European Organisation for Rare Diseases) and medical associations (ESGCT: European Society of Gene and Cell Therapy and EBMT: European Blood and Marrow Transplantations). The CAT will be responsible for preparing a draft opinion on the quality, safety and efficacy of each ATMP for which an MA (marketing authorisation) application is submitted. The CAT opinion will then be submitted to the EMEA's committee for Medicinal Products for Human Use (CHMP) for final approval. CAT is also involved in developing the classification and certification procedures in relation to ATMPs. The CHMP has three working parties involved in the development of new guidance on ATMPs: The Biologics Working Party (BWP); the Gene Therapy Working Party (GTWP) and Cell-based Medicinal Products Working Party (CBMP).

The common framework for the marketing of ATMPs is contained within Regulation (EC) No 1394/2007 of the European Parliament and the amending Directive 2001/83/EC, originally adopted in 2007. The most recent recommendations were introduced and accepted by the European Parliament in 2014. The overall aim of the new regulation is: *“to improve patient access to safe and effective ATMPs of good quality; to provide a legal basis to promote development in the European Biosciences Industries; and to harmonise market access in the European Union by establishing a comprehensive regulatory framework which, includes the centralized procedure for Marketing Authorisations (MA) for ATMPs”*

### **1.8.3 Gene Therapy Clinical Trials**

Rosenthal and colleagues performed the first human gene therapy trial using a retrovirus to treat advanced melanoma in 1989 (Rosenthal, Kornhauser, Donoghue, Rosen, & Merlie, 1989). Thus far, the development of GTMPs have been slow despite over 1800 gene therapy clinical trials being conducted worldwide in 31 countries (Ginn *et al.*, 2013). In 2012, there were 39 active trials and as illustrated in Figure 1.25 below, 1,843

gene therapy clinical trials have been carried out utilising 11 different gene types. However, despite the activity, only a small percentage of these gene therapy approaches have made it to market.

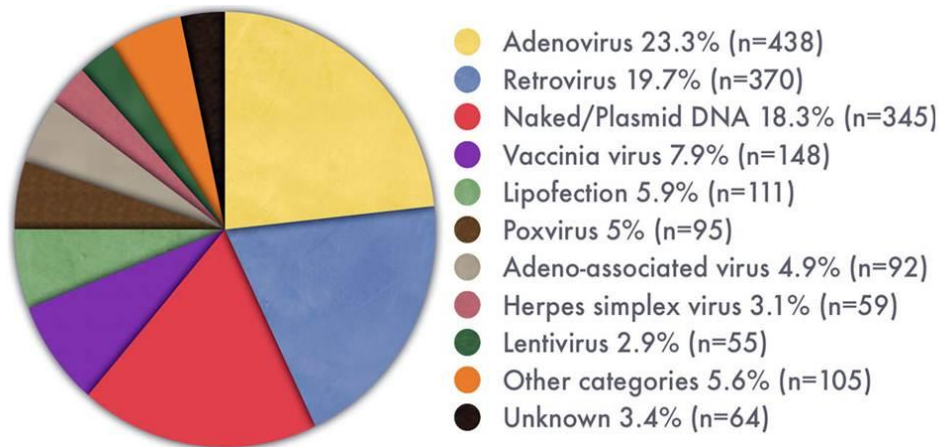


**Figure 1.25:** Gene Therapy clinical trials (1989-2012). Journal of Gene Medicine. Wiley *et al.*, 2012. n = number of clinical trials.

In 2012, a gene therapy medicine called Glybera (alipogene tiparvovec developed by uniQure, a Dutch Biotech) was recommended for authorisation in the 27 EU member states for the first time, for the treatment of a genetic disorder lipoprotein lipase deficiency (LPLD), using a recombinant adeno-associated virus. The European Medicine’s Agency (EMA) recommended the authorisation on the proviso that the company would be required to carry out post-marketing surveillance, carefully monitoring all outcomes in patients receiving the treatment.

To date, only one other gene therapy product (Gendicine®) is commercially available and implemented in clinical practice, to treat cancer of the neck. There are currently seven projects in Phase III Clinical Trials. Table 1.2 captures the active clinical trials (as of 2010) that have resulted in a commercial presence.

	Product Name	Company	Target Disease
Commercialised in China only	Genocidine™	SiBiono Genetechnologies	p53 adenovirus for the treatment of head- and neck squamous cell cancer is used in combination with radiotherapy
	Oncorine™	Sunway Biotech	nasopharyngeal cancer, combination treatment with chemotherapy
In Phase III Clinical Trials	Collatogene	AnGes MG	HGF Gene Therapy for Peripheral Artery Disease
	Glybera®	AMT	AAV-based gene therapy for LPLD
	Cerepro®	Ark Therapeutics	Adenovirus-based therapy for treatment of operable malignant glioma
	Generx®	Cardium Therapeutics	Adenovirus-based therapy for treatment of CAD
	TNFerade™	GenVec Inc	Adenovirus-based therapy for treatment of oesophageal and pancreatic cancers
	TK008	MoIMed	Haematopoietic Stem Cell Transplant Therapy (High-risk leukemia)
	XRP0038	Sanofi-Aventis	Critical Limb Ischemia with skin lesions (TAMARIS)
	Allovectin-7®	Vical	Non-viral plasmid/lipoplex treatment for Metastatic Melanoma

**Table 1.2:** Status of ATMPS commercially available in Phase III Clinical Trials, BioPortFolio, August 2010.

Knowledge of this regulatory pathway is essential for the development of a GES for market and will input at a very early stage into critical path decisions to progress this potential product from concept to commercialisation.

## 1.9 Research Summary

Against the background of gene therapy and gene-eluting stents overviewed in the preceding sections, the aims and objectives of the present research are set out below.

The removal of endothelium during an angioplasty procedure causes the underlying medial layer to change phenotype, thus inducing the formation of neointimal hyperplasia in certain patient populations. It is envisioned that promoting re-endothelialisation at a very early stage will stimulate the exposed SMC medial layer to return to a quiescent, non-proliferative state, thus preventing the formation of a hyperplastic SMC mass in the neointima. Specifically, it is proposed that the delivery of a gene vector, carrying a therapeutic gene could achieve this. It is proposed that the delivery of a gene vector, namely a plasmid-lipoplex formulation from a stent platform, carrying the endothelial nitric oxide synthase (eNOS gene), to cells at the site of vascular injury will enable nitric oxide production at the site. Presentation of a GES containing the eNOS gene should result in transduction of the cells at the site of injury but it will also have the potential to target circulatory cells that infiltrate the injury site during the inflammatory response. Localised cell transduction ought to initiate the production of nitric oxide (NO), capable of diffusing through the medial layers and also into the bloodstream. In theory, the production of NO should recruit endogenous progenitor endothelial cells to the site of vessel injury, thus inducing the formation of endothelium. In addition, by re-establishing the endothelial layer post-injury, it returns the non-thrombogenic properties of the intimal layer. This would be a significant event as it is the thrombogenicity of an exposed medial layer that warrants the long-term administration of anti-platelet therapy to prevent late stent thrombotic events.

In the context of the development of a GES, the properties of some polymer coatings used on DES could potentially afford the same control to a biologically active agent, such as a therapeutic gene, as they are currently employed for pharmacological agents on DES platform. DES has primarily focused almost entirely on the anti-proliferative, anti-migratory and anti-inflammatory channels to prevent ISR. In the present work, what is of interest is to explore the GES from a pro-healing approach using a non-viral system.

The principal objective of the research contained within this thesis is to determine a polymer coating/non-viral vector combination that could successfully deliver a therapeutic gene, eNOS, to the site of vascular injury, produce NO and induce re-endothelialisation as quickly as possible, thus arresting the proliferative nature of an exposed SMC medial layer.

The thesis has two main hypotheses:

1. Stent-based non-viral vector delivery can safely target the vector to the site of vascular injury resulting in comparable gene expression to viral gene delivery from a stent.
2. Non-viral mediated Lipo-eNOS delivery to the vasculature of a hypercholesterolemic rabbit model can reduce the incidence of ISR, through enhanced NO production and re-establishment of a functional endothelium.

The work presented in this thesis is divided into two separate phases of investigation as summarised below, and illustrated in Figure 1.26.

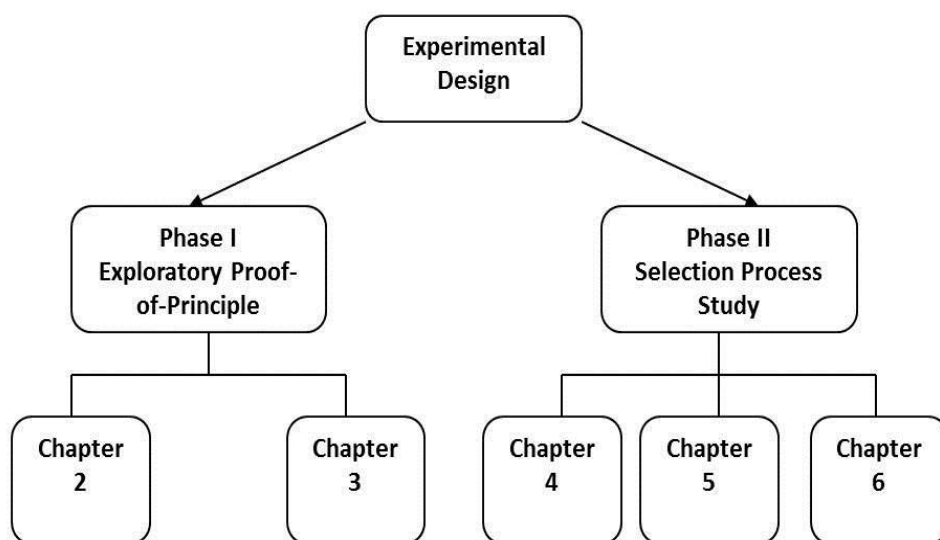


Figure 1.26: Organisation of the thesis.

### 1.9.1 Phase I: Exploratory proof-of-principle study

This phase is documented in chapters 2 and 3 and focused on the proof-of-principle exploration of the development of a non-viral GES.

#### 1.9.1.1 Chapter 2 Experimental Plan

The work contained in this chapter investigated the potential of utilising an amphiphilic block copolymer, Pluronic<sup>®</sup> F127 as a non-viral vector and polymer carrier. This polymer has the ability to load and deliver significant levels of vector to the vasculature and has already been tested extensively for biocompatibility *in vitro* and *in vivo* and could be a potential polymer that would act dually, as a coating and vector. The main advantage of this candidate polymer is that it has already been successfully used in other gene therapy applications as a vector, and that it induces a clinical benefit (Batrakova *et al.*, 2001), (El-Kamel, 2002). It is well-researched that plasmid DNA and Pluronic<sup>®</sup> F127 concentrations and binding ratios can be modulated to produce an optimal release kinetic profile of plasmid DNA in addition to optimal polyplex particle properties. It

is therefore hypothesised that the optimisation of the polyplex encapsulation, coupled with biophysical characterisation, will enable prediction of Pluronic's potential as a suitable dual non-viral vector/polymer carrier for a GES platform.

### **1.9.1.2 Chapter 3 Experimental Plan**

This chapter contains a comparative study to evaluate the use of a commercially available liposome, versus a viral vector (adenovirus) from previously conducted proof-of-principle work (Sharif *et al.*, 2008) to illustrate successful gene delivery to the vessel wall, both delivered from a Phosphorylcholine (PC) coated stent platform. This study looks specifically at elution profiles over a time period and aims to establish if there is a link between elution profiles and transfection efficiencies for both a viral and non-viral vector, in *in vitro* pseudovessels and *ex vivo* rabbit carotid artery explants.

This chapter also explores a more clinically relevant *in vitro* assessment technique by deploying stents in a pseudo-vessel consisting of a silicone tube seeded with indigenous vascular cells, instead of just evaluating the vectors in static 2D *in vitro* plates. This would enable the screening of candidate genes (reporter and therapeutic), vectors (viral and non-viral) and delivery vehicles (polymers/stents) to be more precise and scientifically robust. There is a well-documented "mis-match" between *in vitro* and *in vivo* results in the literature, i.e. therapies may produce a certain result in relation to performance, efficacy and safety *in vitro* and the same therapy does not replicate this result in an *in vivo* situation (Rex *et al.*, 2001), (Krishnan *et al.*, 2003), (Kumaraswamy, Sethuraman, & Krishnan, 2014). *In vitro* results can either "over-predict" successful outcomes that are then not translated to the *in vivo* setting, and also conversely can under-predict *in vitro*, and as a result the therapy never progresses to a pre-clinical animal model to be evaluated. Both results

have significant drawbacks. The aforementioned studies relate primarily to drug dissolution profiles *in vitro* versus *in vivo*. However in 2007, Cirulli and Goldstein produced evidence specifically from *in vitro* transfection studies to illustrate that the *in vivo* functional importance of a polymorphism in the context of human disease (Cirulli & Goldstein, 2007). This study specifically highlighted the need to consider the relationship between temporal regulation, tissue specificity and genetic background when attempting to use *in vitro* data to predict behaviours of vectors *in vivo*. These investigators emphatically concluded that if the expression difference is found in transfected cell lines *in vitro* but not in a tissue of interest *in vivo*, then the evidence from the *in vitro* experiments are close to “meaningless” (Cirulli and Goldstein, 2007). A similar conclusion was drawn by Wang and Sadée a year previously with their *in vitro* experiments comparing polymorphisms affecting transcription and mRNA processing and in turn investigating how the vectors perform *in vivo* when they are exposed to human phenotypic variability (D. Wang & Sadee, 2006).

The major constraint to adequately determine if a vector, which is able to transfect cells *in vitro*, can perform as well when delivered *in vivo*, is the selection of an appropriate assessment environment. Most *in vitro* transfection studies are conducted in static, 2D environments as opposed to a dynamic, biochemically and anatomically correct reproduction of the *in vitro* environment. The 3D pseudo-vessel model proposed here does not address the dynamic and biochemical limitations but it does allow the *in vitro* transfection efficiency experiments to be conducted in a more anatomically and dimensionally realistic environment than what an *in vitro* 2D static experimental set-up can provide. It is proposed that this simple advancement in assessment technique would greatly enhance the performance of the candidate liposomal formulations at this stage of the evaluation process and provide more predictive estimations of how the formulations will perform *in vivo*.

It is expected that evaluating transfection efficiency in a 3D *in vitro* cell culture system, under stent deployment pressures, will provide a more realistic and representative expectation of efficacy, in comparison to current *in vitro* methods, prior to a pre-clinical animal model study assessment. The study described in Chapter 3 investigated if testing, and screened, non-viral vectors in 3D environments (*in vitro* and *ex vivo*) to establish if this system can better predict the performance *in vivo*, than a 2D *in vitro* assessment alone.

### **1.9.2 Phase II: Selection Process Study**

The second phase of this experimental work focused on selecting an optimal liposomal formulation to be coated onto an existing stent platform to successfully deliver a therapeutic gene and induce a clinical advantage *in vivo*. Three potential liposomal formulations were evaluated: Lipofectin™ (commercially available), DDAB/DOPE and DDAB/POPC/Cholesterol (in-house formulations), to determine if they could effectively transfect, first a reporter gene *in vitro*, and subsequently *in vivo*, before selecting the lead formulation to be evaluated in an hypercholesterolemic model *in vivo* with a relevant therapeutic gene.

#### **1.9.2.1 Chapter 4 Experimental Plan**

The work contained within this chapter don the biophysical characterisation, cytotoxicity potential, long-term storage capability and transfection efficiency, of all three candidate liposomal formulations (introduced in section 1.9.2) in an *in vitro* setting. This process of characterisation and transfection assessment, coupled with the information gathered in Phase I, enabled a leading liposomal formulation or “lipoplex”/stent platform combinations to emerge. It was hypothesised that the evaluation of three candidate lipoplexes, in terms of their performance within an ISO controlled testing framework (ISO10993:

Biological evaluation of medical devices), determined which lipoplex should be evaluated further in an appropriate non-diseased *in vivo* animal model.

### **1.9.2.2 Chapter 5 Experimental Plan**

The study in this experimental chapter acted as a validation step in further screening the three liposomal candidates in an appropriate non-diseased (normocholesterolemic) *in vivo* animal model, primarily for its transfection efficiency capabilities, with appropriate reporter genes. This study focused on lipoplex-delivery of a reporter gene to the vessel wall from both a polymer coated (Phosphorylcholine) stent and a bare metal stent. The BMS acted as a control arm to verify if a polymer coating enhances transfection efficiency *in vivo*. It was hypothesised that the lead lipoplex (bare metal vs. PC coated stent) from the previous chapter 4 *in vitro* studies would be validated by a gene expression study in an appropriate normocholesterolemic *in vivo* animal model.

### **1.9.2.3 Chapter 6 Experimental Plan**

This chapter investigated the therapeutic effect of the delivery of a clinically relevant therapeutic gene (eNOS) and used the leading lipoplex, determined from the data generated in chapters 4 and 5. The study examined and quantified the delivery of the eNOS to the vessel wall in a diseased (hypercholesterolemic) animal model. It was proposed that the timely delivery of this lipoplex containing eNOS (Lipo-eNOS) to the vessel wall would induce re-endothelialisation and restore non-thrombogenicity to the luminal surface, by virtue of decreasing the attraction of inflammatory cells to the site of vascular injury. In turn, arresting the inflammatory response prematurely and decreasing the incidence and extent of neointimal hyperplasia formation. Based on previous research (Sharif *et al*, 2008), it was hypothesised that eNOS delivery from a PC coated stent would re-endothelialise better than delivery from a BMS.

In summary, the completion of the outlined experimental plan will sequentially address the predictions postulated by the original hypothesis. If the predictions that:

1. Stent-based non-viral vector delivery can safely target the vector to the site of vascular injury resulting **in comparable gene expression** to viral vector delivered genes and
2. Non-viral mediated Lipo-eNOS delivery to the vasculature of a hypercholesterolemic rabbit model **can reduce the incidence of ISR,** through enhanced NO production and **re-establish a functional endothelium,**

were supported by the results of experiments outlined in the two phases then the hypotheses of this study will be proven.

## **1.10 Specific study aims**

The specific aims of each chapter are summarised below.

- **Chapter 2**

To investigate the feasibility of Pluronic<sup>®</sup> F127 as a potential stent coating/vector construct for the delivery of a therapeutic gene to the vasculature.

- **Chapter 3**

To characterise and compare the following key parameters: elution kinetic profiles, transfection efficiency capabilities and gene expression patterns for both a viral and non-viral vector in *in vitro* pseudovessels and *ex vivo* rabbit carotid artery explants.

- **Chapter 4**

To evaluate three candidate liposomal formulations (lipoplexes) for potential use as gene therapy vectors. Both the biocompatibility and transfection efficiency of all three candidate lipoplexes will be assessed as per ISO10993: Biological evaluation of medical devices.

- **Chapter 5**

To evaluate the *in vitro* transfection efficiency of the three candidate lipoplexes when applied to a stent surface (bare metal vs. PC coated stent) in an appropriate *in vivo* model (normocholesterolemic NZW rabbit model). This process should determine the leading lipoplex formulation/stent platform (bare metal vs. PC coated stent) combination to be further assessed in a pathological model.

- **Chapter 6**

To evaluate the efficacy of localised stent delivery of the leading lipoplex, (identified from Chapter 5) to the vasculature of an appropriate *in vivo* hypercholesterolemic animal model.

- **Chapter 7**

Conclusions and future directions are presented in this chapter. The overall goal of this chapter is to critically appraise if the results of the experimental plan produced results that support the predictions outlined in the original hypothesis of this thesis, to elucidate the limitations of the study and to provide recommendations for future work.

**2. Evaluation of non-viral Pluronic®F127 (PF127) as a potential coating/vector for delivery of a reporter gene *in vitro***

## 2.1 Introduction

As previously described in the research summary of the introductory chapter the work presented in this chapter forms part of the proof-of-principle phase of this thesis. This chapter investigates the overall feasibility of a non-viral amphiphilic polymer Pluronic<sup>®</sup>F127 (PF127) to function as both a stent coating and a non-viral vector for gene delivery to a vessel wall. The polymer family of Pluronics have already been used extensively in gene therapy applications (Gebhart *et al.*, 2002), (Gaymalov, Yang, Pisarev, Alakhov, & Kabanov, 2009) and (Song *et al.*, 2014) but there has been limited evaluation conducted on the polymer as a stent coating, although some research groups have investigated the polymer as a drug-elution vehicle (Lavasanifar, Samuel, & Kwon, 2002), (Grassi *et al.*, 2006), (Batrakova *et al.*, 2001) and (Kraynov *et al.*, 2011). The work presented here aims to independently characterise both the biophysical properties of the PF127 (complexed with plasmid DNA) and the plasmid DNA elution kinetics profiles of the PF127. The study investigates if there is any relationship between biophysical characterisation and elution kinetic profiles and if these parameters can help predict *in vitro* transfection efficiencies (2D). Finally, the work also examines if there was merit in evaluating the *in vitro* transfection efficiency of PF127 from a stent in a 3D system (cell-lined silicone tube).

To contextualise this work, the following introduction briefly explores the following subjects: Non-viral vectors; Pluronic and its use in general medical applications and specifically its use in gene therapy applications; and PF127, the specific Pluronic examined in this study. The introductory section concludes with the experimental rationale and specific objectives of the work contained herein.

### 2.1.1 Non-viral vectors

As discussed extensively in section 1.7, gene therapy strategies have been successfully used to treat a range of diseases (Morgan & Anderson, 1993), (Armbruester *et al.*, 2002) , (Miller, 1990), (Partridge & Oreffo, 2004), and (Naldini *et al.*, 1996). Although non-viral gene therapy strategies are less efficient than that of their viral counterparts *in vivo*, they are a more attractive modality as they circumvent bio-safety concerns of immunogenicity, virus-mediated random integration and recombination wild-type viruses (I. Matsumoto *et al.*, 2001) and (R. Y. Chen *et al.*, 2003).

Non-viral vectors, based on cationic polymers and cationic lipids, can transfect cells efficiently by: (1) binding with plasmid DNA, (2) condensing plasmid DNA, (3) protecting plasmid DNA from nuclease degradation, and (4) enhancing the transport of plasmid DNA into the target cell (Boussif *et al.*, 1995), (Wagner, 2008), (Gebhart *et al.*, 2002), (Gaymalov *et al.*, 2009), (Tang *et al.*, 2011) and (Ramgopal, Mondal, Venkatraman, & Godbey, 2008). Among these non-viral contenders is the family of amphiphilic (containing both hydrophilic and hydrophobic domains) tri-block copolymers referred to as Pluronics.

### 2.1.2 Pluronics

Pluronics, a family of commercially available block co-polymers, have been extensively studied and reviewed for their potential use in the pharmaceutical and biomedical field for a diverse range of applications because of their proven *in vivo* transfection capabilities (Kabanov (Batrakova *et al.*, 2001), (Gebhart *et al.*, 2002), and (Moghimi & Hunter, 2001).

This family of polymers are sometimes referred to as synperonins or poloxamers in the literature. However, they are most often referred to by their trade name Pluronic<sup>®</sup>. Pluronics are composed of PEO (polyethylene

oxide) and PPO (polypropylene oxide) blocks in a 2:1 ratio and often denoted by their generic nomenclature EO<sub>x</sub>PO<sub>y</sub>EO<sub>x</sub>. The significance of this classification system is that it enables users to select from a wide variety of Pluronic formulations with different molecular weights (MW) and hydrophilic-lipophilic balances (HLB).

This polymer family exhibits many interesting characteristics including water solubility, low toxicity and thermo-reversible gelation properties. Of the aforementioned characteristics, thermo-reversible gelation has a significant impact on how efficiently an agent (drug or a biologic) can be loaded into the polymer. Thermo-reversible gelation is governed by two parameters: concentration and temperature. In aqueous solutions, at concentrations above their critical micelle concentration (CMC), Pluronics self-assemble into micelles, the diameters of which range from 10-100nm (Gebhart *et al.*, 2002). Figure 2.1 illustrates the morphology of unimers (single copolymer molecules) of Pluronic and their self-assembly capacity to form micelles. The micellar core is hydrophobic and is separated from the aqueous exterior by a hydrated hydrophilic PEO corona.

The hydrophobic core has the capacity to absorb large quantities (20-30%) of water-soluble drugs. The function of the hydrated, crystalline PEO shell is to ensure that the micelles remain in a dispersed state, protecting the agent payload from degradation, minimizing the agent's exposure to tissue and enhancing its transport across cellular barriers into target cells (Batrakova *et al.*, 2001).

Similarly, with respect to temperature, it is postulated that the gelation phenomenon in Pluronic occurs because of micelle formation at critical temperatures (CMT) resulting in the dehydration of the

hydrophobic PPO core and the mechanism of micellar packing at increased temperatures (Bohorqueze *et al.*, 1994) and (Cabana *et al.*, 2001).

In addition to thermoreversible gelation properties, the amphiphilic nature of Pluronic, is also a distinctive characteristic. It affords the polymer a unique capability to interact with hydrophobic surfaces of biological membranes (Gaymalov *et al.*, 2009). This is a very important consideration for polymer selection in the context of DNA encapsulation. This non-ionic, water-soluble polymer, although it is not known to bind or condense plasmid DNA, has significantly enhanced the expression of transgenes *in vitro* and *in vivo* (Felgner, 1997), (Gebhart *et al.*, 2002).

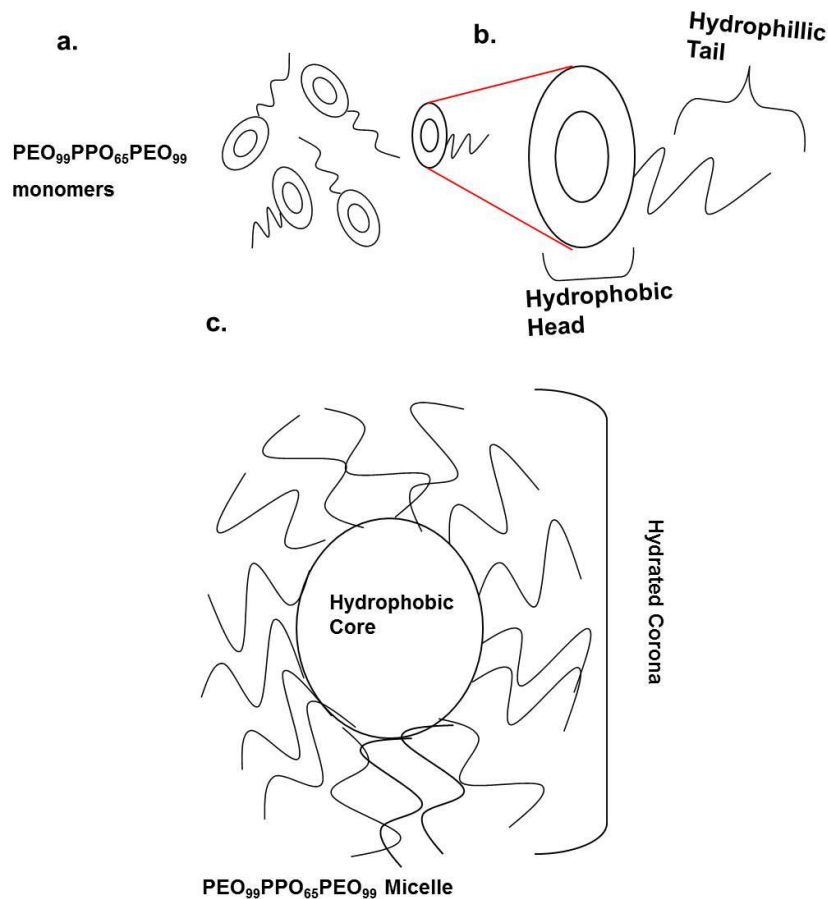


**Figure 2.1:** Morphology of Pluronic<sup>®</sup> F127 (a) Schematic of individual monomers Pluronic<sup>®</sup> F127 (b) Magnified schematic of a monomer illustrating hydrophilic/hydrophobic regions (c) Representation of chain conformations in micelles formed by tri-block copolymers like Pluronic<sup>®</sup> F127 (Adapted from Booth & Attwood, 2000).

### 2.1.3 Pluronic - medical applications

Pluronics are an important class of materials and have evolved over the decades from being used exclusively in commercial applications to their adaptation to the medical/pharmaceutical arena, primarily due to the fact that they can “self-assemble”. Self-assembled structures have been studied and used extensively in the pharmaceutical industry to exploit their useful properties, including nanoparticle size range (10-100nm), hydrophobic drug solubility and low toxicity values (Jeon, Kim, & Kim, 2003), in the areas of drug delivery, drug stability and controlled release of drugs.

From a clinical perspective, Pluronic has primarily been used for, and has had the most success in, the treatment of cancer. It has been used to positively influence the transport and activity of anti-cancer agents in MDR (multi-drug resistant) tumour cells (Venne, Li, Mandeville, Kabanov, & Alakhov, 1996). This Pluronic treatment is often administered after an oncology patient experiences a cancer recurrence post-chemotherapy administration. It is postulated that the Pluronic micelles encapsulate the anti-cancer agents, enabling them to be endocytosed by the tumour cell membrane. A particular Pluronic formulation (a blend of Pluronic<sup>®</sup>L61 and Pluronic<sup>®</sup>F127) loaded with doxorubicin was used in Phase II clinical trials where it illustrated its potent ability to sensitize MDR cancer cells (Kabanov (Batrakova *et al.*, 2001). It was this landmark study in 2003 that initiated a thorough investigation into the complex mechanisms and specific cascade of cellular events which mediated this successful response in MDR cancer cells. What was most remarkable about this particular study was that these effects were more notable in polymer concentrations below the critical micelle concentration (CMC) (Miller, 1990) and (Batrakova *et al.*, 2001) indicating that unimers and not self-assembled micelles, characteristic of higher concentration solutions, are responsible for these fascinating biological modifying properties. This had been previously postulated by

Batrakova and colleagues (1997 and 2001), i.e. that it was the unimers (monomers) and not the micelles that had the ability to traverse the cellular membrane. Both the cell membrane lipid bilayer and the Pluronic are amphiphilic in nature thus the hydrophobic segments of the membrane are the ideal target for the immersion of the hydrophilic section of the Pluronic unimer. In contrast, formation of micelles at high concentrations results in shielding of the hydrophobic PPO chains in the micellar core which diminishes Pluronic's availability to affect the cellular membrane. Figure 2.2 illustrates how a polyplex, formed between naked plasmid DNA and a block copolymer, such as Pluronic, may be taken up by the cellular membrane and endocytosed. Most importantly, certain molecular weight classes of Pluronics, including PF127, have already been approved by the FDA for clinical use (Gebhart *et al.*, 2002), (Mei, Sun, & Song, 2009), (F. Liu, Qi, Huang, & Liu, 1997) and (R. Wang *et al.*, 2013).

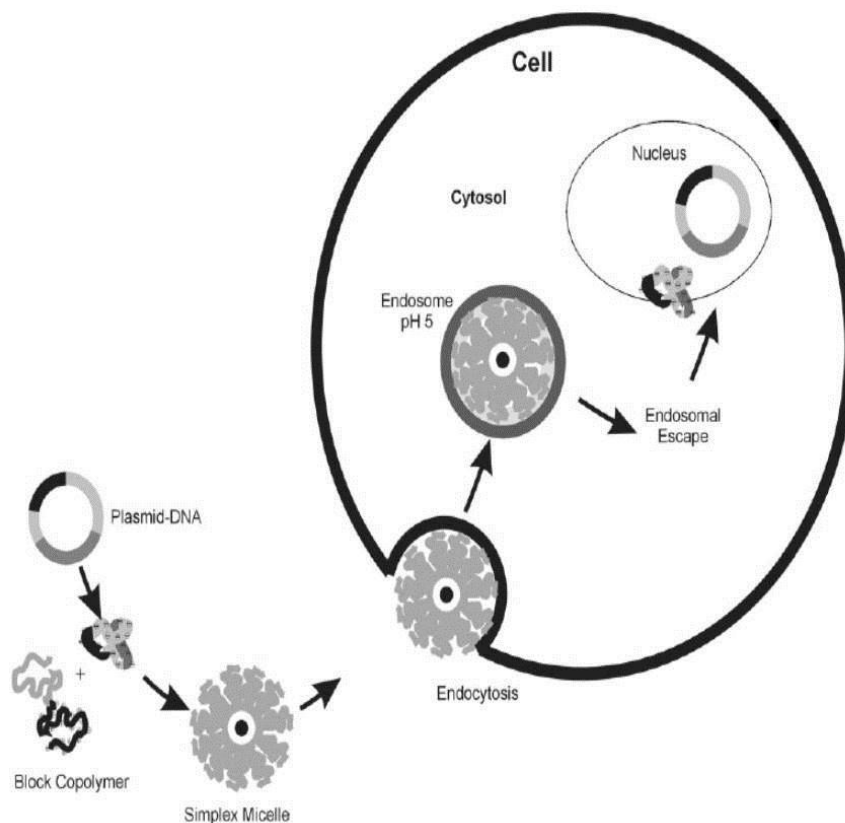


**Figure 2.2:** Schematic of the mechanism of cellular uptake of a triblock copolymer/plasmid DNA polyplex by endocytosis (Konrad and Förster, 2003).

#### 2.1.4 Pluronic - gene therapy applications

As discussed in section 2.1.3 above, Pluronic is very suitable for gene delivery in terms of gene therapy and vaccination strategies. It is well documented that delivery of plasmid DNA could be a potential modality to generate meaningful levels of gene expression to induce a clinically relevant therapeutic effect. Pluronic gels display low toxicity, and low clinically-useful doses have not induced an increase in serum triglycerides and cholesterol in animal models (Blonder *et al.*, 1998). As mentioned in section 2.1.2, amphiphiles are compounds that have both hydrophilic and hydrophobic domains. Pluronic and plasmid DNA are both amphiphiles. DNA is a macromolecule that consists of a hydrophilic, polar,  $\delta$ -negative phosphate backbone and a hydrophobic non-polar,  $\delta$ -positive internal bases. This duality has a stabilising effect on the DNA double helix structure.

These compounds are also characterised by hydrogen bonding and bonds via electrostatic attraction. Figure 2.3 illustrates the chemical structure of plasmid DNA. Part a) demonstrates the classical Watson and Crick double helix model and illustrates the polar phosphate groups of the backbone which confers hydrophilicity to the structure, and part b) gives an illustration of the b-form conformation of plasmid DNA (used in this study) and how they further expose the hydrophilic part of the sugar-phosphate backbone. This is particularly important in the context of complexing with an amphiphile, such as PF127, to produce DNA loaded, non-viral vectors.

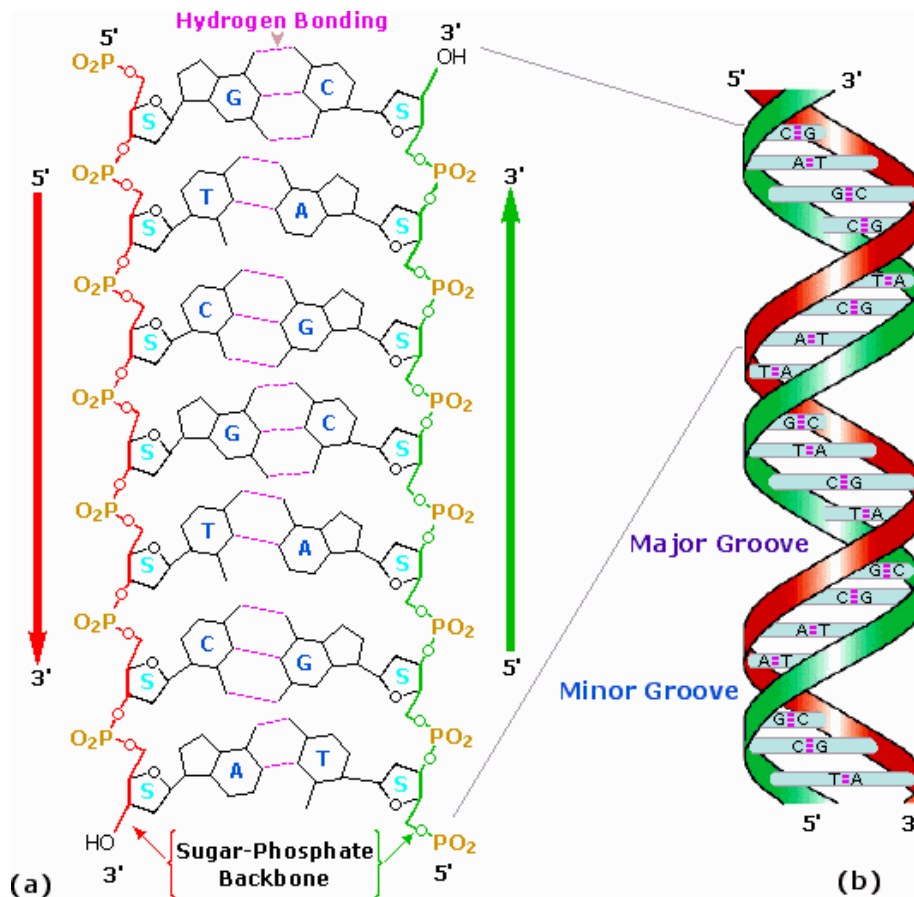


**Figure 2.3:** Chemical structure of plasmid DNA (a) Watson and Crick Double Helix structure in which DNA strands are arranged anti-parallel to one another i.e. with opposite 3' and 5' ends (b) Right-handed B-form plasmid is favoured in aqueous solutions. These conformations leaves an exposed phosphate backbone resulting in two groove formations: major (20Å) and minor (12Å). Source: <https://worldofbiochem.wordpress.com/2014/04/11/reflection-10-nucleotides-and-ucleic-acids-2/>

Plasmid DNA does not freely cross the cell membrane because in a free state (i.e. not condensed) its hydrophilic, negatively-charged surface attracts nucleases causing rapid degradation (Chiou *et al.*, 1994), (Roques *et al.*, 1995) and (Demaneche, Jocteur-Monrozier, Quiquampoix, & Simonet, 2001). It has been shown that interaction between Pluronic formulations and DNA are mediated by the central hydrophobic block copolymer (Bello-Roufai, Lambert, & Pitard, 2007) which forms a protective capsule around the DNA. Complexes of DNA and block copolymers (or polyplexes) have been used to successfully deliver DNA to cells (Arigita, Zuidam, Crommelin, & Hennink, 1999).

### 2.1.5 Pluronic® F127

Pluronics are available in a wide variety of molecular weights. Pluronic® F127 (PF127) is an ABA-type tri-block copolymer and has a nomenclature of PEO<sub>99</sub>PPO<sub>65</sub>PEO<sub>99</sub>. Figure 2.4 gives a graphical representation of PF127.

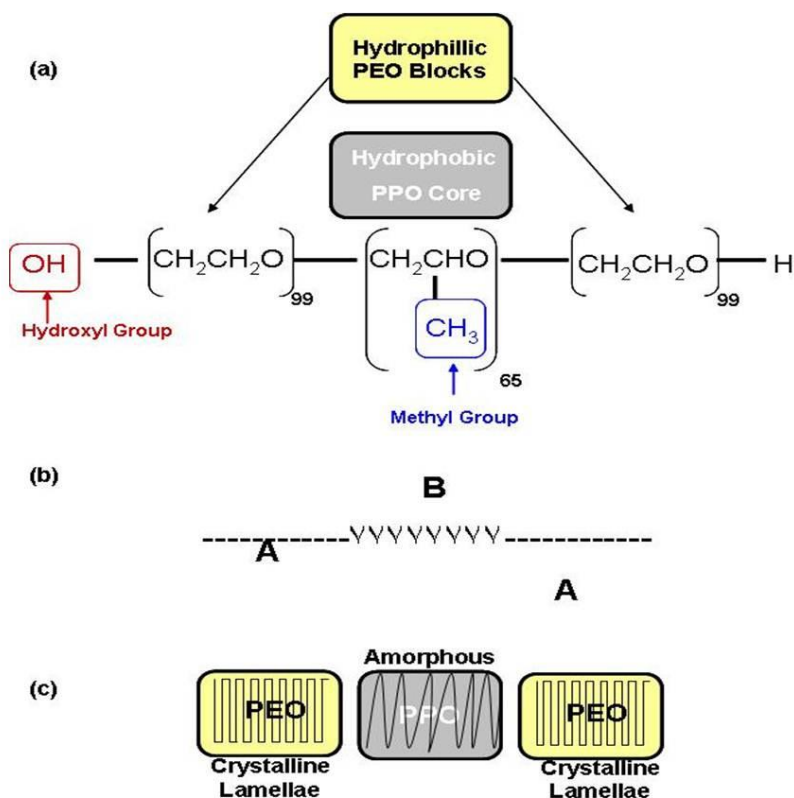


**Figure 2.4:** Graphical representation of Pluronic® F127 (a) Chemical structure of Pluronic® F127 – PEO<sub>99</sub>PPO<sub>65</sub>PEO<sub>99</sub> (b) Molecular architecture of a linear tri-block copolymer (ABA) (c) Schematic diagram illustrating the theoretical model of symmetric crystalline-amorphous tri-block copolymer morphology (Hong *et al*, 2001).

Moderately concentrated solutions of PF127 in water are micellar liquids at low temperatures (4°C) and form a gelatinous substance as the temperature increases. Specifically, an increase in temperature of an aqueous solution of PF127 results in the copolymer molecules aggregating to form spherical micelles which are composed of a dehydrated polyoxypropylene core and outer hydrated polyoxyethylene corona (Jain (Jain, 2000). PF127 forms semi-solid gels at room temperature and across the physiological temperature range (20-40°C) (Prud'homme, Draghia-Akli,

& Wang, 2007). In aqueous solutions at concentrations of 15-20% or higher, it exhibits the unique property of thermo-reversible gelation (Schmolka, 1994).

### **2.1.6 Experimental Rationale**

The primary aim of this study is to establish if PF127 has the potential to be used as a stent coating to efficiently deliver gene products to the vasculature *in vivo*. As both a potential stent coating and a vector, PF127 has a two-fold function and this is taken into consideration when designing the experiments. As a stent coating, it is important to use a Pluronic solution that has the ability to encapsulate a “therapeutic” payload concentration of naked plasmid DNA while remaining gelatinous at 37°C. It is also important that it can also be applied to the surface of a stent without difficulty. Due to the self-assembly nature of Pluronic at higher concentrations, a 20% Weight/Volume (w/v) Pluronic solution is used in the following experiments. Capitalising on its “thermoreversible” nature, the unencapsulated plasmid DNA is loaded and mixed with the 20% w/v PF127 in its liquid form at 4°C to ensure that a homogenous formulation is produced for the experimental work.

From a gene vector perspective, in advance of transfection efficiency assessment, it is critical to ascertain the optimal pDNA:PF127 ratio to ensure that there is complete encapsulation of the pDNA into nano-sized micelle particles that can be effectively released over a specified time course (elution kinetic profile) and readily endocytosed to effect gene expression in cells. To this end, prior to conducting any *in vitro* transfection efficiency experiment, three formulations (different pDNA:PF127 ratios) are biophysically characterised as it is expected that there will be significant changes to the structure, size and charge of the polyplexes (i.e. pDNA loaded PF127 micelles).

*In vitro* transfection efficiency studies will include both 2D and 3D experimental set-ups. From the literature, although Pluronics perform well *in vivo*, they are not known to transfect well *in vitro* (2D systems) and often require an amplifier or “adjunct” to ascertain if there is transfection capability. The rationale of screening any candidate vector *in vitro* first, is to determine which vector merits further examination. 2D *in vitro* assessment alone (without an adjunct) would eliminate Pluronic as a candidate at the first test, even though there is successful *in vivo* transfection efficiency precedence. Without an adjunct in a 2D experiment, it would be difficult to differentiate between the candidate formulations. Therefore, for the purpose of this screening process, an amplification protocol is employed to ascertain which Pluronic formulation progresses for examination in a 3D *in vitro* system. Details of the amplification protocol is described in the material and methods section of this chapter.

The lead formulation which emerges from the above characterisation then has its elution kinetics profiled over a 14 day period (to determine the plasmid DNA elution out of the polymer vector). Thereafter, the lead PF127 formulation is coated onto a commercially available bare metal stent (i.e. with no polymer coating) platform and deployed in a cell-lined tubular 3D *in vitro* system to assess if transfection efficiency can be obtained without the use of a transfection agent adjunct and to determine if the experimental set-up can favourably impact the *in vitro* screening process.

### **2.1.7 Experimental Objectives**

**Overall goal:** To investigate the feasibility of PF127 as a potential stent coating/vector construct for the delivery of a therapeutic gene to the vasculature.

### **Specific objectives:**

- To establish the binding mechanism that exists between plasmid DNA macromolecules and PF127.
- To investigate the effect on the biophysical, structural and morphological properties of PF127 with the addition of a therapeutic payload of unencapsulated plasmid DNA.
- To characterise the elution profile of plasmid DNA, eluted from PF127, over a specific time-course (14 days).
- To investigate if there is any correlation between biophysical characteristics, elution kinetic profiles and the transfection efficiency capabilities of PF127 in a standard VERO cell line (2D system).
- To preliminarily explore if there is any advantage in evaluating transfection efficiency in a 3D *in vitro* system as part of the screening process for the development of a GES.

## **2.2 Materials and Methods**

### **2.2.1 Preparation of PF127**

Cell culture-grade Pluronic<sup>®</sup>F127 (CAS no. 9003-11-6) was purchased from BASF (BASF Corp., New Jersey, USA) and used as received without an additional purification step. Stock solutions of the polymer, in serial concentrations, were prepared (5, 10, 15, 20 and 25% w/v) as per the cold method (Schmolka *et al.*, 1972), carefully adding small quantities of either cold double-distilled Milli-Q water, for biophysical characterization tests, or minimal essential medium (MEM, Invitrogen Corp., Oregon, USA), for transfection efficiency experiments. PF127 solutions were then gently inverted to mix over ice at 4°C and stabilisation was allowed to occur with overnight refrigeration on a roller plate (Schmolka *et al.*, 1972). The solutions were then filtered slowly through 0.45µm Millex- HV syringe

driven filters (Millipore Corp., Cork, Ireland) and incubated on ice to prevent premature gelation.

### **2.2.2 Plasmids**

The plasmids pCMV-Luc, coding for Luciferase, and pCMV-eGFP, coding for green fluorescent protein (Clontech, Palo Alto, CA, USA), controlled by the human cytomegalovirus (CMV) immediate-early gene promoter, were purified from recombinant *Escherichia coli* DH5 $\alpha$  using an Endofree QIAGEN plasmid purification column (QIAGEN Ltd, Dublin, Ireland). The concentration and purity of the DNA was measured on a Nanodrop Spectrophotometer ND-1000 (Thermo Scientific, Dublin, Ireland).

### **2.2.3 Synthesis of DNA loaded PF127 formulations**

PF127 formulations (complexed with pDNA as polyplexes) were required for both 2D transfection and elution kinetic experiments. The pDNA concentration requirements are different for both sets of experiments and the construction of the specific polyplexes are described in the following sections.

#### **2.2.3.1 PF127 Hydrogel synthesis - elution kinetics experiment**

The fabrication of PF127 hydrogels loaded with plasmid DNA for the elution kinetic study was performed in the following manner. Plasmid DNA (pCMV- Luc) at a concentration of 1mg/mL was dissolved in the PF127 (20% w/v) as described in section 2.2.1, at 4°C. 300 $\mu$ l aliquots of the PF127/DNA solutions were prepared in the following pDNA ( $\mu$ g):PF127 (nmole) ratios: 1:1; 1:3 and 1:5, so that each sample hydrogel contained 0.1mg (100 $\mu$ g or 10,000 ng) of plasmid DNA. Each aliquot was delivered to pre-warmed CrownCell™ inserts (BD Biosciences, Dublin, Ireland) (to ensure immediate gelation) suitable for 24-well plates (NUNC, BD Biosciences, Dublin, Ireland)

and allowed to solidify overnight under humidified conditions at 37°C/5% CO<sub>2</sub> before being utilised in experiments.

#### **2.2.3.2 PF127 Hydrogel synthesis -2D transfection experiment**

The hydrogels for the 3D transfection study were prepared in the same manner as described in section 2.2.3.1 above, but only 100 µl aliquots were loaded with 0.2 mg of plasmid DNA.

#### **2.2.4 Stent preparation**

For this work, 3.0 x 15mm L605 Cobalt Chromium stents (Multi-link Vision™, Guidant) were coated with the leading pDNA/PF127 formulation only (i.e. a particular ratio either 1:1, 1:3 or 1:5 determined from the biophysical characterisation data). The selected Pluronic formulation, containing 100µg of dissolved plasmid DNA (eGFP prepared as described in section 2.2.2) in a 200µL volume of 20% w/v PF127, was prepared under sterile laminar flow conditions, at 4°C. The stent coating process needed to be performed over ice to keep the PF127 formulations liquid during stent coating. The coating solution was deposited in 20µl aliquots and allowed to dry in between additions. After coating, stents were stored in sterile eppendorfs at 4°C.

#### **2.2.5 Cell culture**

VERO (Green African Monkey Kidney Epithelial Cells, ATCC®, CCL-81™) cells were expanded and cultivated in T-75 flasks in Dulbecco's Modified Eagle Medium (DMEM) (Sigma Aldrich, Dublin, Ireland) supplemented with 10% (v/v) FBS (Sigma Aldrich, Dublin, Ireland) at 37°C/5% CO<sub>2</sub>, penicillin/streptomycin (5,000 U/mL) and additional L-glutamine (200 mM), sub-culturing every 2-3 days up to passage 20. Figure 2.5 below illustrates the HERA incubator used for culturing VERO cells and subsequent transfection studies.



**Figure 2.5:** HERA incubator for tissue culture and bioreactor experiments programmed to 37°C and 5% CO<sub>2</sub>. Image courtesy of Dr. Siobhan Gaughan, National Centre for Biomedical Engineering Science (NCBES).

## **2.2.6 *In vitro* transfection**

### **2.2.6.1 - 2D transfection efficiency**

Cells were seeded into NUNC 24-well plates with 13 mm diameter wells (BD Biosciences, Dublin, Ireland) with an initial density of  $1.2-1.6 \times 10^5$  cells per well, and were ready for transfection in 1 or 2 days, after reaching 70-80% confluency. Once confluency was reached, the culture medium was exchanged with serum-free medium prior to the addition of a transfection agent. Although Pluronic is well documented to successfully induce gene expression *in vivo*, it cannot transfect cells at detectable levels alone *in vitro*, rendering it very difficult to optimise Pluronic combinations *in vitro* prior to pre-clinical assessment. Therefore, in 2D *in vitro* settings, it is necessary to enhance PF127 formulations with another cationic vector carrier, such as liposomes, to establish its potential as a stand-alone vector for use *in vivo*. In this experiment, a commercially available transfection agent, Lipofectamine2000™, was used in conjunction with PF127 hydrogels to ascertain if the amplifier effect could provide a promising result *in vitro*.

Each PF127 hydrogel (1:1, 1:3 and 1:5 combinations) were synthesised to contain 2µg of DNA within the CrownCell™ insert. The

inserts containing the plasmid-loaded PF127 hydrogels were placed on top of the adherent cells of each well and incubated for 3 hours. Figure 2.6 below illustrates the experimental set-up.

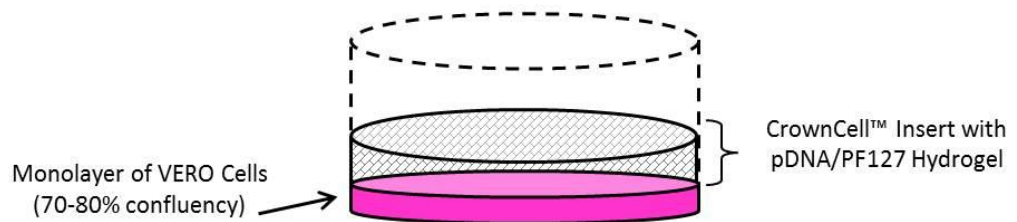


**Figure 2.6:** Schematic of a single well of a 24-well plate to illustrate pDNA/PF127 hydrogel in a CrownCell™ positioned adjacent to a Vero cell monolayer.

Thereafter, the transfection agents (the Pluronic hydrogels within the CellCrown™ inserts) were removed and the underlying cells incubated with fresh medium for 2 days. After a 24 hour incubation period the cells were washed (1x PBS) and suspended in 200 $\mu$ l of lysis buffer (RLB, Promega) and allowed to incubate at room temperature for 5-10 minutes. The cells were then subjected to one freeze-thaw cycle at -80°C. The thaw cycle was exercised on a rocker at room temperature. 40 $\mu$ l of supernatant from each sample was transferred to a black round-bottomed plate (samples are light-sensitive) and assayed for luciferase activity on a Wallac plate reader (10s Luminescence protocol). The luminescence was measured in arbitrary relative luminescence units (Alenius, Hammarlund-Udenaes, Hartvig, & Lindstrom, 2010) on an automated Wallac plate reader. Peak emission was measured at room temperature for 30 seconds. Each transfection was conducted in triplicate. ExGen200, a sterile solution of linear 22 kDa polyethyleneimine (PEI) with a N/P ratio of six, was used as a positive control for luciferase activity (measured in relative light units) and plasmid DNA was used as a negative control in this experiment.

### **2.2.6.2 - 3D transfection efficiency (stented silicone tubes)**

Sections (2 cm in length) of medical grade silicone tubing (Goodfellows Ltd, Cambridge, UK) were washed in 100% alcohol and subsequently sonicated in sterile HBSS (Sigma Aldrich, UK) for 30 minutes. Under sterile laminar flow hood conditions, the 2 cm tube sections were stoppered at one end and filled slowly (to ensure that there are no air bubbles) with a fibronectin solution (concentration 8µg/mL, Sigma Aldrich, UK) and then stoppered at the other end. The fibronectin filled silicone tubes were then incubated at 37°C/5% CO<sub>2</sub> for 90 minutes. Media was aspirated from a 90-95% confluent T75 flask of VERO cells (cultured as per section 2.2.5 containing approximately  $8.5 \times 10^7$  cells). The cell monolayer was gently washed with 10 mL of PBS, supernatant aspirated and discarded (twice), and then given a final of 10 ml wash with a D-PBS solution (PBS without Ca<sup>2+</sup>/Mg<sup>2+</sup>).

The cells were then treated with 1 mL Trypsin/EDTA solution and allowed to incubate for 5 minutes at 37°C to accelerate cell detachment. T75 flask was gently tapped to encourage complete cell detachment and the trypsinisation process neutralised with the addition of 2 mL of fresh media. The final 3 mL solution was deposited into a clean 15ml tube and pelleted in a centrifuge at 1500 rpm. The supernatant was then aspirated and the pellet resuspended in 1 ml volume of media. 10 µL was deposited on a haemocytometer (under the coverslip) to count the number of cells in the 1 mL volume (cells/mL). Approximately 400,000 VERO cells were required for each 2 cm section. The fibronectin filled tubes were then removed from the incubator and the solution discarded prior to filling the tubes with the VERO cell suspension (in a 200 µL aliquot). Figure 2.7 illustrates the tubes at this stage of preparation prior to incubation. The cell-filled tubes were incubated for 24 hours at 37°C/5% CO<sub>2</sub> to ensure cell adherence to the tube wall. After 24 hours the pDNA/ PF127 coated stents (prepared as described in 2.2.4 ), each containing 100µg of plasmid DNA,

were deployed in the cell-lined silicone tubes, filled with fresh media and returned to the HERA incubator for a further 48 hours before transfection efficiency assessment.

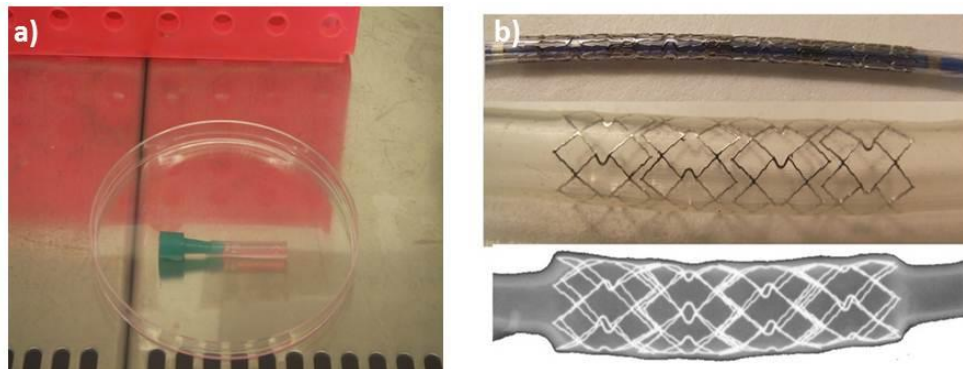


**Figure 2.7:** 3D *in vitro* transfection efficiency assessment (b) Image of an undeployed stent on its balloon catheter, below this lies a fully deployed stent in a silicone tube and an x-ray image of the deployed stent in a silicone tube.

### 2.2.7 Elution kinetic profiling

Plasmid DNA-loaded PF127 hydrogels (166  $\mu$ l volume at 1:1 ratio of pDNA to PF127) were immersed in 0.5mL of TE Buffer (10mM Tris-HCL, 1mM EDTA, pH 7.4) at 37°C. This experimental set-up is illustrated in Figure 2.8 below.

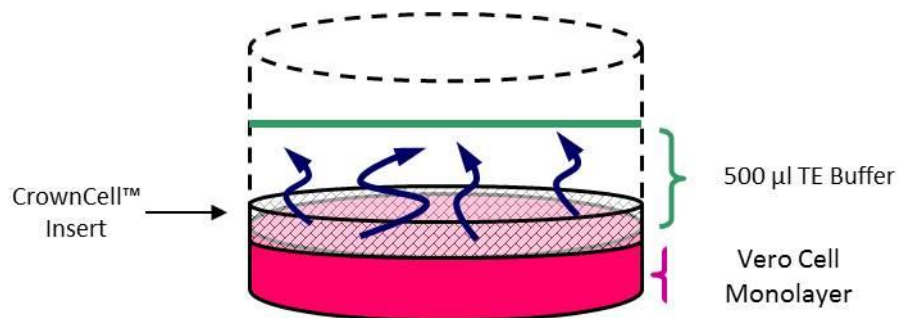


**Figure 2.8:** Schematic pDNA/PF127 hydrogel elution kinetic experimental set-up using a modified Franz cell apparatus (Förster and Konrad, 2003).

The release medium was collected and replaced with fresh medium at specified time-points (20, 40, 60 minutes, 4, 8, 12, 24 hours, 2-14 days). After careful removal of the debris and other impurities, the amount of DNA eluted was determined by PicoGreen™ dsDNA Quantitation assay (Molecular Probes, Invitrogen Corp., Oregon, USA) according to the

manufacturer's instructions. Released DNA in the release medium and the working reagent of PicoGreen assay kit (1:1 v/v) were thoroughly mixed and incubated at room temperature for 5 minutes. Fluorescence of the sample was measured at an excitation wavelength of 488nm and an emission wavelength of 530nm (Molecular Probes, Invitrogen Corp., Oregon, USA). The gel was subsequently analysed for retained plasmid DNA using an adaptation of a protocol used to remove Ethidium Bromide (EtBr) from DNA gels (Maniatis, 2012). A 200 µl volume of 1-butanol saturated with Isoamyl alcohol was added to the residual PF127 /pDNA gel and the resultant solution was centrifuged at 1500 RPM/3minutes at room temperature. Using a Pasteur pipette, the lower aqueous phase was transferred to a clean eppendorf and the procedure repeated another 3 times. PF127 was removed from the aqueous pDNA solution by diluting with three times the volume of water and the DNA precipitated by adding 400 µl of ethanol for 15 minutes at 4°C. The solution was then centrifuged at 10,000g for 15minutes/4°C and the resultant DNA precipitate dissolved in 1mL of TE buffer prior to measuring the concentration on a spectrophotometer.

### **2.2.8 Differential Scanning Calorimetry (DSC)**

Differential Scanning Calorimetry was performed on a DSC-60 (TA instruments, Shimadzu, Japan) with thermal analysis software TA-60WS (TA instruments, Shimadzu, Japan). The scanning rate was set at 1°C/min. This heating rate was selected as a compromise between the need for a condition close to the equilibrium and an acceptable signal/disturbance ratio. The signals were recorded, and after a properly designed baseline subtraction procedure, were used to localise the micellisation phenomenon. Spectra were obtained for three samples for each condition on the heating and cooling cycle with an empty pan as reference. The 20µl volume samples were placed in aluminium pans, and subsequently crimped and hermetically sealed. The following thermal history was performed:

heating at 1°C/min from -75°C to 140°C, followed by a 140°C for 10 minutes before cooling sample to ambient room temperature.

### 2.2.9 Transmission Electron Microscopy (TEM)

TEM allows real-time imaging of objects at a nanometer scale. TEM sample preparation and image acquisition procedures followed those described previously (Horcas *et al.*, 2007). 5 µl aliquots of the sample solutions (pDNA/PF127 at a concentration of 1mg/mL) were applied to carbon-coated Formvar 200 copper grids; the excess was blotted away with filter paper and allowed to stand for 15-30s. The samples were negatively stained with 2% (w/v) uranyl acetate and allowed to dry. Specimens were maintained at a temperature of 37°C and observed under an H-7600 transmission electron microscope (Hitachi, Japan) operating at 75kV and at a nominal magnification of 50,000 x under low dose conditions. Images were recorded with a 2K x 2K Gatan slow scan CCD camera. All samples were performed in triplicate. Figure 2.9 below displays the TEM used in these experiments.



**Figure 2.9:** Hitachi Transmission Electron Microscope. Image courtesy of Dr. Eadaoin Timmins, National Centre for Biomedical Engineering Science (NCBES), National University of Ireland, Galway.

### 2.2.10 FTIR Spectroscopy

Fourier Transform InfraRed (FTIR) spectroscopy was conducted on both plasmid DNA (pCMV-eGFP) samples and pDNA complexed with Pluronic. FT-IR spectra were obtained with a FTIR-8300 (Shimadzu, UK) equipped with a mercury-cadmium-telluride detector using a diamond

attenuated total reflectance (ATR) method. Figure 2.10 below illustrates the FT-IR 8300 used for these experiments. Spectra were obtained under dry air purge by co-addition of 256 interferograms which were then apodised using the Happ-Genzel function, with no zero filling to give a resolution of  $4\text{cm}^{-1}$ . The association band of water at  $2200\text{ cm}^{-1}$  was used as a reference for subtraction of water. Baseline corrections ( $1804\text{-}904\text{ cm}^{-1}$ ) and seven-point Savitsky-Golay smoothing were applied to the spectra. Peak positions were assigned by an algorithm in AIMView software.



**Figure 2.10:** FT-IR 8300. Image courtesy of Dr. Eadaoin Timmins, National Centre for Biomedical Engineering Science (NCBES), National University of Ireland, Galway.

### 2.2.11 Dynamic Light Scattering (DLS)

Particle sizing was performed using a Malvern Spectrophotometer Autosizer 4800 (Malvern Instruments Ltd, Worcestershire, UK) equipped with a Uniphase 75 mW Argon laser operating at 488 nm with vertically polarized light. Prior to measurement, each pDNA/Pluronic® F127 formulation was diluted with 50 mL distilled water. This dilution ensured that the pDNA was dispersed homogeneously. For each run, each time correlation function was obtained by a digital auto-correlator PCS7132 from Malvern Instruments. The autocorrelation function was analysed using the methods of cumulants (Koppel, 1972), and the resultant mean translation diffusion co-efficients were converted to mean hydrodynamic radii by the Stokes-Einstein equation. Each sample was measured three times with the mean and standard deviation reported.

### **2.2.12 Zeta Potential – Surface Charge Analysis**

The zeta potential surface charge of pDNA/PF127 samples was assessed using a Zetasizer 3000HSA apparatus with Horiba LA-920 software (Malvern Instruments Ltd, Worcestershire, UK). The zeta potential measurement based on laser Doppler Interferometry was used to assess the electrophoretic mobility of DNA, either naked or complexed with Pluronic in different ratios (1:1, 1:3 and 1:5). Measurements were performed for 20 seconds using a standard capillary electrophoresis cell with zero field correction, a dielectric constant of 79 and the Helmholtz Smoluchowsky equation to convert measurements into zeta potential values. All experiments were performed in triplicate and conducted at 37°C.

### **2.2.13 Statistical Analysis**

The data, presented as means and standard deviation, were calculated over at least three independent experiments. Significant differences between any two groups were evaluated by Student's t-test with  $p < 0.05$ .

## **2.3 Results**

### **2.3.1 Physical characterisation – DSC**

The thermal history, consisting of a complete heating and subsequent cooling cycle of PF127, is depicted in Figure 2.11. The thermogram graph clearly exhibits a small endothermic peak at 1.3°C, confirming the temperature at which unimers begin to form. The micellisation transition temperature occurs at 8.9°C. This is a first order endothermic phenomenon which indicates the energy required for this particular concentration of PF127 (20% w/v) to begin to aggregate polymer unimers into micelles, commonly referred to as the self-assembly process. The onset of micellisation can be observed at approximately 12°C and thereafter a plateau of activity is noted in which gelation and close micellar

packing continues to occur, consistent with what an increase in temperature should generate for a block copolymer. At approximately 57.12°C, a second order endothermic peak is detected (extracted panel - Figure 2.11) and associated with the glass transition ( $T_{\text{glass}}$ ) and relaxation events which occur in the amorphous section of the block copolymer (i.e. the PPO block). The thermogram also exhibits the characteristic peak of water evaporation at 100°C, another endothermic reaction requiring significant energy or heat-flow (mW) to occur. On the cooling cycle, the PF127 illustrated a relatively large exothermic peak at 35.5°C, illustrating the temperature at which unimers begin to form, approximately 8°C below the  $T_m$ . The onset of micellisation can be calculated from the area between the  $T_m$  and the  $T_{\text{glass}}$  at approximately 12°C.

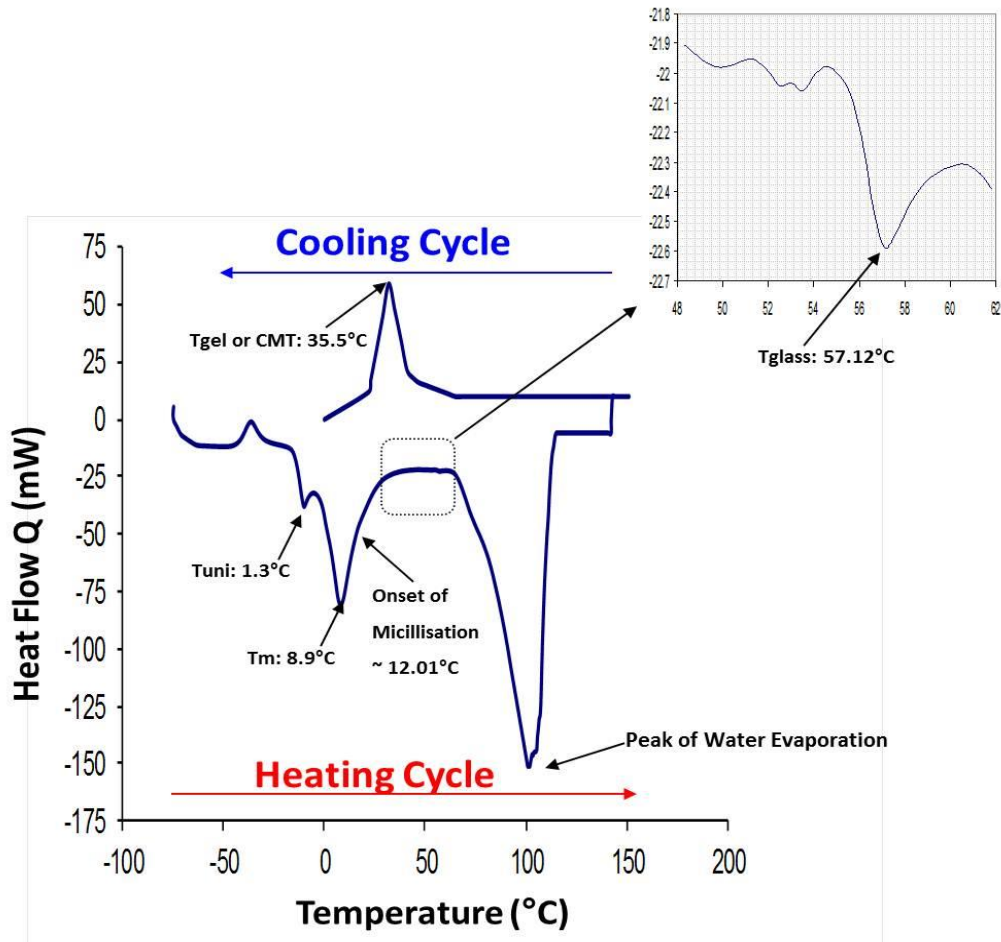


**Figure 2.11:** DSC thermogram of PF127 (20% w/v), recording thermal history (Heat Flow Q in mW) endothermic and exothermic phenomena through one entire heating/cooling cycle.

This result is in agreement with previous calorimetry studies of unmodified Pluronics (Miles, 1994), which demonstrated that the broad peak at low temperatures is due to micellisation while the peak at higher temperatures, only observed in higher concentrations, corresponds to gelation, an athermal process. In the cooling phase, an exothermic peak is detected at approximately 35°C which is consistent with the melting temperature T<sub>m</sub>, or gel-liquid crystal transition temperature of the crystalline PEO parts of the polymer. Figure 2.11 acts as baseline fingerprint of thermal activity of an unloaded vector.

Further DSC profiles are depicted in Figure 2.12 below which clearly illustrates the changes which occur when 3 different concentrations (Low =

0.5 mg/mL, Medium = 1.0 mg/mL and High = 2.0 mg/mL) of plasmid DNA are complexed with PF127.

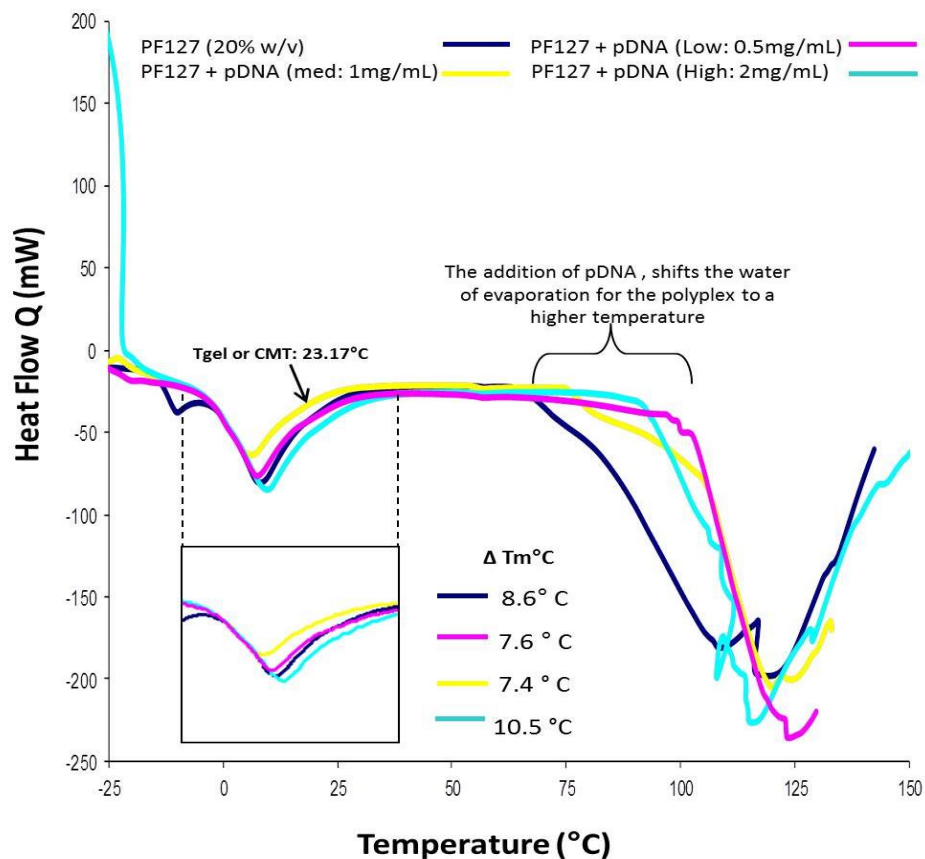


**Figure 2.12:** DSC thermograms of PF127 polyplexes recording the thermal history of PF127 alone and loaded with pDNA at three different concentrations (0.5 mg/mL, 1 mg/mL and 2 mg/mL).

The most significant change is the shift of the peak of water evaporation to a higher temperature of the polyplexes (Pluronic complexed with pDNA) in comparison to an uncomplexed or unloaded Pluronic. In other words, the plateau area is extended with the addition of plasmid DNA (all three concentrations) indicating that the biological macromolecule complexes very strongly with the block copolymer, making it more difficult to break and requiring more energy to release the water in the latent heat of vaporisation phase. Figure 2.12 also shows that the micellisation temperatures of the polyplexes are affected. The unloaded PF127 sample in Figure 2.12 begins to form micelles at approximately 8.6°C.

PF127 Formulations	Unimer Formation (°C)	Tgel or CMT (°C)	Onset of Micellisation ( $\Delta J/g$ )
PF127 alone (20% w/v) Alexandridis <i>et al.</i> , 1994	1.9 ± 0.36	20.6 ± 1.6	10.6 ± 0.6
PF127 alone (20% w/v) Figure 2.11	1.3	35.5	12.01
PF127 alone (20% w/v) + 1 mg/mL pDNA Figure 2.12	0.33	23.17	7.4

**Table 2.1:** Comparison of experimental data with previously published DSC measurements of PF127 (Alexandridis *et al.*, 1994).

The thermogram graph then shows that the addition of both low (0.5mg/mL) and medium (1.0 mg/mL) concentrations of pDNA causes the micellisation temperature to decrease to 7.4°C and 7.6°C respectively. Conversely, by increasing the pDNA payload to a higher concentration (2.0 mg/mL) it causes the micellisation temperature to increase to 10.5°C. This result would indicate that there is an optimal binding ratio of pDNA to polymer to produce polyplexes. It would be reasonable to assume that an overload of pDNA makes it more difficult for the block copolymer to self-assemble and also results in the presence of unencapsulated plasmid DNA, which is not a therapeutically desirable option. Further data is presented in Table 2.1 below, illustrating that the addition of plasmid DNA (at a 1mg/mL concentration) reduces the temperature at which unimer formation occurs and also reduces the temperature at which micellisation or self-assembly occurs. The data generated during this study is consistent with previously published work (Alexandridis *et al.*, 1994).

### 2.3.2 Chemical characterisation – FTIR

Figure 2.13 illustrates the FTIR absorbance spectrum of plasmid DNA, i.e. free-state, uncomplexed pDNA. This absorbance spectral fingerprint is consistent with data other investigators have previously reported in the literature (values in brackets on Figure 2.13) (Banyay, Sarkar, & Graslund, 2003) and illustrates the characteristic IR bands of

hydroxyl groups and phosphate groups at  $3280\text{ cm}^{-1}$  and  $1240\text{ cm}^{-1}$  respectively.

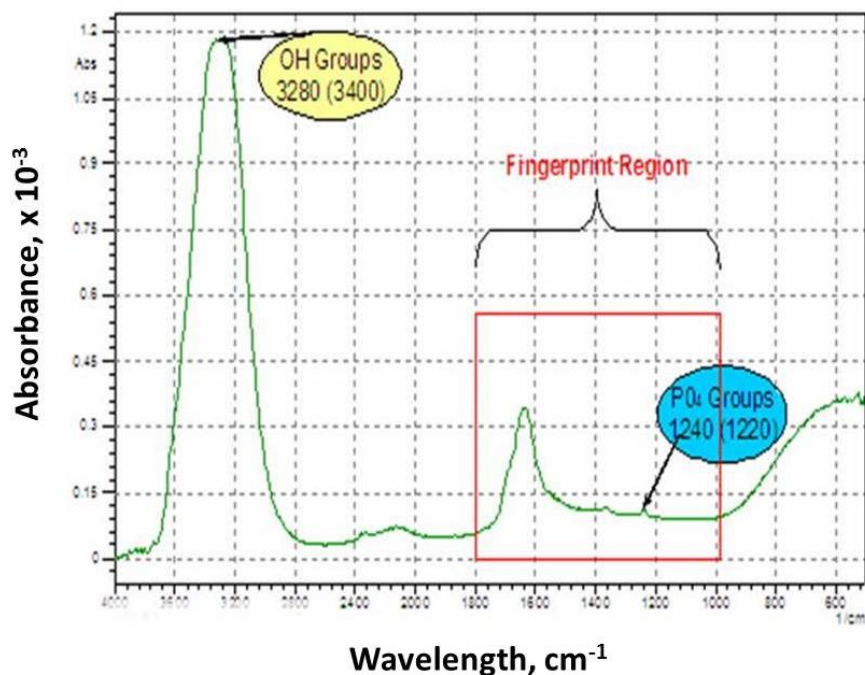


**Figure 2.13:** FTIR absorbance spectral data. Graph illustrates the characteristics IR bands of plasmid DNA with the data from the literature (in brackets). Banyay *et al*, Journal of Biophysical Chemistry, 2003.

From the previous DSC analysis, a plasmid DNA payload of 1.0mg/mL was selected for the FTIR analysis to assess the chemical changes that occur when plasmid DNA is complexed with PF127. Figure 2.14 depicts the absorbance spectra of PF127 (green line), plasmid DNA alone (grey line) and plasmid DNA complexed with PF127 (pink line). The carbon (C-O-C) stretching band double bond at  $1078\text{ cm}^{-1}$  is a characteristic absorbance band for PF127 which broadens significantly when complexed with the plasmid DNA, confirming that hydrogen bonding occurs between the delta negative phosphate backbone of plasmid DNA and the delta positive hydrated corona of the PF127 micelle. The DNA fingerprint region highlighted in the plot is the area of interest in this experiment, this fingerprint region chemically represents the phosphate backbone of the DNA molecule. When pDNA is complexed with the Pluronic, chemical

changes are expected to occur in this region if the Pluronic can successfully encapsulate the DNA.

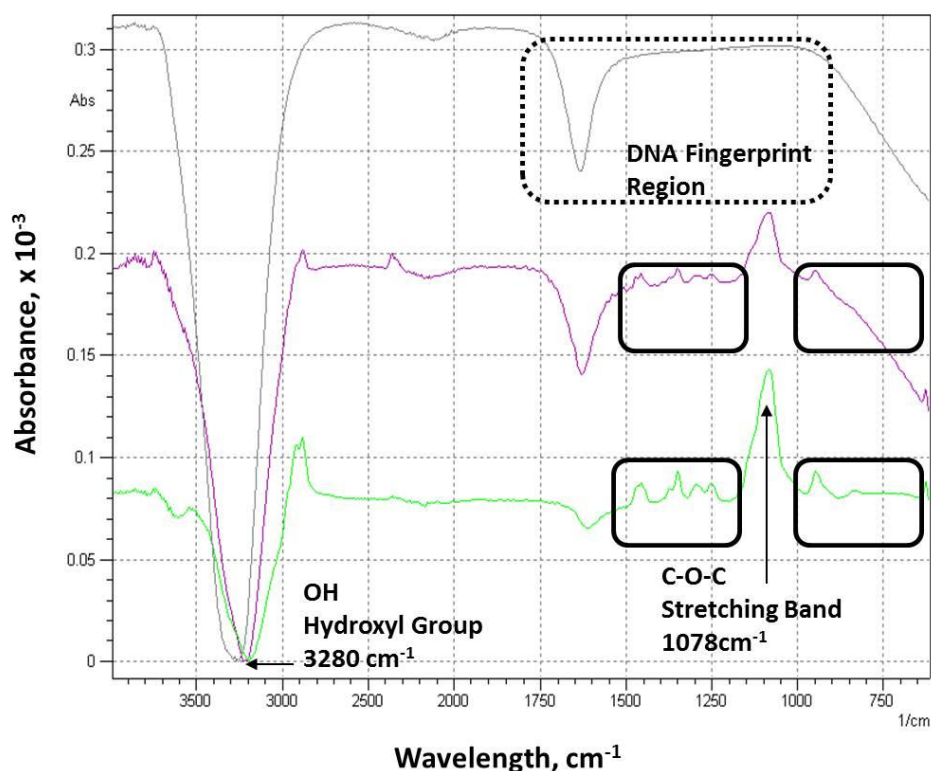


**Figure 2.14:** FTIR analysis of pDNA alone 1 mg/mL (grey line), PF127 alone - 20% w/v (purple line) and the pDNA/PF127 polyplex (green line).

### 2.3.3 Charge Analysis – Zeta Potential

The charge analysis of the outer membrane of polyplexes of varying pDNA:PF127 ratios: 1:1; 1:3 and 1:5 (each formulation with an overall pDNA concentration of 1mg/mL) is illustrated in Figure 2.15. Zeta potential experiments are always preceded with a calibration solution to ensure that the electrophoresis cell can detect both positively charged and negatively charged particles simultaneously (Figure 2.15 (a)). Plasmid DNA in its free uncomplexed form is more commonly referred to as “b-form” plasmid DNA. This particular form supercoils into a figure eight configuration to expose the negative portions of its backbone. These exposed portions are more commonly referred to as the delta negative portions of DNA. As expected, plasmid DNA alone (aqua blue line) registers only a negative population peak, consistent with the exposed delta negative surface of

free-state, uncomplexed plasmid DNA. When plasmid DNA is complexed with a polymer, it is expected that the delta negative portion interacts with the positively charged parts (i.e. PPO blocks) of the Pluronic, thus complexing with the plasmid DNA to form smaller, neutrally charged particles.

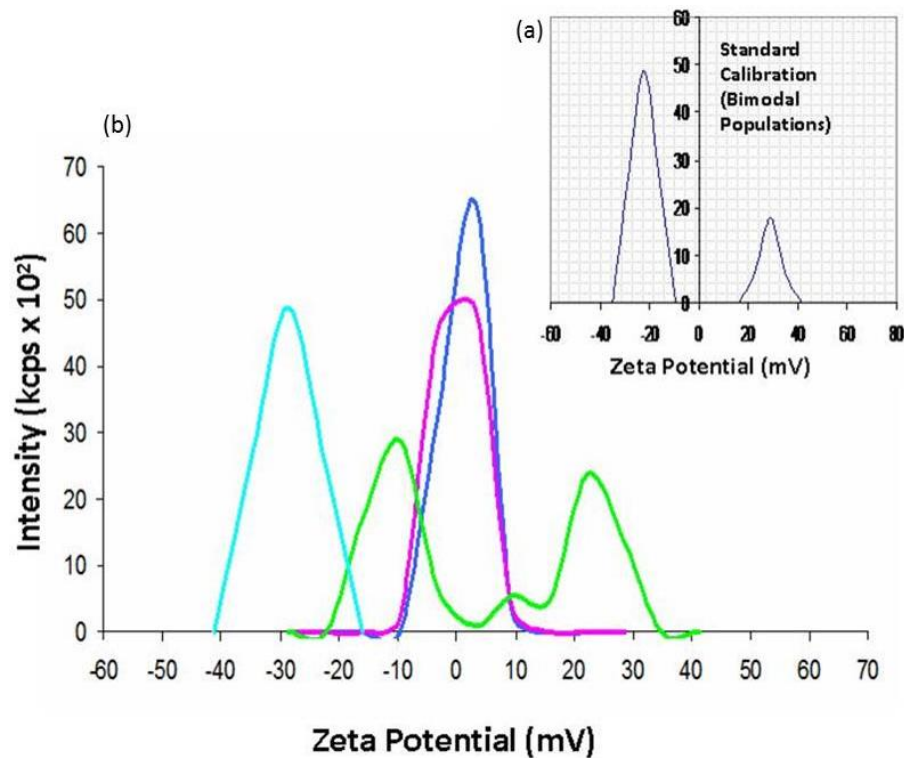


**Figure 2.15:** Zeta-size charge analysis (mV) of pDNA alone and PDNA/PF127 polyplexes. (a) Standard calibration (b) Zeta potential measurements of pDNA alone (light blue), pDNA/PF127 polyplexes 1:1 (dark blue line), 1:3 (pink line) and 1:5 (green line).

The results in Figure 2.15 illustrate that when Pluronic is complexed with plasmid DNA in 1:1 and 1:3 ratios, a neutralized population peak is detected. This indicates the complete encapsulation of the plasmid DNA by the Pluronic. However, when the Pluronic component is increased to 5 parts, 1:5 formulation, the significant neutral populations detected with the other two formulations are not evident and two distinctive negatively and positively charged populations exist. This would indicate that there are both free delta negative plasmid DNA particles and Pluronic micelles with an exposed hydrophobic, positively charged surface present in the 1:5

formulation. Reviewing the profiles of all three formulations would indicate that there is complexation equilibrium phenomenon governed by the availability of delta negative head groups of the plasmid DNA.

### **2.3.4 Morphological characterisation – DLS, TEM**

DLS particle size measurements and population distribution histograms of all pDNA:PF127 ratios: 1:1; 1:3 and 1:5 are presented in Figure 2.16. The most homogeneous population distribution is the 1:1 formulation (Figure 2.16 (a)) with a dominant 34.9% of the sample population with a particle size of approximately 120nm (119.9nm) and a combined 89.3% of the sample with a particle size between 75.6 and 150.9 nm. The 1:3 ratio (Figure 2.16 (b)) presents a dominant sub-population (51.5%) with a mean particle size of 2.2 nm but has a combined 45.8% of the sample population of particles ranging in size between 78.3 – 95.2 nm. The sub-population is significant as several investigators have shown the hydrodynamic diameter of Pluronic unimers within a range of 20-25 Angstrom, or 2-2.5 nm, depending on the Pluronic formulation (Foster *et al.*, 2008, Alexander *et al.*, 2012). These recent findings corroborate observations from a review paper published by Alexandriadis and colleagues in 1995. In this review paper, the investigators collated the results of 22 studies (both light- and neutron-scattering) across a range of Pluronics, including PF127. All the studies illustrated that Pluronic unimers exhibited a hydrodynamic diameter of approximately 1nm and micellar Pluronics measured in at approximately 10nm, irrespective of their concentration.

Figure 2.16 (c) depicts the most inhomogenous sample (1:5 formulation) with the dominant population consisting of particles with a mean diameter of 1.2 nm. There was a negligible population (<1%) of a particle size consistent with nano-sized particles (70-150 nm) capable of being endocytosed across the cellular membrane. Most significantly

though in the 1:5 formulation is the presence of a population of particles measuring between 900 and 1500 nm in diameter, representing 15.1% of the population.

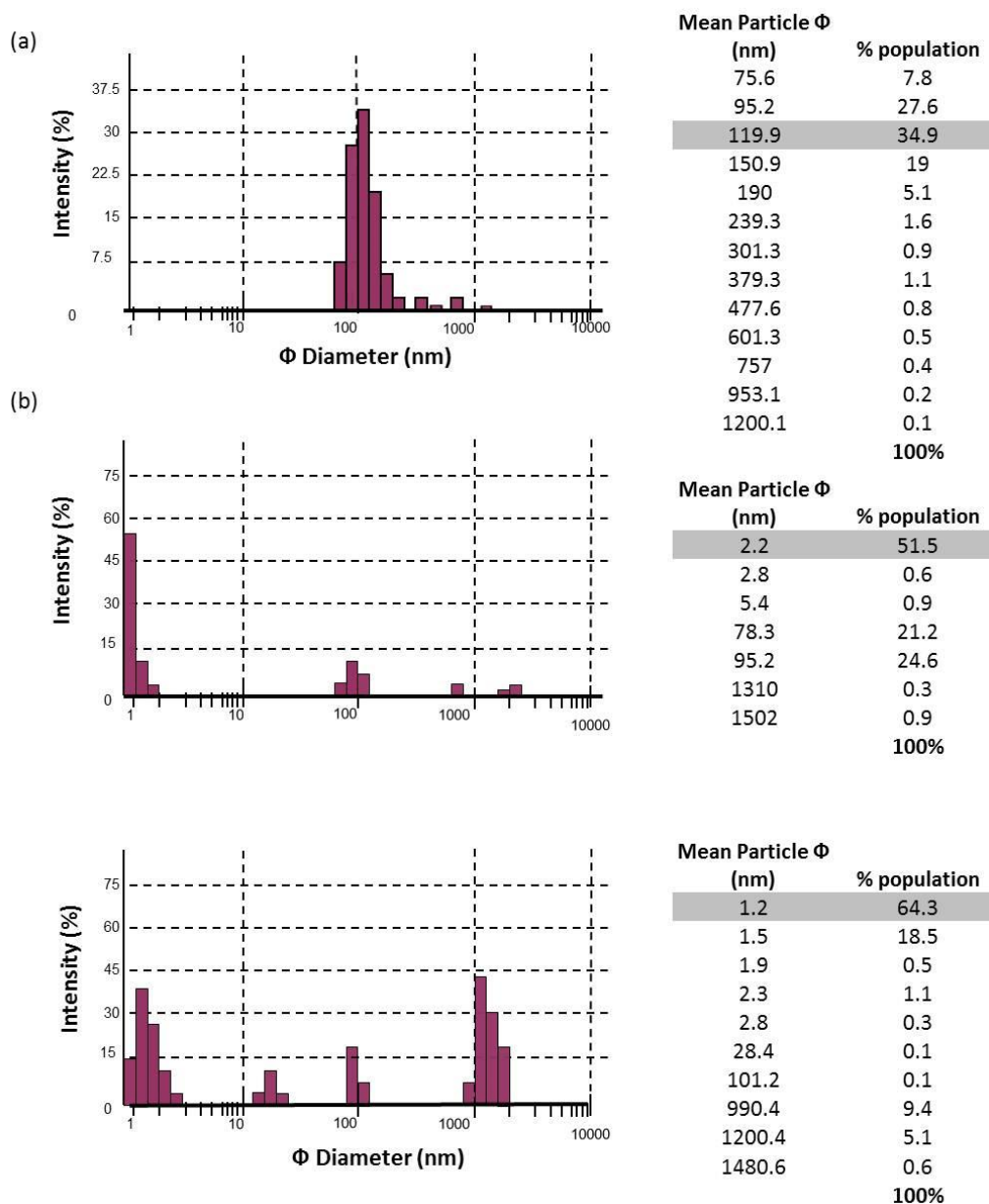


**Figure 2.16:** Size distribution of PF127 polyplexes in volume in histograms by Dynamic Light Scattering (DLS) (a) 1:1 (b) 1:3 and (c) 1:5. Grey fill indicates weighted dominant particle size.  $\Phi$  denotes diameter.

TEM was conducted on each of the three pluronic formulations (1:1, 1:3 and 1:5). The images produced by the TEM were of poor quality due to the viscous nature of the polymer formulations and the difficulty for

the electron beam to penetrate the substance. However, the TEM has the capability to detect the outer boundary of particles and the software can be used to measure the polyplex diameters *in situ*. Selected representative images of these TEM investigations are given in the appendices and serve to validate the presence of polyplex particles in all three formulations. The selected TEM particle measurements correlate well with the mean diameter population distributions determined by the DLS examinations (Figure 2.16). Formulations 1:1 and 1:3 produced polyplex particles with diameter measurements (70-150nm) consistent with what is documented in the literature for similar polyplexes (Koping-Hoggard, Mel'nikova, Varum, Lindman, & Artursson, 2003), (Dhanoya, Chain, & Keshavarz-Moore, 2011) and (S. Zhang, Prud'homme, & Link, 2011). The 1:5 formulation illustrates significantly lower diameter measurements (one of the largest particles detected registered at 39.5nm).

It is important to comment at this point that it was very difficult to coat the stent with the pluronic formulation (section 2.2.4). The gelatinous coating could be sheared off the stent substrate very easily and great care was required during preparation and storage of the stents, prior to deployment in the 3D cell-lined silicone tubes.

### **2.3.5 Elution kinetics**

The results presented in Figure 2.17 (a) depicts the elution profile of plasmid DNA released over a 14 day time period from PF127 hydrogels under physiological conditions (37°C/5% CO<sub>2</sub>). The graph illustrates a characteristic burst release followed by a plateau for the remainder of the experiment.

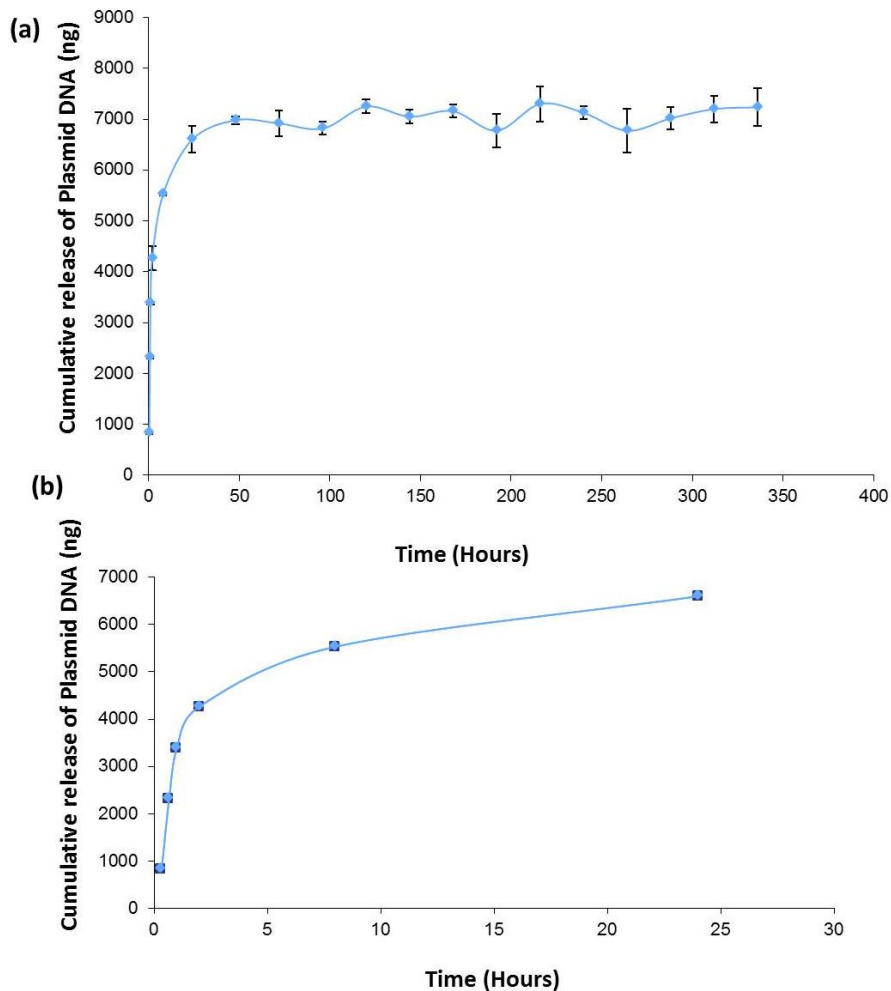


**Figure 2.17:** Polyplex elution kinetic profiles: (a) 14 day - cumulative DNA release from PF127 (20% w/v) hydrogels in 10 mM Tris-EDTA Buffer (pH 7.4). (b) 24 hour burst profile. Hydrogels were cured for 24 hours at 37°C before addition of buffer. DNA was quantified using PicoGreen assay. Each point represents average  $\pm$  standard deviation (n =3).

Approximately 72% of the initial payload (1mg/mL) was eluted over 14 days. Figure 2.17 (b) further illustrates the burst effect and the confirmation that the majority of the plasmid DNA was eluted in the first 72 hours. This is validated by the fact that almost 12% ( $11.42 \pm 0.57\mu\text{g}$ ) of the original plasmid DNA payload was detected in the residual hydrogels after the 14-day time course experiment. The presence of this residual plasmid DNA in the hydrogels confirms the theoretical assumption that the concentration gradient is required in order for diffusion to occur.

Thus, the collective plasmid DNA detected in the experimental data shown in Figure 2.17 accounts for almost 85% of the initial plasmid DNA payload. This is considered an acceptable capture if there is a +/-5% error built into both the DNA elution profile experiment (~72% of plasmid DNA payload) and the residual DNA detection test (~12%).

### **2.3.6 Transfection efficiency – 2D and 3D**

As described in section 2.2.6.1, Pluronic alone *in vitro* cannot transfect cells efficiently and therefore it is important that the amplification effect of introducing an adjunct transfection agent is taken into account when interpreting the transfection efficiency results. As graphically illustrated in Figure 2.18, negligible levels of gene expression were detected with the luciferase assay across all three plasmid DNA/Pluronic formulations (1:1; 1:3 and 1:5) when PF127 was used alone, < 3%. The relative luminescence units (Alenius *et al.*, 2010) were amplified significantly (36%, 29% and 24% respectively) when used in conjunction with Lipofectamine 2000™, a commonly used transfection agent used to amplify the transfection efficiency so that it is more representative of what the formulation would be capable of transducing *in vivo* (Gebhart *et al.*, 2002).

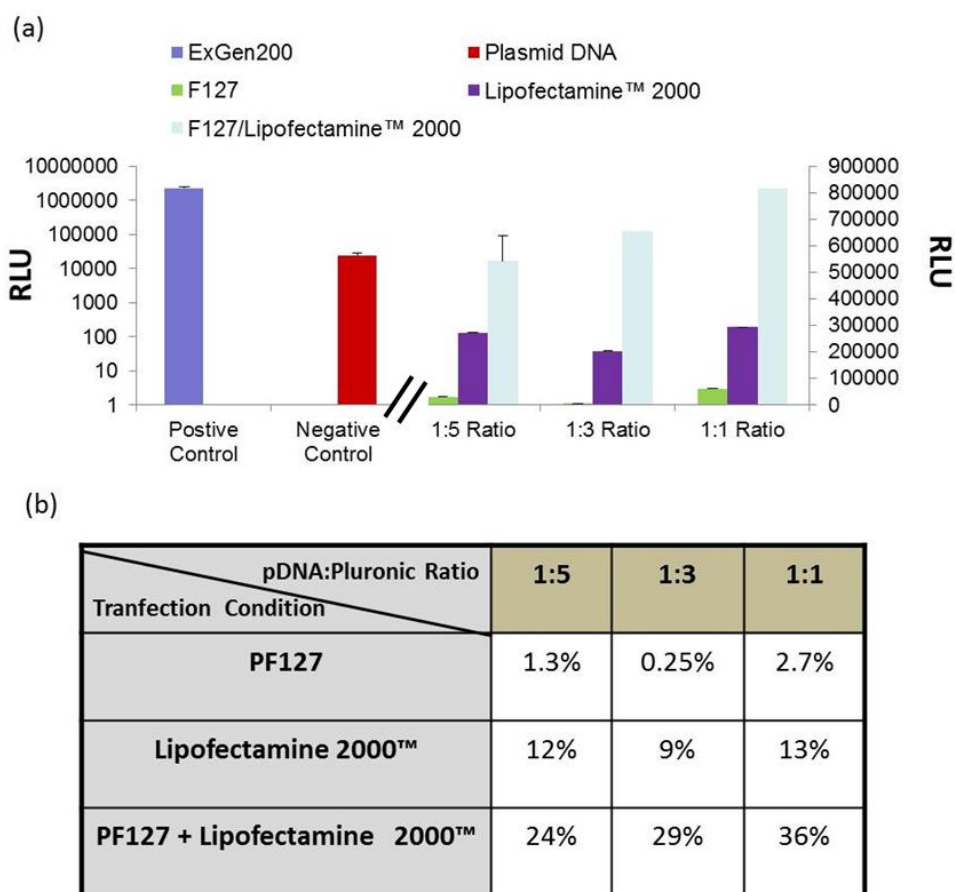


**Figure 2.18:** Luciferase expression - Vero cells with PF127 alone, Lipofectamine 2000™ alone and PF127 enhanced with Lipofectamine 2000™ post 48 hour exposure (a) GFP expressing cells with PF127 20% (w/v) in 1:5, 1:3 and 1:1 Transfection agent:pDNA ratios respectively, (b) Table illustrating comparative percentage expression across the transfection conditions in 2D static *in vitro* culture conditions.

However, even with the amplification, the expression levels were still weak and not statistically significant or comparable to the experiment's positive control (ExGen200 compound – a commonly used liposomal formulation for transfection efficiency experiments across a broad range of cell lines). As expected the results presented in Figure 2.18 for the 2D *in vitro* assessment of PF127 were difficult to reliably quantify or predict Pluronic's true transfection capability. To fully explore this limitation, a preliminary investigation of assessing transfection efficiency in a 3D *in vitro* environment was also conducted. The purpose of this experiment was to determine if there was any significant advantage in examining the

transfection capability of the PF127 (coated onto a stent) in a 3D *in vitro* environment as part of the screening process.

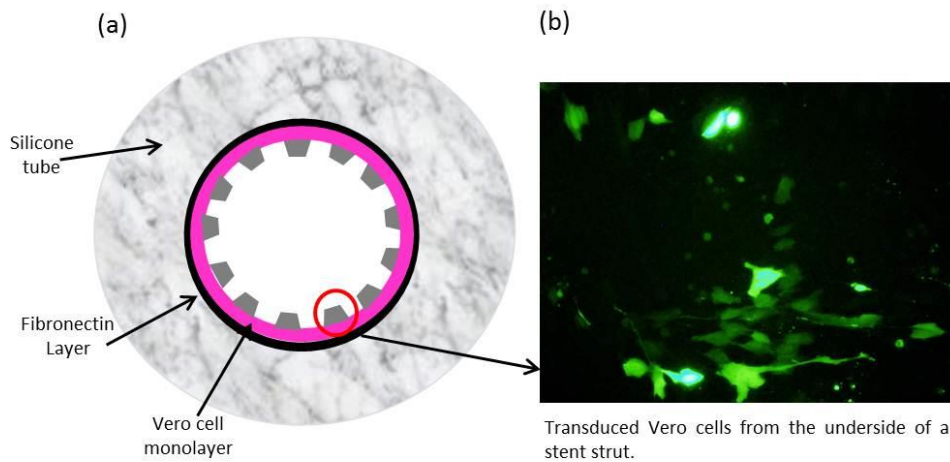


**Figure 2.19:** 3D *in vitro* experimental set-up. (b) eGFP expressing Vero cells imaged on the inside of a silicone tube post stent deployment *in situ* for 36 hours in 3D *in vitro* static culture conditions with PF127 alone.

Figure 2.19 (a) illustrates how the stent is deployed in a 3D system with the struts aligned with the Vero cell monolayer adhered to the inner lumen of a silicone tube. Figure 2.19 (b) clearly illustrates significant gene expression (green cells) along the underside of the vessel (36 hours post transduction) without the use of any additional agent, i.e. Lipofectamine 2000™, unlike the 2D *in vitro* system results presented in Figure 2.18.

## 2.4 Discussion

To maximise the ability of any delivery vehicle vector to deliver a therapeutic gene *in vivo*, it is highly desirable to characterise the vector, as comprehensively as possible *in vitro*, prior to assessment in a pre-clinical model. This characterisation ought to include evaluating the potential vector's inherent biophysical properties when plasmid DNA is introduced, its elution kinetics and its transfection capabilities. With DES, the elution kinetics of a pharmacological agent out of the "carrier" and the mechanism of action by which the agent is taken up by the cell is a vitally important aspect in its design. The same principles apply in the development of a

potential GES platform. This type of characterisation methodology enables vector optimisation to occur in both a time- and cost-effective manner.

One of the critical aspects investigated in this chapter was the mechanism by which plasmid DNA complexes with PF127. To this end, it was important to establish the most therapeutically relevant plasmid DNA concentration loading and to determine the volume ratio of plasmid DNA to PF127 that can ensure the most efficient transfection *in vitro*. A step-wise approach, through physical, chemical and morphological characterisation, was employed to determine which component combination produced the most optimal polyplex. These characterisation techniques enabled all relevant aspects of the polyplex to be investigated prior to selecting a leading polyplex for evaluation in the elution kinetic and transfection efficiency experiments.

Firstly, the most optimal plasmid DNA concentration to induce the best transfection results was established and whether or not a dosing concentration effect occurs was also examined. To this end, 3 concentrations (0.5mg/mL, 1mg/mL and 2mg/mL) of plasmid DNA were selected to be thermally examined by DSC. The subsequent results illustrated that both 0.5mg/mL and 1mg/mL concentration marginally decreased the temperature at which micellisation thus enabling complexation or “binding” with the plasmid to occur more efficiently. At the higher concentration (2mg/mL), the results illustrated an increase in micellisation temperature, making it more difficult for the polymer to self-assemble and form a gelatinous substrate, necessary for a stent platform coating. Upon consideration, the 1mg/mL concentration was selected to be used in the remainder of the experiments, and this also aligns with the concentration most widely used in other gene therapy transfection efficiency experiments (Cherng *et al*, 1996, Fischer *et al*, 1999, Mao *et al*, 2001 and Kunath *et al*, 2003). The 1 mg/mL payload of plasmid DNA was

then evaluated to ascertain the chemical changes that occur when it binds with the 20% w/v PF127 that confirms that efficient binding occurs. This was illustrated sufficiently through FTIR analysis presented in Figure 2.14 and validated that the 1mg/mL plasmid DNA dose complexes with the 20% w/v PF127.

At a morphological level, the size of polyplex particles produced has a direct impact on how they will be endocytosed and ultimately on their transfection efficiency capabilities. The experiments reported in this chapter (both DLS and TEM) have shown that plasmid DNA successfully complexes with PF127 to form polyplex particles at a nanoscale range (70-150 nm), suitable for endocytosis by a cell membrane. In addition, the volume ratio at which the PF127 complexes with plasmid DNA affects the both the size and charge of the polyplex particles, which in turn plays an important role in determining the level of cellular and tissue uptake. This study illustrated that a 1:1 ratio produced a greater proportion (89.3%) of the most suitably sized nanoparticles for endocytosis than the 1:3 formulation (45.8% nanoparticles) and 1:5 formulation (< 1% of the population was of a nano-scale size). This nano-particle sizing in agreement with other investigators that nano-particles (approximately 100nm) have a greater uptake (2.5 fold greater) than their micro-particle ( $\mu\text{m}$ ) counterparts (Desai *et al.*, 1997), (Kreuter *et al.*, 2003) and (Roque *et al.*, 2008). In addition to particle size, the surface charge of nanoparticles plays a pivotal role in cellular uptake and subsequent gene expression (Couvreur, Barratt, Fattal, Legrand, & Vauthier, 2002). It has been documented that the more positively charged a nano-particle is, preferably more than 30mV, the greater its transfection efficiency (Govender, Jacobs, Bredenkamp, & Swart, 2005).

The biophysical characterisation experiments in this chapter indicated that the 1:1 polyplex formulation should perform the best *in*

*vitro* as it had the most optimal characteristics of all three formulations with the highest proportion (81.5%) of nanoparticles suitable for cellular endocytosis (90-150 nm) as confirmed by DLS and TEM. The binding capabilities of different concentrations of plasmid DNA, to ascertain if a dosing plateau existed, was also examined. This experiment confirmed that plasmid DNA payloads, greater than 1 mg/mL, had a negative impact of micellisation temperatures, thus affecting their binding capabilities.

These results validated that the 1:1 formulation produced the most positively charged polyplex (greater than 30mV across the most dominant particle population), with a mean diameter of 199.9 nm across the dominant sub-population. Thus it is expected that this formulation would perform the best *in vitro*. To this end the experimental results presented above (DSC, FTIR, TEM, DLS,  $\zeta$  potential) have addressed the first two objectives outlined at the beginning of the chapter.

However, modulating polyplex formulations to produce nanoparticles to have the most optimal surface charge and mean diameter so that they can be theoretically endocytosed by the cellular membrane is only one part of transduction success. The elution kinetics of plasmid DNA out of a polymeric carrier also governs its capability to be an efficacious vector. Drug elution kinetic profiles are primarily governed by diffusion mechanisms and this can be modulated by the drug molecule size and charge, concentration of the drug on the stent and dissociation constants. However, the mechanisms which govern gene elution kinetics are not as well understood as their drug counterparts. In the work presented here, the objective to characterise and profile PF127 formulations was executed successfully. However, the true value of this information, from a vector screening perspective, is yet to be determined. Figure 2.17 clearly illustrated an initial burst driven by a concentration gradient. It was established that the majority of the plasmid DNA payload (1 mg/mL) eluted

during this phase. If this was a drug, it would be expected that this payload would be metabolised within the first 72 hours, however this cannot be extrapolated for a gene product, i.e. that the plasmid DNA eluted out of the polymer is transduced into the target cells and illustrates transfection efficiency *in vitro* within the first 72 hours. The elution kinetic experiment itself was a difficult one to set up, the 14 day profiling was time consuming and the experiment required significant trouble-shooting before meaningful results could be obtained. What can be deduced is that the 14 day timeframe is unduly lengthy considering the burst profile exhibited in the first three days and so for future profiling a reduced timeframe will be employed (Chapter 3). This work addressed the third objective of this chapter.

As previously discussed, Pluronics have been extensively investigated as vehicles for gene delivery and have exhibited enhanced expression of naked plasmid DNA in skeletal muscle, cardiac muscle skin and in tumours (Richard *et al.*, 2005), (J. P. Yang & Huang, 1997), Gebhart (Gebhart *et al.*, 2002), (Lemieux *et al.*, 2001), (Pitard *et al.*, 2004) and (Liaw *et al.*, 2002) at relatively high levels for a non-viral modality. The grafting of PEO-containing block copolymers onto liposome surfaces has resulted in improving their survival in the circulating blood stream, therefore affording them “stealth” characteristic that protects them from immunogenic attack and making them an ideal candidate for drug delivery vehicles (Lasic & Papahadjopoulos, 1995). However, difficulty has always resided with the fact that Pluronics alone do not enhance gene transfer *in vitro*. This study also illustrated this when the 2D *in vitro* system only showed negligible transfection *in vitro* (<3% across all formulations). Several previously conducted studies have shown that an adjunct, such as a cationic polymer or liposome, is required to be present in order for Pluronics to transfect effectively. This study also illustrated this phenomenon with a significant enhancement in gene expression with the presence of a liposome

(Lipofectamine 2000™), in the 2D *in vitro* study. However, one of the reasons why Pluronic was selected for examination was because of its potential to act as both a vector and stent coating.

The mechanism for transfection by Pluronic is largely not understood however it has been proposed that it acts as a biological response agent by selectively activating transduction pathways (Alakhov (Batrakova *et al.*, 2001), Sriadibhatla and colleagues proposed, and subsequently confirmed, that Pluronic significantly enhanced gene expression (Luciferase and GFP with CMV promoters) in fibroblast, myoblast and adenocarcinoma cell lines. (Sriadibhatla, Yang, Gebhart, Alakhov, & Kabanov, 2006) That study attributed the transfection efficiency, in part, to the activation of the nuclear factor kappa beta (NF- $\kappa$ B) signalling pathways. NF- $\kappa$ B is a protein complex that controls DNA transcription and is found in almost all cell types and is involved in a multitude of cellular responses which respond to stimuli such as stress, presence of cytokines, free radicals, UV irradiation, oxidized LDL, and bacterial or viral antigens (Tian & Brasier, 2003), (Gilmore, 2006), Brasier *et al.*, 2006 and (Perkins & Gilmore, 2006). The fact that Pluronic has the ability to effectively transduce cells *in vivo* but is unable to transfect *in vitro*, without enhancement of an adjunct, may be due to the fact that, unless one of the aforementioned stimuli are present, this particular signalling pathway is not activated *in vitro* and the poor gene expression results.

To date, *in vivo* gene delivery using Pluronic has almost always utilised injection methods for gastrointestinal and skeletal muscle applications. This affords a gentle pressure and sustained exposure of the vector against the target tissue. It is important to consider if sustained pressure *in situ* is a factor which greatly enhances the vector's (in this case Pluronic) capability of transfection *in vivo*. In this study, the deployment of

a PF127 coated stent in a 3D *in vitro* system favourably enhanced gene expression in an *in vitro* system compared to its 2D counterpart.

Overall, the biophysical characterisation did help screen in terms of optimal DNA encapsulation and the determination of the most optimal ratio of plasmid DNA to PF127 to produce dominant populations of nano-scale particles. However, the ability to combine any of this empirical information to help predict *in vitro* elution profile kinetics and/or the transfection capabilities of any of the vectors did not prove substantially insightful. Nevertheless, the stepwise approach of characterisation that was employed is very useful and merits further investigation to explore if correlations between biophysical characterisation, elution kinetic profiles and *in vitro* transfection efficiencies can be drawn.

Although the transfection capabilities of the vector were not remarkable *in vitro*, even with an adjunct, it is reasonable to suggest that elution “out” of the polymer vector does not correlate directly with efficient transduction of the plasmid DNA in the cells. So although the elution kinetic profile of a 1mg/mL plasmid DNA payload encapsulated in a 1:1 ratio with PF127 could be established, the profiling itself did not offer any accurate predictions for its transfection capabilities.

The purpose of the study outlined in this chapter was to evaluate if Pluronic could efficiently deliver genes to cells *in vitro* and to assess its potential to act as both a stent coating and a vector. Based on a 2D *in vitro* evaluation system, Pluronic would not be considered any further. However with the knowledge of its successful performance *in vivo* with other gene therapy applications (GI, Ocular,) it was considered reasonable to investigate if, in the more clinically/anatomically relevant 3D *in vitro* setting, the transfection efficiency evaluation would be more reliable and accurate. Hence the decision to deploy a Pluronic (with encapsulated

pDNA) coated stent in a pseudo-vessel (cell-lined silicone tube) to investigate if this minor adaptation could enhance gene expression *in vitro*.

The results presented in Figure 2.19 gave a preliminary indication that the transfection efficiency capability of Pluronic could be far superior in the 3D *in vitro* system compared with its 2D *in vitro* counterpart (visual examination alone – quantification was not possible). More importantly, it produced transfection efficiency without the use of an adjunct which was a very desirable outcome. Therefore the objective of determining the elution profile of plasmid DNA out of the PF127 and its subsequent transfection capabilities were significantly enhanced when the vectors were assessed in a 3D *in vitro* set-up. Thus, this proof of principle experiment warrants inclusion in the next study for further evaluation of other non-viral vector contenders for the development of a GES and also validates that correct *in vitro* experimental design is a valuable input when screening potential vector candidates.

It is important to emphasise at this juncture that substantial difficulty was encountered when coating the stents with PF127 and subsequently deploying the coated stent in a cell-lined tube. Extreme care was required to ensure that the coating did not shear off the stent surface during this process. So although proof-of-concept was achieved by deploying a coated stent in a 3D set up the practical constraints of an *in vivo* deployment would not be achievable with PF127 as a stent coating. Its naturally viscous nature, at 20 % w/v alone would deem it an impractical stent coating thus rendering this proposed “dual” system as inefficient and not suitable for further scientific pursuit in this instance.

In summary, so although no definitive relationship between biophysical characterisation, elution kinetic profiles and transfection efficiency capabilities could be established the experiments individually did

provide vital information from an *in vitro* pre-screening perspective, i.e. lead formulation in terms of optimal pDNA loading, optimal Pluronic:pDNA ratios, most favourable charge and particle diameter for cellular uptake etc.

## 2.5 Conclusion

The purpose of the work contained in this chapter was to investigate the feasibility of PF127 as both a potential stent coating and vector for the delivery of a therapeutic gene to the vasculature. In order to achieve this, specific objectives, outlined at the beginning of the chapter, needed to be investigated and their outcomes examined in the context of the overall thesis hypotheses. The specific objectives of this chapter were achieved in this study: the binding mechanism and optimal encapsulation ratio were established, the leading candidate was characterised and the elution kinetics over a 14 days was determined. It was confirmed that transfection efficiency could, albeit at low levels, be achieved with a 2D *in vitro* set-up and that the intensity was amplified by using another non-viral vector adjunct (Lipofectamine™ 2000). Furthermore, it was established that evaluating the PF127 coating in a 3D system was a better option than its 2D counterpart, and most importantly, generated significant transfection efficiency without the use of an adjunct. In conclusion, correlations between biophysical characterisation and optimal nanoparticle determination for theoretical endocytosis could be generated but no clear relationship between biophysical characterisation and elution kinetics and/or transfection efficiency could be adequately established in this study.

When plasmid DNA is complexed with PF127, it was confirmed in this study that they produce nano-scale particles that have the ability to successfully deliver gene products to a target cell or tissue. In addition, the deployment of a coated stent in a 3D *in vitro* system introduces the

possibility that sustained pressure can favourably enhance gene expression in an *in vitro* system and is certainly more representative of what occurs *in vivo* with stent deployment.

PF127 can successfully deliver a reporter gene to a target cell and therefore has the potential to be a suitable vector for a stent platform. It was postulated that this amphiphilic polymer could act as both a delivery system and a vector, thus eliminating the requirement of an additional polymeric coating. It was found throughout the course of this study, that although PF127 could effectively encapsulate plasmid DNA in quantities that subsequently could transduce cells *in vitro*, that it was very difficult to assess and/or screen the vector in a repeatable and reproducible manner. Furthermore the practical concerns of deploying a coated stent *in vivo* without shearing off considerable amounts of the PF127 from the stent's surface rendered this vector/coating an improbable candidate. However, the extensive knowledge achieved in trouble-shooting the stent-coating process, developing the 3D *in vitro* system protocols and refining the deployment techniques, is extremely helpful for evaluating other non-viral candidates for the subsequent studies presented in this thesis.

So, although it has been established in this study that PF127 would not be suitable stent coating, there is the possibility that there may be an opportunity to evaluate it as a reservoir polymer (used as a filler in hollows or holes within a stent strut). However, in its current configuration it is not a suitable stent coating for further evaluation in this work.

This study has clearly elucidated that performing characterisation tests, biophysical and morphological tests, can act as a good screening tool for selecting candidate formulations to be progressed for further assessment in *in vitro* studies. Elution profiling of gene products could be very useful but for the purposes of this study it will only address the

timeframe of the elution of the gene product and not help predict its uptake into target cells and its associated transfection efficiency capabilities. The study also revealed that conducting transfection efficiency experiments in a more anatomically relevant system (3D silicone tubes) gave rise to greater transfection efficiency results than those obtained in traditional methods of evaluation (2D static cell culture plates). Overall, this study demonstrated that an improved methodology of *in vitro* assessment has a significant impact on the interpretation of the results. If the study had not taken into account the effect of 3D deployment on transfection efficiency then the potential of PF127 as a vector could not have been properly elucidated. Likewise, the elution kinetic profiles did not truly reflect the transfection capabilities, and so when the design of experiments for pre-screening can “rule out” candidates prematurely, that is a significant problem for the development of disruptive technologies in the treatment of disease. Taking everything in to account, these results clearly illustrate the benefit of conducting comprehensive *in vitro* assessments to screen candidate vectors prior to progressing to a pre-clinical testing stage.

It will be further examined during the course of this thesis if a rigorous *in vitro* assessment can help predict performance *in vivo*. If this could be achieved then the evaluation of different types of stents, vectors and polymeric coatings could be performed accelerating the development of new technologies in a timely, efficient and cost-effective manner.

**3. Comparison of viral and non-viral vectors  
delivery from stent substrates *in vitro* and  
*ex vivo***

### 3.1 Introduction

In the previous chapter it was established that, although PF127 has had *in vivo* gene therapy success in the past, for this particular application of stent-based gene delivery to the vasculature, it can no longer be considered as a potential stent coating candidate. While the Pluronic coating could successfully transduce cells *in vitro* when deployed in a short length (2-3 cm) of silicone tubing, it was evident that this gelatinous coating (20% w/v) would shear off the stent's surface immediately at the site of *in vivo* insertion (either trans-radial or femoral) during interventional procedures. This is one of the primary reasons that it was deemed an unsuitable candidate coating for these investigations. In addition, the *in vitro* transfection results observed in Chapter 2 could not be achieved with PF127 alone in a static 2D *in vitro* experimental set-up. This result is consistent with findings in the literature by other investigators where the presence of an adjunct (cationic polymers/liposomes), or the administration of a secondary process such as electroporation, is always required to ensure transfection *in vitro* or to enhance efficiency *in vivo* (Batrakova *et al.*, 2001), (El-Kamel, 2002), (Gebhart *et al.*, 2002), (Jeon *et al.*, 2003) and (Bureau *et al.*, 2012).

However, it was discovered that by altering the *in vitro* experimental environment, i.e. evaluating in a 3D instead of a 2D system, resulted in greater transfection efficiency. Deploying a PF127 coated stent and encoding a GFP reporter gene in a 3D experimental set-up, resulted in a significant increase in gene expression, which had previously only be achieved in a 2D *in vitro* system with the presence of an adjunct and/or a secondary (mechanical or electrical) stimulus. A substantial amount of

insight was gained by trouble-shooting the coating process and evaluating the stent coating in 3D, as well as, a 2D *in vitro* environment and this improved methodology is incorporated into the assessment of coatings in the remainder of the work reported in this thesis.

In a DES, the pharmacological agent or drug is assessed pre-clinically to determine how it might perform *in vivo*. A detailed understanding of drug release kinetics is necessary for the design of stent-based drug delivery systems. The same rationale applies to the development of a GES in order to optimise therapeutic effect and minimise local vascular toxicity.

In the previous chapter it was established that a non-viral delivery vehicle (PF127) could more successfully transduce cells in a 3D *in vitro* system than in its traditional 2D counterpart system, and more importantly, without the use of an adjunct to enhance transfection. Based on this discovery, the focus of the present chapter is to explore how the *in vitro* system can be enhanced to evaluate vectors and coatings, and whether this will have an effect on predicting their performance *in vivo*. Although PF127 was not the ideal vector/coating option for this particular application, a focus will be maintained on continuing to develop a non-viral delivery vehicle to apply to a stent. To this end, it is very important to assess potential non-viral vector candidates against the leading viral vector that has already successfully delivered a therapeutic gene to the vasculature from a stent platform.

The study presented in this chapter aims to characterise and compare elution kinetics, transfection efficiency capabilities and gene expression patterns for both non-viral and viral delivery vehicles in *in vitro* pseudovessels and *ex vivo* rabbit carotid artery explants. To contextualise the proposed experimental plan, this chapter reviews: *in vitro* versus *in*

*vivo* performance, the rationale for using advanced *in vitro* systems, and the basics of pharmacological Elution kinetic profiling. To this end, it is postulated that this chapter aims to produce data and other information that could be used collectively to help select non-viral delivery vehicles for further examination through *in vivo* models in the subsequent phases of the thesis.

### **3.1.1 *In vitro* versus *in vivo* performance**

Evidence exists that there is often a mismatch between *in vitro* and *in vivo* results in the literature across pharmacological and biological interventions (D. Wang & Sadee, 2006) and (Cirulli & Goldstein, 2007). *In vitro* results can sometimes be unrealistically good and prove difficult to translate into an *in vivo* setting. This type of occurrence was observed in a recent study (Ahmed & Ayres, 2011), where investigators had established the “ideal” elution kinetic profiles established for a drug loaded pectin-ethylcellulose bead. However, the dissolution rates *in vivo* were completely different from those measured *in vitro* and non-efficacious results ensued. Conversely, agents can under-perform *in vitro* and as a result never make it to a pre-clinical animal model to be evaluated. This is exactly the situation encountered in Chapter 2, where Pluronic alone did not transfect well *in vitro*, in a 2D transfection system. Hence there is a need to improve transfection systems, as well as, the need to investigate other means to predict how a vector should perform *in vivo*. Both under-performance and over-prediction of performance has significant drawbacks. The inability of current *in vitro* assessment systems to accurately predict or simulate behaviour *in vivo* incurs significant economic costs as well as unnecessary animal experimentation. In a worst-case scenario, this can mean that devices fail in clinical trials because the materials and/agents do not perform *in vivo* as expected from the *in vitro* data generated.

### 3.1.2 Advanced *in vitro* systems

The cardiovascular tissue engineering community has become proficient in creating 3D co-culture systems to develop its products (Jockenhoevel, Zund, Hoerstrup, Schnell, & Turina, 2002), (B. K. Mann & West, 2001), (Perry & Roth, 2003), (Oh & Lee, 2013) and (Smit & Dohmen, 2015). Specialist simulated environments, more commonly referred to as “Bioreactors”, are employed to develop constructs for implantation and have evolved significantly over the last few years. Several investigators have contributed to the evolution of anatomically realistic simulation environments over the last 15 years (Niklason *et al.*, 1999), (Seliktar, Black, Vito, & Nerem, 2000), (Minuth, Schumacher, Strehl, & Kloth, 2000), (Fuchs, Nasser, & Vacanti, 2001), (Hoerstrup *et al.*, 2001), (Mitchell, Sanders, Garbini, & Schuessler, 2001), (Jockenhoevel *et al.*, 2001), (Jockenhoevel *et al.*, 2002), (Zimmermann *et al.*, 2002), (Mertsching, Walles, Hofmann, Schanz, & Knapp, 2005), (Dvir, Benishti, Shachar, & Cohen, 2006), (Mironov *et al.*, 2006), (Flanagan *et al.*, 2006), (M. A. Brown, Iyer, & Radisic, 2008), (Grayson, Martens, Eng, Radisic, & Vunjak-Novakovic, 2009), (Hollweck *et al.*, 2011) and (Lim *et al.*, 2012). Bioreactors for cardiovascular cell and tissue growth have particularly focused on the development of biomechanical and biochemical properties to produce functional tissue engineered constructs. In 2003, Barron and colleagues reviewed the evolution of bioreactors for tissue engineering applications in a comprehensive review and provided a succinct definition of a bioreactor “*a system that simulates physiological environments for the creation, physical conditioning, and testing of cells, tissues, precursors, support structures, and organs in vitro*” (Barron, Lyons, Stenson-Cox, McHugh, & Pandit, 2003). Since then, the functionality of bioreactors has evolved considerably and the introduction of new technologies, such as microfluidics, has proved advantageous in cell culturing applications. Microfluidics have the capability to provide a high degree of control over cell culture conditions, particularly in aspects such as dynamic control of temperature and gas

concentration, the precise measurement of media exchange and the automation of cellular tasks (Mehling & Tay, 2014).

Several research groups have developed different micro-bioreactors and have successfully demonstrated their value as novel *in vitro* biomimetic tools for a variety of applications including high throughput cell screening, drug development, protein production, therapeutic development, mRNA amplification and to better understand cell physiology and behaviour (Martin, Root, & Spence, 2006), (S. K. Das, Chung, Zervantonakis, Atnafu, & Kamm, 2008), (Khnouf, Beebe, & Fan, 2009; Lindstrom & Andersson-Svahn, 2010) and (Funamoto *et al.*, 2012). Advanced *in vitro* environments, such as bioreactors, have the potential to enable more effective and accurate transfection efficiency assessments. These more precise *in vitro* evaluations will enable more accurate predictions of *in vivo* performance of potential therapeutic solutions. A 2011 review specifically investigated how microfluidic bioreactors for cell culturing are an essential progression in assessing the micro-environment (Rahman, Pasirayi, Auger, & Ali, 2009). This review places particular emphasis on how effective *in vitro* cell culturing should be to reliably and reproducibly mimic the *in vivo* micro-environment of the cell. More realistic, predictive *in vitro* results will produce speedier and more cost-effective product development cycles. This improvement can help reduce pre-clinical animal experimentation requirements with an overall goal of expediting the commercialisation of future therapeutic agents and devices.

In 2007, Punchard and colleagues utilised the “micro-fluidic” principles in the development of a bioreactor to specifically assess how native, human coronary endothelial cells re-align in the direction of the stent placement (Punchard *et al.*, 2007). This gives an indication that stent deployment methodology has implications on the outcomes of *in vitro* assessment. Advanced *in vitro* systems have the potential to act as a stage-

gate process for R&D engineers and scientists to determine whether or not a particular therapeutic solution should be progressed for further assessment *in vivo*.

### 3.1.3 Elution kinetics

When designing a DES, one of the most important parameters analysed is the *in vitro/in vivo* correlation (IVIVC). The United States Pharmacopoeia (Chatrchyan *et al.*, 2014) defines IVIVC as “*the establishment of a relationship between a biological property, or a parameter derived from a biological property produced from a dosage form, and a physicochemical property of the same dosage form*” (Leeson *et al.*, 1995). Typically, the parameter derived from the biological property is AUC (area under the curve) or C<sub>max</sub> (maximum concentration of the drug) and are both quantified from blood plasma, while the physicochemical property is the *in vitro* dissolution profile (Raje, Cao, Newman, Gao, & Eddington, 2003).

However, the FDA defines IVIVC as “*a predictive mathematical model describing the relationship between an in vitro property of a dosage form and an in vivo response*” (U.S. Department of Health and Human Services - September 1997). This methodology of evaluation is very useful for developing and improving pharmacological products.

With gene therapy applications, however, there are different challenges to overcome. In the first instance, there is very little experimental data available on gene elution studies. It is also more difficult to quantify an eluted gene during and after an experiment. Similarly, the mechanism of cellular uptake of a gene when it reaches its destination involves a far more complex cascade of events than that of a pharmacological agent. From a physicochemical perspective, the drug is characterised by its *in vitro* dissolution profile. It is then assumed that the

amount of drug eluted is representative of how much drug is absorbed by the tissue and subsequently metabolised. This property does not exactly translate to the situation at the cellular interface when a gene is in use. Unlike a drug, the concentration gradient is not the only factor that can impact uptake of a gene in the cell. Measuring the quantity of gene eluted out of a polymeric stent coating fulfils the *in vitro* kinetic profile. This quantification alone does not reliably predict transfection efficiency. Therefore, it is important to quantify subsequent gene expression in cells.

#### **3.1.4 Experimental Rationale**

Although researchers have investigated both viral gene delivery and non-viral gene delivery from stents to the vasculature, the work presented in this study focuses on the independent characterisation of the elution of a gene “out of” a polymeric carrier and the subsequent gene expression quantification in both an optimised 3D *in vitro* system and rabbit carotid explants.

To date, no known study has been conducted to directly compare the elution profiles and the transfection efficiency of a viral versus a non-viral gene-eluting stent in either *in vitro*, *in vivo* or *ex vivo* experimental models. Traditionally, elution profiles of any agent, pharmacological or biological, are quantified *in vivo* by its detection and examination in organs such as the liver, kidneys, bowel and spleen for distal spread of the agent. However, because of the inherent differences between pharmacological product and therapeutic gene approaches, already described in section 3.1.3, it is important to quantify the following:

- i. The amount and rate of gene that elutes “out” of the polymer coating, and,
- ii. The subsequent transfection efficiency of the eluted gene into target cell population.

Therefore in the first instance, the study focuses on characterising the elution kinetic profiles of both vectors (over a 7 day period) and examines the results in a traditional 2D *in vitro* system to evaluate transfection efficiencies. As illustrated in the previous chapter, the importance of evaluating potential gene therapy solutions in a clinically relevant environment is critical to the development of a GES. So, in addition to the 2D *in vitro* assessment, the vectors are also evaluated in both 3D *in vitro* systems and rabbit carotid explants. It is anticipated that collectively this type of quantitative information could help predict a vector's performance when traversed to a pre-clinical *in vivo* model in subsequent phases of development.

On a final note on the experimental rationale, despite unsuccessful attempts with PF127 in Chapter 2, there is a continued focus on developing a non-viral delivery vehicle in the form of a GES. In previous work conducted by Sharif and colleagues in 2008, it was illustrated that a non-viral liposome coated stent was as efficacious in delivering a reporter gene to the vasculature as its viral counterpart in a normocholesterolemic rabbit model (Sharif *et al.*, 2008). In the study, the purpose of the inclusion of a liposome-coated stent (non-viral delivery system) acted as an additional control to a adenov-viral coated stent. Both vectors were applied to Phosphorylcholine (PC) coated stents (not bare metal stents) and the experimental design hypothesised that the viral stent delivery would have significantly greater transfection efficiencies compared to the liposome coated stent control. Therefore, it was an unexpected result that the non-viral stent performed so well *in vivo* and one which would not have been predicted by traditional *in vitro* evaluation methodologies. Given the successful indications in the aforementioned study with the use PC coated stents as platforms for both non-viral and viral vectors, the subsequent studies in this thesis will use this stent type for the vector evaluation and use bare metal stents as their controls, to maintain consistency across the

studies contained within this thesis and to also enable results to be directly compared to relevant prior studies.

### 3.1.5 Experimental Objectives

**Overall goal:** To characterise and compare the following key parameters: elution kinetic profiles, transfection efficiency capabilities and gene expression patterns for both a viral and non-viral vector in 3D *in vitro* pseudovessels and *ex vivo* rabbit carotid artery explants.

Specific objectives:

- To characterise the elution profile of adenovirus (Ad-βgal) and lipoplexes (Lipo-βGal) from a PC coated stainless steel stent *in vitro* over 7 days.
- To evaluate the efficacy of both of these systems to deliver and target a reporter gene (βGal) to the synthesised smooth muscle cell monolayer of an *in vitro* pseudovessel and the injured smooth muscle cell medial layer of the explant post-stent deployment.
- To compare *in vitro* and *ex vivo* gene expression patterns with *in vivo* delivery.

## 3.2 Materials and Methods

### 3.2.1 Cell culture

Vero cells were cultured as previously described (section 2.2.5) and plated on 24-well (section 2.2.6.1) plates for viral vector optimisation and elution kinetic experiments for both viral and non-viral vectors. Human coronary artery smooth muscle cells (hCASMCs) were purchased from Clonetics®/Cambrex Biosciences, Lonza, USA and maintained in EGM-2 basal medium (SmBM™ CC-3181) supplemented with accompanying SingleQuots™ (SmGm™) containing hEGF, Insulin, hFGF-B, Gentamicin/Amphotericin-B and 10% FBS. Cells were seeded at an initial

density of 10,000 cells/cm<sup>2</sup> in T75 flasks or 24 well plates and allowed to reach 80% confluency prior to conducting any experiments.

### **3.2.2 Vector Preparation**

#### ***3.2.2.1 Preparation of non-viral delivery vehicles (liposomal vectors)***

Commercially available liposomes were used in this study. Lipofectamine 2000™ was complexed with pDNA in a 2:1 charge ratio to produce 300ul aliquots of lipoplexes containing 100 µg of pDNA. pCMV-βGal was complexed with Lipofectamine 2000™ for elution studies, *in vitro* transfection efficiency studies (2D and 3D) and *ex vivo* explant protocols.

#### ***3.2.2.2 Preparation of viral delivery vehicles (adenoviral vectors)***

Two viral vectors were constructed for this study. As described in section 1.7.3 a number of viral vectors exist. However, for the purposes of this study, replication-incompetent adenoviral vectors were selected for evaluation. Adenoviral vectors encoding β-galactosidase (Ad-βgal) and humanised fluorescence protein (Ad-eGFP), both under the transcriptional control of the cytomegalovirus immediate early promoter (CMV), were generated through homologous recombination (E1, E3 deletion) in the vector core facility at the Regenerative Medicine Institute (REMEDI, NUI Galway). An Ad-Null (an empty vector control with E1-deletion but no therapeutic insert) was also generated and used as a control. Viral particle number was determined by lysing the adenovirus in a lysis buffer (10mM TE buffer with 0.5% SDS in double distilled H<sub>2</sub>O) and virus concentration was determined by a plaque assay (Plaque forming units, pfu). Serial dilutions were made and incubated at 56°C for 5 minutes. Optical density ratio (OD) 260/280 and protein concentration was measured spectrophotometrically (ND-1000 UV-Vis, NanoDrop Technologies, USA). The number of viral particles per ml was calculated using the following formula:

$$\text{OD}_{260} \times \text{dilution factor} \times 1.1 \times 10^{12}$$

**Equation 3.1**

Titres of Ad-eGFP, Ad-Null and Ad-βgal stocks were  $10^{11}$ ,  $2 \times 10^{11}$  and  $2 \times 10^{12}$  pfu/ml respectively. Virus was subsequently disrupted in 0.1% NP40 and sonicated for 5 minutes prior to the viral vector optimisation study.

### **3.2.3 Viral vector optimisation study**

In order to use adenoviral vectors encoding different reporter genes, it is important to standardise the infectivity capability of a single, baseline viral vector across a range of multiplicity of infections (MOIs). This is an essential empirical baseline to establish so that viral vectors from different stock solutions (with sometimes different concentrations) can be interchanged throughout the study. The nature of using viral vectors is that experiments may require the use of several reporter genes depending on the type of assays required. MOI is the ratio of viral particles to target cells; the lower the MOI that can be used, the more optimal the result. Optimisation of adenovirus transduction of Vero cells was conducted with the Ad-eGFP viral vector. Vero cells were cultured and plates seeded as previously described in section 2.2.5. Vero cells were transduced with Ad-eGFP at a range (50, 100, 250, 500, 1000) of MOIs to ascertain the most optimal MOI for successful transduction with minimal cell death. In order to use adenoviral vectors encoding different reporter genes, it is important to standardise the infectivity capability of the viral vectors across a range of MOIs so that different stock solutions, with different concentrations, can be interchanged throughout the study. Vero cells were analysed after 1 hour and 4 hour exposure to the viral vector, the infectivity media was then removed and fresh media was added and the cells were cultured for a further 24 hours. The percentage of cells expressing GFP was then calculated by flow cytometric analysis. Once the optimal viral vector MOI

was established with an Ad-eGFP vector, an equivalent MOI for both the Ad-Null and Ad-βgal viral vectors was calculated from the stock concentrations determined in the previous section (3.2.2) and utilised throughout the study where appropriate.

### **3.2.4 Viral vector cellular response**

#### ***3.2.4.1 Exposure protocol***

Vero cells were cultured in 24-well plates as previously described in section 2.2.5 at an initial density of  $1.2-1.6 \times 10^5$  cells per well, and were ready for transduction in 1 or 2 days, after reaching 70-80% confluence. Cells were exposed to the following viral vectors: Ad-Null, Ad-eGFP and Ad-βGal, at an MOI of 500 for a period of 1 hour. After this exposure time had elapsed, the infectivity media was removed and replaced with fresh media. The cells were then allowed to culture before a cell viability assay was conducted. Experiments were performed in triplicate.

#### ***3.2.4.2 Cell viability – Alamar Blue™ assay***

Cell viability after exposure to viral vectors was assessed using an Alamar Blue™ assay (Biosciences, USA). Non-transduced Vero cells acted as a negative control for acceptable cell death levels (i.e. 100 % baseline level). Alamar Blue™ is a safe, non-toxic aqueous dye that is utilised to assess cell viability and/or cell metabolism. The assay involves the addition of a flurogenic redox indicator to growing cells in culture (Westby, Nakayama, Butler, & Blair, 2005). In brief, the media was removed from the wells and the cells rinsed with sterile PBS (1X). A 10% Alamar Blue™ and sterile Hanks' balanced salt solution (HBSS) mixture was added to each well (500µl) and the plates incubated at 37°C with 5% CO<sub>2</sub> for 1 hour. 100 µl aliquots from each well were then transferred to a black 96-well plate and cell metabolism was evaluated by measuring the fluorescence intensity (530nm excitation/590nm emission) on a micro-plate fluorescence reader (FLX800, Biotelution kinetic Instruments, Inc., Ireland). In this assay the

number of viable cells correlates with the magnitude of dye reduction and is expressed as percentage of Alamar Blue™ reduction (J. O'Brien, Wilson, Orton, & Pognan, 2000), (Horobin, 2001) and (Abe, Takahashi, & Fukuuchi, 2002) and The calculation of the percentage of AB reduction (% AB reduction) is given as follows according to the manufacturer's protocol:

$$\% \text{ AB reduction} = \frac{(\varepsilon_{ox} \lambda_2)(A\lambda_1) - (\varepsilon_{ox} \lambda_1)(A\lambda_2)}{(\varepsilon_{red} \lambda_1)(A\lambda_2) - (\varepsilon_{red} \lambda_2)(A\lambda_1)} \times 100$$

**Equation 3.2**

### **3.2.5 Stent coating procedure**

Figure 3.1 schematically illustrates the addition of complexed vectors (either liposome or adenovirus) to the surface of PC-coated stents (Abbott Vascular Trimaxx™ 3.0 x 15mm). The vector formulations were deposited manually by micropipette in 30 µl aliquots under sterile laminar flow conditions as previously described in section 2.2.4.

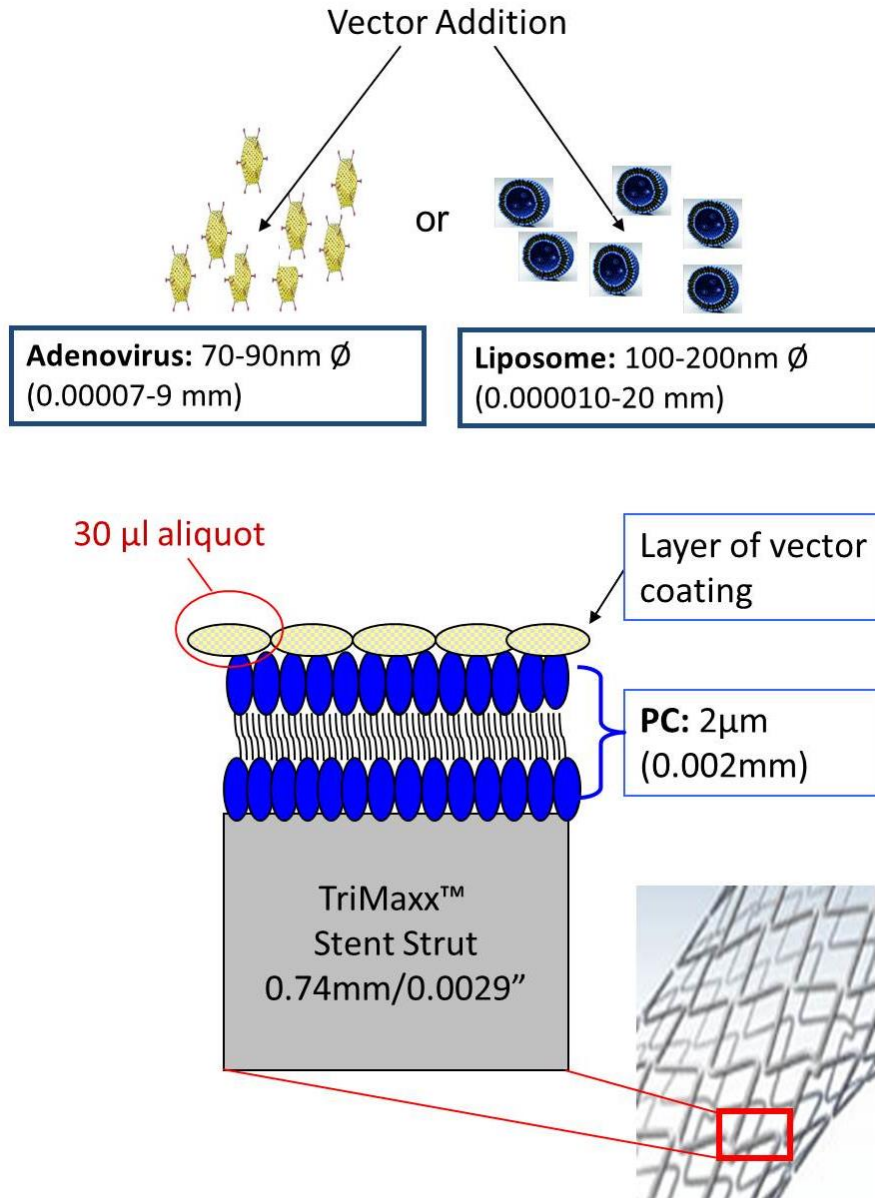


**Figure 3.1:** Vector stent coating (Adenoviral or Liposomal particles) to a commercially-available PC-coated stent- Abbott Vascular Trimaxx™.

Additional precautionary steps were employed with the viral vector coating procedure, ensuring that the process occurred in dedicated hoods and that the viral Gilson pipette tips were disposed of as per in-house biohazard protocols. Once completely dry, the stents were retracted back into their sterile tubular packaging, resealed in laminated pouches and stored at 4°C until required for use.

### 3.2.6 Elution kinetics

In order to determine the elution kinetic profiles of the cumulative DNA release for 2 different time-points, the experimental set-up remained the same for the exposure part (section 3.2.4.1). Comparison of cumulative DNA release elution curves were calculated via PicoGreen<sup>®</sup> assay for the liposomal profile and with real-time PCR QIAGEN™ DNAeasy for the Adenoviral profile.

#### 3.2.6.1 PicoGreen<sup>®</sup> assay

hCASMCS were cultured in a 24 well plate until they reached 90% confluence. The media was collected at each time-point over a seven-day period and the untreated control and stored at 4°C for further processing. On each day the supernatant from each well was removed and replaced with fresh media. On day 7, media was removed and the cells were gently rinsed cells with HBSS. 250µL aliquots of double distilled water were added to each well. Plates were then subjected to 3 freeze-thaw cycles to desiccate the cell and release the DNA. While cells were subjected to the final freeze-thaw cycle a standard curve was constructed in a 96 well plate from a 2µg/mL and 50ng/mL DNA stock solutions. Each dilution was made in triplicate.

Final DNA concentration (ng/mL)	Volume (µL) of TE buffer	Volume (µL) of 2ug/mL DNA stock	Final DNA concentration (ng/mL)	Volume (µL) of TE buffer	Volume (µL) of 50ng/mL DNA stock
1000	0	100	25	0	100
500	50	50	10	60	40
100	90	10	5	80	20
50	95	5			
0	100	0			

**Table 3.1:** Standard curve serial dilutions for PicoGreen<sup>®</sup> assay

A 100µL aliquot from each well of the 24 well was added into a well of a 96 well plate for the standard curve. A 100µL aliquot from the kits PicoGreen<sup>®</sup> solution was also added to each well. The 96-well plate was

incubated at room temperature for 2-5 minutes in the dark before placing in the Wallace plate reader at 1.0sec fluorescein.

### **3.2.6.2 Synthesis of cDNA and RT-PCR**

Adenoviral elution profiling was performed by synthesising cDNA from the transduced cells and reverse transcriptase polymerase chain reaction (RT-PCR) was subsequently performed. 2 µg samples of RNA, in the presence of DNase 1, oligo dT (Invitrogen Corp., Oregon, USA), 20 U AMV reverse transcriptase (Sigma Aldrich Irl, Dublin, Ireland) were used. The cDNA (complementary DNA) product was subjected to 25-35 cycles of PCR using primers specific to the LacZ gene (Forward primer: 5' GCGTAAGTGAAGCGACCCG 3'; Reverse primer: 5' GCGTGCAGCAGTGGCGATGG 3'). GAPDH primers (Forward primer: 5' ACCACAGTCCATGCCATC 3'; Reverse primer: 5' TCCACCACCTGTTGCTG 3') were used as an endogenous standard, unchanged between treatments. The PCR products were visualized on 1.5% agarose gels in 1x TAE with 10,000 x SYBR Safe™ DNA gel stain (Molecular Probes, Invitrogen Detection Technologies). Gene expression data was normalised against GAPDH (Glyceraldehyde 3-phosphate dehydrogenase) and expressed as the relative fold change in gene expression relative to untreated controls.

### **3.2.6.3 Cell preparation for Guava flow cytometry**

The media was removed from each well and subsequently washed with PBS. A 200µl aliquot of trypsin-EDTA was added to each well and allowed to incubate for 5 minutes at 37°C. After this time period, approximately 300 µl of media was added to each well to neutralise the trypsin solution. The contents of each well were aspirated and transferred to 1.5 ml eppendorfs and spun for 5 minutes at 1000 rpm, removing the supernatant carefully without the disturbing the cell pellet. Pellets were re-suspended in 500 µl of 4% PFA and left to acclimatise to room temperature for 10 minutes. Following another spin at 1000 rpm for 5 minutes, the PFA

supernatant was removed and pellets were each washed in 500  $\mu$ l of PBS. Eppendorfs were spun for a third time and then re-suspended in 200  $\mu$ l of fresh PBS. The contents of each eppendorf were transferred to a 96 well round bottomed plate for flow cytometry analysis.

#### **3.2.6.4 Flow cytometry**

Cytometric analysis was performed on a desktop EasyCyte™ from Guava® Technologies in combination with Cytosoft software (v3.1). The 96 well plate prepared from section 3.2.6.1 above was loaded into the flow cytometry analyser and allowed to acclimatise for 15 – 20 minutes prior to acquiring the samples. The ExpressPlus™ programme was used to count the single cells expressing GFP fluorescence, using a negative control (untransduced cells) to adjust the gates and parameters. To eliminate cell debris, a quadrant gate was selected from a dot plot that represented all cells and debris in a sample cell population.

#### **3.2.6.5 Confocal imaging and Image J software**

An inverted confocal laser scanning microscopy, (Zeiss LSM 510 Axiovert) equipped with Millennia V Tsunami Multiphoton lasers, was used for capturing the confocal fluorescent images. The same microscope settings were employed to all images to simplify comparison of results. The argon laser (488 nm) was set at 5.0% and helium–neon laser (543 nm) was set at 25%. Emitted fluorescence from Alexa 488 and 555 was detected through a dichroic 405/488/543 and a BP505–525 filter for the green channel and a BP560–620 filter for the red channel. The pinhole was set to 105  $\mu$ m (1.0 Airy unit), and the PMT detector, gain, and offset were 680, 1.0%, and 6% for both green and red channels. Fluorescence pixels were recorded as 12-bit images and stored as TIFF files. In this study, Image J software (<http://rsbweb.nih.gov/ij/>) and MATLAB software (2007a, The Mathworks, Natick, MA) were used. Image J software was used to extract

the fluorescent intensity levels of  $\beta$ gal from each confocal fluorescent image.

### **3.2.7 *In vitro* – 2D transfection efficiency**

2D transfection experiments (n=6 per group) for this study were performed as previously described for PF127 in Chapter 2. hCASMCs were used in place of Vero cells. Exposure times for the vectors were 2 hours and 1 hour, for liposomal (Lipo-eGFP) and adenoviral (Ad- $\beta$ gal) formulations respectively, under standard tissue culture conditions (37°C/5% CO<sub>2</sub>). Vector supernatants were subsequently removed after these respective incubation periods and replaced with fresh media for a further 48 hours. Cells from adenoviral transduction were fixed with Formalin for 10-15 minutes at room temperature prior to staining with an X-Gal staining solution ( $\beta$ -Gal Histochemistry protocol adapted from Hughes and Blau, 1992) and were visualised under light microscopy to determine transfection efficiency and subsequently quantified using Image J. Liposomal-mediated transfection was conducted with Lipo-eGFP and GFP positive cells were quantified with the use of flow cytometry as described in section 3.2.6.4.

### **3.2.8 *In vitro* – 3D transfection efficiency**

This part of the study optimised the protocol established in Chapter 2 for the assessment of a PF127 coated stent containing an eGFP-C1 plasmid. Protocol was followed as described in section 2.2.6.2 with the following amendments:

- (1) hCASMC ( $1 \times 10^5$  cells/2cm tubing section) were used to line the fibronectin-coated silicone tubing instead of Vero cells ( $4 \times 10^5$  cells/2cm tubing section);
- (2) cell-filled tubes were rotated at 15 rpm to ensure uniform distribution and adherence of cells to the entire luminal surface of the tube sections.

Vector coated stents (liposome and adenovirus), previously prepared from section 3.2.5, were deployed inside the hCASMC cell-lined silicone tubes ( $3.0 \pm 0.05$  mm internal diameter) using a Demax Medical<sup>®</sup> balloon catheter inflation device. Figure 3.2 illustrates the 3D experimental set up to produce a stented hCASMC lined silicone pseudovessel. Panel (a) shows a 2cm silicone fibronectin lined tube filled with hCASMC-rich media. All the cell-seeded silicone tube sections needed for the experiments were rotated at 15 rpm (b). A silicone tube was filled with media only and processed to act as a negative control. Other controls included a stented silicone tube with no cells (e) and a stented cell lined tube with evidence of cells seeded in between the struts (f).

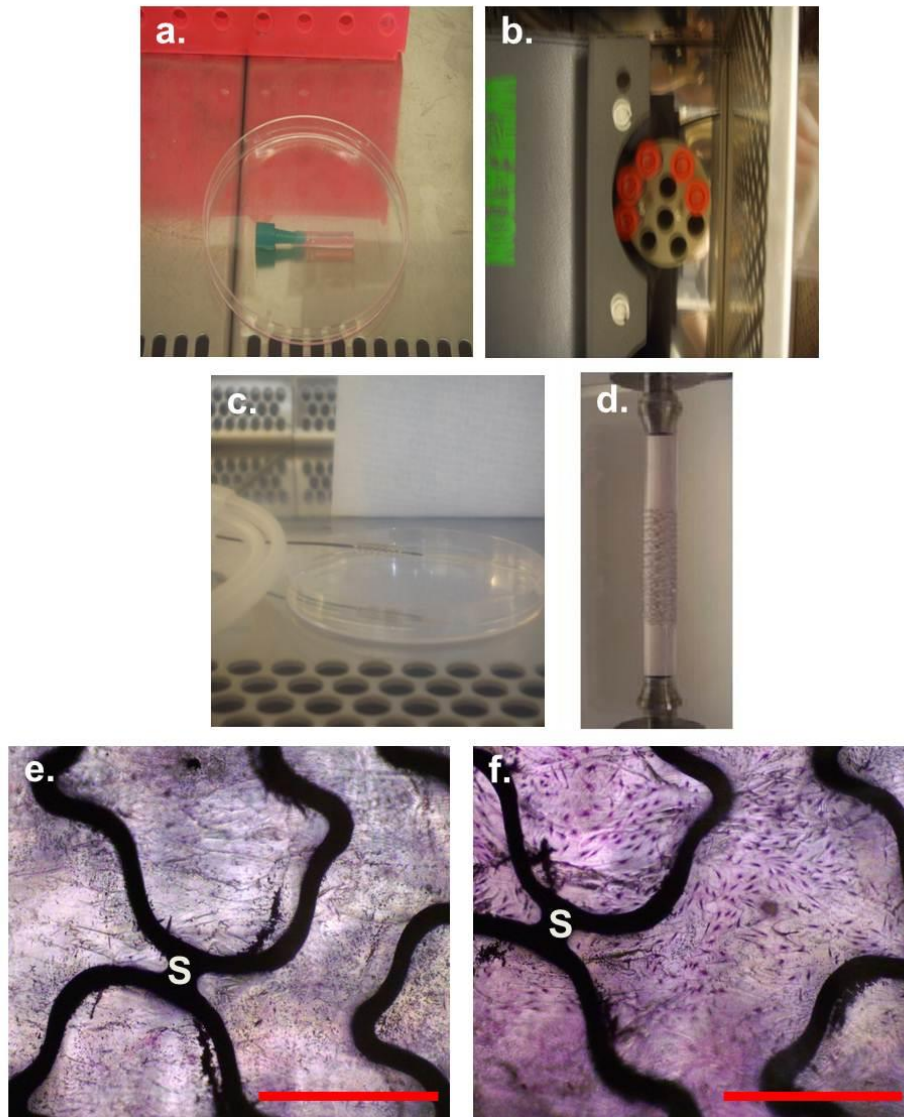


**Figure 3.2:** 3D *in vitro* system protocol with verification images (a) 2 cm silicone fibronectin-lined tubing filled with hCASM-rich media, (b) hCASM cell-lined silicone tubes in rotation phase, (c) expanded vector-coated stent, (d) stented silicone tubing (courtesy of Dr. Marie Puchard), (e) control (stented silicone tube with no cells) and (f) H&E stained confluent monolayer at 4x magnification. Scale bars=500mm. "S" denotes strut.

The stent strut has a PC coating with the vector (viral or non-viral) and when deployed in the pseudovessel this vector coated side was placed in contact with the cell-seed inner lumen.

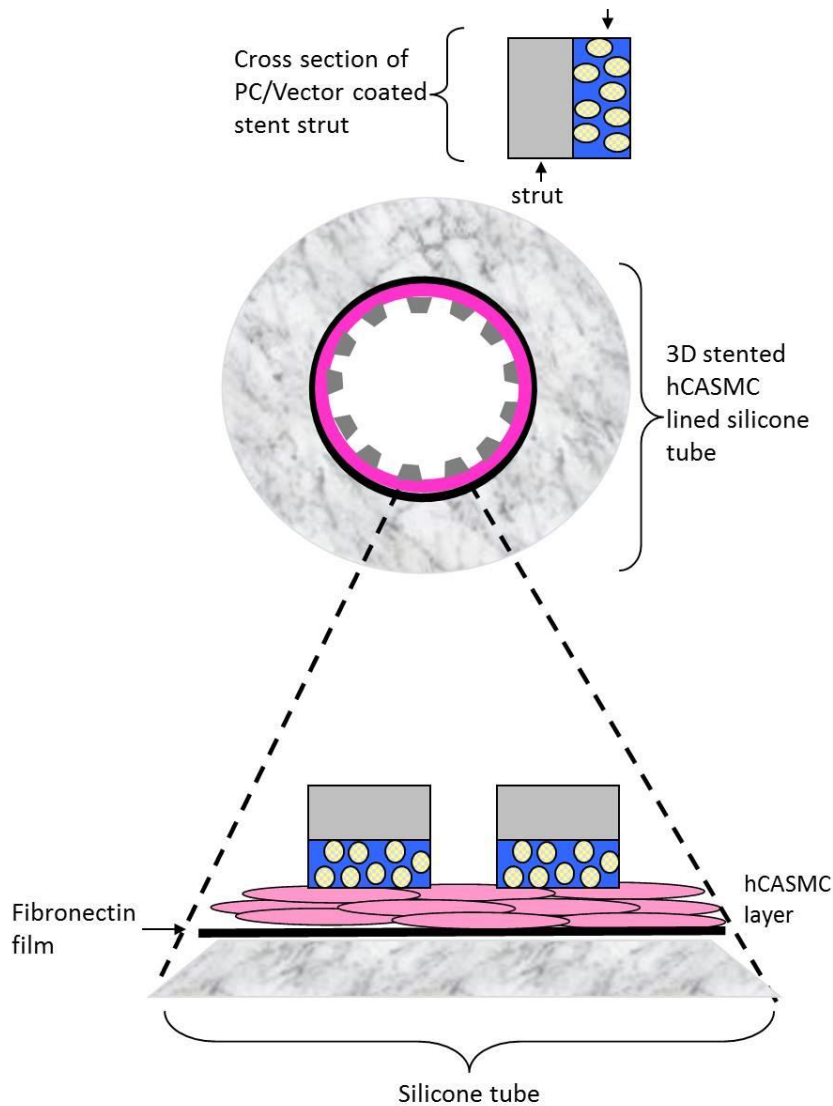


**Figure 3.3:** Schematic of cross-sectional stented hCASMC-lined silicone tube for 3D transfection efficiency evaluation.

All stents were deployed at a pressure of 8bar to ensure a nominal 3.0mm diameter expansion. Stented tubes were then immersed in fresh media housed in 15ml Sardstedt tubes and incubated at 37 °C for a further 48 hours prior to stent removal and visual examination.

### 3.2.9 Carotid artery explant protocol

This protocol was conducted using explants (non-stented control carotid arteries) from normocholesterolemic rabbits. These explants were kindly donated by Dr. Sean Hynes (Department of Pathology, University

College Hospital Galway) and were derived from a non-related performance study. At the time of its conclusion, the organ harvesting protocol corresponded with this experimental study's requirements. No conflict of interest between these two separate studies was raised and the harvesting and use of the explants in this context did not infringe on the ethical approvals granted. At the time of sacrifice, before administering pentobarbital intravenously, the left carotid artery was exposed. This exposed vessel (which had not received any intervention or treatment) was subjected to three successive balloon injuries of 1 minute duration each (6 ATM for 60 second) with a 2.5 x 14 mm commercially available balloon. The injured vessels were then stented with either an Ad- $\beta$ gal or Lipo- $\beta$ Gal-coated Abbott Vascular Trimaxx™ PC stent (3.0 x 15mm). At sacrifice, the left carotid arteries (along with the stented iliac arteries from previous intervention) were carefully excised and immersed in a sterile dissecting medium (DMEM buffered with 20mmol/LHEPES and supplemented with 0.1 mmol/L non-essential amino acids, 1 mmol/L sodium pyruvate, 8 mmol/L L-glutamine, 100 U/mL penicillin and 100  $\mu$ g/ml of streptomycin) at 25 to 35°C. Each vessel was then cleaned and the section slit longitudinally with the use of a sterile surgical blade prior to conducting the  $\beta$ gal histochemistry staining protocol, previously described in section 3.2.6, was then performed on the explants.

The histochemically stained explants were then sectioned into 20 $\mu$ m segments (using a cryostat) and mounted onto poly-lysine-coated slides (Sigma, Dublin, Ireland). The slides were allowed to air dry at room temperature and then fixed with 4% paraformaldehyde for 5 min, washed in phosphate-buffered saline (PBS), dehydrated in 70% and 95% ethanol for 5 min before finally storing in fresh 95% ethanol. In-situ Hybridisation (ISH) was used to quantify the gene expression in the histologically sections. ISH was carried out under RNAase-free conditions. The mineralocorticoid receptor (MR) probe used had the following sequence: 5' TTC GGA ATA GCA CCG GAA ACG CAG CTG ACG TTG ACA ATC T 3'. The probe was end-

labelled with  $^{35}\text{S}$  and incubated at 37°C for one hour. The labelled probe was purified by centrifuging at 3000 rpm for two minutes through a G-50 sephadex micro-column (GE Healthcare, Dublin, Ireland). Appropriate volumes of the labelled probe were added to hybridising buffer and the probes were evaluated for incorporation of the radiolabel by scintillation counting. Probes were hybridised overnight at 44°C and unbound probe was washed with saline sodium citrate twice for 30 min at 55°C followed by 2 min washes with SSC, distilled water, 50%, 70% and 95% ethanol. Sections were allowed to dry at room temperature before exposure to the film. Images (8-bit greyscale TIFF files) were analysed with the NIH Image J software (version 1.37; <http://rsb.info.nih.gov/ij/>). MR receptor expression was quantified by determining the grey levels of the pixels for each section and the background level measured and subtracted for each section and cumulatively evaluated to produce a % gene expression for the cell population.

### **3.2.10 Statistical Analysis**

Experiments were performed in triplicate and results presented as means  $\pm$  standard deviation, unless otherwise stated. Independent Student's *t*-test (two-tailed) was used to detect statistical significance. Significance levels were set at  $p < 0.05$  (\*) and  $p < 0.01$  (\*\*). † denotes no statistical difference.

## **3.3 Results**

### **3.3.1 Adenoviral optimisation**

As previously described, optimising a range of viral vectors MOIs against a baseline viral vector so that any reporter gene can be used throughout the study is central to being able to conduct assays irrespective of the reporter gene or the promoter. Figure 3.4 illustrates the results of adenoviral transduction of Vero cells with Ad-eGFP. Adenoviral transduction was performed in Vero cells for an MOI range of 50-1,000. 2

exposure time periods were employed: 1 hour and 4 hours, respectively, and the resultant cells were analysed by flow cytometry to determine the percentage of GFP expressing cells for each viral vector. Figure 3.4 Graph (a) confirms, as expected, that increasing the MOI induces increasing transduction capabilities. The graph also shows that the longer exposure time (i.e. 4 hours) is not necessary to achieve maximal infectivity of cells and that in fact a lower exposure time of one hour transduces between 10-20% more cells across all MOIs. This graph also illustrates that an MOI of 500 can transduce a comparable percentage of target cells (less than 3% difference) when compared to a MOI of 1000 and therefore should be utilised in the study as the higher the MOI, the greater the cellular death incurred. Part (b) of the figure presents representative images of Veros, transduced with Ad-eGFP at MOI 50, MOI 500 and MOI 1000 respectively at an overall magnification of 4x.

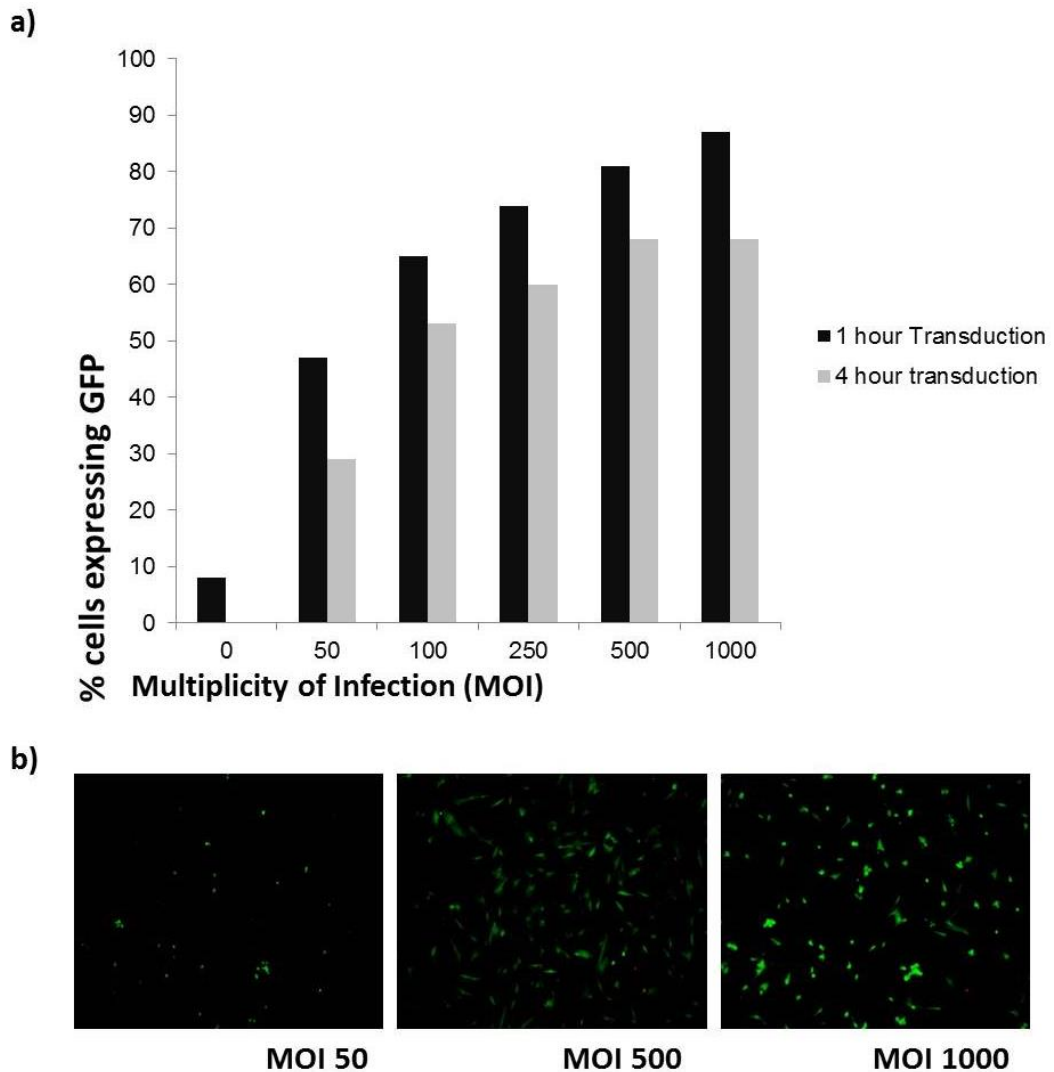


**Figure 3.4:** Optimisation of adenovirus transduction of Vero cells with Ad-eGFP with a range of MOIs (50-1,100) at 1 and 4h. (a) % cells expression GFP vs. MOIs and (b) representative fluorescent images of transduced Vero cells at different MOIs.

### 3.3.2 Adenoviral vector cytotoxicity

An MOI of 500 (i.e. maximal transfection with minimal cell death) was determined from section 3.3.1 to be a comparable MOI to be utilised across a number of viral vectors to establish the level of cellular viability in Vero cells post-adenoviral transduction. At 48 hours, cell viability of Vero cells transduced for 1 hour with Ad-Null, Ad-eGFP and Ad- $\beta$ Gal at an MOI of 500 was assessed by Alamar Blue™ assay. Results in Figure 3.5 illustrate that there is a statistically significant adverse impact ( $p < 0.05$  denoted by \*) on cell death with all adenoviral vectors in comparison to the negative

control (cells not exposed to a vector or untransduced cells). However, the presence of a reporter gene, either eGFP or  $\beta$ gal, does not significantly increase cell death and therefore can be considered an independent variable. Ad-Null induces marginally less cell death but not significantly so. Finally, there is no statistical significant difference (†) in cell death levels between Ad-eGFP and Ad- $\beta$ Gal.

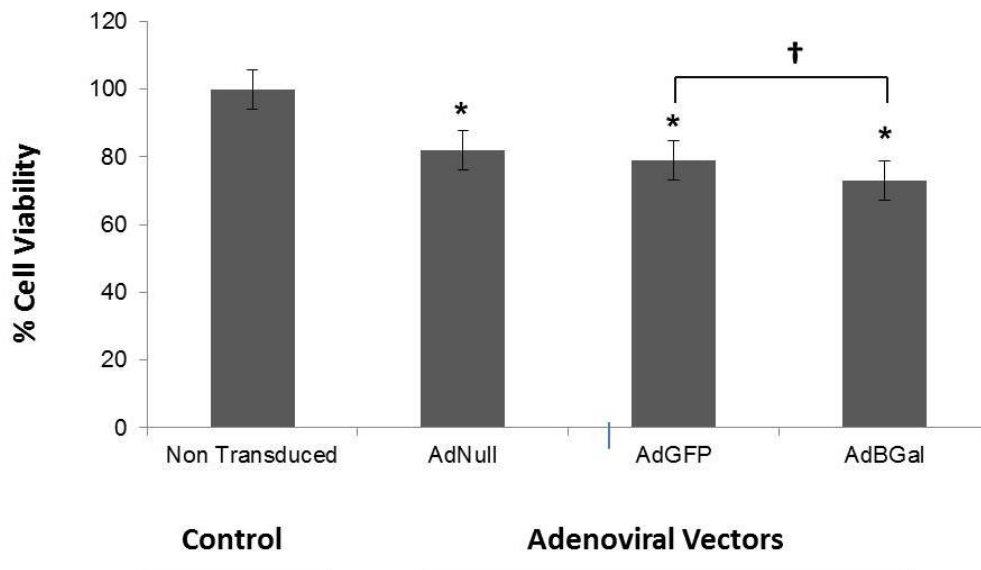


**Figure 3.5:** Assessment of cellular viability following adenovirus transduction of Vero cells. At 48 hours, cell viability of Vero cells transduced for 1 hour with Ad-Null, Ad-eGFP and Ad- $\beta$ Gal at an MOI of 500 was assessed by Alamar Blue™ assay. Results are expressed as a percentage of the mean absorbance of the untreated control cells, set at 100% viability. The values displayed are the means  $\pm$  standard deviation from three independent experiments. A paired student t-test was used where a p-value < 0.05 was considered statistically significant versus the control\*; † no significant difference.

### 3.3.3 Comparison of elution profiles

Figure 3.6 illustrates the elution curves of a viral vector (Ad- $\beta$ Gal) and a non-viral vector (Lipo-eGFP) from a stent platform, over a 7-day period. The figure illustrates clearly that although both vectors plateau in release between day 3 and day 7, there is a different shaped profile for each vector. Ad- $\beta$ Gal presents a steeper burst of viral vector release in the first 24 hours in comparison to its non-viral counterpart. In addition, the liposomal vector releases significantly less cumulative DNA, approximately

32%, over the 7 day period versus approximately 78% released with the viral Ad- $\beta$ Gal.

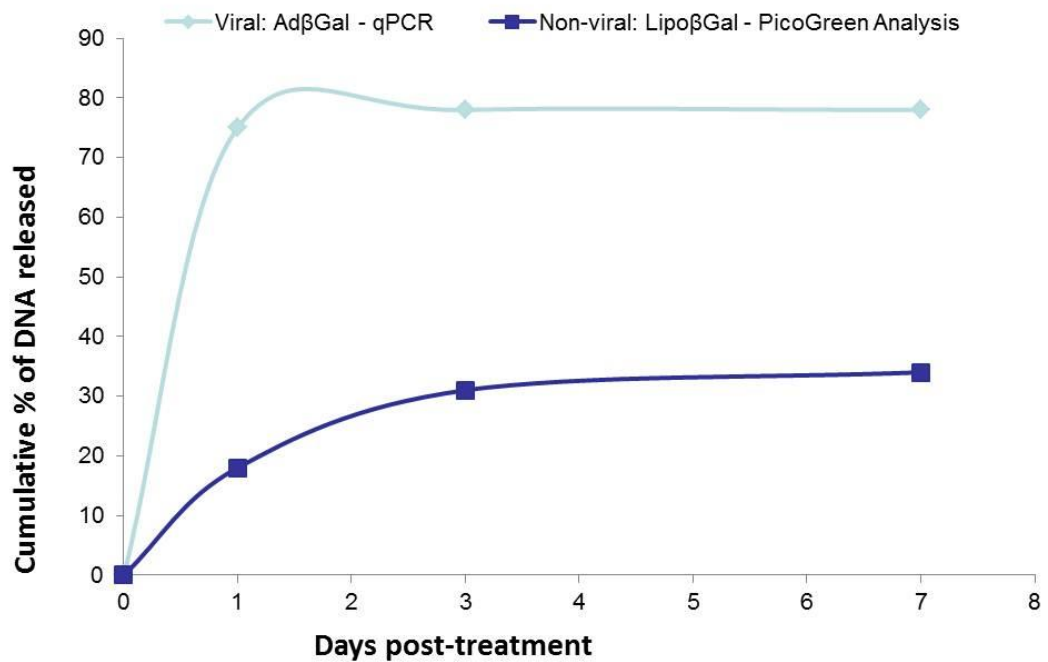


**Figure 3.6:** Cumulative DNA release elution curves. Calculated via PicoGreen<sup>®</sup> assay for the Liposomal profile and with real-time PCR QIAGEN<sup>™</sup> DNAeasy for the Adenoviral profile.

### 3.3.4 *In vitro* transfection efficiency – 2D

For transfection efficiency evaluations (*in vitro*, *in vivo* and *ex vivo*), both qualitative and quantitative assessments were conducted. The quantitative assays used were determined by the reporter gene present. Figure 3.7 illustrates representative images of transduced cells from both viral and non-viral vectors. Images (a) and (c) illustrate light microscopy of control hCASCs. Positive viral transduction (Ad- $\beta$ Gal) of hCASCs is shown in image (b) and positive non-viral transfection (Lipo-eGFP) is illustrated in image (d).

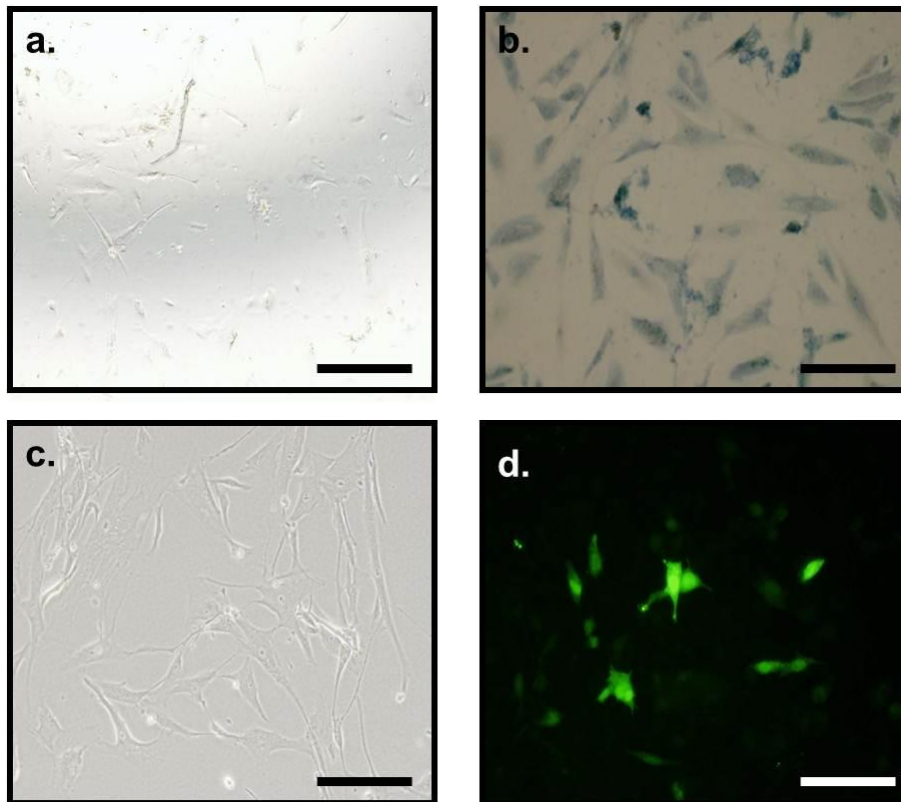


**Figure 3.7:** 2D *In vitro* transfection efficiency results, 28 hours post-vector exposure. (a, c) Light microscopy of hCAMCs at 70-80 confluence in a 24 well plates (b) Viral transduction (Ad-βGal) of hCAMSCs and (d) Non-viral transfection (Lipo-eGFP) of hCAMSC. 10x magnification, scale bars = 200 μm.

The visual examination of the 2D *in vitro* samples validates that both vectors are capable of transducing the hCASMCS, albeit the viral vector has much greater transfectivity capability under the microscope. The quantitation of the 2D *in vitro* transfection is graphically depicted in Figure 3.8 and corroborates that the Ad-βGal vector performs, as expected, with relatively high transduction rates in a 2D system ( $41.98\% \pm 4.7$ ). The non-viral vector also exhibits anticipated results of  $5.66\% \pm 0.67$ . These results are concurrent with transfection efficiency rates for both viral and non-viral modes of transduction in hCASMCS.

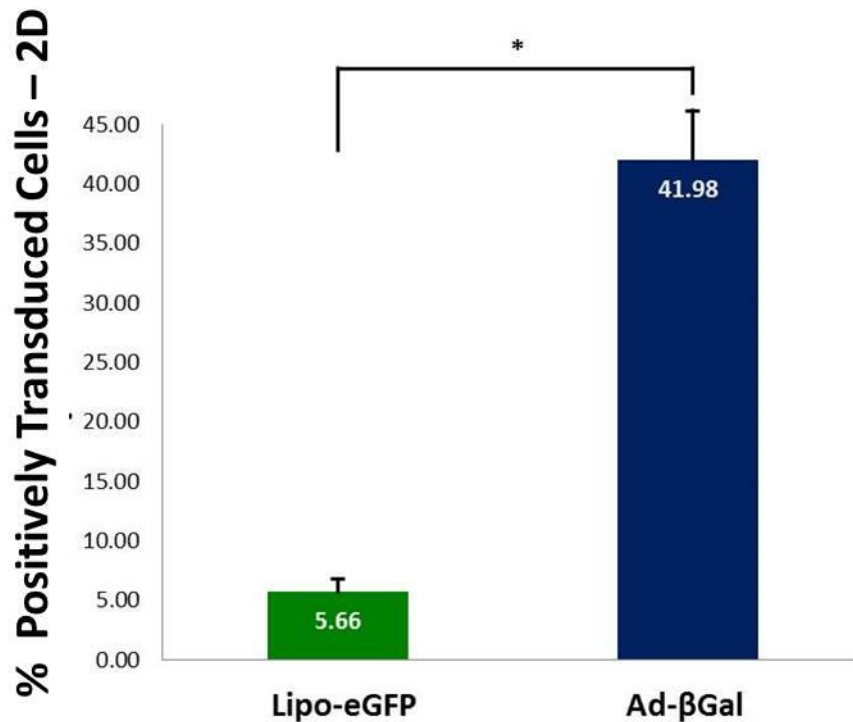


**Figure 3.8:** Comparison of % positive gene expression in a 2D *in vitro* system. Non-viral (Lipo-eGFP) and viral (Ad-βGal) transduction efficiencies. \* =  $p < 0.05$ .

### 3.3.5 *In vitro* transfection efficiency – 3D

Figure 3.9 presents results for vector coated stents following deployment in a 3D *in vitro* pseudovessel. Image (a) is a Multiple Image Alignment (MIA) of an opened pseudovessel post Ad-βGal stent deployment. All cells positively transduced cells with β-galactosidase can be detected by their distinctive blue colour. This image illustrates the distinctive gene expression pattern directly underneath the stent struts and is of particular interest as the pattern has been previously observed in an *in vivo* animal model but to date has not been shown to be replicated in an *in vitro* system. Images (b) and (c) are examples of magnified sections of the MIA in shown in image (a). Superimposed lines are placed on the margins of transduced areas to emphasise the stent pattern (formed by the positive transduction of cells) and further consolidates the evidence that greater under-stent strut gene expression can be replicated *in vitro* when

conducted in an anatomically relevant experimental set-up compared with the 2D transfection results demonstrated in Figure 3.8.

Images (d) and (e) are representative images of the inner luminal surface of a pseudovessel in which a Lipo- $\beta$ gal stent was deployed. There is little evidence of the distinctive open cell stent strut pattern composed of  $\beta$ -galactosidase expressing cells evident in the Ad- $\beta$ Gal stented pseudovessel (images a, b and c). Images d and e only illustrates a sparse, diffuse distribution of positively transduced cells and no evidence of clean lines which characterises the Ad- $\beta$ Gal pseudovessel. Visual examination alone deems the Lipo- $\beta$ gal mediated transduction to be negligible in comparison to its viral counterpart.

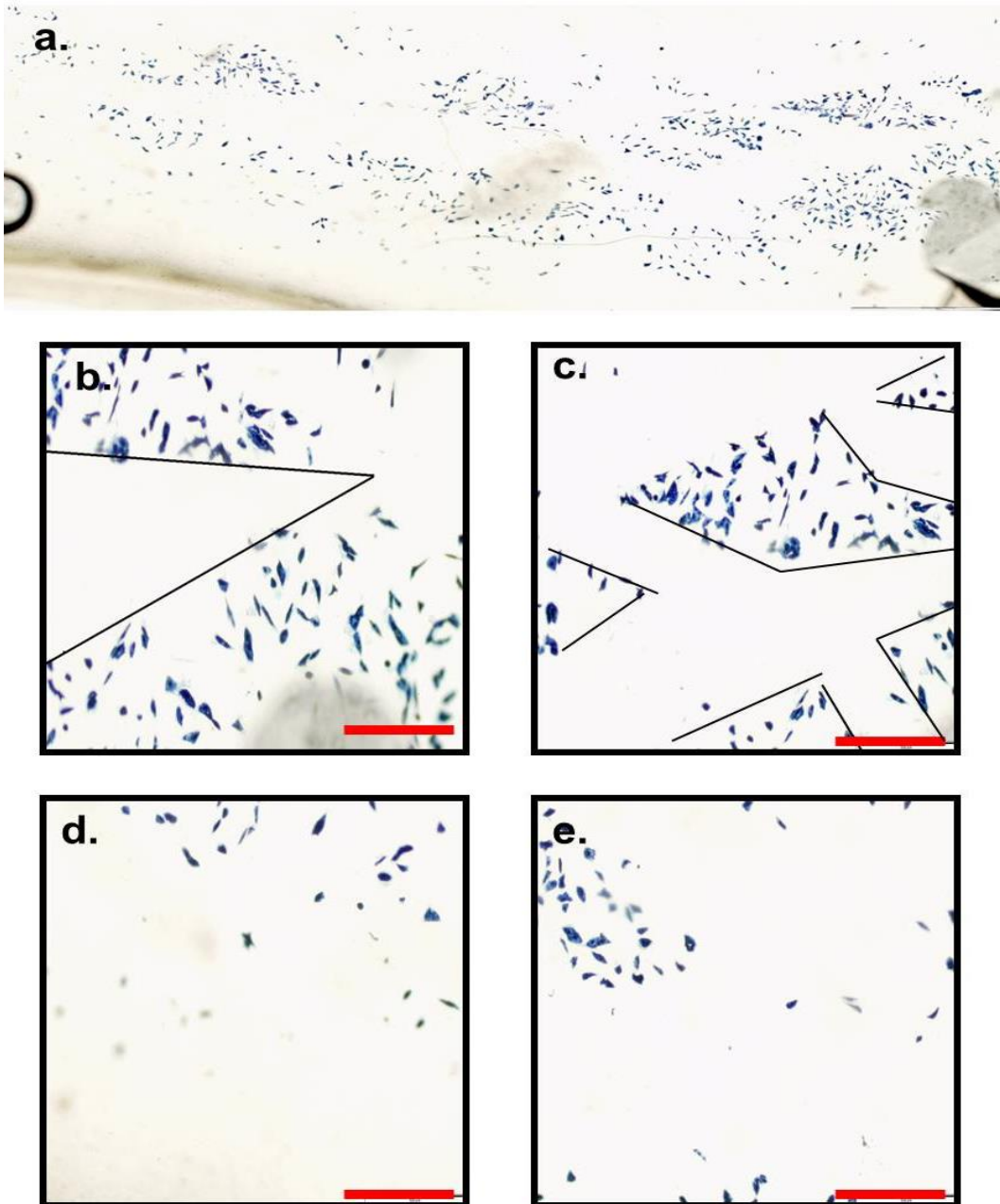


**Figure 3.9:** 3D *In vitro* transfection efficiency results, 48 hours post-vector exposure. (a) Multiple Image Alignment (MIA): (Lipo-eGFP) Ad- $\beta$ Gal stented pseudo-vessel. 40x magnification; scale = 2000  $\mu$ m. Representative images of hCASMCM stained cells on the inner surface of pseudovessel (b,c) Ad- $\beta$ Gal; (d,e) Lipo- $\beta$ gal. Scale bars = 500 $\mu$ m.

The quantitation of the 3D *in vitro* transfections is graphically depicted in Figure 3.10. As established with the 2D *in vitro* results, the Ad- $\beta$ Gal vector is capable of inducing high transfectivity in the 3D system (53.33%  $\pm$  4.09), although not significantly greater than the 2D transfection evaluation (41.98%  $\pm$  4.7). The non-viral vector performs marginally better

in the 3D system ( $7.8 \% \pm 0.57$ ) compared with the 2D system ( $5.66\% \pm 0.67$ ). However, the comparison between the Ad- $\beta$ Gal and Lipo-eGFP in the 3D system illustrates a statistically meaningful difference ( $p < 0.05$ ).

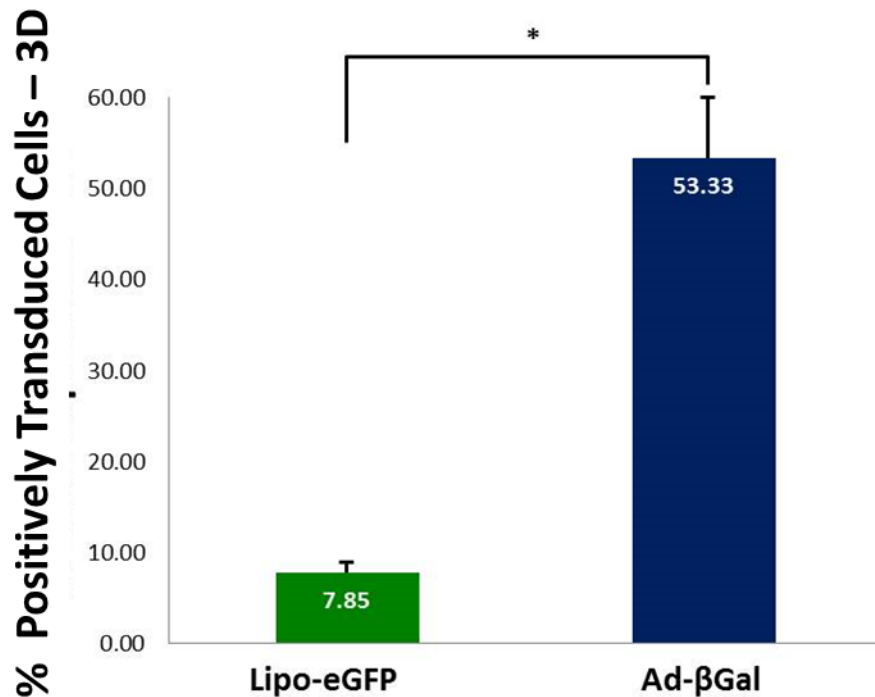


**Figure 3.10:** Comparison of % positive gene expression in a 3D *in vitro* system. Non-viral (Lipo-eGFP) and viral (Ad- $\beta$ Gal) transduction efficiencies. \* =  $p < 0.05$ .

### 3.3.6 *Ex vivo* transfection efficiency

Deployed stents in excised carotid explants are shown in Figure 3.11. Like the preceding 2D and 3D *in vitro* assessments, the images in this figure provide qualitative evidence of successful transfection efficiency. Image (a) shows a control, un-stented vessel with no evidence of the characteristic blue cells, indicative of successful transduction. An excised vessel stented with an Ad-Null coated stent is presented in image (b). The expanded stent is clearly visible *in situ* however there is no visual detection of positive blue cells. In image (c) a faint blue hue can be visually detected in the tissue in the stented part of the vessel but does not exhibit any distinctive pattern. Image (d) is the excised vessel following deployment of

the Ad-βgal stent. This explant exhibits significant cell transduction with a substantial surface area presenting blue indicating a very high infectivity and successful transduction.

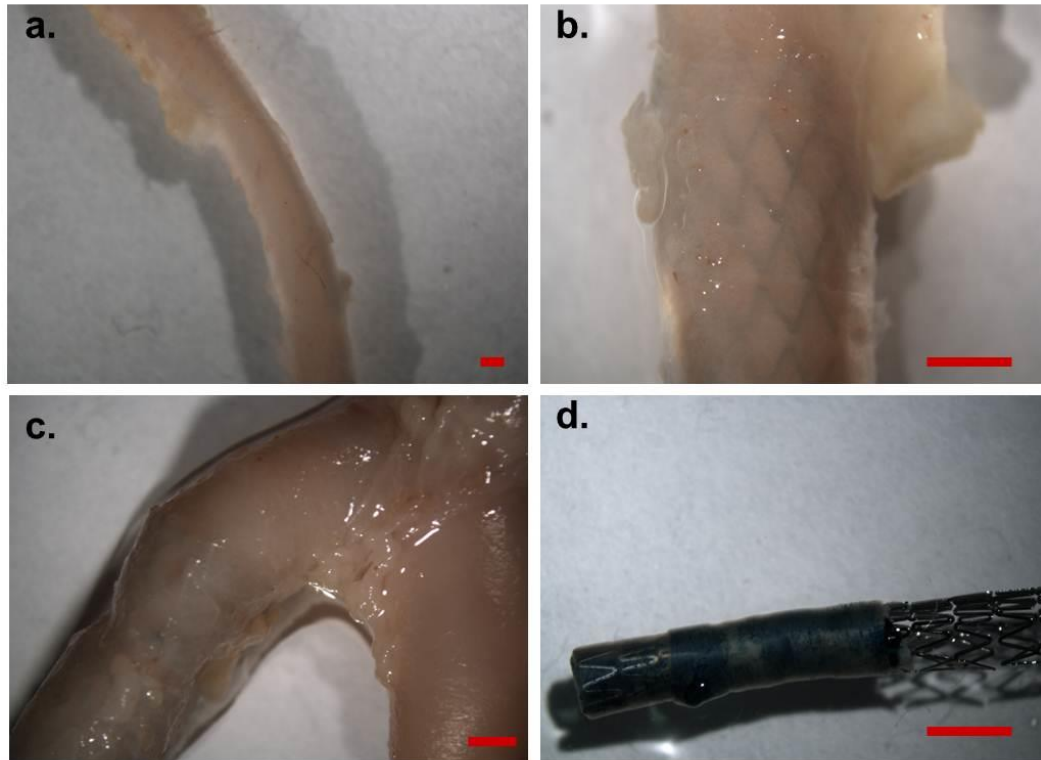


**Figure 3.11:** 3D *Ex vivo* transfection efficiency results, 48 hours post-vector exposure. (a) control vessel – no stent (10x) (b) Control vessel – stent with no vector (4x) (c) Lipo-βgal (4x). Scale bars = 1500μm. Representative images of vessel sections.

When the vessels are processed and subsequently quantified using the methods described in section 3.2.9, the quantitation of the transfection efficiency is graphically depicted in Figure 3.12. As established with both the 2D and 3D *in vitro* results, the Ad-βGal vector is capable of inducing high transfectivity in an explant ( $63.90\% \pm 5.98$ ), although not appreciably greater than the 3D transfection efficiency evaluation ( $53.33\% \pm 4.09$ ). Non-viral Lipo-eGFP performs significantly better in the explant assessment ( $31.73\% \pm 3.13$ ) compared with either the 2D ( $5.66\% \pm 0.67$ ) or 3D ( $7.85\% \pm 0.57$ ) systems. This 4/5-fold increase is significant and further validates the need to utilise quantitative measurements of transfection efficiency when assessing potential therapeutic agents. The visual examinations,

demonstrated in Figure 3.11 alone would not have elucidated the extent of transfection efficiency capability.

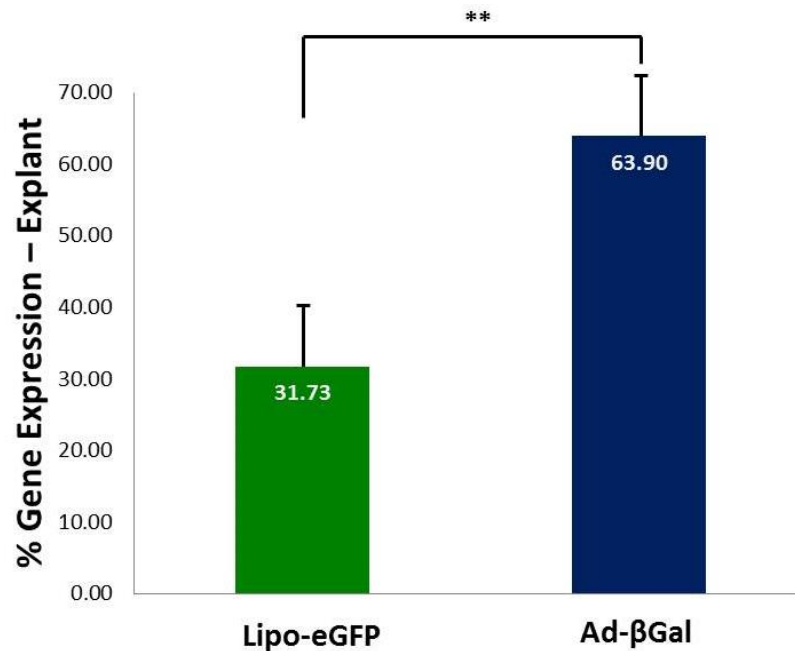


**Figure 3.12:** Comparison of % gene expression in explants. Non-viral (Lipo-eGFP) and viral (Ad-βGal) transduction efficiencies. \*\* =  $p < 0.01$ .

Figure 3.13, demonstrates a comparison of the gene expression across 2D, 3D and explant systems. Significant differences in gene expression exist across all systems. However, there is no significant difference between the 2D and 3D *in vitro* systems for the Lipo-eGFP evaluation (5.66% versus 7.85%). The most prominent result is the difference observed between the Lipo-eGFP in the 3D *in vitro* system ( $7.85\% \pm 0.57$ ) and the transfection efficiencies quantified in the explant system with the non-viral vector ( $31.73\% \pm 3.13$ ).

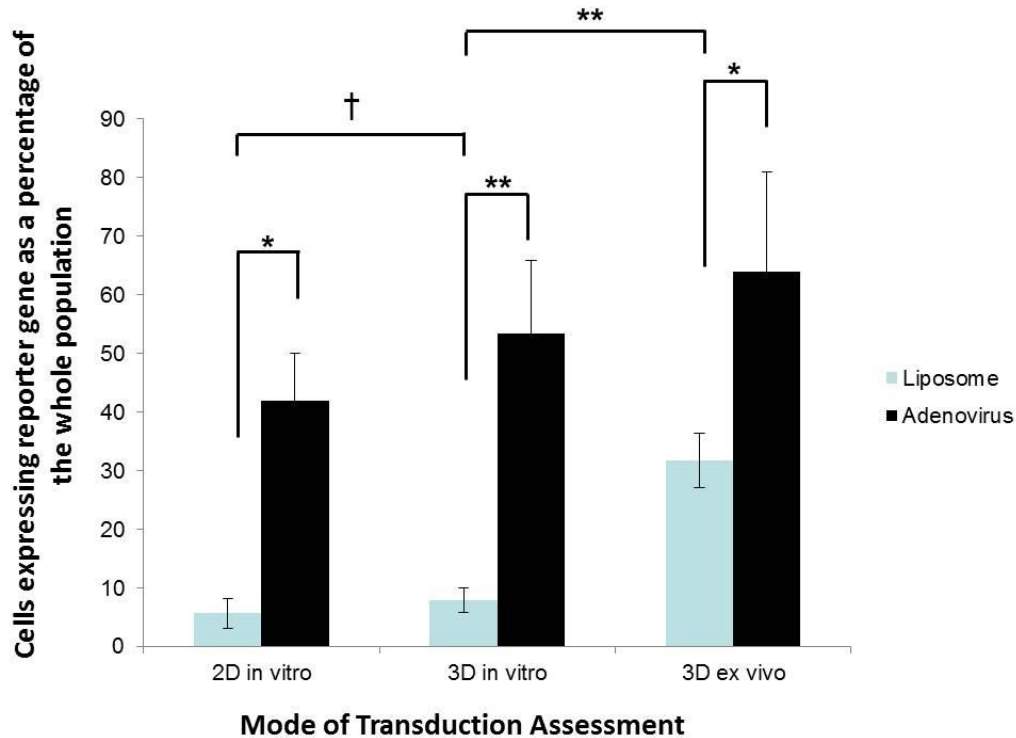


**Figure 3.13:** Comparison of non-viral and viral transfection efficiencies across 3 modes of assessment: 2D *in vitro*, 3D *in vitro* and *ex vivo*. \* =  $p < 0.05$ ; \*\* =  $p < 0.01$  and † denotes no significant difference.

### 3.4 Discussion

As comprehensively discussed in Chapter one, non-viral gene delivery systems are much less efficient than their viral counterparts, specifically in terms of delivering genes into target cells. However, non-viral vectors are considerably less immunogenic than any of their viral counterparts. Furthermore, they do not induce the risk of insertional mutagenesis, a catastrophic outcome at a genetic level which in the worst-case scenario can lead to the development of fatal malignancies or other serious adverse effects (Hacein-Bey-Abina, de Saint Basile, & Cavazzana-Calvo, 2003), (Sadelain, 2004) and (Romano *et al.*, 2009). So notwithstanding the unquestionable effectiveness of viral vectors in transducing cells, the primary barrier to their successful commercialisation to date has resided in substantial concerns about their biosafety. Therefore, designing more sophisticated non-viral vectors, that could transfect tissue as efficiently as viral vectors, is an approach that would be welcomed by all industry

stakeholders. In order to achieve this evolution in non-viral vectors, the design of their optimal performance characteristics needs to closely align with their viral equivalents. To this end, the overall objective of this study was to further understand, characterise and compare the fundamental governing factors (primarily elution kinetic profiles and transfection efficiency capabilities) that enable vectors to successfully transduce cells and produce a therapeutic effect. Therefore, both non-viral and viral vectors were evaluated comparatively in each experiment.

As demonstrated in Chapter 2, it was also clearly elucidated that the accuracy of transfection efficiency capability could potentially be more precisely evaluated in more superior *in vitro* systems. The evaluation of the PF127 coated stent in 2D static cell culture conditions failed to reveal the full transfection capability of the system. It was only when the PF127 coated stent was deployed in a cell-lined silicone tube that gene expression was observed. This proof-of-concept evidence instilled confidence that continued vector assessment should include a 3D system. In an effort to build on this theme of generating more clinically relevant *in vitro* data prior to transitioning a potential vector into an *in vivo* model, this study evaluated both vector types, head-to-head, in an *ex vivo* assessment system. This *ex vivo* system (rabbit carotid arteries) was introduced to the evaluation process to ascertain if its inclusion could provide additional predictive insight into the potential performance of vectors *in vivo*.

The singular, limiting challenge that currently prevents non-viral vectors from achieving clinical translation, is their inability to fulfill the conflicting requirements of adequately protecting the DNA protection while having efficient release kinetics *in vivo*. A 2009 review, examining these juxtaposed characteristics, concluded that future, efficacious non-viral gene therapy will depend on the combination of intelligent material design, innovative imaging techniques and sophisticated *in vitro* model

systems to facilitate the rational design of gene-delivery vectors (Grigsby and Leong (2010). In the work presented here, some of the aforementioned factors (materials and *in vitro* model systems) were examined and directly compared to a viral vector in an effort to develop improvements in non-viral vectors while preserving viral vector performance characteristics as both an efficacy and performance benchmark.

The first specific objective addressed in the results focused on characterising and comparing the elution profiles of Lipo-eGFP (non-viral) to Ad-βgal (viral). It was previously established in Chapter 2 that a 14 day experiment was excessively long and reducing the timeframe to a 7 day experiment would be an adequate period to establish the EK profile for both vectors. Figure 3.6 demonstrated that the vectors exhibited different release profiles over the 7 day period. The most noticeable difference is the rate of release in the first 72 hours. Ad-βGal eluted the majority of its therapeutic payload (78.2%) in the first 24 hours which is approximately 4 times greater than the release of Lipo-eGFP (18.6%) in the equivalent period. The elution kinetics for the Lipo-eGFP vector begins to plateau at Day 3 with 30.3% of the original DNA payload detected, increasing marginally to 32.2% in total by Day 7. There is a significant difference between the viral and non-viral vectors in the amount of DNA released over 7 days, with almost 2.5 times more eluted from the viral vector (78.2% versus 32.2%). The differences in the amount and rate of DNA release may be two-fold. In the first instance the modes of action between viral and non-viral vector cell transduction are fundamentally different.

Viral vectors essentially “attack” and invade the host cells, integrate into their DNA and directly replicate into the progeny; by contrast non-viral vectors, such as liposomes, employ a more stealth-like modality of cellular transduction by utilising the host cell’s mechanism of endocytosis – the

process by which cells absorb molecules (such as liposome encapsulated DNA) from outside the cell by engulfing it with their cell membrane. This phenomenon of nano-particle encapsulation, such as liposomes used in this study, has been routinely used as a means to manipulate the pharmacokinetic profile of drugs (Bandak, Goren, Horowitz, Tzemach, & Gabizon, 1999), (R. L. Hong, Huang, *et al.*, 1999), (M. E. O'Brien *et al.*, 2004), (Narayanan, Nargi, Randolph, & Narayanan, 2009), (Gibbons *et al.*, 2011) and (Hamblin *et al.*, 2014). Liposomal encapsulation of doxorubicin is a specific example, where preclinical studies have consistently shown that the liposome-encapsulated doxorubicin outperformed conventional doxorubicin at equivalent doses in mouse tumor models (R. L. Hong, Sheen, *et al.*, 1999), (M. E. O'Brien *et al.*, 2004). When the drug is encapsulated by the liposome it dramatically increases the drug's half-life *in vivo*. This is most likely due to the liposome's ability to condense the size of the drug molecule to a particle size, 100nm or less and serves to shield its detection and ultimately its uptake by the cell's reticulo-endothelial system, which free, untethered drugs would be subjected to very quickly *in vivo*. Hendriks and co-workers postulated from this that optimal kinetic parameters relate specifically to physicochemical liposomal properties, such as size or  $\zeta$  potential (Hendriks *et al.*, 2012) and this is a theory that the studies in Chapter 2 also supported, and is further substantiated by the results in this chapter in relation to Lipo-eGFP elution kinetic profile and transfection efficiency.

Secondly, although the rate of release of Lipo-eGFP is most likely retarded by how the liposome structure induces physicochemical changes, it is possible that the amount of DNA actually released over the 7 day period may be under-reported. A limitation of this part of the study was that the DNA release for both vector platforms required different analysis. A PicoGreen<sup>®</sup> assay was used for the Liposomal elution kinetic profile whereas PCR QIAGEN DNAeasy was employed for the viral elution kinetic

profile because it was a necessary biosafety measure. However, the use of different methodologies does not allow for comparable analysis. The PicoGreen<sup>®</sup> assay detects unbound DNA and, as was uncovered during this work, the nature of lipoplexes is that the pDNA is condensed into the micellar core and therefore may not be accurately detected by this methodology. Investigators have since explored this under-detection and have standardised a more accurate methodology for nano-particle quantification *in vitro* (Holladay *et al.*, 2010). However, this discrepancy alone does not account for the variance observed between the terminal non-viral elution value (32.2% of the original DNA payload) and the subsequent 2D *in vitro* results (less than 6% transduction of the target cell population). This indicates that, even though the 2D *in vitro* transfection studies for both the non-viral (Gao and Huang (1991), (M. D. Brown, Schatzlein, & Uchegbu, 2001), (Oku *et al.*, 2001), (Dalby *et al.*, 2004) and viral vectors (Klingel *et al.*, 2000), (Karra & Dahm, 2010) are comparable with previous studies, comparison of the respective Elution profiles do not give any conclusive indication of a direct relationship between gene elution profiles and 2D *in vitro* transfection efficiency. This highlights even further that the mode of action in cellular transduction may contribute more prominently to transfection efficiency capability than the amount of gene eluted. Further examination of the potential correlation of elution profiles with transfection efficiency proved to be more relevant as the study transitioned into assessment in a 3D system (*in vitro* and *ex vivo*).

The second objective in this study sought to evaluate the efficacy of both viral and non-viral vectors to deliver and target a reporter gene to the synthesised smooth muscle cell monolayer of an *in vitro* pseudovessel (3D *in vitro*) and the injured smooth muscle cell medial layer of an explant (*ex vivo*) post-stent deployment. To verify the difference between the definitions: *In vitro* involves the use of artificial media which resemble biological fluids while *ex vivo* involves the use of biological tissue.

Although the non-viral transfection efficiency is modest compared with the viral vector (terminal gene elution value  $\sim 78\%$  with a corollary cellular transduction rate of  $41.98\% \pm 4.7$ ), it is difficult to ascertain if the gene elution profile generated is relevant as there is minimal data published on the subject matter. To recapitulate, when the vectors were evaluated in a 3D system there was a slight increase in transfection but this was not statistically significant for either: Viral:  $53.33\% \pm 4.09$  (3D) versus  $41.98\% \pm 4.7$  (2D); Non-viral:  $7.8\% \pm 0.57$  (3D) versus  $5.66\% \pm 0.67$  (2D). However, when the non-viral vector was transitioned to an *ex vivo* system, there was a remarkable increase in quantified cellular transduction. The non-viral vector performed significantly better in the explant assessment ( $31.73\% \pm 3.13$ ) compared with either the 2D ( $5.66\% \pm 0.67$ ) or 3D ( $7.85\% \pm 0.57$ ) systems. This 4/5-fold increase is significant and further validates the need to utilise quantitative measurements of transfection efficiency when assessing potential therapeutic agents. The elution kinetic profiles generated in this study for both vectors did not accurately predict successful transduction *in vitro* (albeit there were limitations to the study detection methodologies as discussed previously). Furthermore, the visual examination alone, as demonstrated in Figure 3.11, would not have elucidated the extent of transfection efficiency capability, and on that basis alone would not have warranted further examination in the context of the development of a GES. It has been well recognised that *in vitro* gene transfer assays are poor indicators of transduction efficacy observed *in vivo* (D. Wang & Sadee, 2006),(Cirulli & Goldstein, 2007) and (Ahmed & Ayres, 2011). In 2004, Arap and colleagues designed and optimised an intermediate model for assessing and quantifying unidirectional transduction *ex vivo*. This study illustrated versatility and also enabled inter-changeability between different viral vectors (adenovirus and AAV) and different reporter genes ( $\beta$ -galactosidase and green fluorescent protein). In their results, they demonstrated that *ex vivo* transduction assays could correlate better with *in vivo* gene transfer results (Arap *et al.*,

2004). The results presented here also corroborate this with more accurate predictions when utilising an *ex vivo* system. This also further validates that a combination of *in vitro* and *ex vivo* assessment provides the most optimal evaluation of candidates vectors and reporter genes during the proof of concept development phase of a GES.

The third specific objective within this work aimed at comparing *in vitro* and *ex vivo* gene expression patterns. Figure 3.13 illustrates a comparison of the gene expression across 2D, 3D and explant systems. The most significant result of the entire study was the difference observed between the Lipo- $\beta$ gal in the 3D ( $7.85\% \pm 0.57$ ) and the explant ( $31.73\% \pm 3.13$ ) systems, respectively. The presence of *ex vivo* tissue, and by association certain cell types (e.g. macrophages, T-cells, residual endothelial cells), that could mediate cellular uptake and gene expression, seems to be the only differentiating factor that could explain the substantial difference between the *in vitro* and *ex vivo* transfection efficiency results. Interestingly, the visual examination of the viral vector (3D *in vitro* and *ex vivo* results) clearly illustrated that the gene expression adopted the pattern of the stent struts. Figure 3.9 (b,c) demonstrates linear patterns for the viral Ad- $\beta$ Gal stent, whereas the non-viral Lipo- $\beta$ Gal stent produced irregular, inconsistent patterns of gene expression in the 3D *in vitro* assessment (Figure 3.9 d,e). Although the gene expression for the non-viral Lipo- $\beta$ gal stent was almost 4 times greater in the explant system, the visual detection/quantification of the cellular transduction proved extremely difficult because it only presented as a diffuse blue-green hue (Figure 3.11 c) which has an appreciably different appearance to the distinctive blue lines presented in Figure 3.9 and Figure 3.11 d. These results further substantiated the suggestion that the presence of cell-based factors in the explants must contribute to the increase in the mediation of cellular transduction and that the different mode of actions that the vectors utilise to express genes also has an impact on transfection

efficiency capabilities. It is important to note at this juncture that performance evaluation of the non-viral vector in an *in vitro* system (2D and 3D) alone would not have adequately revealed its true transfection efficiency potential, and this further emphasises the necessity to technically appraise any vector candidate in more clinically relevant systems prior to pre-clinical evaluation. Given the fact that a vector's mode of action is an important element in cellular transduction, one which can impact transfection efficiency specifically; the *in vitro* and *ex vivo* data generated in this study clearly justifies further exploration in an appropriate *in vivo* model.

To truly understand the implications that some of the results presented from this study may have, it is important to provide some context with precedent studies that exist pertaining to non-viral stent based gene delivery to the vasculature. In 2003, Perlstein and colleagues conducted a porcine pre-clinical coronary study that compared denatured-collagen-PLGA-coated stents containing plasmid DNA (encoding GFP) to coated stents without DNA (Perlstein *et al.*, 2003). This group had previously demonstrated that DNA-PLGA-coated stents could successfully deliver genes to the arterial wall (Klugherz *et al*, 2000). Interestingly, the *in vitro* part of the study illustrated a relatively high transfection capability ( $7.9\% \pm 0.7\%$  vs.  $0.6\% \pm 0.2\%$  control) but when the non-viral vector was transitioned *in vivo* the transduction capability declined to approximately 1%. This research work provided a firm scientific basis for the 2003 study where Perlstein and colleagues further investigated the mechanism of non-viral gene delivery to the vasculature by incorporating denatured collagen into the DNA-stent coatings. This study postulated that the denatured collagen would enhance gene transfer due to adhesion molecule interactions and actin-related mechanisms. Again, the preliminary *in vitro* results proved that the denatured collagen conferred significantly greater transfection compared to the control ( $18.3 \pm 1.2\%$  to  $2.9 \pm 0.2\%$ ,  $P=0.001$ ).

When transitioned to the *in vivo* model (3D), positive transduction occurred at the site of stent deployment, albeit at lower levels than preliminary *in vitro* results (10.8%). The authors concluded that the denatured collagen increased the level of gene expression *in vitro* and *in vivo* because of integrin-related mechanisms and associated changes in the arterial smooth muscle cell actin cytoskeleton (Perlstein *et al.*, 2003). This was a reasonable scientific deduction as the study performed appropriate immunohistochemistry assays to substantiate the claims. Although this was not the approach taken in the study presented here, nonetheless the criticality of non-viral cellular transduction (specifically the differences of the mode of action compared to its viral counterparts) has emerged as a common theme for both studies. It was also noted in both the Klugherz and the Perlstein studies that in the *in vivo* results, the positive reporter gene expression was largely concentrated in the areas adjacent to the stent struts but when visually examined didn't exhibit the distinctive pattern that the study presented here demonstrated with the viral vector.

Similarly, in a more recent publication, Brito and colleagues progressed to using a therapeutic gene (eNOS) (as opposed to a reporter gene that the other studies have used) from a PLGA/gelatin coated stent platform and the results clearly demonstrated re-endothelialisation in approximately 45% of the surface area of the exposed stent struts (Brito, Chandrasekhar, Little, & Amiji, 2010b). The importance of this result is that successful gene transduction at the site of gene delivery subsequently provided efficacious therapeutic results (i.e. evidence of re-endothelialisation). Although the gene expression patterns are not discussed explicitly in any of these papers, it is reasonable to surmise that the pressure conferred by the stent struts to the arterial wall is a contributory factor in the positive cellular transduction results as demonstrated in both the 3D *in vitro* and *ex vivo* experiments. This evidence further supports the argument that employing an extensive *in*

*vitro* assessment is necessary to accurately evaluate potential vectors in the development of a GES.

*In vivo* experiments enable the complete evaluation of a potential therapy in an environment that has a full spectrum of cellular interactions. However, proof-of-concept work needs to be conducted in a validated *in vitro* environment prior to this transition to pre-clinical and clinical assessment. A broad range of models exist between the *in vitro* and *in vivo* extremes, from cell lines to *ex vivo* tissue samples. So, the rationale for testing the potential therapeutic vectors in an *in vitro* (2D and 3D) and explant systems was justified. This stage-gate process of *in vitro* assessment has helped to establish and validate that the vectors are worth further investigation in an *in vivo* model.

### **3.5 Conclusion**

The purpose of the work contained in this chapter was to characterise and compare the key parameters for both viral and non-viral vectors. These included the evaluation of gene elution profiles and transfection efficiency capabilities in conventional 2D *in vitro* systems as well as the level of transduction and gene expression patterns in both 3D *in vitro* pseudovessels and *ex vivo* rabbit carotid artery explants. In order to achieve this, specific objectives, outlined at the beginning of the chapter, needed to be addressed and the outcomes of the study examined in the context of the overall thesis hypotheses.

Each of the specific objectives outlined at the beginning of this chapter were achieved in this study: Characterisation of both viral and non-viral gene elution profiles from a PC coated stainless steel stent followed by the evaluation of both systems to efficaciously deliver a target reporter gene to (a) the synthesised smooth muscle cell monolayer of an *in vitro* pseudovessel and (b) the injured smooth muscle cell medial layer of rabbit

carotid artery explant post-stent deployment, as well as directly comparing their respective *in vitro* and *ex vivo* gene expression patterns. The results produced in this work confirmed that each vector produced a different type of gene elution profile. The results also provided empirical data, over a 7 day period, which allowed comparable analysis of the release kinetics between the vector systems. In this study, the stents were PC-coated (a non-degradable polymer) and the vectors were adhered to its surface. Therefore, the polymer/vector complex is classified as a “matrix” not as a “reservoir”. A reservoir-type polymer coated stent, by definition, refers to those with an inert coating material, which functions as a rate-controlling membrane where the release rate remains relatively constant and is not affected by concentration gradient, but most likely is related to the thickness and permeability of polymeric membrane (Fu & Kao, 2010).

However, because the stent coatings in this study are classified as matrix, it was expected that both the viral and non-viral gene release profiles would be, to some extent, governed by Fickian diffusion which is specifically associated with concentration and diffusion distance (Siepmann, Herrmann, Winter, & Siepmann, 2008). The gene elution profiles generated for both did exhibit a mix of first order (initial burst) and zero order (plateau region) characteristics but neither vector expelled the entire DNA payload. The gene elution profiles generated verified that the viral delivery system eluted its DNA payload much more rapidly (within first 24 hours) than the non-viral delivery system, by contrast, eluted less of its DNA payload (2.5 times less) more gradually over a 72 hour period. However, despite the successful determination of gene elution profiles for both and the validation that they possess different gene elution profile characteristics, neither gene elution profile could accurately predict transfection efficiency capability *in vitro* or *ex vivo*. Both delivery systems were shown to have the capability to transfect cells, albeit at varying levels, with reporter genes ( $\beta$ Gal and eGFP) in both 2D static cell culture systems,

3D cell lined *in vitro* pseudovessels and rabbit carotid artery explant systems. However, neither the 2D nor 3D *in vitro* results could have predicted the significant increase in transfection efficiency capability of the non-viral delivery system in the explant. This particular result provided critical insight into the importance of utilising as many as possible clinically-relevant *in vitro* assessment systems prior to any *in vivo* evaluation. Furthermore, the non-viral transfection detected in the *ex vivo* system fully corroborates the point made at the outset in relation to the risk of prematurely eliminating potential viable therapeutic agents at the *in vitro* screening stage.

This study has clearly elucidated that conducting a comprehensive assessment prior to evaluation of potential vector candidates in *in vivo* models is a beneficial process when developing a GES. The gene elution profiles provided data that could help develop some models of gene elution kinetics out of the PC coating. However, the profound disparity that existed between the amount of DNA eluted out of the vectors and the subsequent transfection efficiency verified that directly applying the release kinetic methodologies used to DES will not help predict *in vivo* performance for a GES. The primary reason for this non-transferability is that the mode of transduction used by vectors to gain access to target cells is fundamentally different to how drugs are metabolised at the cell surface when delivered from a stent platform. Similarly, as the mode of transduction is fundamentally different between vector types, in that endocytosis is probably the predominant mechanism by which non-viral vectors enter the cell, the presence of necessary tissue factors in the *ex vivo* system probably explains why the non-viral vector performed at much higher efficiency *ex vivo* than in the *in vitro* experiments.

The overall learning in this study is that an improved methodology of *in vitro* assessment has a significant impact on the interpretation of the

results. If the study had not taken into account an *ex vivo* system then the potential of the non-viral vector could not have been properly elucidated. Likewise, the gene elution profiles did not truly reflect the transfection capabilities and so when the design of experiments for pre-screening can eliminate candidates prematurely. This is a significant problem for the development of disruptive technologies in the treatment of disease. In combination, these results clearly illustrate the benefit of conducting comprehensive *in vitro* assessments to screen candidate vectors prior to progressing to a pre-clinical testing stage.

The results presented in this chapter undoubtedly contribute toward the first thesis hypothesis which is that stent-based non-viral vector delivery can safely target the vector to the site of vascular injury resulting in gene expression that has the potential to induce a clinical benefit, comparable to viral gene delivery. Comparable refers to the ability to transduce cells at a level that could potentially induce a therapeutic effect *in vivo*. Historically, non-viral vectors have not been seriously considered as an efficacious gene delivery choice for the vasculature with the last decade dominated by viral efficacy studies (Hayase *et al.*, 2005), (Belke *et al.*, 2006), (Kholova *et al.*, 2007), (Dwarakanath *et al.*, 2008), (Breen, O'Brien, & Pandit, 2009), (Wei *et al.*, 2011) and (Pecora *et al.*, 2012).

This study successfully compared performance capability and clearly illustrated that the non-viral vector has the capability to transduce cells at a level (in excess of 30% of cells in the *ex vivo* model) that has the potential to rival a viral vector's performance *in vivo*. As previously discussed, a recent publication demonstrated 10.8 % transfection efficiency *in vitro* with a non-viral vector, encoding a  $\beta$ -Gal reporter gene (Perlstein *et al.*, 2003). This system when transitioned to an *in vivo* model with a therapeutic gene (eNOS), instead of a reporter gene, translated the performance to a clinically meaningful result: approximately 45% re-

endothelialisation (Brito *et al.*, 2010b). The work contained in this chapter has contributed toward the development of an experimental characterisation template to evaluate candidate vectors in an effort to address the overall hypothesis of stent based non-viral gene delivery to the vasculature.

In conclusion, this chapter's results complete the proof-of-concept phase for the development of a non-viral GES. It can be surmised that a non-viral (liposome-based) vector is a viable option for a GES and needs to be further evaluated for efficacy, performance and safety requirements in the context of developing a commercial product. Given the promising *ex vivo* results with the non-viral vector, the rationale to transition any further evaluation to an appropriate *in vivo* model is a reasonable step to take at this stage of the product development process. The next phase of experimental work will focus on selecting the most optimal liposomal formulation to successfully deliver a therapeutic gene to the vasculature *in vivo*. Three potential liposomal formulations will be evaluated to determine if they can effectively transfect DNA *in vitro* containing a reporter gene and subsequently in a normocholesterolemic *in vivo* model. The lead liposomal formulation will then be evaluated in a hypercholesterolemic *in vivo* model with a relevant therapeutic gene.

**4. *In vitro* characterisation study of  
candidate non-viral lipoplexes from a  
coronary artery stent substrate**

## 4.1 Introduction

The use of a non-viral vector in a GES is preferable to using a viral vector. The results from the previous chapters have offered an indication that non-viral stent delivery could perform as well as its viral counterpart. Most importantly the transduction levels achieved by the non-viral vector, particularly in the *ex vivo* system, could have the potential to induce a clinically relevant effect *in vivo* if a therapeutic gene replaced the reporter gene. The preceding chapters also established that although gene elution profiling could provide some indication of transfection efficiency capability for a viral vector, a predictive correlation for a non-viral vector couldn't be ascertained. This prominent disparity between the vectors is postulated to be because of their inherently different gene expression modalities. However, this proof-of-concept phase did establish merit in comprehensively characterising vectors from a biophysical perspective prior to *in vitro* assessment. In addition, Chapter 3 definitively determined that comprehensive *in vitro* assessment is critical to appraise a potential vector prior to pre-clinical evaluation, and it transpired from this work that liposomal delivery from a PC coated stent has the potential to be an efficacious GES.

As outlined in Chapter 1, the design and development of a medical technology has to be conducted within an internationally accepted framework such as an ISO 10993 standard (Biological evaluation of medical devices). This standard contains 20 parts of which biocompatibility and biophysical characterization are two of the fundamental evaluations. The foundation work conducted in the preceding phase (Chapters 2 and 3) has established that biophysical characterisation could provide reliable, pre-screening information to help predict transfection efficiency capability. Likewise, determining the biocompatibility of potential vector candidates is an important consideration in the overall context of developing a potential

commercially viable product. Both of these aspects are addressed in the ISO 10993 standard (parts 5 and 19).

Therefore, the next phase of development of a GES focuses on the selection of an optimal liposomal formulation to be coated onto an existing stent platform to successfully deliver a therapeutic gene and induce a clinical advantage *in vivo*. This product is referred to as “Lipostent”. Chapter 4 reports the examination of three potential liposomal formulations are evaluated: Lipofectin™ (commercially available), DDAB/DOPE and DDAB/POPC/Cholesterol (in-house formulations) to determine if they could effectively transduce, first a reporter gene *in vitro* and subsequently *in vivo*, before selecting the lead formulation to be evaluated in an hypercholesterolemic model *in vivo* with a relevant therapeutic gene in Chapter 5.

In order to contextualise this work, the following section will concisely examine lipoplexes and medical device evaluation (ISO 10993), specifically biocompatibility and biophysical characterisation. This section concludes with the experimental rationale and specific objectives of the work contained herein. It is important to note at this point that the thesis focus transitioned from proof-of-concept (Phase I) to a commercialisation stage (Phase II). See opening section of thesis for details of funding for Phases I and II, respectively.

#### **4.1.1 Lipoplexes**

As previously explained in Chapter 1, the formulation of DNA/cationic lipid complexes are referred to as lipoplexes. It is necessary to encapsulate plasmid DNA in a protective material such as a polymer, or cationic lipids, to protect the macromolecule from degradation *in vivo* and to facilitate cellular uptake by the target cell. Cationic lipid transfection was first pioneered by Felgner and colleagues in 1987 and since then

substantial progress has been made in the development of synthetic gene delivery systems, particularly in novel cationic lipids (Felgner *et al.*, 1987), (Stephan *et al.*, 1996), (E. R. Lee *et al.*, 1996) and (Felgner, 1997). Despite promising results with the first generation cationic lipids, successive generations didn't transcend the technical challenges that always faced non-viral vectors, even though numerous research groups continued to conduct studies, particularly on understanding the structure-activity relationship (Antimisiaris *et al.*, 2000). Some potential for therapeutic capacity for lipoplexes was established in the mid-nineties when various research groups successfully and safely treated conditions like Melanoma (G. J. Nabel *et al.*, 1993) and Cystic Fibrosis (Ferrari, Geddes, & Alton, 2002) with locally delivered lipoplexes directly to the site of interest. By 2003 there were 57 cationic lipid based clinical trials on-going targeting a range of diseases (Coronary Artery Disease, Peripheral Artery Disease, Cancers, Cystic Fibrosis) however despite the research activity, non-viral approaches have never been successfully commercialised. The common lesson that most of these researchers documented during these studies was that a definitive discrepancy existed between *in vitro* and *in vivo* transfection conditions and that successful *in vivo* transfection efficiency is completely dependent on the administration route (G. M. Huang *et al.*, 2002). With oral and intravenous administration of lipoplexes, they rarely made their destination at levels that could transduce a therapeutic effect. However local delivery, like the stent platform under examination in this work, could prove to be a more attractive modality to deliver therapeutic doses.

#### **4.1.2 Medical device evaluation - ISO 10993**

The application of lipoplexes, as a non-viral gene vector, to a commercially available stent-loaded balloon catheter, immediately transposes it from a Class III medical device to an ATMP. As no current guidelines exist to direct the process of proof-of-principle testing of ATMPs from a performance, efficacy or safety perspective, the current testing

methods to evaluate Class III medical devices are employed here to construct a baseline for the assessment of non-viral gene vector delivery from a stent platform, both polymer and non-polymer coated.

ISO 10993 is a set of guideline documents which entails a series of standards for evaluating the biocompatibility of a medical device prior to a clinical study. The list of standards is subdivided to address every given biocompatibility aspect (Figure 4.1) and acts as a framework for test selection to assess biological responses to a device. Biological testing must be performed to exclude possible deleterious effects of the materials and also to assess the functionality of the device in its biological environment (C. J. Kirkpatrick *et al.*, 1990).

- **Part 1:** Guidance on selection of tests
- **Part 2:** Animal welfare requirements
- **Part 3:** Tests for genotoxicity, carcinogenicity and reproductive toxicity
- **Part 4:** Selection of tests for interactions with blood
- **Part 5:** Tests for cytotoxicity: in vitro methods
- **Part 6:** Tests for local effects after implantation
- **Part 7:** Ethylene Oxide sterilization residuals
- **Part 8:** Clinical investigations
- **Part 9:** Degradation of materials
- **Part 10:** Tests for irritation and sensitization
- **Part 11:** Tests for systemic toxicity
- **Part 12:** Sample preparation and reference materials
- **Part 13:** Identification and quantification of degradation products from polymeric medical devices
- **Part 14:** Identification and quantification of degradation products from ceramics
- **Part 15:** Identification and quantification of degradation products from metals and alloys
- **Part 16:** toxicokinetics study design for degradation products and leachables
- **Part 17:** Establishment of allowable limits for leachable substances
- **Part 18:** Chemical characterization of materials
- **Part 19:** Physico-chemical, mechanical, morphological and topographical characterization of materials

**Figure 4.1:** Overview of ISO 10993 Standard: Biological evaluation of medical devices ([www.iso.org](http://www.iso.org)).

For the purposes of this investigation, the testing adheres to the scope and practices outlined in ISO 10993 Biological evaluation of devices-

Part 5: Tests for *in vitro* cytotoxicity and Part 19: Physico-chemical, morphological and topographical characterisation of materials.

#### **4.1.2.1 Biocompatibility: ISO 10993-5**

The concept of biocompatibility has evolved from the *status quo* of it being acceptable for an implanted material to just be inert, to the concept of the ability of a material to perform with an 'appropriate' host response in a specific environment (Williams, 1989). ISO-10993-Part 5 describes the test methods to assess *in vitro* cytotoxicity of medical devices using cultured cells in contact with a device and/or extracts of a device. These cytotoxicity tests are designed to determine the biological response of mammalian cells *in vitro* using appropriate biological parameters (ISO 10993-5:1999- 2<sup>nd</sup> Edition). For a medical device, and specifically in the context of a stent platform, its biocompatibility will be governed by the surface properties of the contacting surface (be that the metal, polymer or vector) and not the bulk characteristics of the metal or polymer exposed.

Establishing the biocompatibility of any medical device is governed by two fundamental questions: 1) Does the device elicit an undesirable biological affect when introduced to human mammalian cells and 2) do the product constituents have the necessary properties to perform its proposed function?

When the ISO10993 standard was first introduced, users could employ qualitative methods to assess the condition of mammalian cells once they had been exposed to, or were placed in direct contact with, the candidate material. Traditionally, how the cells reacted to the material was based solely on the examination of cell morphology and the grading of the intactness of the cell monolayer after its exposure to the material (Sims-Williams, 1988) and (Srivastava, Gorham, & Courtney, 1990). However, as the standard evolved to address harmonisation and to aid reproducibility,

quantitative methods were added to the standard to act as a comparison technique to the qualitative cell morphology examination methods to evaluate cytotoxic effects. Objective, quantitative methods employed in this study include cell metabolism (AlamarBlue™ - mitochondrial activity) and cell proliferation (PicoGreen®-DNA synthesis).

#### **4.1.2.2 Biophysical Characterisation: ISO 10993-19**

From the experimental work performed in Chapters 2 and 3, it is clear that conducting some level of bio-physical characterisation assessment on candidate vectors is a useful way of evaluating if a vector should be progressed for further assessment. To this end, for the work presented in this chapter the biophysical characterisation profile that each of the lipoplexes exhibits when coated onto a stent platform substrate (medical grade stainless steel 316L) is also investigated. The adhesion process to an implanted device *in vivo* is almost entirely governed by the device's surface characteristics, mainly its surface morphology, surface charge, chemical composition, surface roughness and wettability values. ISO 10993- Part 19 pertains to the parameters and test methods that can be useful in the identification and evaluation of the physico-chemical, morphological and topographical (PMT) properties of materials in finished medical devices (ISO 10993-19: 1999-2<sup>nd</sup> Edition).

#### **4.1.3 Experimental Rationale**

Given that the focus here is on non-viral gene delivery, the primary aim of this study is to establish if the vector constituent of a GES, the lipoplex, could fulfil the basic regulatory requirements as outlined in ISO 10993: Biological evaluation of devices. Three potential candidate lipoplexes (Lipofectin™ (DOTMA/DOPE), DDAB/DOPE and DDAB/POPC/Cholesterol) are considered as described below.

A commercially available stent-based catheter delivery system (PC-coated TriMaxx™ or a bare metal CoCr Multilink Vision™ coronary stent crimped onto an ePTFE balloon catheter) are used in this, and subsequent, experimental chapters to further optimise the development of a GES system. The purpose of this chapter is to establish that the lipoplex formulations that are manually applied to the surface of commercially available stents do not adversely impact biocompatibility (ISO10093:5), to profile the variation in biophysical characteristics (ISO10993:19) of the candidate lipoplexes and to determine if such variations modulate the transfection efficiency of the vectors *in vitro*.

The cytotoxicity assessment and the *in vitro* transfection efficiencies of the lipoplexes were conducted in both an ISO 10993 approved cell line (Vero CCL81) and an indigenous vascular target cell line hCAsMCs. In this case the addition of lipoplexes to the surface of a stent, PC coated or BMS, will affect the aforementioned surface properties and thus the consequences must be explored in the context of overall biocompatibility.

#### **4.1.4 Experimental objectives**

**Overall goal:** To evaluate three candidate liposomal formulations (lipoplexes) for potential use as gene therapy vectors. Both the biocompatibility and transfection efficiency of all three candidate lipoplexes will be assessed as per ISO10993: Biological evaluation of medical devices.

**Specific objectives:**

- To determine the biocompatibility of all three candidate liposomal formulations.
- To profile the biophysical properties of the liposomal formulations.
- To determine the transfection efficiency of liposomal formulations in both standard and indigenous vascular cell lines.

- To assess the effect of long-term storage (-80°C/12 months) on both cytotoxicity and transfection efficiency in both standard and indigenous vascular cell lines.

## 4.2 Materials and methods

### 4.2.1 Plasmids

The reporter plasmids EGFP-C1 & SV40-Luc were used for assessment of transfection efficiency. Plasmid DNA encoding either an eGFP gene driven by the CMV promoter or luciferase driven by a SV40 promoter were isolated from *Escherichia coli* bacteria and prepared according to Endofree Plasmid Giga Kit manufacturer's instructions (QIAGEN Ltd, Dublin, Ireland). Both plasmids were obtained from Clontech, Palo Alto, USA. Isolated DNA was stored in TE Buffer (100mM NaCl, 10mM Tris-HCl) at a concentration of 2 mg/mL after verifying its purity by UV spectrometry.

### 4.2.2 Candidate liposomes

For the experiments conducted in this study three candidate liposomal formulations (DOTMA/DOPE, DDAB/DOPE and DDAB/POPC/Chol) were compared. DOTMA or DDAB (Dimethyldioctadecylammonium) are cationic lipids which help in binding the negatively charged nucleic acids, and DOPE is a so-called 'helper-lipid' which allows the entrapped nucleic acid to escape the endosomes after cell entry by endocytosis. Cholesterol aids in forming stable, gel-phase ("waxy") liposomes. POPC (1-Palmitoyl-2-Oleoyl-sn-Glycero-3-Phosphocholine) is a derivative of naturally occurring phospholipids (phosphatidylcholines) that form the cell membranes of eukaryotic cells. The amount of cationic lipids and the amount of helper lipids can vary from a 1:1 to a 1:5 molar ratio. The ratio of cationic lipid amount (nmole) to plasmid amount ( $\mu\text{g}$ ) may vary from approximately 3:1 to 6:1 in these formulations.

The DOTMA/DOPE liposomal formulation is commercially available as Lipofectin™ (Invitrogen Corp., Oregon, USA) as a 1:1 molar mixture. The two DDAB based formulations were prepared by Dr. Udo Greiser (Hayes *et al*, 2006), with the following modifications: chloroform solutions containing either: 2 μmol dimethyldioctadecylammonium bromide salt (DDAB, Avanti Lipids), 5 μmol 1-Palmitoyl-2-Oleoyl-sn-Glycero-3-Phosphocholine (POPC, Avanti Lipids) and 6.5 μmol Cholesterol (Chol, Roche) or 5 μmol dimethyldioctadecylammonium bromide salt (DDAB, Avanti Lipids) and 5 μmol dioleoylphosphatidylethanolamine (DOPE, Avanti Lipids), were mixed in glass tubes. The organic solvent was then subsequently removed in a Büchi rotary evaporator at 100-200 mbar, at greater than 65°C for 45 min to achieve lyophilisation of the lipids under vacuum conditions. The resulting lipid films formed from the lyophilisation process were resuspended in 400 μl of 50% EtOH solution, sonicated in a waterbath for 15 minutes before being mixed with 200 μl pDNA solutions, as described below.

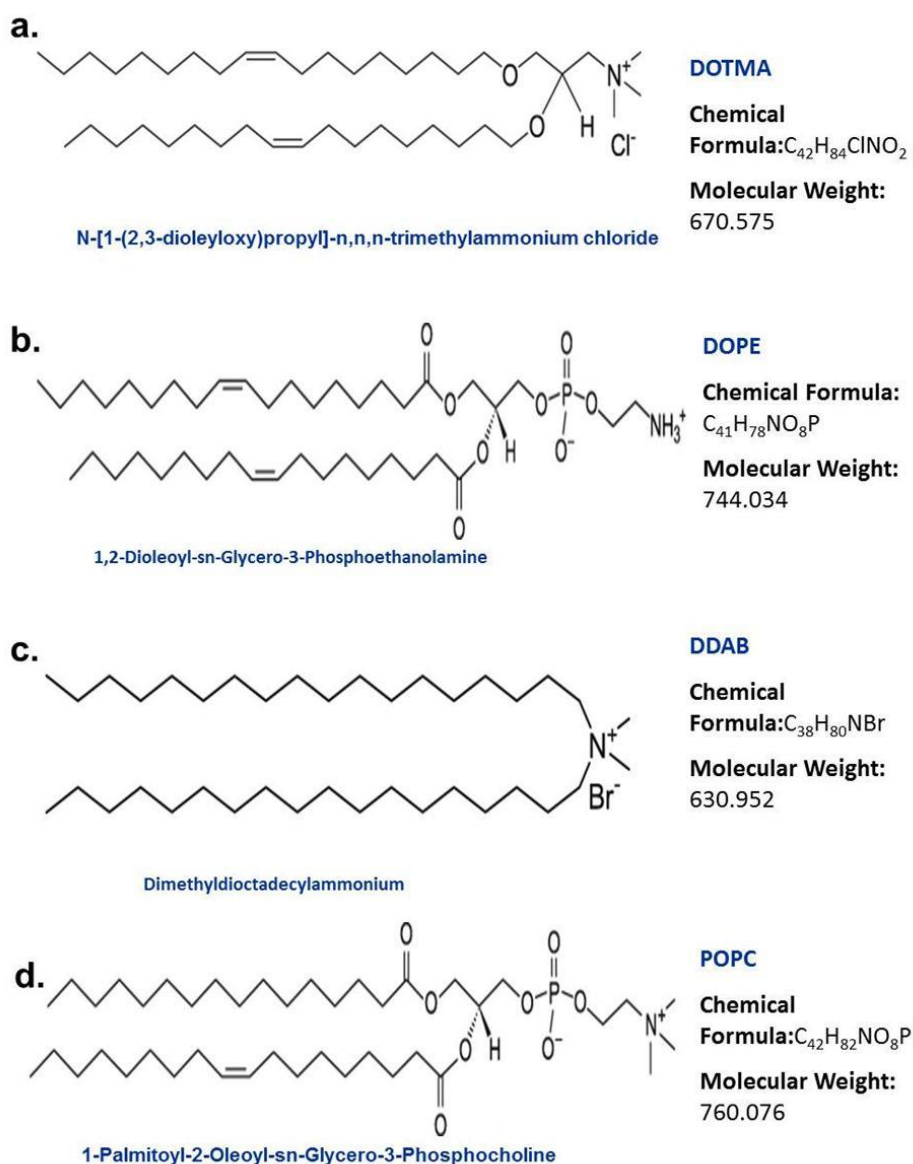


**Figure 4.2:** Chemical structures of liposomes constituents (a) DOTMA (b) DOPE (c) DDAB and (d) POPC – adapted from Avanti Lipids ([www.avanti.com](http://www.avanti.com)).

### 4.2.3 Coupon preparation

10mm diameter stainless steel 316L coupons (Goodfellows Ltd, Cambridge, UK) were polished using a Metaserv 2000 grinder and polisher (Buehler Ltd., Illinois, USA). Each coupon underwent serial polishing steps with increasing grades of SiC grit paper (600, 800 and 1200). After each polishing step, the coupons were soaked in 3 $\mu$ m diamond suspension polish and metadi lubricant wash.

#### **4.2.4 Construction of lipoplexes**

Lipoplexes were constructed in the following way for the experiments described in this study. 50  $\mu\text{l}$  of a 2 mg/ml plasmid solution (100 $\mu\text{g}$  plasmid DNA encoding Luciferase or eGFP) was diluted to a total volume of 100  $\mu\text{l}$  with endotoxin free TE buffer (Invitrogen) in an eppendorf. 200  $\mu\text{l}$  of each 1mg/ml liposomal solution was added to the plasmid solution and mixed several times by inverting the eppendorf. The components were allowed to form lipoplexes for 1 hour at room temperature followed by 4°C incubation overnight.

#### **4.2.5 Preparation of Lipo-coupons**

The prepared stainless steel 316L coupons (section 4.2.3) were washed several times with distilled water, rinsed with ethanol, dried with medical wipes (Kimberley Clarke, USA) and were subsequently placed under a laminar flow hood for 30 minutes to dry, prior to coating with lipoplexes (section 4.2.4). Lipoplexes were applied to the sterilised coupons using a micropipette in 30  $\mu\text{l}$  droplets. Lipoplex application was conducted aseptically in sterile conditions. The majority of lipoplex coated coupons were used in transfection studies within a few hours. However, the potential for efficient gene delivery after long-term storage was also examined in this study.

#### **4.2.6 Long-term storage of Lipo-coupons**

A sample (n=3) of all three lipoplex-coated coupons were stored at -80°C storage conditions for a period of one year. Each coupon (10mm  $\varnothing$ ) was placed in an individual well of a 24-well plate. The plates were sealed with parafilm and placed in a -20°C freezer for 24 hours. All samples were then transferred to -80°C for long term storage (12 months). Following long-term storage, specimens were allowed to defrost at room temperature 24 hours prior to assay. By comparing lipoplexes, pre- and

post-freeze storage step, it is possible to determine if freezing adversely affected the biocompatibility and/or the transfection capabilities. This is an important consideration when assessing if the GES can be manufactured and determining life-shelf of a potential commercial product.

#### **4.2.7 Lipoplex release studies from coupons**

Lipoplex-coated coupons were incubated with 100µl of DMEM, 10% FBS and penicillin/streptomycin (P/S) on the surface at 4°C for 0, 1, 7, 10, 14, 21 or 28 days. The collected supernatant at each time point was mixed with Quant-iT™ PicoGreen® (Invitrogen Ireland). Five minutes after mixing the supernatant with the PicoGreen® solution, the fluorescence intensity was measured using Varioskan Flash multi-reader (Thermo Scientific) with an excitation of 480nm and an emission of 520nm. Metal coupons coated with 100 µg of Gaussia luciferase plasmid DNA were used as positive controls.

Microscope images of fluorescently labelled surfaces: 100µl of DMEM, 10% FBS and (P/S) were added to the lipoplex coated coupon surfaces and incubated for one day at 4°C. The medium was then replaced with 100 µl of PicoGreen®, incubated for 5 minutes at room temperature and removed by pipetting before visualization. Images were taken with Fluorescein isothiocyanate filter functionalized Olympus Ix81 inverted microscope.

#### **4.2.8 *In vitro* cell seeding and culture**

Cell culture studies were performed to assess cellular responses (cell viability) to the lipoplexes and their transfection efficiency for both Vero and hCASMCS. All cells were cultivated at 37°C in a humidified atmosphere with 5% (v/v) CO<sub>2</sub>. Vero cells (Green African Monkey Kidney Cells), as described in Chapter 2, were obtained from the American Type Culture Collection, Virginia, USA and cultivated in Dulbecco's Modified

Eagle Medium supplemented with 10% FBS, (P/S) and additional L-glutamine. Vero cells were chosen for ISO compliance testing. hCASMCs were purchased from Clonetics™/Cambrex Biosciences and maintained in EGM-2 supplemented with 10% FBS (as previously described in section 3.2.1). hCASMCs were tested to establish the ability of lipoplexes to transduce smooth muscle cells – a main target cell population for therapeutic intervention.

#### **4.2.9 *In vitro* transfection**

Cells were plated in 24-well plates at a density of  $3 \times 10^4$  cells and  $9 \times 10^3$  cells for Vero and hCASMCs respectively. Simultaneously, lipoplexes were prepared in duplicate with two different reporter genes, luciferase and eGFP. Lipoplex-coated coupons were each placed in 0.5 mL of medium and incubated at 37°C in a humidified atmosphere with 5% (v/v) CO<sub>2</sub> for 24 hours. After this time period in culture the cells were washed with 0.5 ml of PBS, and 0.5 ml of fresh growth medium was added to each well. The extract solution containing the lipoplexes were then added to the sub-confluent cell monolayer of each well and incubated with the cells for 24 hours at 37°C in 5% (v/v) CO<sub>2</sub>.

##### **4.2.9.1 *Luciferase™ reporter assay***

To monitor the transfection rate, both Vero and hCASMCs were transfected with individual lipoplexes containing the luciferase gene. After a 24 hour incubation period the cells were washed (1x PBS) and suspended in 200ul of lysis buffer (RLB, Promega) and allowed to incubate at room temperature for 5-10 minutes. The cells were then subjected to one freeze-thaw cycle at -80°C. The thaw cycle was exercised on a rocker at room temperature. 40µl of supernatant from each sample was transferred to a black round-bottomed plate (samples are light-sensitive) and assayed for luciferase activity on a Wallac plate reader (10s Luminescence protocol).

The luminescence units were normalised with respect to protein content of the cells, which was determined by the Bradford assay.

#### **4.2.9.2 eGFP assessment**

The transfection efficiency of the lipoplexes for eGFP expression was determined optically using fluorescence microscopy and represented as a percentage of the total area of adherent cells. Flow cytometric analysis for GFP fluorescence was also performed using a 4-color FACS - Calibur (Becton Dickinson, Ireland) equipped with an argon laser exciting at a wavelength of 488 nm. For each sample, 10,000 events were collected by list-mode data that consisted of side-scatter, forward scatter and fluorescence emission centered at 530 nm (FL1). The GFP fluorescence was collected at a logarithmic scale with a 1024 channel resolution. Cell Quest Pro Software (Becton Dickinson, Ireland) was applied for the analysis of the data. For sample preparation, 48 hours post-transfection, the cells were subjected to a single wash step (2ml PBS), subsequently trypsinised, pelleted and washed with 1ml PBS, and resuspended in 300µl of PBS. The cell suspension was analysed within 30 minutes.

#### **4.2.10 Assessment of cellular response**

The cytotoxicity induced by the application of lipoplexes to sterilised stainless steel coupon surfaces was examined using extraction test methods (see Figure 4.3) according to International Standard 10993-5: Biological Evaluation of Medical devices- Part 5: Tests for Cytotoxicity: *In vitro* methods (ISO 10993-5: 1999- 2<sup>nd</sup> Edition). The standard states that a user can use either a direct contact or elution method when evaluating cytotoxicity. Figure 4.3 illustrates that when a coupon is put in direct contact with a cell monolayer it causes additional cell death, not because it is cytotoxic, but because it blocks nutrient diffusion. Therefore, an extraction methodology was employed by placing each lipoplex coated coupon in 500µl (surface area to extraction volume ratio of approx

3cm<sup>2</sup>/mL) of media and incubated at 37°C in a humidified atmosphere with 5% (v/v) CO<sub>2</sub> for a period of 24 hours. This media is then removed and added to cells to assess cellular response to the lipoplex. High-density polyethylene (HDPE, US Pharmacopeia, USA) served as the negative control and organo-tin-stabilised poly(vinylchloride) (Portex Ltd., UK) as the positive control, both of which were chosen based on ISO reference standards. The polymers were sterilised by soaking in 70% ethanol for 30mins followed by rinsing in Hank's Buffered Salt Solution (HBSS, Sigma).

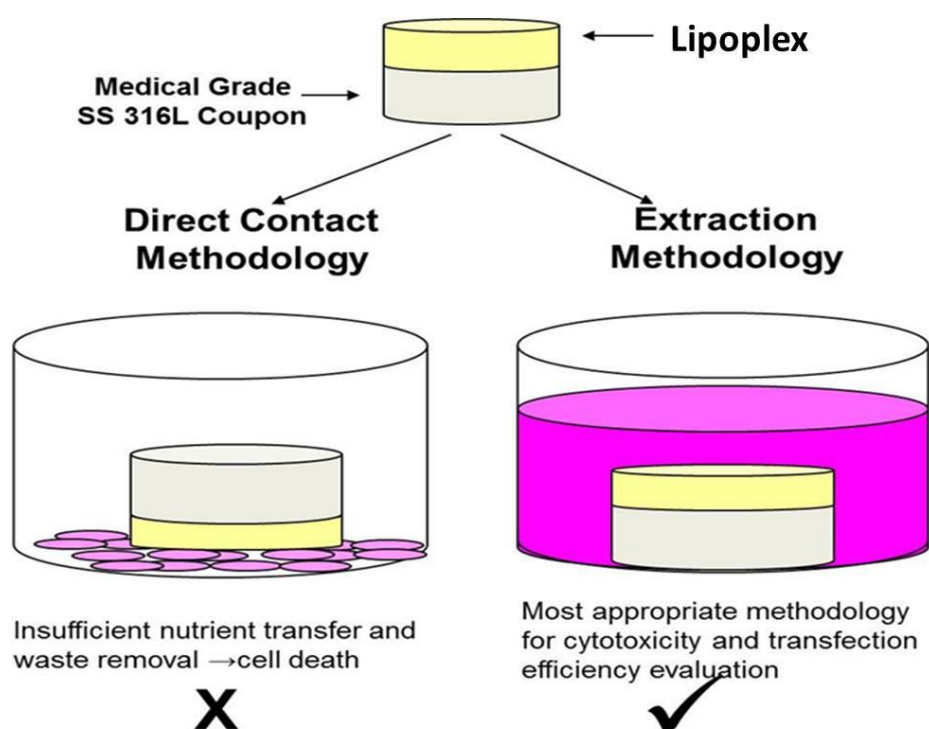


**Figure 4.3:** ISO 10993-Part 5 methodology selection for cytotoxicity assessment.

#### 4.2.10.1 Cell metabolism

Cell metabolic activity was then examined using an AlamarBlue™ assay (Biosciences, USA) as per the protocol described in previous chapters. The lipoplex formulations were also evaluated by an independent pre-clinical service (Charles River Laboratories, Ireland) to determine their cytotoxic effect, if any, by cytopathic morphological evaluation (qualitative assessment).

#### **4.2.10.2 Cell proliferation**

Cell proliferation assays measure actively dividing cells within a sample cell population. The measurement of DNA synthesis is a prominent parameter, as a specific marker for replication, for analysing cell proliferation. A PicoGreen<sup>®</sup> (Molecular Probes, USA) assay was employed to detect the amount of dsDNA as a quantitative measure to assess cell number. The plates used to examine cell metabolism with the AlamarBlue™ assay were subsequently subjected a wash step and three freeze-thaw cycles (as discussed in section 4.2.11.1) to lyse the cell membranes and release the DNA for quantification in solution. A standard curve of DNA concentrations was constructed and 100µl aliquots of the lysed solutions and the standard curve samples were combined with 100µl aliquots of the PicoGreen (dilution 1:200) working solution. Fluorescence was measured at an excitation wavelength of 485nm and an emission wavelength of 535 nm using a Wallac 1420 Victor 3 plate reader (Perkin Elmer Inc., Ireland).

#### **4.2.11 Biophysical characterisation**

##### **4.2.11.1 Atomic Force Microscopy (AFM)**

The surface topography or the depth analysis of the lipoplex-coated stainless steel 316L coupons were evaluated on a Digital Instrument Dimension 3100 system within 24 hours of their preparation. The surface topography was imaged using Tapping Mode (RMS 2V, Frequency 100-500 kHz). This mode involves using a sensitive stylus over the coupon surface and analysing the vertical changes. This technique enables the thickness and uniformity of the coating material, in this case lipoplexes, to be determined on the order of 10–100 nm. Experiments were performed in triplicate for each sample, using a J-tube scanner (scan size: 10 x 10 mm, vertical range: 5 mm). To eliminate imaging artefacts, the scan direction was varied to ensure that a representative image was obtained.

#### **4.2.11.2 Transmission Electron Microscopy (TEM)**

TEM sample preparation and image acquisition procedure was followed as described previously (Horcas *et al.*, 2007). 5 µl aliquots of the individual lipoplexes were deposited onto a holey carbon-coated Formvar 200 copper grid; the excess was blotted away with filter paper and allowed to stand for 15-30s. The samples were negatively stained with 2% (w/v) uranyl acetate and allowed to dry. Specimens were maintained at a temperature of 37°C and observed under an H-7600 transmission electron microscope (Hitachi, Japan) operating at 75kV and at a nominal magnification of 50,000x under low dose conditions. Images were recorded with a 2K x 2K Gatan slow scan CCD camera. All samples were performed in triplicate.

#### **4.2.11.3 Scanning Electron Microscopy (SEM)**

The surface morphology of lipoplex-coated stents was examined by Scanning Electron Microscopy (SEM). Lipoplex-coated stents were attached to carbon adhesive discs on an aluminium stub. The samples were coated with a thin layer of gold under an argon atmosphere and imaged using a scanning electron microscope (Model S-4700 with EDX (Energy Dispersive X-ray Analysis), Hitachi, Japan) operating at 10kV, 20°C and  $10^{-5}$  torr.

#### **4.2.11.4 Dynamic Light Scattering (DLS)**

The mean particle size of the lipoplexes was measured by Dynamic Light Scattering (DLS) using a Spectrophotometer Autosizer 4800 from Malvern Instruments equipped with a Uniphase 75 mW Argon laser operating at 488 nm with vertically polarised light. Prior to measurement, each lipoplex formulation was diluted with 50 mL distilled water and dispersed homogeneously. Scattered light was measured at 160° and at an operating body temperature of 35-40°C. For each run, each time correlation function was obtained by a digital auto-correlator PCS7132 from Malvern Instruments.

#### **4.2.11.5 Contact Angle Measurement**

The sessile method of contact angle measurement was performed by a Data Physics confocal microscope (model OCA 20) equipped with a video CCD-camera and SCA 20 software. Static contact angles were measured by placing a water droplet (2-5 $\mu$ l) onto the lipoplex coated stainless steel 316L coupons at a dispensing speed of 1  $\mu$ l/min. The angle was measured within 4 s of water contact with the sample. All samples were performed in triplicate.

#### **4.2.11.6 Zeta-Potential Measurements**

The zeta potential surface charge of the liposomal formulations was assessed using a Zetasizer 3000HSA apparatus (Malvern Instruments). The zeta potential measurement based on laser Doppler Interferometry was used to assess the electrophoretic mobility of DNA, either naked or complexed with liposomes. Measurements were performed for 20 seconds using a standard capillary electrophoresis cell with zero field correction, a dielectric constant of 79 and a Helmholtz Smoluchowsky constant  $F(\kappa a)$  of 1.5. All experiments were performed in triplicate and conducted at 37°C.

#### **4.2.12 Statistical Analysis**

All assays were performed in triplicate and results presented as means  $\pm$  standard deviation. Independent Student's *t*-test was used to detect statistical significance. Significance levels were set at  $p < 0.05$  (\*) and  $p < 0.01$  (\*\*).\*, \*\* to denote the respective significance in the following results figures.

### **4.3 Results**

#### **4.3.1 Cytotoxicity evaluation**

As described in chapter 3, all three candidate lipoplexes were evaluated to determine the level of cytotoxicity they would elicit *in vitro*.

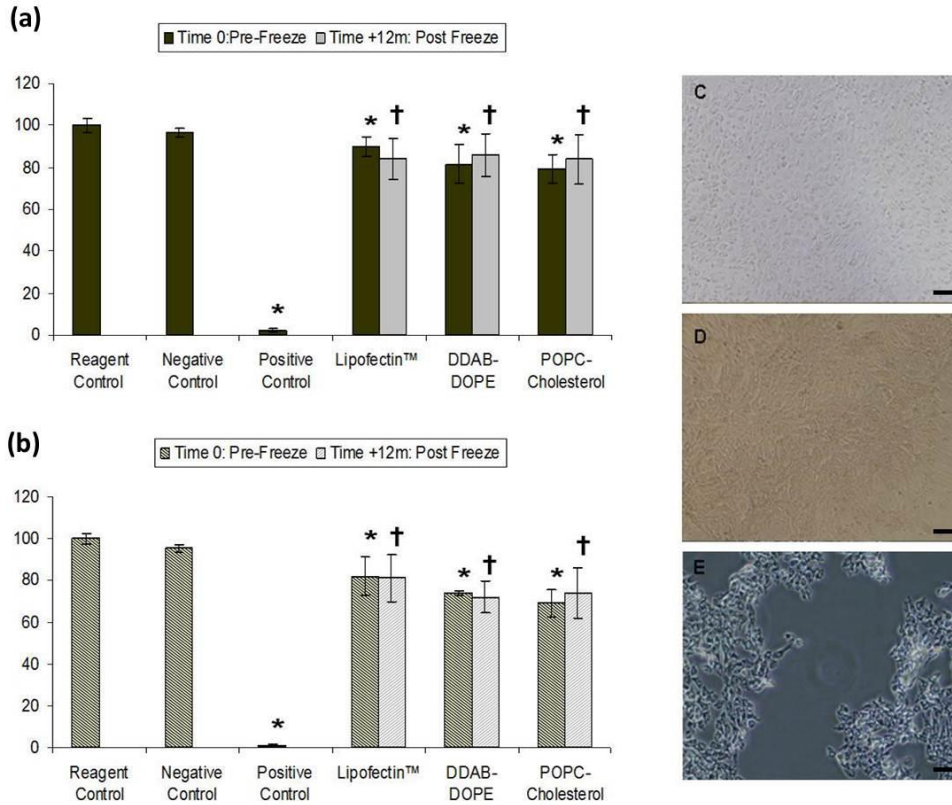


**Figure 4.4:** Cell Viability Assay -after incubation with all three lipoplexes before (Time 0) and after storage (Time +12months) against ISO standard positive, negative and reagent controls. All *In vitro* cytotoxicity tests were performed using the extraction methodology in compliance with ISO 10993-5. Cell metabolic activity was assessed using AlamarBlue™ assays (a) Vero, Cercopithecus aethiops (monkey, African green kidney cells), ATCC CCL81 (b) hCAMSCs. (C-E) Representative phase contrast images of Vero cells at 10x magnification to examine cell death (cytopathic observation) (C) Reagent control – media only Grade 0 (D) Negative control – Borealis HDPE beads, Grade 0 (E) Positive control – Cadmium Chloride 10µg/ml, Grade 4. A paired student t-test was used where a p value < 0.05 was considered statistically significant \*; † no significance difference. Time 0 vs, Time + 12months. Bonferroni/Dunns test showed significant better cell viability for all three lipoplexes compared with the positive control (p = 0.001) and DDAB/POPC/Chol lipoplexes are significantly worse than the reagent or negative control (0.0019).

Cytotoxicity of all three lipoplexes was examined in an *in vitro* assay using both an industry-recommended Vero cell line as well as hCAMSCs. Cytotoxicity was examined as per the elution methodology (liposomal preparations eluted from stainless steel coupons into media to model release from a metallic stent surface) determined by the ISO 10993 standard. This was performed both pre- and post-freezing to examine any contributory effect of a freeze-thaw cycle, which is an important practical aspect to consider in a “real world” application of liposomes to stent surfaces. Figure 4.4 shows that all liposomal formulations were significantly

less cytotoxic than the positive control and that moreover, no liposomal formulation was more toxic than the other. In addition, no significant differences in cell viabilities were observed when freshly prepared versus freeze thawed, stored coupons were used for transfection experiments. Figure 4.4 illustrates that the application of a freeze thaw cycle to the coated coupons did not render the formulations more or less toxic in comparison to either standard cell line.

Vero (Figure 4.4a), or the relevant vascular cell, hCASMC (Figure 4.4b) indicating the stability of these formulations. Interestingly, there was a slight increase in cytotoxicity associated with the application of these liposomes to smooth muscle cells compared to the Vero cell line. In the context of liposomal delivery from a stent, this could potentially be a desirable property, acting in a similar manner to drug eluting stents inhibiting smooth muscle cell proliferation. An independent pre-clinical service (Charles River Laboratories, Castlebar, Ireland) confirmed these findings by cytopathic morphological evaluation. No significant changes in the morphology of the Vero cells were detected when treated with the reagent control (serum containing medium without lipoplexes) as demonstrated in Figure 4.4 (c) or in Figure 4.4 (d) with negative control (Borealis HDPE beads, Grade 0). A positive cytotoxicity control (Cadium Chloride 10  $\mu\text{g}/\text{ml}$ , Grade 4) however resulted in significantly altered cell morphology with evidence of cell death and detachment (Figure 4.4 (e)).

#### **4.3.2 *In vitro* transfection efficiency**

As stated previously, all three liposomal formulations, carrying either eGFP or luciferase reporter genes, were applied to stainless steel coupons. The coupons were placed in growth medium and allowed to incubate for a period of 48 hours. Both Vero and hCASMC cells were transfected with supernatant obtained from lipoplex-coated coupons. Vero cells were treated with freshly prepared lipoplexes (i.e no freeze cycle) and

hCASMCs were treated with lipoplexes that had previously been eluted and stored at -80°C for 12 months. Figure 4.5 demonstrates that all three lipoplexes retained their ability for efficient transfection of Vero cells (Figure 4.5 B-D) and hCASMC cells (Figure 4.5 F-H). Although results varied depending on the cell type and on the lipoplex formulation, Vero cells were more susceptible to transfection by Lipofectin (Figure 4.5 B) and DDAB/DOPE (Figure 4.5 C), in comparison hCASMC (Figure 4.5 F-G). Overall, Lipofectin and DDAB/DOPE- based lipoplexes gave better transfection results than DDAB/POPC/Chol-based formulations (Figure 4.5 D, H) for all cell types tested when liposome-encapsulated eGFP or Luciferase reporter gene pDNA (Figure 4.5 I) were eluted from coupons.

No statistically significant differences in any *in vitro* transfection assay were found between Lipofectin and DDAB/DOPE (Figure 4.5 I). Furthermore, the comparison between freshly prepared, lipoplex coupons (Figure 4.5 I, solid bars) and coupons thawed after a 12 month period (Figure 4.5 I, hatched bars) showed no adverse effect on the biological activity of any liposomal formulations. Lipoplexes eluted from the coupon into the incubating media had demonstrable uptake and expression when examined visually and using a standard assay for Luciferase activity. In Figure 4.5, *in vitro* transfection efficiency post-long term storage conditions (+12months/-80°C) is illustrated to ensure that the lipoplexes could withstand both the temperature and duration of storage without adversely affecting their transfection capabilities. This is an essential requirement for the feasibility of a gene eluting stent to be up-scaled and manufactured commercially. Interestingly, using two different methodologies to assess transgene expression, all three lipoplexes delivered transgene equally effectively under standardized *in vitro* conditions.

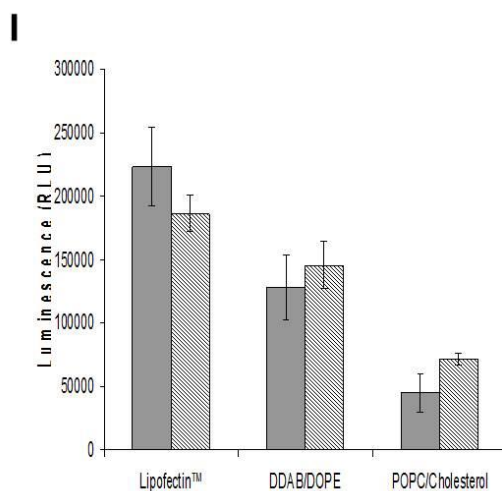
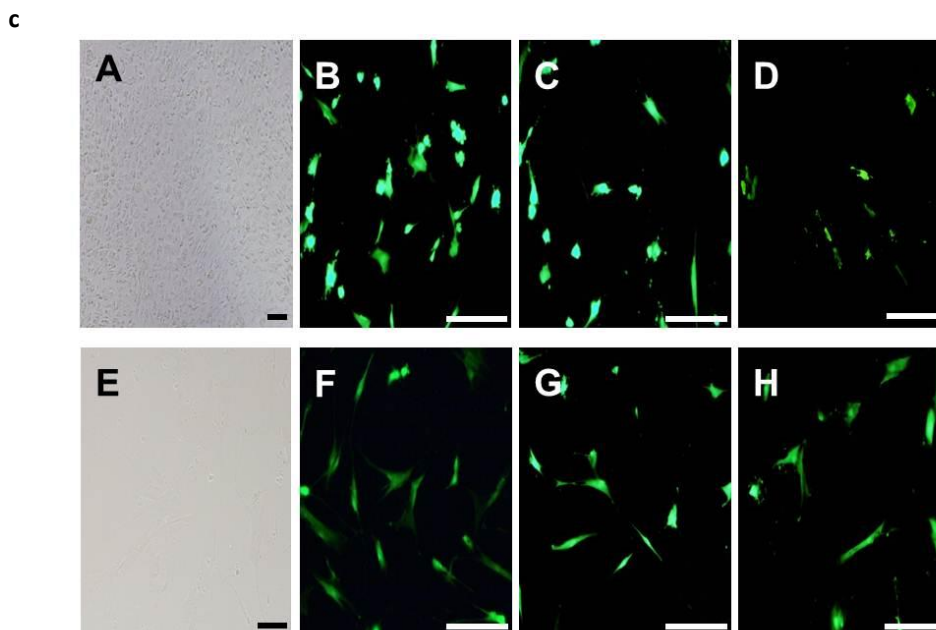


**Figure 4.5:** Phase Contrast Cell Images (A-D Vero cells treated with media supernatant derived from coupons coated with lipoplex-eGFP. Phase contrast (10x). Vero cells untreated controls. (B) Lipofectin™ (C) DDAB/DOPE and (D) POPC-Cholesterol. Images (E-H) hCASM cells treated with media supernatant (E) Phase contrast (10x) hCASM untreated controls (F) Lipofectin™ (G) DDAB/DOPE and (H) POPC-Cholesterol. All examined under fluorescence microscopy 48hours post-supernatant application (I) Luciferase activity measured in Relative Luminescence Units.

### 4.3.3 Biophysical characterisation of lipoplexes

The point of this study was biophysical characterisation of the liposomal formulations as a basis on which to compare them and elucidate their mechanisms of action *in vivo*. Figure 4.6 demonstrates representative AFM and TEM images of all three lipoplexes, establishing that all liposomal formulations produced nano-sized particles with mean diameters of less

than 100nm. The AFM images confirmed the adherence of the liposomal solutions to the surface of the stainless steel coupons.

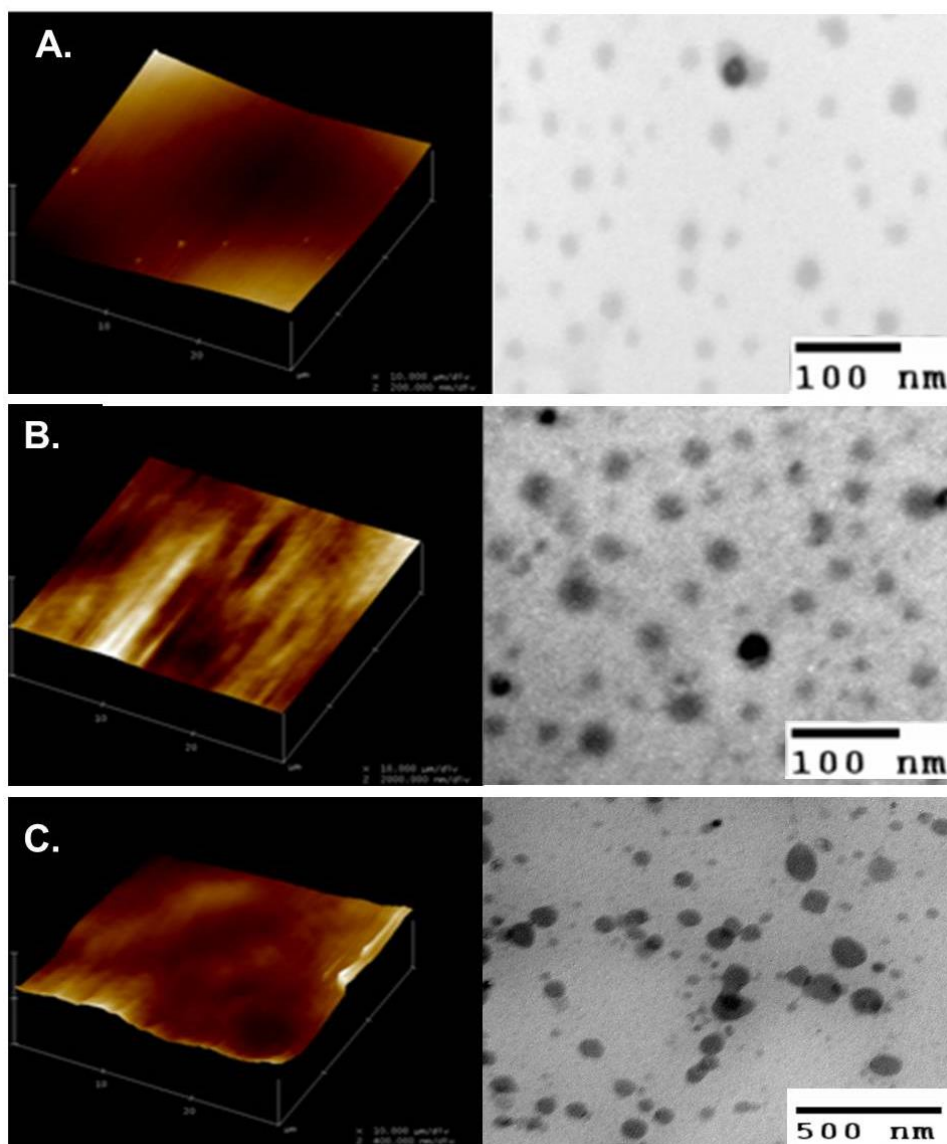


**Figure 4.6:** AFM surface roughness plots of lipoplexes coated on stainless steel 316L coupons and corresponding TEM micrographs of lipoplex solutions (A) Lipofectin <sup>™</sup>(B) DDAB/DOPE and (C) DDAB/POPC/Cholesterol.

Figure 4.6 compares and contrasts the diameters of lipoplex particles in solution with the corresponding behaviour when the particles are applied to a stainless steel substrate. The larger particle sizes and the evidence of large aggregates are supported by the higher surface roughness values confirmed by AFM.

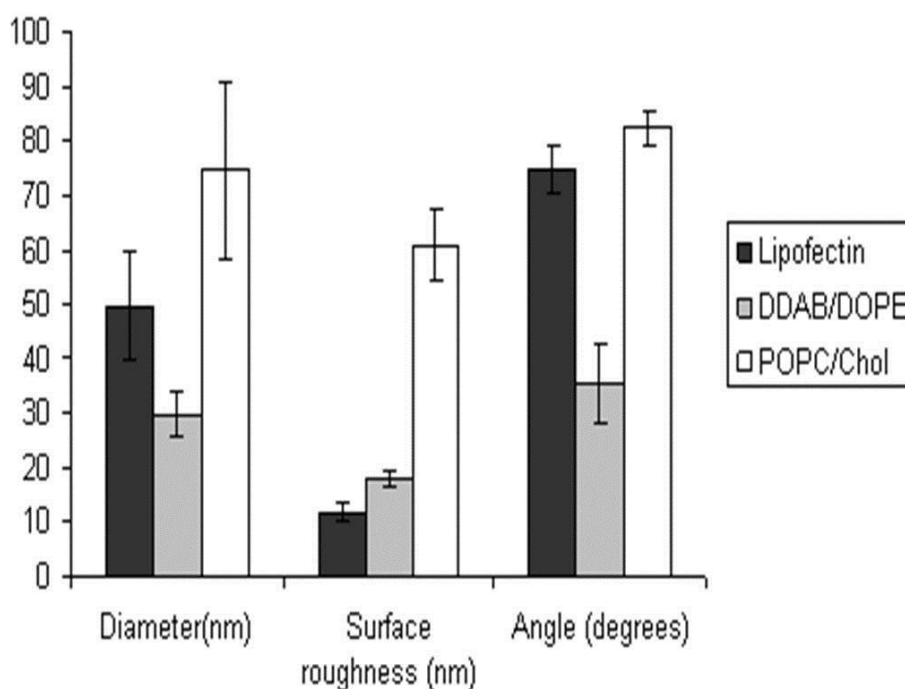


**Figure 4.7:** Biophysical comparison of the diameter (nm), surface roughness (nm) and contact angle measurement (degrees) for Lipofectin™, DDAB/DOPE and POPC/Chol.

Biophysical Characterization			Lipofectin™	DDAB/DOPE	POPC/Chol
Size	TEM	<b>Diameter (nm)</b>	49.8 ± 10.21	29.7 ± 4.15	74.8 ± 10.21
Surface Charge	Zeta Potential	<b>Charge (mV)</b>	-47.6	34.9	9.5
Surface Morphology	AFM	<b>Surface Roughness (nm)</b>	11.62 ± 1.69	18.02 ± 1.46	35.36 ± 6.56

**Table 4.1:** Tabulated biophysical data comparing all three lipoplexes.

Figure 4.7 and Table 4.1 both demonstrate that DDAB/DOPE had the smallest diameter followed by Lipofectin™ and then DDAB/POPC/Cholesterol. The variation in diameter ranged from 30 to 75 nm. Although, as expected, DDAB/POPC/Cholesterol had the largest diameter, and also the greatest surface roughness, diameter was not shown, with the other coatings, to correlate directly to surface roughness. However, the relative diameters of the liposomal formulations could be directly correlated with their surface wettability based on contact angle

measurements. These results suggest that Lipofectin™ and DDAB/DOPE form homogeneous layers when interacting with a stainless steel surface.

With regard to lipoplex particle charge, Figure 4.8 illustrates that both Lipofectin™ and DDAB/POPC/Cholesterol had a bimodal distribution of charge indicating a major and minor peak of charge. However, unlike Lipofectin™, which had a predominantly negative charge (-47.6mV), both the other lipoplexes had an overall positive charge (34.9mV for DDAB/DOPE and 9.5mV for DDAB/POPC/Cholesterol). The plasmid DNA used to form the lipoplexes, as is well documented, had a net negative charge; this is confirmed in by zeta charge analysis in Figure 4.8.

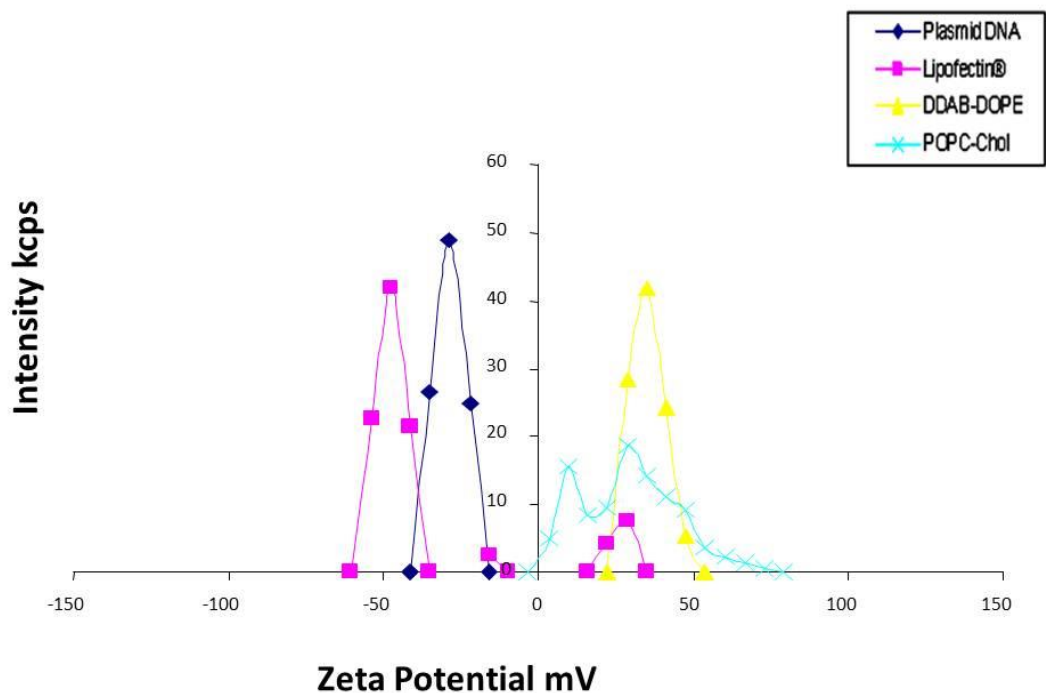


**Figure 4.8:** Zeta charge analysis of lipoplex formulations. Symbol representation : ■ = Lipofectin™; ◆ = Plasmid DNA; ▲ = DDAB/DOPE ; X = POPC Cholesterol.

In Figure 4.9, SEM micrographs illustrate the interaction of the lipoplexes with the PC-coated stents. The lipoplex coating on both the Lipofectin™ and DDAB/DOPE stents is very homogenous and uniform. This correlates well with their respective wettability and zeta charge values demonstrated

in Table 4.1. In addition, while coating both of these lipoplexes onto PC stents, it was noted how relatively quickly they dried in comparison to the DDAB/POPC/Cholesterol lipoplex. Aggregates are clearly observed on the images and also by the naked eye during the coating procedure. The phenomenon of “beading” is very prevalent on the POPC/Cholesterol stents; this indicates its hydrophobicity. Figure 4.7 confirms POPC/Cholesterol’s hydrophobicity by its relatively high contact angle values (in comparison to the controls and the other lipoplex candidates) as determined by contact analysis. Because of its viscous nature, it is difficult and lengthy (~7hours) to coat the PC stents with DDAB/POPC/Cholesterol. The SEM images confirm its tendency to coat non-homogenously and the visible presence of aggregates correlates well with the small population of large diameter particles detected in the TEM analysis of DDAB/POPC/Cholesterol in solution.

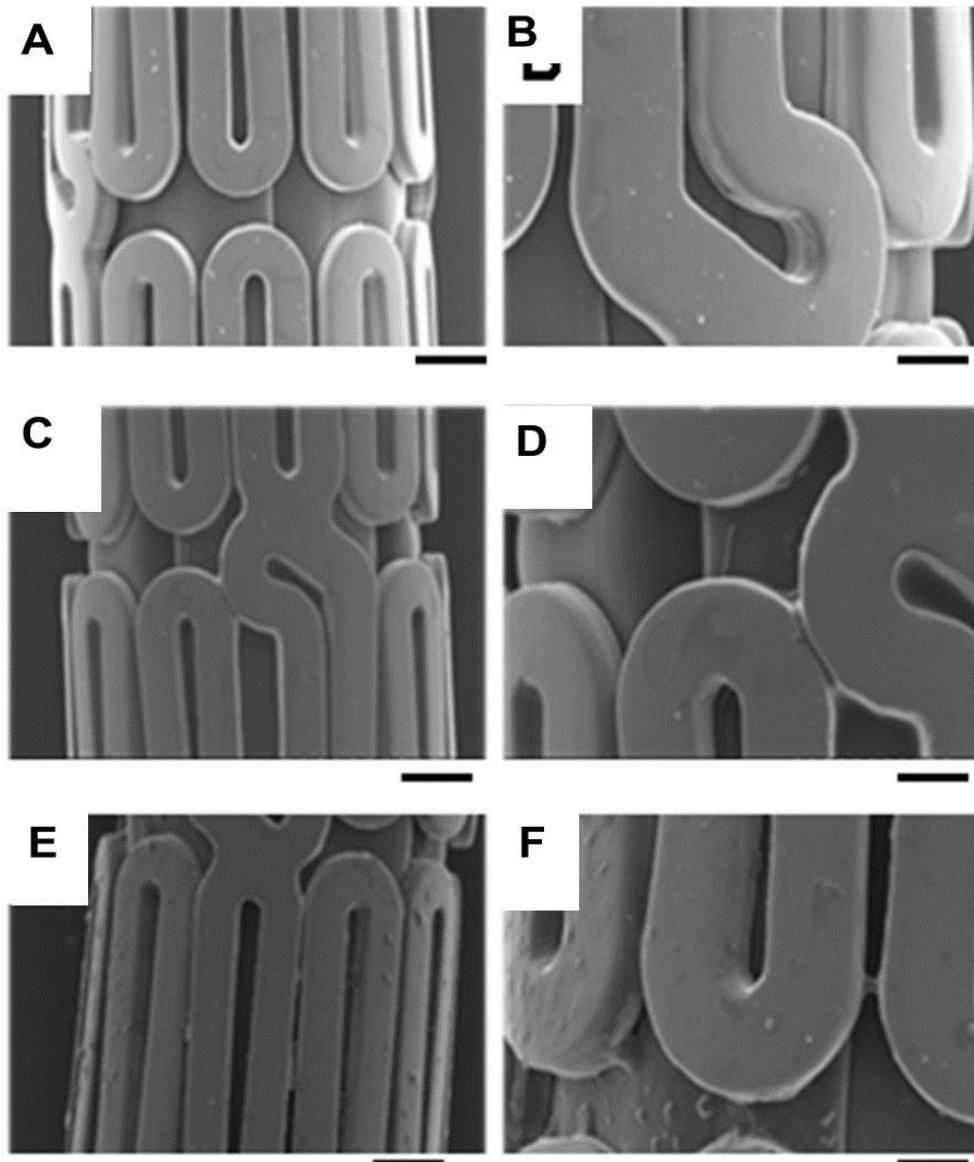


**Figure 4.9:** Scanning Electron Micrographs. Top row (A-B): SEM micrographs of Lipofectin™ coated PC stents. Middle Row (C-D): SEM micrographs of DDAB/DOPE coated PC stents. Bottom Row: SEM micrographs of DDAB/POPC/Cholesterol coated PC stents. Scale Bars: A 500  $\mu\text{m}$ ; B: 200  $\mu\text{m}$ ; C: 500  $\mu\text{m}$ ; D: 200  $\mu\text{m}$ ; E: 500  $\mu\text{m}$ ; F: 200  $\mu\text{m}$ .

## 4.4 Discussion

Medical devices are an extremely diverse cluster of healthcare products ranging from bandages to drug-eluting stents. Medical devices can utilize a variety of mechanical, electronic, chemical, pharmacological or biological actions in isolation or in combination, to address a particular clinical need (Tobin and Walsh, 2008). A clinical need can be addressed by

employing numerous methodologies, but depending on the constituents of the methodology, the regulatory path can be very different.

In light of the current landscape as previously explained in Chapter 1, Europe has a more evolved regulatory pathway than the USA for ATMPs via the Committee for Advanced Therapies (CAT) for Market Authorisation (MA). This pre-clinical study, and resultant discussion, focuses on the European jurisdiction and therefore was conducted in accordance with the European guidelines.

The complexity of the manufacturing process differs for all types of ATMPs but GTMPs such as a GES will face challenges in the areas of quality, safety, efficacy and manufacturability. The completion of the initial *in vitro* characterisation, presented in this chapter, was essential in order to establish baseline feasibility for the production of a GES.

With respect to toxicology, in addition to cytotoxicity (ISO10993:5), the aspect of biocompatibility investigated in the current study, a PC coated stent has been documented as having successfully passed the other biocompatibility metrics. These include: sensitisation (ISO10993:10); acute intracutaneous reactivity (ISO10993:6); acute systemic toxicity (ISO10993:11); haemolysis (ISO10993:4); complement activation (ISO10993:3) (tests performed by North American Life Science Associates and Huntingdon Research Ltd., on behalf of Biocompatibles Ltd, Whelan *et al* specifically looked at the biocompatibility of PC-coated stents in the porcine model in 2000 (Whelan *et al.*, 2000).

The two greatest challenges to the progression of a gene therapy medicinal product to clinical practice lie in safety and efficacy (Hu *et al.*, 2004). The potential components of 'Lipostent', namely the lipoplexes, as the delivery device is already an approved device, were examined in the

context of their ability to efficiently transfect cells without inducing high levels of cell death. This study enabled the first milestone to reach completion on this regulatory pathway, i.e. achieving satisfactory results in both *in vitro* transfection efficiency and cytotoxicity testing.

In this study, the results demonstrated that none of the candidate lipoplexes elicited unacceptable cytotoxicity in vascular and/or standard cell lines as stipulated by ISO 10993:5. The acceptance criterion for this test would be typically 80% cell viability (damage threshold criteria ISO 10993-5), which all three candidates reached. In addition, the physicochemical, morphological and topographical properties of the lipoplexes were determined on both polymer and non-polymer coated stent platforms in compliance with ISO10993:19. This characterisation profiling will also prove helpful in explaining the *in vivo* transgene expression results in the remaining chapters in the thesis.

A comparative analysis of transfection efficiency and cytotoxicity of three liposomal formulations was also performed. The lipoplexes were formulated in a 1:2 ratio of plasmid DNA to cationic lipid (-/+), this ratio was documented by Faneca and colleagues to be the most optimal in terms of protecting the DNA from nuclease degradation (Faneca, Simoes, & de Lima, 2002). In order to examine their efficacy, as would be experienced via local gene delivery to the vasculature from a coronary stent *in vivo*, it was decided to carry out the following protocol: a bare metal substrate was coated with the same quantity of liposome formulation that had been applied to a stent, for the *in vivo* section of the study (Chapter 5 and 6). This was subsequently immersed in serum-free medium for 24 hours the resultant supernatant utilised to treat cultured cells *in vitro*. Gene transfer in hCASMC and Vero cells was carried out in the absence of serum. The results showed both that transfection efficiency and low cytotoxic effects could be achieved with all three lipoplexes ranging from 1.98%, 4.67% to

9.85% in DDAB/POPC/Cholesterol, DDAB/DOPE & Lipofectin™, respectively. These results correlate well with the GFP cytometric analysis in which the autofluorescence was gated with control cells (not treated with a transfection agent) at less than 1%. A transfection efficiency of approximately 3.5% has been recorded by other investigators for commercially available Lipofectin™ mediated transfection in hCASMCS (Kiefer, Clement, Garidel, & Peschka-Suss, 2004) but those experiments were performed in serum-supplemented medium and with a DNA/TR (-/+ charge ratio of 1:3. For the purpose of this study, tissue culture conditions for transfection were maintained serum-free, as dictated by Felgner *et al*, in their protocol for cationic lipid mediated transfection protocol (Felgner, 1997). A pre-incubation step was also incorporated to improve the transfection efficiency protocol which may account for the slightly higher value attained.

Lipoplexes were also tested after a 12 month storage period at -80°C to assess the impact, if any, of long term storage on the transfection efficiency and/or cytotoxicity of the formulations on mammalian cells. This is a critical hurdle to overcome in order to demonstrate the commercial feasibility of the therapy in a clinical application. All three lipoplex formulations, both pre and post- a freeze cycle, showed a significant increase ( $p < 0.01$ ) in transfection efficiency in comparison to the negative control (cells treated with plasmid DNA but not liposomes). It was also noted that both in-house formulations (DDAB/DOPE and DDAB/POPC/Cholesterol) illustrated a trend, though not statistically significant, that improved the transfection efficiency *in vitro* after a freeze-thaw cycle. This may be due to the possibility that a freeze-thaw cycle could disassemble aggregates of lipoplex particles (>1400) that would be resistant to endocytosis by the cellular membrane as previously shown by other investigators (Kawaura, Noguchi, Furuno, & Nakanishi, 1998).

The evaluation of cytotoxicity between lipoplex formulations, pre- and post- long-term storage at -80°C, resulted only in minor differences in cell viability, which indicated that the severity and duration of the freeze cycle did not induce deleterious effects on the lipoplexes.

Although all three lipoplex formulations proved to be capable of transfecting mammalian cell lines, each lipoplex formulation however exhibited different biophysical properties, including a variation in charge and size. It is documented by investigators that intrinsic factors such as the size and charge of cationic lipoplex particles have a significant impact on transfection efficiency in mammalian cells (Resina, Prevot, & Thierry, 2009) and (Koynova, Wang, & Macdonald, 2008).

## 4.5 Conclusion

As previously described, the primary aim of this experimental study was to establish if the “vector” constituent of a lipoplex/stent delivery system (“Lipostent”) would fulfil the basic regulatory requirement of biocompatibility. To this end, the results have demonstrated that none of the candidate lipoplexes elicited unacceptable cytotoxicity as stipulated by ISO 10993-5 while all were capable of transfecting mammalian cells at levels consistent with other *in vitro* liposomal transfection rates. In addition, the physicochemical, morphological and topographical properties of the lipoplexes were characterised on both polymer and non-polymer coated stent substrates as stipulated by ISO 10993:19.

Collectively, the results demonstrate that the selection of a non-viral vector can be an efficient delivery vehicle in the vasculature when delivered from a stent scaffold. The biophysical properties and biological efficacy of both the commercially available Lipofectin™ and DDAB/DOPE make them interesting for further assessment as a coating material, whereas the third liposomal candidate, DDAB/DOPE/Cholesterol, with its

“waxy” properties, may be more suitable as a delivery vehicle from material surfaces where delamination would not be an issue, e.g. orthopaedic applications. The completion of this essential *in vitro* characterisation process enables the establishment of a baseline feasibility for the production of a GES platform.

However, it is well documented that *in vitro* performance does not always correlate with or reliably predict *in vivo* performance (Cirulli & Goldstein, 2007) and so to this end, it is vital to validate and further examine the *in vitro* results of all three lipoplex candidates in an appropriate *in vivo* model.

Prior to selecting a lead liposomal formulation, all three candidates were further examined in a normocholesterolemic rabbit model (Chapter 5) to determine the most optimal formulation from both a polymer coated (PC) and non-coated stent platform before subsequently examining the lead formulation for its therapeutic effect in a clinically relevant animal model- hypercholesterolemic NZW rabbit model (Chapter 6).

**5. A comparison of liposomal gene delivery  
*in vivo*, from bare metal and PC coated,  
coronary stents in a  
normocholesterolemic rabbit model**

## 5.1 Introduction

It has already been established that GES offer an ideal platform for local delivery of a smaller, more efficient dose of therapeutic genes. Early pioneering work on the release of genes from coated stents by R.J Levy's group (Klugherz *et al.*, 2002), (Perlstein *et al.*, 2003), (Fishbein *et al.*, 2008) demonstrated feasibility for plasmid-DNA or adenoviral-mediated gene delivery. The initial strategies for delivering therapeutic genes to the vessel wall included direct introduction through catheters at the time of angioplasty (E. G. Nabel *et al.*, 1990), (Fischer *et al.*, 2002) or via gel-coated surfaces of the balloon (Riessen *et al.*, 1993), (Asahara *et al.*, 1995). However, this type of catheter-based delivery did not produce clinically favourable outcomes (i.e. reduced ISR) to merit further investigation and hence the move to stent-mediated gene delivery. The introduction of stents to deliver genes has since proven to be far more clinically beneficial since this early pioneering phase in vasculature gene delivery.

In 2007, a review conducted by Takahashi and colleagues consolidated all the findings from major studies relating to stent-mediated gene delivery to the vessel wall (Takahashi, Letourneur, & Grainger, 2007). Interestingly, the researchers concluded that two of the primary factors for successful *in vivo* delivery, with subsequent transgene expression, from cardiovascular stents, related to 1) the layer-by-layer DNA deposition on the stent surface and 2) the prolonged direct contact with the vascular bed at the site of implantation (Takahashi *et al.*, 2007). The more recent Brito and Sharif studies, where they successfully demonstrated that focal, localised delivery of transgenes using non-viral liposomal delivery is feasible and efficient from stents (Sharif *et al.*, 2008), (Brito *et al.*, 2010b), also supported the conclusions from the Takahashi review.

Up to the present point in this thesis, assessment of potential GES options has been conducted in *in vitro* (2D, 3D) and *ex vivo* systems. The

information gathered in this phase of development has been immensely insightful and enabled the primary work in Chapter 4 to concentrate on biocompatibility and transfection efficiency aspects. Chapter 4 consolidated the view-point that precise *in vitro* assessment can help accelerate the decision-making process in early phase product development and can also effectively enable several GES candidates to be evaluated in parallel. Thorough safety and efficacy testing of potential GES technologies in pre-clinical models is paramount for successful clinical translation. The preliminary biocompatibility testing in Chapter 4 initiated this important process and provided baseline information on cytotoxicity risks. However, testing potential GES candidates in an appropriate *in vivo* pre-clinical model is an essential, progressive step. There is no single, animal model which is optimal for stent testing. The porcine model is recognised as the gold standard pre-clinical evaluation model for cardiovascular devices because of its anatomical similarities to the human cardiovascular system. However, it is prohibitively expensive to use a porcine model in this context and would be more suitable further downstream in the product development process. There are relevant smaller, rodent models available such as the Zucker rat (McMahon, Zreiqat, & Lowe, 2008) and several genetically modified mouse models (Yin, Wang, & Li, 2002), (Kuhel, Zhu, Witte, & Hui, 2002), (R. S. Schwartz *et al.*, 2004) and (De Angel, Smith, Glickman, Perkins, & Hursting, 2010). However, for rodents even as large as rats, specially modified equipment including specifically manufactured stents must be used which would not reflect the dimensions of the human cardiovascular system. In addition, reproducibly injuring the vessel wall is a significant technical challenge in such small calibre vessels. As a compromise, a cost-effective rabbit model will be used in this study to evaluate the efficacy of stent-based reporter gene delivery. Furthermore, the size of the rabbit common iliac arteries allow for the use of equipment compatible with humans (including stents), albeit in a more muscular, vascular environment than observed in the human coronary bed.

The results in Chapter 4 gave important baseline performance information (transfection efficiency) and fundamental biocompatibility indicators (cytotoxicity) but not enough measurable differences existed between the candidate lipoplexes to select a lead at this stage. Therefore, this chapter will continue to examine all three lipoplexes as the GES development transitions to evaluation in an appropriate *in vivo* model. Also, although it has been well documented that PC stents have the capability to elicit promising results in several gene delivery studies (E. S. Chan *et al.*, 2006), (Zhen, Fang, Zhou, Li, & Dong, 2006) this study will examine each lipoplex candidate on a PC coated stent versus a bare metal control for continuity and validation purposes. This study will also seelution kinetic to further investigate the technical elements (stent coating methodology and site of implantation, i.e. prolonged contact with vascular bed) postulated by the 2007 Takishari review as being important aspects for successful localised gene therapy applications.

To recapitulate, Phase I (Chapters 2 & 3) clearly demonstrated the importance of DNA encapsulation in a vector to protect it from ubiquitous nuclease digestion, the impact of vector/polymer combinations on release kinetics, stent coating technicalities and the distinct disparity between 2D *in vitro*, 3D *in vitro* and *ex vivo* transfection efficiency capabilities. These aforementioned aspects may have significance *in vivo*, and therefore the work contained in this chapter will focus on further examining the development of a GES in a pre-clinical environment. In order to provide further background to this next body of work, the following section will examine the history of stent-mediated gene delivery and specifically PC stents, stent coating methodologies and implantation sites. This section concludes with the experimental rationale and specific objectives of the work contained herein.

### 5.1.1 Stent-based gene delivery to the vasculature

A number of research groups have previously reported successful localised and sustained stent-based gene delivery to the vasculature (Klugherz (Klugherz *et al.*, 2002), (Yoneda *et al.*, 2001), (Perlstein *et al.*, 2003), (Oberfell *et al.*, 2004) (Takahashi *et al.*, 2007). In a recent review of gene therapy for cardiovascular disease, Fishbein and colleagues (Fishbein, Chorny, & Levy, 2010) and (Fishbein *et al.*, 2013) proposed that one of the primary reasons for limited progress to date, is the lack of gene delivery systems which can localise gene delivery to specific sites. They concluded that most pre-clinical studies performed to date have done so *in vivo* and have focused on the specificity of local delivery and the corresponding elution kinetics.

The Fishbein research group that conducted this review in 2010 had already previously established efficacy with bulk immobilisation of pDNA techniques from stent platforms (Fishbein *et al.*, 2008). In their study they compared denatured collagen stents (1500µg pDNA/stent) and PLGA stents (1mg pDNA/stent) in a porcine coronary model. At day 7, they demonstrated significant GFP expression levels in the neointima, notably a 9-fold difference between the denatured collagen/DNA coated stents compared with the PLGA/DNA stents ( $10.4 \pm 1.23\%$  vs.  $1.14 \pm 0.7\%$ ). This is particularly significant as the denatured collagen/DNA stents contained only 500µg of pDNA, in comparison to the PLGA/DNA stent which was loaded with 1mg of plasmid DNA. In other words the denatured collagen stent exhibited nine times more transfection efficiency than the PLGA stent, with half the plasmid loading. In the same study the authors also compared their non-viral stents with an antibody-tethered adenoviral loaded stent ( $5 \times 10^{10}$  viral particles/stent). At day 7, they demonstrated 17% transduction rate in the neointima with expression of 7% and 1% in the medial and adventitial layers, respectively (Fishbein *et al.*, 2006). This

work further substantiates the overall hypothesis of feasible, non-viral gene delivery to the vessel wall at levels that could transduce vascular cells.

### 5.1.2 PC Stents: Gene delivery

As described in Chapter 3, PC coated stents positively contributed to the successful non-viral delivery of a reporter gene to the vessel wall. Furthermore, the biophysical characterisation of the lipoplexes in Chapter 4 provided visual and quantifiable evidence of lipoplex adhesion to the PC stents. Previous studies (J. S. Chan, Wang, Zhang, Chen, & Carriere, 2000), Zhen *et al.*, 2006) have demonstrated the advantage of utilising PC stents when delivering macromolecules to the vessel wall. Chan and colleagues also demonstrated the efficient delivery of c-myc antisense (c-myc is a cytokine involved in the formation of NIH) from PC-coated stents in a porcine model. The group illustrated efficient delivery and therapeutic benefit after 28 days with significantly increased lumen patency (30.5% greater than the control,  $p < 0.01$ ), and a significant reduction in neointimal area and thickness was observed (17.5% and 19.5%, respectively,  $p < 0.01$ ). This group attributes their success to the fact that the oligodeoxynucleotides (ODNs) are a much smaller molecule than plasmid DNA and it was easier to diffuse out of the cationic polymer into the arterial tissue. They concluded that “the *in vivo* delivery efficiency study demonstrated ODN uptake was restricted to a distance of 1-2 smooth muscle cells from the lumen”. They postulated that this was more than likely because of the “increased loss from the stent prior to deployment” and suggested that further modification to the polymer was required to improve antisense retention.

Zhang repeated a similar study (*in vitro* only) to establish the efficiency of delivery of antisense ODNs from modified PC films (S. Zhang, Chan, Prud'homme, & Link, 2012). They concluded from their results that the electrostatic attraction between the anionically charged DNA and the

cationically charged choline groups is the driving force for DNA loading (J. Zhang & Zhu, 2006). From this work, in conjunction with the substantial proof-of-concept evidence from Phase I of this thesis, it is reasonable to deduce that PC has an overall positive effect on *in vivo* clinical outcomes, despite the fact that the exact mode of action is still not clearly elucidated. Therefore, this study will specifically investigate the performance of PC coating versus a bare metal control in an *in vivo* model.

### **5.1.3 Stent coating methodology**

Another important aspect of the experimental requirements of this study is the stent coating methodology. As illustrated in Chapter 2, coating the stent proved very difficult with the Pluronic, as its viscous nature made it impossible to coat with any repeatability. In comparison, the coating of the stents with both adenovirus (viral) and Lipofectin (non-viral) was significantly easier. Good transfection efficiency results ensued with both. This indicated that this more controlled coating process may have a positive impact on the vector's ability to transduce cells *in vivo*. Two coating methodologies will be examined in this chapter: 1) a layering methodology, as previously described (chapter 4) and utilised by other research groups, and 2) aerosolisation as a potential alternative to layering.

#### **5.1.3.1 Layer-by-layer (LBL) methodology**

It is well documented that a layering methodology (i.e. allowing the formulation to be deposited in discrete amounts with adequate drying time in between applications) induces a controlled release mechanism when deployed against a vessel wall *in vivo*. Several research groups have reported the use of layer-by-layer (LBL) film deposition techniques on stent surfaces. Numerous studies have established that DNA (an anionic polyelectrolyte) in solution can be used to fabricate ultrathin multi-layered films on surfaces using a variety of both natural and synthetic cationic polymers (Yamauchi, Koyamatsu, Kato, & Iwata, 2006) (Ouyang, Wang,

Zhu, Zou, & Chung, 2004),(Michel *et al.*, 2005), (Ramgopal *et al.*, 2008), (Saurer, Jewell, Kuchenreuther, & Lynn, 2009), (Cini, Tulun, Decher, & Ball, 2010), (Addison, Cayre, Biggs, Armes, & York, 2010),(Kim *et al.*, 2012) and (Kekicheff, Schneider, & Decher, 2013). Jewel and co-workers stated that the layer-by-layer procedure that they employed in their study provided a straightforward mechanism for the fabrication of films constructed using multiple layers with multiple DNA constructs (Jewell *et al.*, 2006). The group postulated that the development of ultra-thin films without the use of an organic solvent (as with the lipoplex formulations in the present study) reduced the need for polymer substrates to immobilise the DNA for kinetic release. The rationale behind the construction of multiple layers of coating is that this inherently controls the DNA release kinetic mechanism from the coating. The LBL methodology was also investigated by Yamauchi and colleagues by assembling alternate cationic lipid and plasmid DNA layers onto gold surfaces (Yamauchi *et al.*, 2006). The multi-layer film consisted of a cationic lipid-plasmid complex (cationic assembler) and free plasmid (anionic assembler). This combination was also used in the construction of lipoplex layers for previously-described work of this thesis, and is also be used in the present study.

Yamauchi and colleagues primed their inert gold substrate with a SAM (self-assembled monolayer) of carboxylic acid-terminated alkanethiol (COOH-SAM), whereas in the present study, the effect of priming with PC (which had lipophilic properties similar to that of SAM) is studied by applying lipoplex formulations to either a PC-coated stainless steel substrate or an untreated cobalt chromium substrate. This methodology, i.e. the creation of a SAM (self-assembled monolayer), has been studied in a variety of biomedical applications (Thierry, Winnik, Merhi, Silver, & Tabrizian, 2003), (Khademhosseini *et al.*, 2004) and (N. Zhang, Chittasupho, Duangrat, Siahaan, & Berkland, 2008). The primary benefit of this technique is that an active molecule, such as plasmid DNA, can be

absorbed into a vector (viral or non-viral) under standard GLP conditions in an aqueous medium. This is particularly advantageous for plasmid DNA delivery because no cross-linking or irradiation techniques are necessary to immobilise the vector. In addition, the layered approach provides enough protection from nuclease degradation. This LBL approach yielded very positive results, showing that cells (endothelial and HELUTION KINETIC293) directly cultured onto the multi-layered gold wire could successfully transduce the cells and yield exogenous eGFP (endothelial (30%) and HELUTION KINETIC293 (80%)). What was particularly noteworthy about the Yamauchi study was that the efficiency increased with an increase in number of layers applied, not with an increased plasmid DNA loading.

Interestingly, Yamauchi and co-workers also characterised the *in vitro* release kinetics of the plasmid DNA from the gold wires. They observed a burst release in the first 8 hours followed by a slower release over 6 days irrespective of the number of layers. They subsequently investigated the release of DNA under simulated arterial flow conditions (shear rate  $\sim 500\text{s}^{-1}$ ) and found that this did not affect the release kinetics, thus confirming the protective effect of layering as opposed to single dose application (Yamauchi *et al.*, 2006).

### **5.1.3.2 Aerosolisation**

One of the practical aspects of stent preparation that emerged through the experiments conducted in Chapter 4 is that it takes substantial time and effort to coat stents with vector solutions (viral and non-viral). This process could be automated but the current standard of applying an active ingredient is the use of a spray coater or an aerosolisation device. With DES, aerosolisation of the drug on to the stent surface is a standard practice to produce this product commercially. One of the reasons that life-sciences products often do not progress to market is that, although it may be scientifically competent, manufacturability and scaling-up to

commercial production levels is technically challenging. Having established, in Chapter 4, that the layering process of coating stents results in positive transfection efficiency *in vitro*, it is important to ascertain if an aerosolisation process could adversely affect the transfection capabilities of a lipoplex formulation. Given the sensitive biological nature of a gene product, it is important to elucidate if this processing step can be used to produce a GES as opposed to the manual pipetting technique employed thus far. To this end, the commercially available liposome, Lipofectin™, will be used to illustrate initial proof-of-principle data.

#### **5.1.4 Deployment pressure and implantation site**

Some of the fundamental Phase I testing of gene delivery vectors was conducted using stainless steel coupons. Two fundamental differences exist in gene delivery from both the stent and the coupon platforms: the deployment pressure and the site of implantation. The effect of deployment pressure is an aspect contributing to transgene expression, which was elucidated in Chapter 2 when *in vitro* transfection (2D static culture) alone with an amphiphilic block co-polymer (PF127) could not be achieved, although there were numerous successful reports for *in vivo* applications. Moreover, transfection was achieved when a stent (coated with an eGFP-loaded Pluronic) was deployed in a pseudovessel system *in vitro* (3D static culture). This raises the question as to the effect of pressure: does the deployment pressure (particularly the sustained pressure afforded by a deployed stent *in situ*) have an effect on transfection efficiency outcomes. It could be argued that both sustained pressure and prolonged contact with the vessel wall may have a similar effect to that of other physical transfection agents, such as electroporation, microinjection, biolistic gene gun, impalefection and soniporation. These transfection methodologies can transduce a cell by forcing the cell membrane to become temporarily permeable and allowing the vector particle (be it polymeric, viral or liposomal) to be internalised by the cell.

The deployment pressure of approximately 6-8 atmospheres (88.17-117.56 psi) is higher than the pressure applied to cells in hydrostatic pressure techniques (1-2 atmospheres/14.6-29.2 psi). This type of pressurised vascular delivery demonstrates improved transfection of unencapsulated DNA *in vivo* (Andrianaivo, Lecocq, Wattiaux-De Coninck, Wattiaux, & Jadot, 2004) and (G. Zhang, Budker, Ludtke, & Wolff, 2004).

The aforementioned study illustrated that when a large volume of unencapsulated DNA was systemically delivered into the tail vein of a 20g mouse (~2.5ml over 3-5 seconds) it resulted in high transfection efficiency in the liver. This group hypothesised that the rapid influx of a relatively large volume of fluid systemically induced a transient decrease in heart function and a rapid increase in venous pressure leading to the temporary enlargement of the hepatic fenestrae (hydroporation) to allow plasmid DNA entry. Several other authors have corroborated this (Alino, Benet, Dasi, & Crespo, 2003), (Andrianaivo *et al.*, 2004), (Kobayashi *et al.*, 2004) and (Velasco, Menendez, Alonso de la Campa, Pinto, & Crespo, 2005).

Several other investigators have also established that the optimisation of both delivery rate and volume (affecting the resultant pressure at the target site) were the most critical parameters in achieving high levels of transgene expression in the livers of mice (F. Liu, Song, & Liu, 1999), (W. Zhang *et al.*, 1997), (G. Zhang, Budker, & Wolff, 1999). To this end, it is important to establish, throughout the course of this present study, if the deployment pressure is conferring an advantage to transfection efficiency and positively influencing the process *in vivo*. In the present study, coated coupons were implanted into subjects, in a non-pressurised anatomic location, as a control experiment.

### 5.1.5 Experimental rationale

The ultimate objective in the present study is to validate *in vitro* transfection efficiency results from Chapter 4 by assessing if localised delivery and expression of a reporter gene can be achieved by each of the candidate lipoplexes (Lipofectin™, POPC-cholesterol and DDAB-DOPE) in a New Zealand White (NZW) normocholesterolemic rabbit iliac artery model. The study also examines efficacy from both a PC coated stent (316LSS TriMaxx™ stent, Abbott Vascular) compared to a BMS without a polymer (a L605 Cobalt Chromium Multi-link Vision™, Guidant). This part of the experiment should determine if PC is necessary for successful gene delivery to the vasculature or if a BMS platform could be employed instead. From these experiments, the most optimal liposomal formulation/stent platform combination should emerge and be progressed to the next stage for examination in a final study which focuses on the transition to a therapeutic gene (eNOS) in a diseased hypercholesterolemic rabbit model (Chapter 6).

In addition to the major objective outline above, this study also assessed additional important aspects, which have been repeatedly emphasised by other stent-mediated studies and corroborated in the *in vitro* assessment of this work. These include: the importance of prolonged contact and sustained pressure with the vessel wall that the stent confers versus a non-pressurised implantation site; the significance of the stent-coating methodology; comparative analysis of 28 day *in vivo* expression kinetics between viral (adenovirus and adeno-associated) and a non-viral vector. These supplementary proof-of-principle experiments will help elucidate any prospective manufacturability challenges in advance and will also provide further understanding of the potential clinical outcomes. To this end the following specific objectives will be investigated.

### **Specific objectives:**

- To assess if localised delivery and expression of a reporter gene could be achieved by each candidate lipoplex in a NZW normocholesterolemic rabbit iliac artery model from both a polymer PC coated stent (316LSS TriMaxx™ stent, Abbott Vascular) and a BMS without a polymer (a L605 Cobalt Chromium Multi-link Vision™, Guidant).
- To analyse the kinetics of expression of the non-viral vector (versus its viral vector counterparts) over a 28 day time course.
- To determine the expression capability of liposomal formulations from a stent coupon implanted subcutaneously.
- To further examine the importance of stent coating protocols in the context of GES commercialisation.

## **5.2 Materials and methods**

### **5.2.1 Plasmids**

Plasmid DNA encoding the LacZ gene driven by the CMV promoter was used as previously described (section 4.2.1).

### **5.2.2 “Lipocoupon” and Lipostent preparation**

All three lipoplexes: Lipofectin™, DDAB/DOPE or DDAB/POPC/Cholesterol were each complexed with a plasmid DNA solution (1:2 ratio) to produce a 300µl lipoplex aliquot. Each lipoplex solution, containing 100µg of plasmid DNA, was applied to the surface of a 316L PC-coated Stainless Steel (TriMaxx™ stent, Abbott Vascular), a L605 Cobalt Chromium (Multi-link Vision™, Guidant) bare metal stent, and a non-polymer coated stainless steel coupon (“Lipo-coupon”). As part of this process, the stent loaded balloon catheters were opened aseptically in a laminar flow biosafety cabinet and the packaging was removed to allow the stent portion to be exposed. The internal wire stylette (part of the pre-packaged stent-deployment system) was used to balance and suspend the

stent portion across a sterile plate without contacting it. A micropipette methodology (Figure 5.1) was utilised to deliver 30  $\mu$ l droplets to the stent surface. After each lipoplex application, the stents were allowed to air-dry under sterile conditions before rotating to the next lipoplex bolus to ensure uniform distribution.

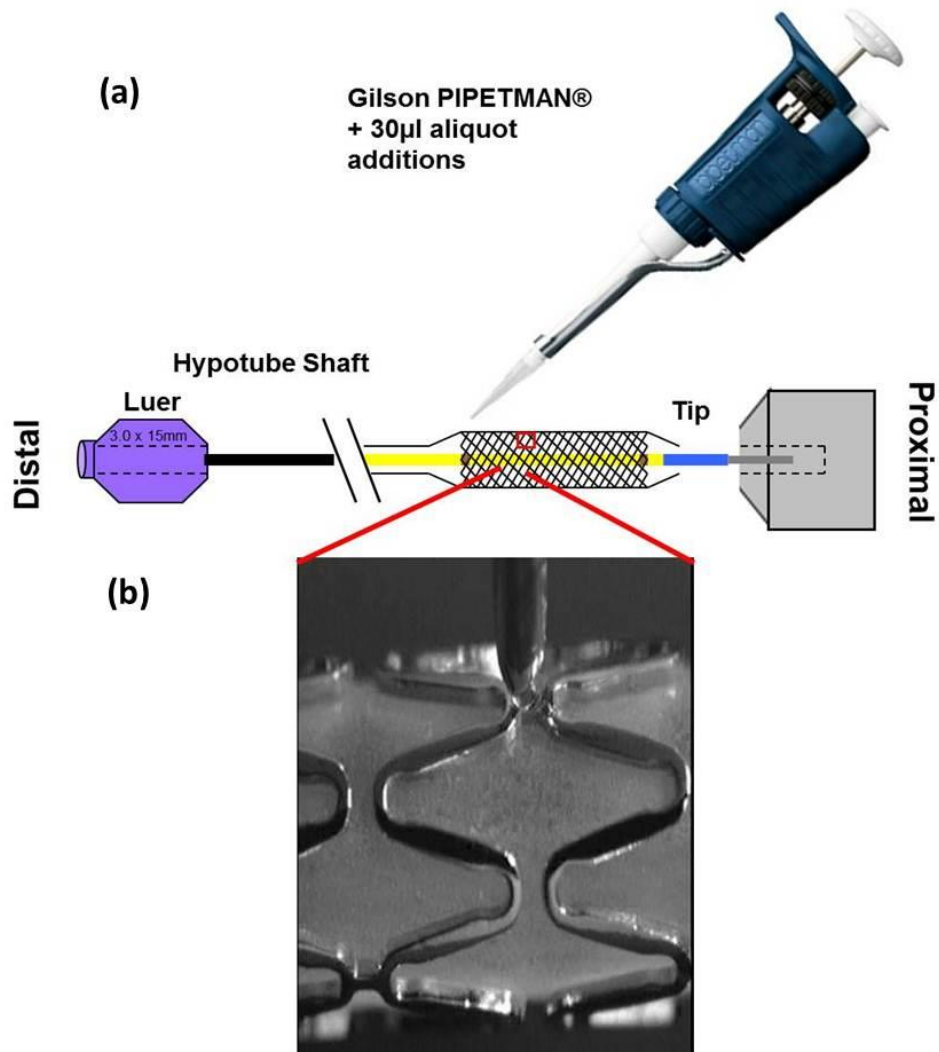


**Figure 5.1:** (a) Micropipette lipoplex deposition onto the surface of a PC coated TriMaxx™ stent. (b) Magnified image of manual pipetting of lipoplex solution onto stent strut.

### 5.2.3 Aerosolised Stents

A small number of PC coated 316L stainless steel TriMaxx™ stents were also coated with liposomal formulations using an aerosolisation

device. Figure 5.2 illustrates how the balloon catheter was loaded and secured into a sterile 50ml vulcan tube.

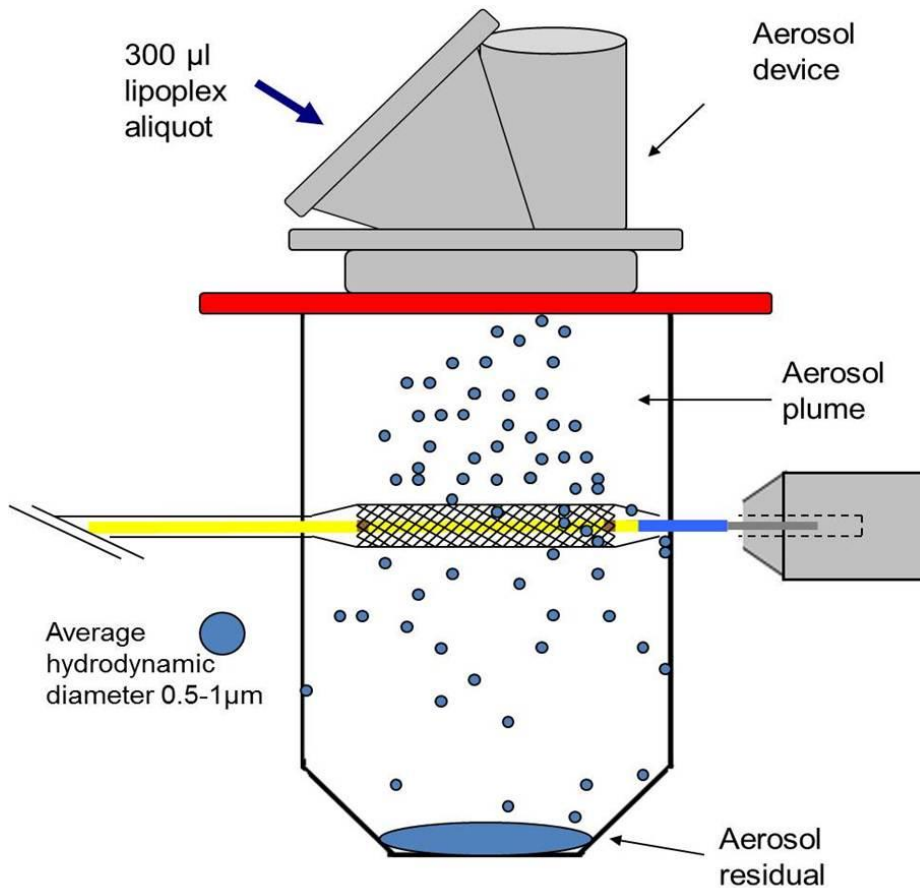


**Figure 5.2:** Aerosolisation process onto the surface of a PC coated TriMaxx™ stent.

The stent was positioned approximately 25mm down the length of the tube to ensure that the length of the stent (15mm) was aligned with the part of the aerosol plume that maximises stent coverage. The sterile cap was removed and the aerosol attachment is placed on top of the Vulcan tube. The aerosolisation device used contained OnQ™ vibrating mesh technology (Aerogen, Ireland) which contains a unique dome-shaped aperture plate containing over 1,000 precision-formed tapered holes surrounded by a vibrational element, which vibrates at over 100,000 times per second producing a low velocity aerosol.

#### **5.2.4 Animals**

The animal studies were carried out with ethical approval from the institutional animal care committee (NUI Galway) and within guidelines laid down by national legislation. A preclinical animal model was developed to assess the efficiency of liposome-mediated gene delivery to the blood vessel wall. Male New Zealand White rabbits (Harlan Ltd., UK) weighing 2.5 to 3.5 Kg were used. Animals were individually housed with a 12 hour light-dark cycle and had food and water *ad libitum*. All animals received low dose aspirin for seven days prior to intervention and thereafter until euthanasia. Animals were sacrificed at time-points from 3-42 days post-stenting with a high dose of phenobarbitone which was administered intravenously following sedation.

#### **5.2.5 Animal model**

The animal model used in the current expression study was previously developed by Sharif *et al* to deliver stents unilaterally to an injured normocholesterolemic rabbit common iliac artery via the common carotid artery (Sharif *et al.*, 2006). All animal work in this study was carried out by Dr Faisal Sharif and Dr Sean Hynes. As before, the stent was delivered over a 0.0014” guidewire using fluoroscopic guidance. Figure 5.3 shows the C-arm used for these procedures. In this experimental study, animals underwent bilateral stenting (stenting both carotids; not just one side), with post-deployment angiography used to assess patency and to ensure no acute thrombus formation.



**Figure 5.3:** GE C-arm (9800 system) used for fluoroscopic guidance of stenting procedures in the current study.

Bilateral stentings halved the number of animals required for this experimental study, thus making the pre-clinical study more ethically acceptable. In all cases only stents with the same liposomal formulations were used in the same animal. Where control stents were deployed in the same animal as a Lipostent, the control stent was deployed first to avoid any cross contamination from the introducer sheath or aorta. Lipoplex-coated stainless steel coupons were implanted subcutaneously, adjacent to blood vessels, in an animal with the same type Lipostent deployed. Mortality for the bilateral stenting procedure was approximately 10%.

### 5.2.6 *In vivo* catheter procedures

As described above, all procedures were performed under fluoroscopic guidance. Prior to the procedure, all animals were given a stat dose of 1000 units of unfractionated heparin intravenously. Animals were anaesthetised with isoflurane after sedation with ketamine (35mg/kg), xylazine (5mg/kg) and acepromazine (1mg/kg). Figure 5.4 shows the interventional set-up which was performed under sterile conditions. The right carotid artery was surgically exposed by blunt dissection and a 5 Fr introducer sheath (Radifocus, Terumo) was introduced into the artery (annotated as Common Carotid Artery in Figure 5.4) and advanced to the lower abdominal aorta. All wires and catheters were passed through this sheath.

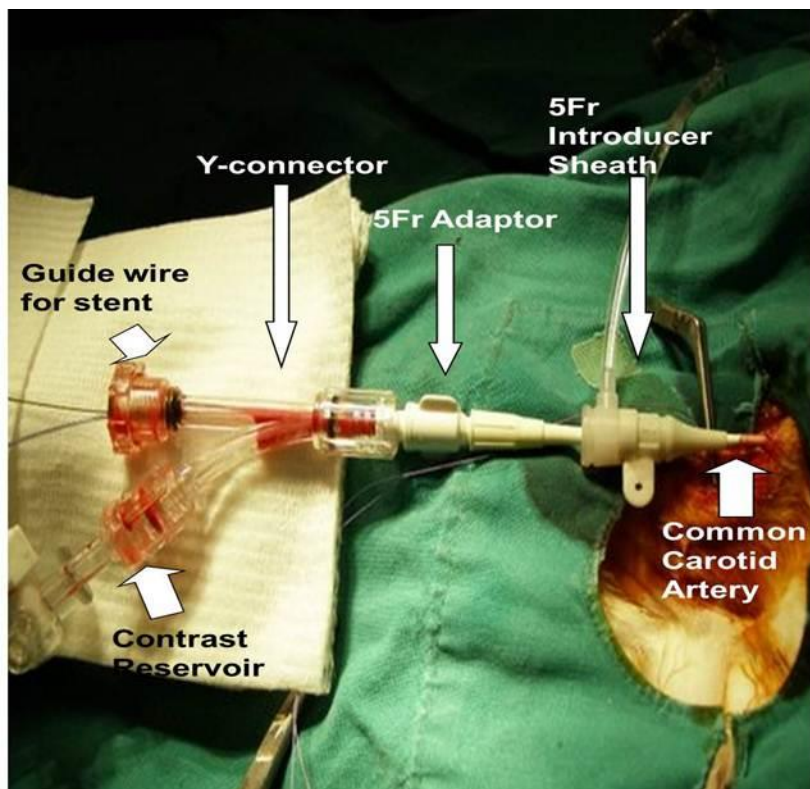


**Figure 5.4:** Stenting of rabbit common iliac arteries via the common carotid artery through a 5Fr introducer sheath (Terumo) and 5FR adaptor for a Y-connector. Normocholesterolemic animals were used for expression studies.

Figure 5.5 (a) illustrates the placement of the balloon on a 0.0014" monorail guidewire (as indicated with the stent markers pre-deployment).

Three consecutive balloon injuries were performed with a 2.5 x 14 mm commercially available balloon which was placed in either external iliac artery. Each balloon injury consisted of applying a pressure of 6 ATM for 60 seconds, with a one minute interval of deflation allowed between each injury. After balloon injury, either a 3.0 x 15 mm Abbott Vascular PC Coated TriMaxx™ stent or a 3.0 x 15 mm Guidant Cobalt Chromium Multilink Vision™ was deployed at the injury site (6 ATM for 30 second). This procedure was repeated for the left iliac artery to facilitate the bilateral stenting. Post-stent deployment angiography was carried out in all animals to exclude any acute thrombus formation at the site of stent deployment as shown in Figure 5.5 (b).

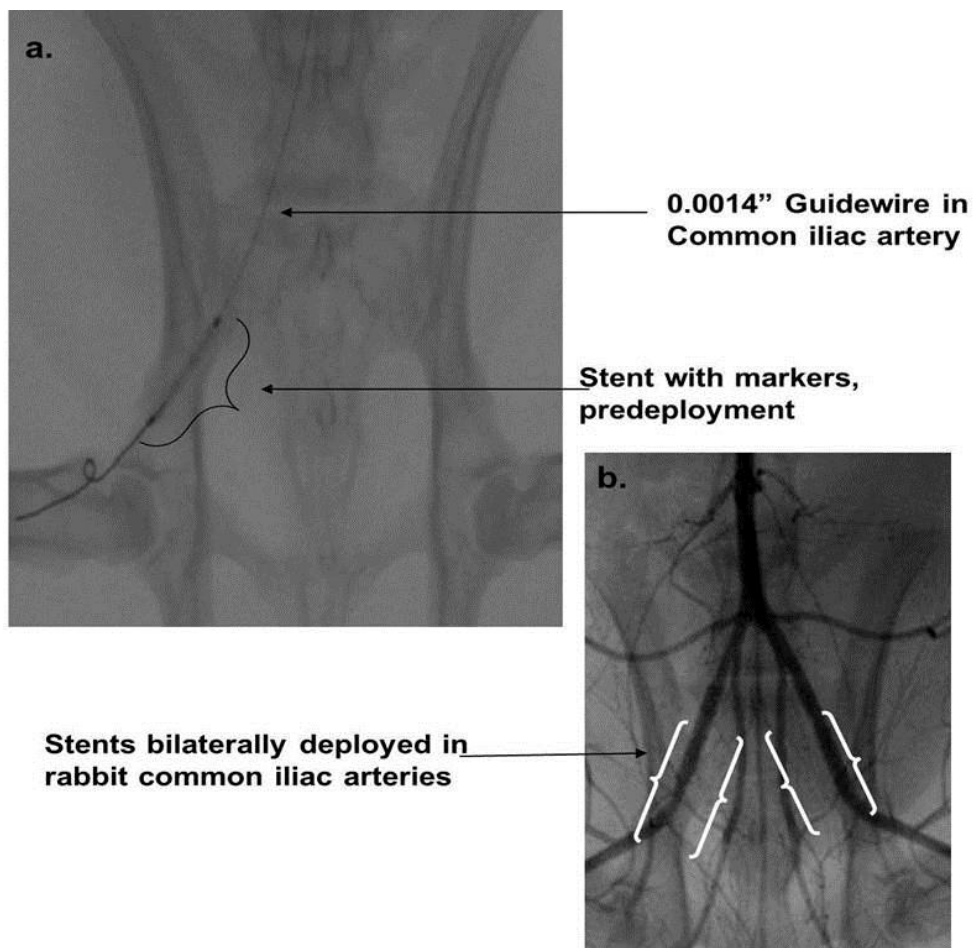


**Figure 5.5:** (a) Stent predeployment *in situ* on monorail 0.0014" guidewire in right common iliac artery. (b) Angiography of stents deployed bilaterally in common iliac arteries.

### **5.2.7 Histochemical analysis of gene expression**

$\beta$ Gal expression was demonstrated in the following manner. Following sacrifice, stented arteries were exposed, retrieved and cut longitudinally with the stent removed prior to staining of arteries. A significant neointimal formation inside the luminal face of the stent was noted at day 28 which was stripped from the luminal face of the stent and stained separately for  $\beta$ Gal expression. All stented arteries were fixed with 4% paraformaldehyde for 30 minutes at 4°C and then rinsed twice with Phosphate Buffered Saline (PBS). Arteries were then immersed in a solution of 500 $\mu$ g/ml 5-bromo-4-chloro-3-indolyl- $\beta$ -D-galactopyranoside (X-Gal; Boehringer-Mannheim Biochemicals, Mannheim, Germany) overnight at 37°C. Following staining, the arteries were then frozen in optimum cutting temperature compound. Sections (5  $\mu$ m) were then cut, placed on slides and stained with haematoxylin and eosin. Positive expression was indicated by the presence of characteristic Prussian blue cells under light microscopy.

### **5.2.8 Image analysis of Lipo- $\beta$ gal transduced vessels**

The luminal surface of all the stained arteries was photographed *en face* using a dissecting microscope. Quantification of positively stained tissue was performed using Java Image processing programme software (Image J) from the National Institute of Health. At days 3 and 7, neointimal formation could not be visualised or separated from the medial layer allowing only the vessel wall to be stained and quantified. However, at day 28 there was a significant neointimal formation observed which could be removed, stained and imaged separately to the vessel media.

### **5.2.9 Statistical Analysis**

Data for all experiments (n=3-5) were expressed and graphed either as the mean or a median value +/- standard deviation. Statistical analysis was performed using a paired student t-test for comparisons between the

groups, where \*p value <0.05 and \*\*p value <0.001 was considered statistically significant. Bonferroni-Dunnett's post-hoc testing was performed, where indicated, to analyse the effects of different lipoplex-coatings on cell viability and transfection efficiencies.

## 5.3 Results

### 5.3.1 *In vivo* Lipostent efficacy evaluation

All three lipoplex formulations were examined on both stent platforms (PC vs BMS) in the normocholesterolemic rabbit iliac artery model, at both 28 days and 42 days. The results presented in Figure 5.6 exhibit a peak of transfection efficiency at 28 days post-deployment and demonstrate persisting but declining gene expression out to 42 days. Notably all three formulations on PC coated stents demonstrated expression at 28 days from both platforms. Equal distribution of transgene expression was achieved in both the neointima (which forms around day 14) and the media of the treated vessels. Transgene expression was assessed as expression per unit area of media and neointima, and quantified using image J software from longitudinally opened arteries stained for LacZ expression using Xgal staining. Bars indicate standard deviation. Statistical analysis was performed using a paired t-test for comparison between groups. Bonferroni/Dunnett's analyses showed no difference in gene expression between stents (PC vs CoCr) for all three lipoplex-coatings, and also that the DDAB/POPC/Chol lipoplex coating is significantly worse than Lipofectin™ (0.0159) for gene expression in the media. No such effect was observed for neointima gene expression data, where the PC stent did confer an advantage over the BMS. Surprisingly, there was evidence of higher levels and more sustained *in vivo* gene delivery from metal surfaces (CoCr) as found for any given DOTAP- or DDAB-based lipoplex vs. previously reported studies that used DOTAP lipoplex (Brito *et al* (a) and (b), 2010). Overall, lipoplex-mediated gene

delivery from stents was found to be very efficient, particularly when compared with previously reported gene-eluting stent platforms.

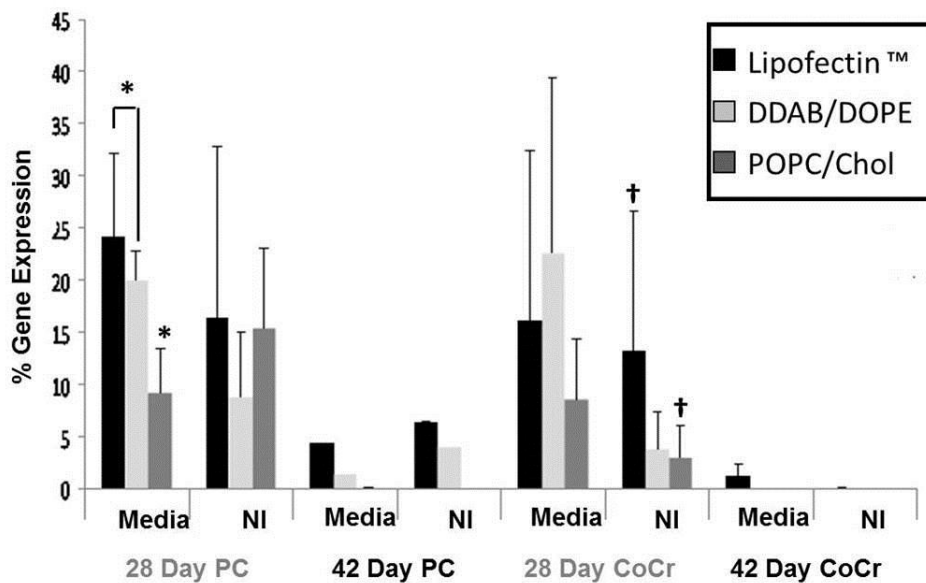


**Figure 5.6:** *In vivo* time course for transgene expression for lipoplexes (Lipofectin™, DDAB/DOPE and DDAB/POPC/Cholesterol) carrying the LacZ reporter gene from both phosphorylcholine stainless steel (PC) and cobalt chromium bare metal (CoCr) stents harvested at 28 and 42 days after deployment in the common iliac artery of New Zealand White Rabbits. Transgene expression was assessed as expression per unit area of media and neointima (NI) and quantified using image J software from longitudinally opened arteries stained for LacZ expression using Xgal staining.

### 5.3.2 Transgene expression - *in vivo*

Based on the results reported in Figure 5.6 (PC stents only) and previously published data using adenoviral and adeno-associated viral delivery from a PC stent (Sharif *et al*, 2006), a time profile for Lipofectin™ delivery from a PC coated stent for a head-to-head comparison was generated. Figure 5.7 graphically presents *in vivo* gene expression over 3, 14, 28 and 42 day time-points post stent deployment, quantified in terms of % area of transgene expressing tissue.

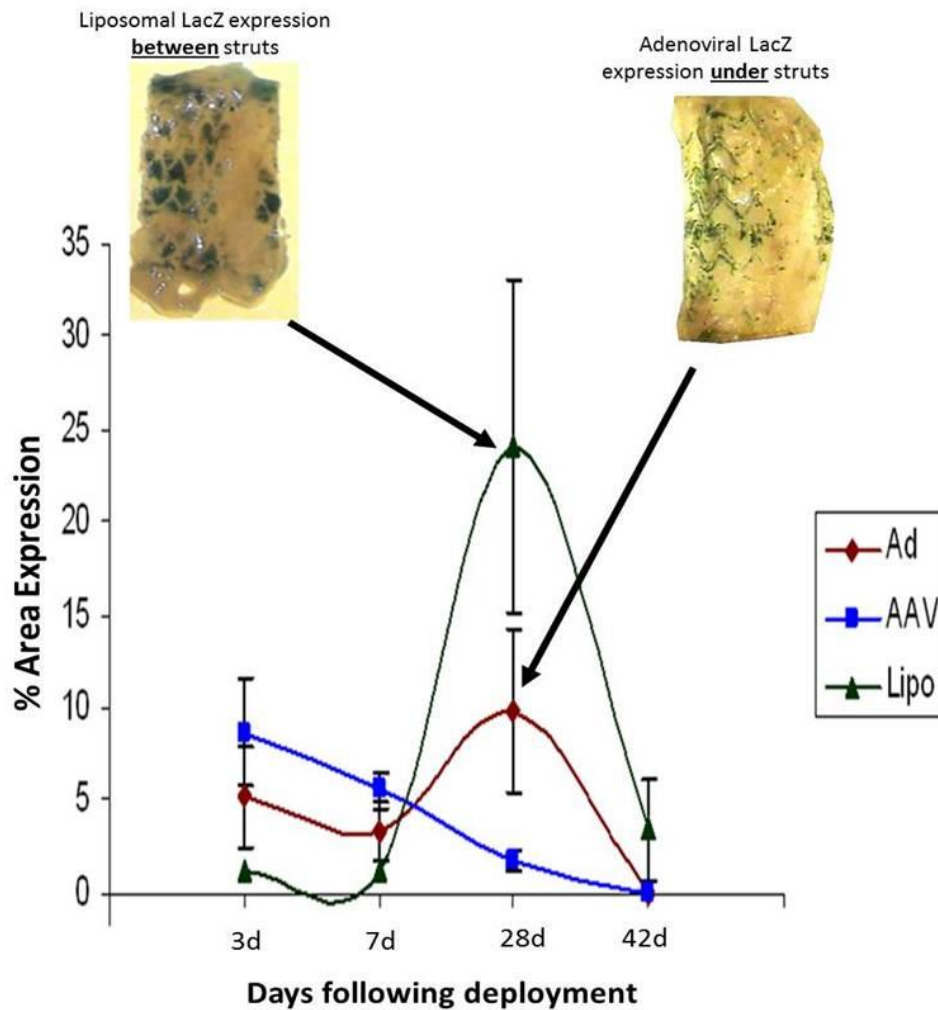


**Figure 5.7:** Comparison of expression between adenoviral, adenoviral associated and liposomal (Lipofectin™) vectors carrying the LacZ reporter gene, at 28 and 42 days post-deployment in NZW common iliac arteries, of a gene eluting stent. The viral vector data is derived from previous work reported (Sharif *et al*, 2006).

Adenoviral vector expression peaked at day 28 at 9.73% while the adeno-associated virus exhibited an entirely different type of expression profile, peaking on Day 3 and declining to 0% by day 42. Liposomal delivery of the reporter gene exhibited the same gene expression profile as the Adenovirus but has significant (24.79%) expression at day 28. Day 28 post-stenting is a significant time-point because this is when neointima formation can be best detected and visualised post injury. When directly compared to the previous findings using viral vectors (Ad-βGal) from PC stents, better efficiency (up to a 2.5 fold increase) at 28 days post-deployment for transgene expression was detected in this study for the

non-viral vector (Lipofectin™) from a PC stent platform relative to its viral counterparts.

### 5.3.3 Subcutaneous Lipocoupon mediated transgene delivery *in vivo*

Figure 5.8 illustrates subcutaneously implanted coupons retrieved with the surrounding connective tissue intact at 28 days post implantation. Liposomal expression in the surrounding connective tissue was detected by using the Histochemical staining protocol described in section 5.2.7. When the gene expression was assessed as a percentage of tissue area with transgene expression (using Image J analysis) the transfection efficiency was less than 5% for all candidate liposomes delivered from the coupon substrate.

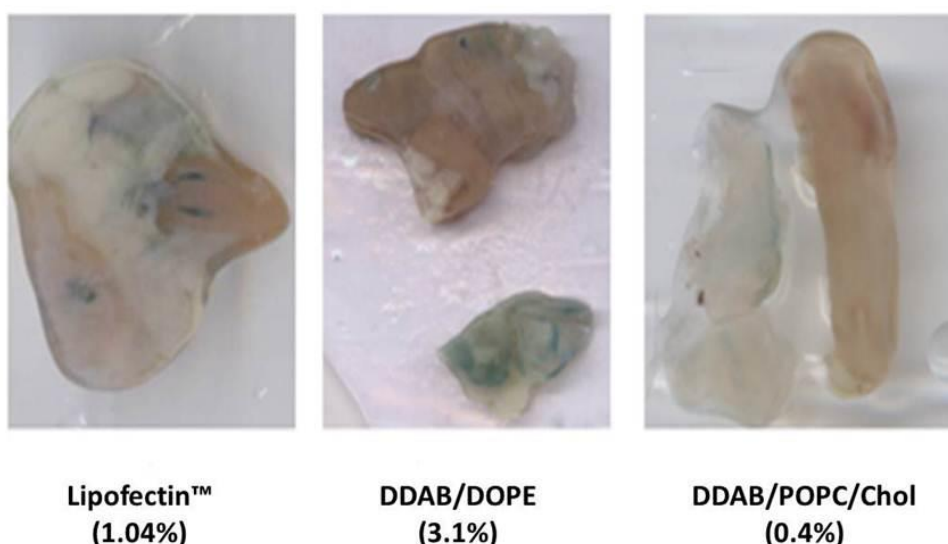


**Figure 5.8:** Tissue explants (Lipofectin™, DDAB/DOPE and DDAB/POPC/Chol) 28 days post-Lipocoupon implantation subcutaneously adjacent to iliac arteries. % area of transgene expression calculated using Image J software.

### 5.3.4 Alternative coating methodology: Aerosolisation

A minor part of this study was to explore the practicality of using aerosolisation as a potential stent coating methodology. As previously described, a small number of stents were coated using an aerosolisation device, akin to the process utilised in GMP facilities for the production of a

DES. The aim of this experiment was to establish that liposomal formulations could survive an aerosolisation process without adversely impacting the transfection capability. Figure 5.9 (a) illustrates the aerosolisation set-up and part (b) demonstrates comparative analysis of gene expression of the reporter gene at 28 days. The aerosolised PC-coated stent could successfully transfect both the neointima (5.05%) and media (1.17%) but at much lower levels compared to the results obtained from manual pipetting (17.18% vs. 24.67% in the NI and media respectively).

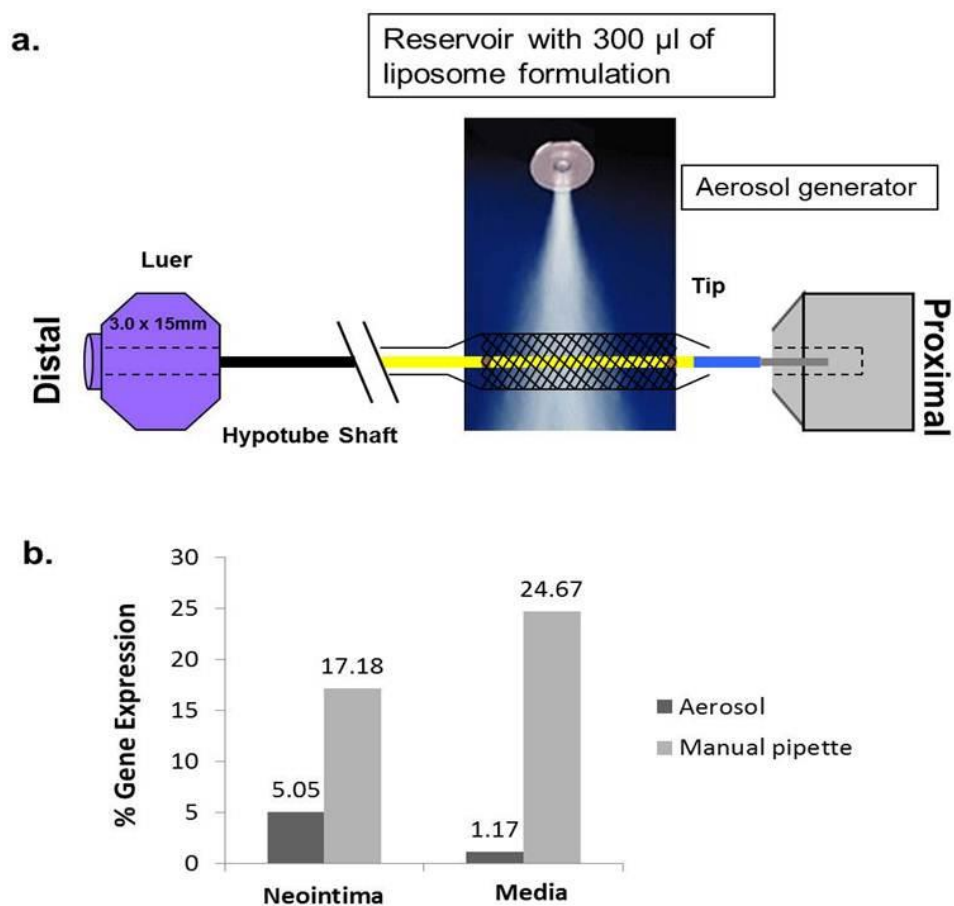


**Figure 5.9:** (a) Aerosol delivery quantification of Lipofectin™ onto the surface of a PC coated TriMaxx™ stent. (b) LacZ expression at 28 days in the media and neointima of normocholesterolemic rabbit iliac arteries with both the aerosolisation and manual pipetting methodologies.

## 5.4 Discussion

The primary aim of this study was to establish if different liposomal formulations, applied to both polymer coated (316LSS PC TriMaxx™) and BMS (CoCr Multi-link Vision™) stent systems, could be successfully delivered to the vasculature of an appropriate animal model. Using a well-established model (NZW normocholesterolemic rabbit), which was optimised further to enable the routine use of bilateral stenting, transgene expression was successfully achieved from a metallic vascular stent surface (with and without a PC coating) *in vivo*. The results presented will be discussed in the context of the preceding experimental work (Chapters 2-4) and previously conducted stent-mediated gene delivery research.

To this end, the results in this chapter will be discussed comprehensively under five specific headings: (i) *In vivo* Lipostent evaluation and the relative levels of expression for *in vitro* versus *in vivo* gene delivery; (ii) time course comparison with other vectors; (iii) impact of site implantation on transfection capabilities (iv) aerosolisation coating evaluation and (v) implantation of subcutaneous Lipocoupons.

### 5.4.1 *In vivo* Lipostent evaluation

As demonstrated in Figure 5.6, all 3 lipoplexes successfully delivered reporter genes to the vessel wall. Overall, lipoplex-mediated gene delivery from all stents (both PC and CoCr) in this study, were found to be very efficient compared to the previously reported gene eluting stent platforms. Surprisingly however, there was evidence of higher levels and more sustained *in vivo* gene expression from metal surfaces (CoCr), as found for all given DOTAP- and DDAB-based lipoplexes compared with previously reported studies that used DOTAP lipoplex (Brito, Chandrasekhar, Little, & Amiji, 2010a) and (Brito *et al.*, 2010b). This result would indicate that the PC coating does not contribute as much to the significance of the *in vivo* expression as originally thought, and questions

the necessity of the PC coating at all if a BMS would suffice. To further examine this, the interpretation of the other experiments performed in this study (stent coating methodologies and the implantation site) will help elucidate if the PC coating is a significant contributory factor to positive *in vivo* expression or not.

A further, noteworthy outcome of this study relates to the comparison of *in vitro* (Chapter 4) and *in vivo* results depicted in Figure 5.10 below. All 3 lipoplex-coated stents produced *in vivo* expression values in a ranking that matches the results found in the *in vitro* experiments generated in Chapter 4 (1: Lipofectin™, 2: DDAB-DOPE and 3: DDAB-POPC/Cholesterol). But again, no measurable differences were observed to separate a clear lead. However, at this stage, the DDAB/POPC/Cholesterol lipoplex could be potentially eliminated from further examination.

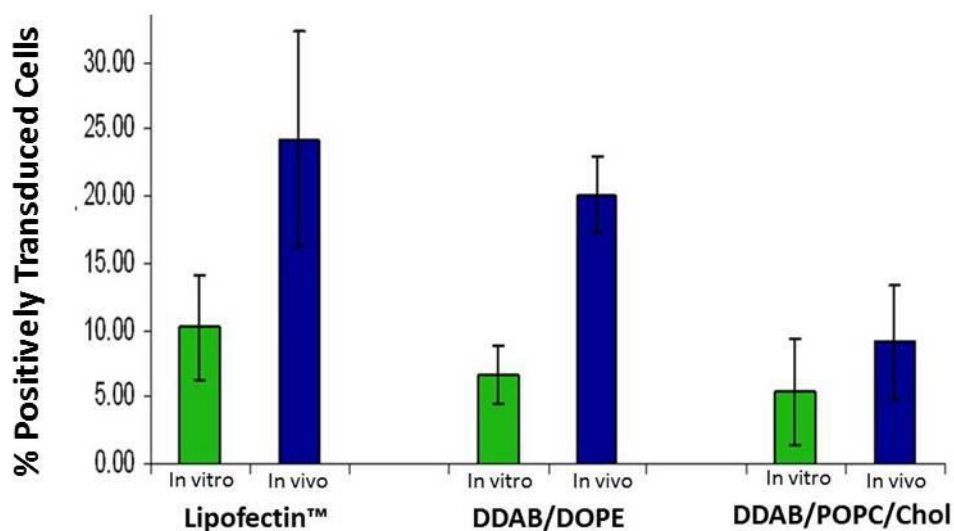


**Figure 5.10:** *In vitro* versus *in vivo* Gene Expression: Illustration of the relative levels of expression for *in vitro* and *in vivo* gene delivery of lipoplexes carrying eGFP (*in vitro*) and LacZ (*in vivo*) at 48 hours (*in vitro*) and 28 days (*in vivo*).

#### 5.4.2 Time course comparison with other vectors

As mentioned the significance of the results generated from this present study are strengthened by comparing directly with previous work conducted by others on gene delivery from PC coated stents to the vasculature (Sharif *et al.*, 2006). The transfection efficiency results discussed above (section 5.4.1) is further amplified when the leading lipoplex formulation (Lipofectin™) is compared head-to-head with both adenoviral and AAV vectors in Figure 5.7. This figure presents a comparison of the performance of adenoviral and adeno-associated coated PC-stents (Sharif *et al.*, 2006) versus the leading lipoplex formulation considered in this study (Lipofectin™ coated PC-stent) at 3, 7, 28 and 42 day time-points, where a significant difference (9.87% versus 24.71 %) in the median peak expression values was detected at day 28. All vectors demonstrated peak expression at 28 days with a steep drop in gene expression thereafter, with no detection of positive expression at day 42. The Lipofectin™ coated PC-stent demonstrated significantly higher expression at day 28 with a non-viral based vector, in comparison to its viral counterparts (adenoviral and adeno-associated coated PC-stents). This result was unexpected, and noteworthy, given that non-viral vectors generally have a relatively inferior performance profile in comparison to viral vector constructs. The result observed here may be due to a more widespread passive non-specific uptake for liposomes, in contrast to a specific uptake requirement for viral vectors. However, when reviewed in the context of the *in vitro* and *ex vivo* results of the previous chapters, there may be a more complex explanation which incorporates a number of factors. The pattern of expression and *in vitro* elution profiles are different (as previously discussed in Chapter 3) and it may be the case that the target cell that mediates transgene expression in viral gene delivery may be completely different to that observed in liposomal delivery.

As mentioned in the introduction (section 5.1), Fishbein and colleagues demonstrated a notable difference (9-fold) in transfection efficiency levels between the denatured collagen/DNA coated stents compared with the PLGA/DNA stents ( $10.4 \pm 1.23\%$  vs.  $1.14 \pm 0.7\%$ ) (Fishbein *et al.*, 2008). At the same time point, the results presented in Figure 5.7 demonstrate approximately 2% transgene expression with Lipofectin™ (100µg/stent). This is an important result because the therapeutic gene payload used in the study presented is only 10% (100µg/stent) of the concentration used by the Fishbein group (1mg/stent). In addition, this reduced therapeutic payload (100µg/stent) continued to induce an increase in expression for another 21 days before diminishing altogether at day 48 of the study.

Figure 5.7 also illustrates an initial burst of expression at day 3 (median value 2.73%; range 1.53-13.6%), gradually decreasing by day 7 (median value 1.65%; range 1.59-6.39%), for an adenoviral stent ( $5 \times 10^{10}$  PFU/Stent). This trend did not continue as maximal expression occurred at day 28 (median value 8.9%; range 1.28-16.93%) followed by a reduction of expression at day 42 (median value 7.31%; range 2.33-22.44%). It would be expected that liposomes would follow a similar expression profile but over a shorter time course than that of an adenoviral vector because liposomes are quickly endocytosed and subsequently eliminated by the body's distal organs. Conversely however, the Lipostent mirrors the time course and profile pattern of the adenovirus vector and also demonstrated prolonged duration of expression out to 42 days. The most significant result of this study relates to the peak gene expression value (24.79%) which the Lipostent demonstrates at day 28, almost 2.5 times greater than its viral counterpart (9.73%), at the same time-point in a normocholesterolemic animal model.

### 5.4.3 Impact of coating methodologies on transfection capabilities

Several different mechanistic processes have been previously described for entrapment and controlled loading of a drug into polymer films (Brazel & Peppas, 1999), (Jain, 2000), (Panyam, Williams, Dash, Leslie-Pelecky, & Labhasetwar, 2004), (Izumrudov, Kharlampieva, & Sukhishvili, 2005) and (Kim *et al.*, 2012). Layer-by-layer deposition has been postulated by many gene eluting strategists (Izumrudov *et al.*, 2005), (Nakano *et al.*, 2009), (Masuda *et al.*, 2011) and (Hossfeld *et al.*, 2013) to have an influential role in releasing bioactive molecules (including genes) in a controlled manner to prevent ISR. So as suggested at the outset of this chapter, it is reasonable to assume that a combination of both chemical interaction and physical construction of layers that determine how a gene product is released *in vivo*. It would appear from the results of this study that the physical layering of the vectors has significantly contributed to the release and subsequent evidence of gene expression *in vivo*.

Perlstein and colleagues successfully delivered plasmid DNA from denatured collagen/PLGA coated stents (Perlstein *et al.*, 2003). This group employed a methodical layering protocol to coat their stents (10 $\mu$ l additions of collagen solution loaded with eGFP plasmid, resulting in the formation of approximately 40 layers), finished with a thin PLGA topcoat to retard the elution kinetics of the DNA. Their study demonstrated that the plasmid DNA release rate from the denatured-collagen only-control stent was far too rapid (all DNA released in 30 minutes) for potential *in vivo* use. The denatured/PLGA coated stents demonstrated a transfection efficiency of 10.8% compared to the 1% transfection efficiently demonstrated in the control group. The authors of the study attributed the increase in transfection efficiency to the integrin-related mechanisms of denatured collagen with the cellular membrane. It is important to note that this group found it necessary to cross-link their collagen matrix in order to maintain the integrity of the stent coating. This process is inherently problematic as

it will deactivate the expression capabilities of the pDNA and may offer an explanation for the poor *in vivo* expression.

However, through the present study, as well as the previous work performed by Sharif and co-workers (Sharif *et al.*, 2006), a coating technique has been established for this study, which ensures a precise layering effect on the stent surface. The lipoplex aliquots (300 $\mu$ l) were substantially greater than the adenoviral aliquots (50  $\mu$ l) in order to hold the same concentrations of pDNA. This larger lipoplex aliquot volume necessitated the lipoplex to be coated in onto the stent surface, in 30  $\mu$ l quantities, with a 30-40 minute drying period between coatings. As the coating layers built up, the stents became more difficult to coat and the aliquots volumes were reduced to 10  $\mu$ l and 5  $\mu$ l respectively until the entire 300  $\mu$ l lipoplex aliquot was loaded onto the stent surface. This coating process inadvertently created “pseudo-layers”, with up to 30 separate additions made during any given coating application. Given the extensive literature on layer-by-layer coating technologies, this coating procedure could have induced a “controlled release” mechanism in the lipoplexes.

This precise coating protocol has been demonstrated to significantly enhance a non-viral (Lipo- $\beta$ gal) stent platform to deliver and express a transgene at a higher level (22.42% media; 16.88% NI) compared to an adenoviral (Ad- $\beta$ Gal) platform (8.87% media; 1.01% NI) at the same time-point (28 days).

It was observed and documented during the stent coating procedure (section 5.1.2), with lipoplexes, that with the first round of lipoplex application there was always a noticeable “beading” effect. The beading effect was more pronounced on the cobalt chromium (BMS) platform than the PC-stents. This is logical as the cationic choline head groups of the PC polymer should bind better with the anionic DNA. The

more pronounced beading or higher contact angle values (45° versus 30°) is indicative of the relative hydrophobicity of the inert metal substrate compared with the PC-coated metal substrate. However, the subsequent applications on both substrates did not exhibit this phenomenon, suggesting that the previous lipoplex layer acts a “primer” coat, so that multiple subsequent layering can be achieved. It was observed and noted during the aerosolisation process that although some lipoplex formulation was successfully adhered to the stent surface, the majority of the volume (>70%) was captured in the receptacle. Considering all aspects of the results presented in this study, the aerosolisation process would need to be significantly modified to be utilised and automated on a large scale to fulfil manufacturability requirements for any potential GES product.

#### **5.4.4 *In vivo* time course of candidate Lipostents**

Figure 5.8 illustrates the transfection efficiency of the candidate liposomes out to 42 days post-deployment. Interestingly, the type of stent used had a significant effect on the gene expression, independent of liposome used. Expression at 28 days in the neointima was statistically better ( $p < 0.05$ ) for all liposomes when a PC-coated stent was used to deliver the liposomes. This is a significant result as it supports the hypothesis that a PC coating positively enhances gene expression *in vivo*, independent of the liposome used. Also, prolonged expression in the NI at 28 days is significant as non-viral techniques normally demonstrate short, transient gene expression post –delivery. This evidence of prolonged gene expression, from a non-viral vector, is important, particularly out to 28 days, the time-point known for NIH formation *in vivo*. It is imperative that that there is continued gene expression at this time-point to ensure that a clinically relevant therapeutic effect can be induced *in vivo*.

#### 5.4.5 Implantation of subcutaneous candidate Lipocoupons

In comparison to their subcutaneous coupon counter-parts, the lipoplex-coated stents deployed in the iliac arteries demonstrated a significantly higher level of transgene expression, across all three formulations. These values were presented for both subcutaneous and vessel delivery in Figures 5.6 and 5.7, respectively, and collated for comparison purposes in Table 5.2 below. There was a significant 6 fold increase in expression, with the application of DDAB/DOPE to a stent, in comparison to the corresponding subcutaneous coupon delivery. The difference was even higher (greater than 20-fold) with Lipofectin™ and POPC/Cholesterol when delivered to the vessel wall.

Lipoplex Formulation	Subcutaneous Coupon %	Iliac artery Stent %	X-Fold Difference
Lipofectin™	1.04	24.9	24
DDAB/DOPE	3.1	19.4	6
POPC/Chol	0.4	9.3	23

**Table 5.1:** Comparison of gene delivery of candidate liposomal formulations from both stent and coupon substrates.

This was quite an unexpected result, as the surface area of the coupon with a 10mm diameter (both sides coated =  $2\pi r^2$ ) is  $157\text{mm}^2$ , enabling the entire 300 $\mu\text{l}$  aliquot (delivering 100 $\mu\text{g}$  of pDNA) of lipoplex to be deposited on the surface of the coupon. In any given stent coating, with the micro-pipette methodology of application, only 60-70% of the lipoplex formulation could ever be successfully applied to the surface of a stent. Despite this, the coupons exhibited much lower levels of transgene expression than that of the corresponding stent (3mm diameter) with a maximum relevant metallic surface of approximately  $16\text{mm}^2$  (calculated from surface area of cylinder ( $2r\pi h$ ) less open cell area for a 15mm stent),

that represents almost 10 times less available surface area than the coupon.

To explore this apparent anomaly, it is important to investigate further two potential factors contributing to these results: firstly, the presence of sustained pressure at the site of deployment of the stent and its absence in the subcutaneous implantation of the coupon, and secondly, the site of implantation of the stent versus that of the coupon. Although in Figure 5.8 all three lipoplexes delivered from coupons illustrated unexpectedly low expression (<5%) this was an isolated experiment and did not have the statistical power to be a significant result. However, it does indirectly support the unexpected finding from Chapter 2, which introduced that the introduction of pressure, particularly sustained pressure from a stent, can positively enhance non-viral gene delivery and expression in an *in vitro* system.

As suggested by the experiments conducted in Chapter 2, pressure, in particular the sustained pressure afforded by the permanent scaffolding nature of a deployed stent *in situ* in the vasculature, is hypothesised to contribute significantly to the high levels of expression of non-viral vectors (amphiphilic polymers and liposomes). This observation was particularly unexpected as non-viral vectors are traditionally poor in comparison to their viral counterparts.

In 1996, Meyer and colleagues also reported that pressure-induced stretching of the arterial wall is a major determinant of arterial mass transport in their experiments of delivery of LDL (26.1 ± 0.9mm) to the rabbit aortic wall (Meyer, Merval, & Tedgui, 1996). The correlation between hydrostatic pressure and transfection efficiency has also been illustrated in cardiovascular tissues. Mann and colleagues (M. J. Mann et al., 1999) illustrated this relationship with their study of pressure-mediated ODN transfection in both human and rat cardiovascular tissues. In this

study, human saphenous veins and rat myocardium were treated in an *ex vivo* setting with controlled, non-distending pressure, 1 atmosphere/14.6 psi and 2 atmospheres/29.2 psi, respectively, without the use of an encapsulating vector. They successfully achieved nuclear localisation of FITC-labelled ODN in both the saphenous vein (90%) and myocardium (50%) tissues respectively. They concluded that pressure-mediated transfection may enhance the hydrostatic movement of ODN through interstitial spaces, delivering it efficiently to the cell surface for internalisation and subsequent transgene expression. Ander and co-workers also employed this pressurised *ex vivo* perfusion technique with a transmural pressure of 400mmHg (0.5 atmosphere/7.73 psi) and reported that the concentration of fluorescently-labelled microspheres (approximately 60-90nm in diameter; comparable to an adenoviral particle) in the intimal layer to be significantly higher ( $p < 0.03$ ) than those that had no pressure applied (Ander, MacLennan, Bentil, Leavitt, & Chesler, 2005). The pressure at a local site, in the case of this study, directly under the stent struts, may physically permeabilise (open channels in cell membrane) and enhance DNA extravasation, followed by DNA uptake, as hypothesised by Budker and colleagues (Budker *et al.*, 2006).

The second factor that may explain the more favourable results from a stent platform relative to than from a coupon surface is the site of implantation: subcutaneous versus arterial. There is very little research performed on the effect of different anatomical compartments on the host response to foreign material implantation. However, a study conducted by Mendes and colleagues (Mendes, Campos, Ferreira, Bakhle, & Andrade, 2007) analysed the inflammatory response to sponges in subcutaneous and in intraperitoneal sites in mice. The metrics they analysed included inflammation, angiogenesis and production of cytokines. They reported that although the level of neutrophil and macrophage accumulation was similar at both sites, the chemokine levels were varied, and most

significantly, there was a 14-fold increase in VEGF surrounding the intraperitoneal implants at day 3. From this it is reasonable to deduce that certain environmental factors, such as implantation site, could affect the biocompatibility of exogenous materials placed at different anatomical sites and therefore their resultant expression capabilities.

The results in this chapter are in line with Brito and colleagues' findings when they successfully delivered lipo (poly) plexes from gelatin covered meshes in an iliac artery restenosis model established in NZW rabbits (Brito *et al.*, 2010a). They detected substantial GFP expression in the medial layer, especially proximal to the stent struts. Their results were comparable to studies that used DNA at 50-100 fold higher concentrations and with viral-based delivery systems (Klugherz *et al.*, 2002), (Fishbein *et al.*, 2006) and (Sharif *et al.*, 2006).

Brito and colleagues found encouraging preliminary transfection efficiency at 24 hours, however the results presented here have shown expression at 28 days and out to 42 days, which is a fitting time-course, as it tracks the natural biological cascade of events post-injury and provides researchers with an opportunity to combine appropriate therapeutic genes, be it for SMC inhibition or re-endothelialisation.

## 5.5 Conclusion

Taking all contributory factors into consideration, the lead formulation from the *in vitro* characterisation (Chapter 4) and the *in vivo* expression studies (Chapter 5) is Lipofectin™ coated onto a PC TriMaxx™ stent. This is most likely due to optimal charge interactions between the lipoplex and the PC coating, enhanced by the layering coating technique, which results in controlled release of the gene vector into the vessel wall.

Even though the stainless steel coupon has a greater surface area, with maximal vector application, the expression levels were between 6-24 fold higher on the corresponding liposomal covered stents (with 60-70% of the DNA quantity applied). In addition, all three lipoplex formulations delivered performed significantly better in the neointima from PC-stent platforms. However, the chemical interaction between the PC coating and the lipoplexes alone does not completely explain the discrepancy observed between the Lipocoupons and Lipostents stents. Therefore, it is important to consider the results in the context of localised stent based gene delivery to date.

Overall, this work highlights the superiority of lipoplex to viral gene therapy and the flexibility of lipoplex formulations in delivering genes from stent platforms. To this end, Lipofectin™, complexed with eNOS delivered from both a PC coated and a bare metal stent, platform will be further explored in the next chapter - preclinical testing of a therapeutic gene (eNOS) in hypercholesterolemic rabbit model.

**6. Liposome-mediated delivery of a  
therapeutic gene, eNOS, to the  
vasculature of a hypercholesterolemic  
rabbit model**

## 6.1 Introduction

DES, as previously discussed, have been associated with a higher frequency of very late stenosis and re-infarction (more than one year) compared to bare metal stents, 1.9% vs. 0.6% per year, respectively (Carter, 2002) and (S. W. Lee, Tam, & Chan, 2011). In addition, animal studies have shown that DES can cause local toxicity to the vessel wall in the form of medial necrosis, intimal proliferation, chronic inflammation and delayed re-endothelialisation of the stents (Chieffo *et al.*, 2008), (Q. Huang, Hong, Xu, & Liu, 2009) and (Towae, Zahn, & Zeymer, 2009). The prevalence of the aforementioned side-effects of DES coupled with the increasing rise of co-morbidities, in an ageing population, necessitates the development of next generation stents that are not reliant on pharmacological interventions. Gene eluting stents fulfil this criteria and an optimal therapeutic approach would involve a strategy which inhibits hyperplasia while promoting re-endothelialisation and suppressing stent- or vector-related inflammatory side effects.

Goh and colleagues recently conducted a comprehensive review of gene technologies for the treatment of ISR (Goh *et al.*, 2013). This review investigates the fundamental principles of gene delivery to the vasculature and comprehensively evaluates the research on gene therapies for CVD over the last decade. The review concludes that *“utilising nanotechnology, sustained and localised delivery of a gene can mitigate the problems of restenosis and late ST by accelerating the regenerative capacity of re-endothelialisation”* (Goh *et al.*, 2013). The study presented in this chapter focuses on sustained and localised delivery of a therapeutic gene to the vessel wall to accelerate re-endothelialisation, thus returning the damaged SMC medial layer to a state of quiescence (i.e. non-proliferating) and preventing the formation of NIH.

The previous chapter investigated if the efficacy of gene delivery was mediated by the underlying substrate (bare metal or PC-coated), or if the method of coating had an impact on how genes are delivered to the vessel wall. This study will investigate the importance of the choice of therapeutic gene. To this end, this study will evaluate the effect of delivering eNOS to the vasculature to stimulate accelerated re-endothelialisation in a hypercholesterolemic rabbit model.

**Overall goal:** To evaluate the efficacy of localised stent delivery of the leading lipoplex (identified from Chapter 5) with a therapeutic gene (eNOS) to the vasculature of an appropriate *in vivo* model.

**Specific objectives:**

- To evaluate eNOS expression in the hypercholesterolemic NZW rabbit model 3, 7, 28 and 42 days after vessel wall gene delivery.
- To measure key parameters such as re-endothelialisation (presence and extent), external elastic lamina (EEL), internal elastic lamina (IEL), lumen area, medial area, percentage neointimal area, % stenosis, injury score and inflammation score.
- To establish a correlation between the extent of re-endothelialisation and percentage neointimal area.

### **6.1.1 Endothelial Nitric Oxide Synthase (eNOS)**

Nitric Oxide (NO) is a pleiotropic diatomic molecule with many diverse roles in the vasculature. It has anti-atherogenic properties including inhibition of smooth muscle cell proliferation and inhibition of platelet aggregation, as well as having vasodilator effects. NO is synthesised normally by endothelial cells and plays a vital role in maintaining homeostasis and vascular tone regulation. When injury occurs to the vessel wall, NO is a critical component in its endogenous defence mechanism

(Lake-Bruse *et al.*, 1999), (Rosanio, Tocchi, Patterson, & Runge, 1999) and (Janero & Ewing, 2000).

NO is synthesised from guanidine nitrogen of L-arginine by one of three nitric oxide synthase (NOS) enzymes: eNOS, nNOS and iNOS. nNOS (neuronal) and eNOS (endothelial) are constitutively expressed and are activated by increasing calcium levels (Ca<sup>2+</sup>) via Calmodulin (Frank, Kolb, Werner, & Pfeilschifter, 1998). The third isoform of NOS, iNOS (inducible), is not constitutively expressed but rather is “induced” in response to microbes, cytokines, hypoxia, thus producing NO (Kibbe *et al.*, 2000).

NO is a free radical, which diffuses freely from its site of production and has a half-life in the order of seconds. NO’s primary function is to regulate vascular tone, inducing relaxation of vascular smooth muscle and dilatation of blood vessels (Schechter & Gladwin, 2003).

Several investigators have previously utilised eNOS expression in the vasculature to increase NO production (Kullo *et al.*, 1997), (Cooney, Hynes, Sharif, Howard, & O'Brien, 2007) and (Sharif *et al.*, 2008). As previously described, Sharif and co-workers have successfully transduced rabbit iliac arteries with a therapeutic eNOS gene (which induces the up-regulation of the eNOS enzyme), using an adenovirus-mediated GES, resulting in enhanced re-endothelialisation with a reduction in intimal hyperplasia at four weeks post-gene delivery (Sharif *et al.*, 2008). However, adenoviral mediated gene delivery to the blood vessel wall has been associated with inflammation which may impede progress of this potential therapy to the clinic (Newman *et al.*, 1995), (Feigenblum, Walker, & Schneider, 1998) and (Perlman *et al.*, 2000).

### 6.1.3 Experimental rationale

As previously described (Chapter 1), the arterial injury response post stent implantation is a classic wound healing response characterised by a three-phase healing process: inflammation, proliferation and maturation (Hofma *et al.*, 2001) and (R. S. Schwartz & Henry, 2002). However, the primary phenomenon that drives the proliferative phase is the removal of the endothelium. Endothelial denudation is a two-fold problem, firstly the vessel lumen is no longer non-thrombogenic with the loss of the endothelial lining, and secondly, the disruption of lining causes the quiescent SMC medial layer to exit G0 of the cell cycle and enter a proliferative phase which becomes exaggerated when re-endothelialisation does not occur to modulate and return the SMC layer to its quiescent, non-proliferative basal state.

In Chapter 5, three liposomal formulations were examined in a normocholesterolemic *in vivo* model to determine the leading option. The aim of the study in Chapter 6 was to evaluate the efficacy and patterns of expression of the lead formulation from the previous chapter, i.e. Lipofectin™, with PC coated stents and on bare metal cobalt chromium stents over a period of time extending to 42 days. The purpose of this experiment is to evaluate the therapeutic potential of utilising lipoplex-mediated delivery of eNOS to the stented vessel wall using neointimal formation (histomorphometric analysis) and endothelialisation (Evans Blue) as primary end-points.

In the course of this study, transgene expression using a nuclear-targeted LacZ was also investigated to ensure that the gene expression observed in the previous chapters is not over-estimated and to further validate the efficacious performance of liposomes that has been reported, in comparison to an adenoviral system. From the hypothesis outlined in Chapter 1, it is proposed that stent-mediated Lipo-eNOS delivery to the

iliac artery of a hypercholesterolemic NZW rabbit will induce re-endothelialisation and decrease NIH. The study proposed here will test this hypothesis, and in addition, establish if the delivery of eNOS from a PC coated stent re-endothelialises better than delivery from a bare metal stent.

## **6.2 Materials and methods**

### **6.2.1 Plasmids**

The following plasmid DNA constructs were amplified in *E.coli* and prepared and purified using Endofree Plasmid Giga Kit manufacturer's instructions (Qiagen): a nuclear-targeted NLS-LacZ ( $\beta$ Gal), a cytoplasmic-targeted CP-LacZ ( $\beta$ Gal), a pcDNA3 empty vector and a CMV-eNOS gene.

### **6.2.2 Cloning of human eNOS**

A human eNOS gene (3.7 Kilobase pairs) was codon optimised and synthesized by GENEART (Germany). The optimised codon, eNOS, was then inserted into the backbone of a pWPTGFP plasmid (Tronolab, Lausanne, Switzerland) by splicing (using restriction enzymes) between the Bam H1 and Sal1 sites in the plasmid's Multiple Cloning Site (Kulldorff *et al.*) as illustrated in Figure 6.1 (a). This plasmid is controlled by an EF1 $\alpha$  promoter. However, the experiments in this study require the plasmids to be under the control of a CMV promoter. For this reason the human eNOS fragment was then excised and ligated from the pWPTeNOS (using BamH1 and Sal 1 restrictive enzymes) into a mammalian eukaryotic expression vector, pcDNA3.1 (5.4 kilobases in size). This plasmid contains the required CMV promoter control as graphically illustrated in Figure 6.1 (b) and therefore the plasmid was linearised with the restrictive enzyme XhoI, blunted and subsequently cut with the BamH restrictive enzyme to allow the excised eNOS gene from the original pWPTeNOS plasmid to be inserted. This eNOS gene is now under the control of the CMV promoter within the pcDNA 3.1 plasmid producing a vector expressing the human

eNOS gene under the immediate early CMV promoter (Figure 6.1 (c)), 9.1kilobase pairs. This insertion could only occur by linearising the pcDNA3.1 vector with an Xho1 restriction enzyme first. Ligated products were transformed into *E.Coli* and the resultant bacterial colonies were screened for the inserted clone.

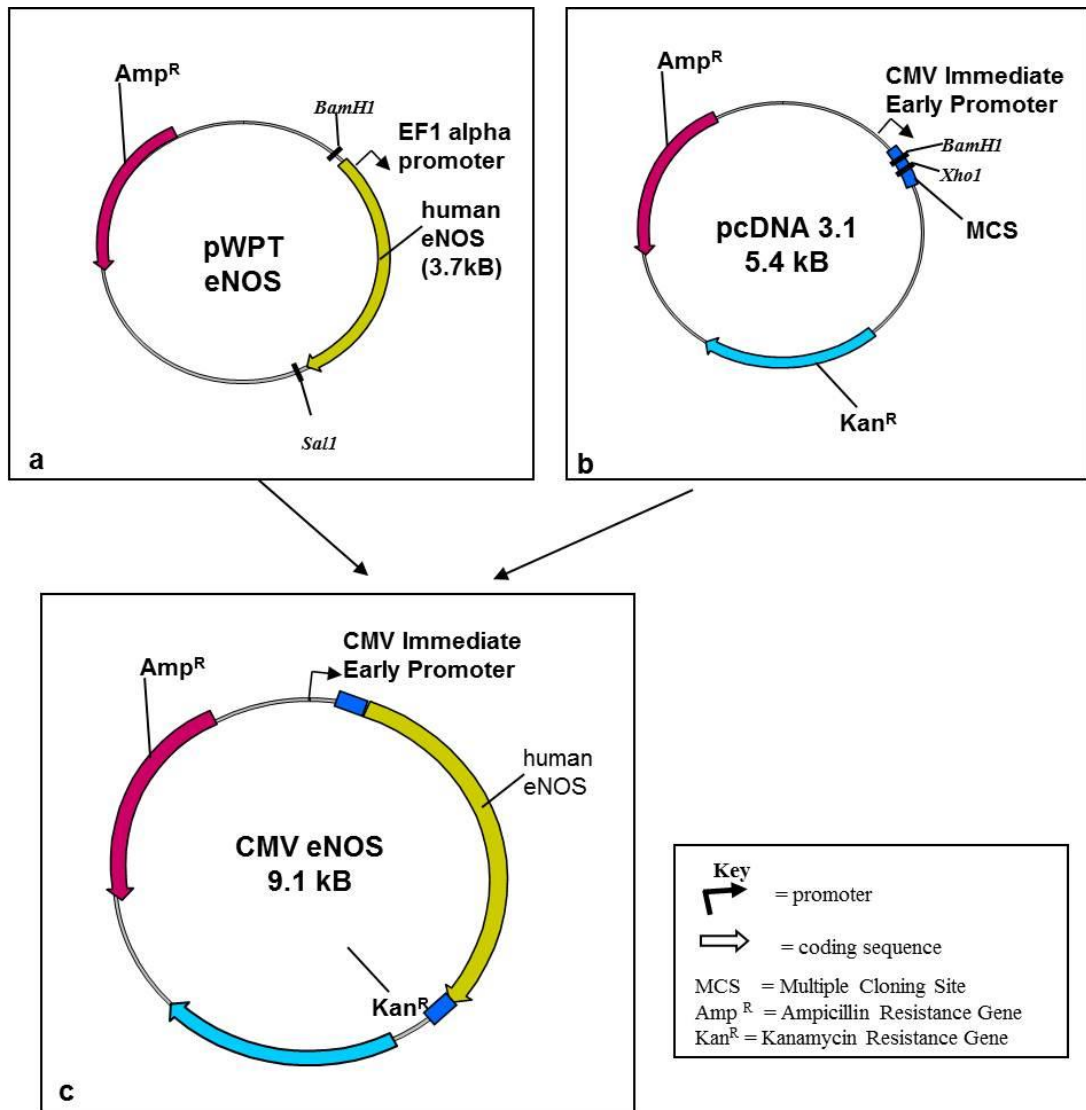


**Figure 6.1:** Plasmid map - pWPTeNOS (a) was previously generated at NUI Galway by cloning a codon-optimised human eNOS gene (synthesised by GENEART, Germany) into the *Mlu* / *Sall* sites of pWPTGFP (Tronolab, Lausanne, Switzerland). The eNOS gene was excised from pWPTeNOS using *BamH1* & *Sall*. This fragment was cloned into pcDNA linearised with *Xho1*, blunted and then cut with *BamH* (b) producing a vector expressing the human eNOS gene under the control of the CMV immediate early promoter (c).

### 6.2.3 Lipostent preparation

Lipofectin™, complexed with the eNOS vector, was employed, as this emerged as the lead liposomal formulation from the *in vitro* and *in vivo* characterisation of the previous chapters (4 and 5). In addition to the therapeutic eNOS vector generated in section 6.2.2, a reporter gene ( $\beta$ Gal) and a null vector were also combined with commercially available Lipofectin™ to produce three formulations identified as: Lipo-eNOS, Lipo- $\beta$ gal and Lipo-Null respectively. Each liposomal combination was then applied to cobalt chromium stents (Multi-link Vision™, Guidant) and PC-coated stents (TriMaxx™, Abbott Vascular) using a Gilson pipette in 30  $\mu$ l droplets followed by a period of air drying under a laminar flow safety cabinet as described in section 5.2.2.

### 6.2.4 Animals

As with the pre-clinical study performed in Chapter 5, the present study conformed to the guide for the care and use of laboratory animals published by the US National Institute of Health (NIH publication no 85-23, revised 1996). Ethical approval for the experiments was obtained from the local institutional animal care committee (NUI Galway) and performed under license, as approved by the Irish Department of Health. A pre-clinical animal model was developed to assess the efficiency of liposome-mediated gene delivery to the blood vessel wall. Male New Zealand White rabbits (Harlan Ltd, UK) weighing 2.5 to 3.5 Kg were used. Animals were individually housed with a 12 hour light-dark cycle and fed either a standard chow or hypercholesterolemic diet one month prior to intervention and given water *ad libitum*. All animals received low dose aspirin for seven days prior to intervention and thereafter until euthanasia. Animals were sacrificed at time-points from 3-42 days post-stenting with a high dose of phenobarbitone which was administered intravenously following sedation. The hypercholesterolaemic diet was continued post-intervention.

Table 6.1 below illustrates the number of animals required for each time-point and demonstrates that each animal was stented bilaterally for maximum efficiency. Lipo-eNOS is the only therapeutic gene delivered and the other permutations (Lipo-Null, Lipo- $\beta$ gal and uncoated PC stents) are for control purposes.

Vector	Time-point: Day 14		Time-point: Day 28	
	Animals	Stents	Animals	Stents
Lipo-eNOS	4	8	6	12
Lipo-Null	4	8	5	10
Lipo- $\beta$ gal	-	-	3	6
PC Stent only	-	-	3	6

**Table 6.1:** Animals and stents, with vector combinations, used in the study.

### 6.2.5 *In vivo* catheter procedures

All procedures were performed under fluoroscopic guidance and performed as previously described (Sharif *et al.*, 2008; Sharif *et al.*, 2006).

### 6.2.6 Histochemical analysis of gene expression

LacZ ( $\beta$ Gal) expression was demonstrated as follows. After sacrifice, stented arteries were exposed, retrieved and cut longitudinally with the stent removed prior to staining. A significant neointimal formation inside the luminal face of the stent was noted at day 28. This neointima was then stripped from the luminal face of the stent from the side of least resistance, and stained separately for LacZ expression. All stented arteries were fixed with 4% Paraformaldehyde for 30 minutes at 4°C and then rinsed twice with Phosphate Buffer Saline (PBS). Arteries were then immersed in a solution of 500 $\mu$ g/ml 5-bromo-4-chloro-3-indolyl- $\beta$ -D-galactopyranoside (X-Gal, Boehringer-Mannheim Biochemicals, Mannheim, Germany) overnight at 37°C. Following staining, the arteries were then embedded in paraffin. Sections (5  $\mu$ m) were then cut, placed on slides,

heated to 60°C overnight, deparaffinized in xylene and rehydrated in graded dilutions of ethanol. Selected sections were counterstained with hematoxylin and eosin, dehydrated and mounted.  $\beta$ -galactosidase-positive cells showed a distinctive Prussian blue colour under light microscopy.

### **6.2.7 Transgene positive cell identification**

Histological sections (5  $\mu$ m) which had previously been positively stained for transgene expression, as described above, were subsequently analysed for smooth muscle or macrophage phenotype. Following Xgal staining and sectioning, slides were deparaffinized and rehydrated, as described above, ready for immunofluorescent staining. Slides were incubated in blocking solution (5% goat serum in PBS) for 30 minutes. Slides were then incubated with either  $\alpha$ -macrophage (RAM11) antibodies (Dako) or  $\alpha$ -SMA antibodies (Abcam) diluted in 5% goat serum in PBS overnight at 4°C. Slides were washed in PBS/1% Tween and incubated with anti-mouse IgG conjugated with Alexa Fluor 488 (Molecular Probes) diluted in 5% goat serum in PBS for 2 hours minimum, in the dark. Slides were washed in PBS and then mounted using Vectashield containing DAPI. Transgene expression and immunostained cell types were assessed visually. All sections had secondary antibody controls run which did not show any staining.

### **6.2.8 eNOS detection in transduced vessels**

eNOS expression at a protein level is important to ascertain the presence, and extent of, regenerated endothelium. The delivery of the eNOS gene vector to the vessel wall is known to induce the up-regulation of the eNOS enzyme, increasing the production of NO which results in endothelium regeneration. To this end both the detection and quantification, of the regenerated endothelium is required to establish the therapeutic effectiveness of the selected gene. Both histological and PCR

techniques were employed to detect and quantify the regenerated endothelium in this present study.

#### **6.2.8.1 Histological techniques**

Both Lipo- $\beta$ gal and Lipo-eNOS S (n=3 in each group) stents were deployed and harvested at 28 days. Histological sections (5  $\mu$ m) were stained as previously described for LacZ transgene expression. Subsequently the same sections were stained for human eNOS expression by immunofluorescence (as above) using a monoclonal antibody generated against human eNOS (BD transduction laboratories).

#### **6.2.8.2 Reverse transcriptase PCR**

RNA was extracted from the rabbit arteries 21 days after exposure to a PC stent with Lipo-eNOS, or a PC stent, alone using the RNeasy kit (Qiagen). Extracted RNA (1 $\mu$ g RNA) was reverse transcribed into cDNA using random primers and the ImProm-II Reverse Transcription system (Promega). Generated cDNA was used as a template to perform standard PCR analysis using ReadyMix Taq PCR reaction Mix with MgCl<sub>2</sub> (Sigma). PCR primers were designed to amplify the human eNOS transgene without amplifying endogenous rabbit orthologues. eNOS primers were forward 5'-GGAGATACGAGGAGTGGAAG-3' and reverse 5'-GCCAAACACCAGGGTCATAG-3' with an expected product size of 449 base pairs. Primers against the rabbit housekeeping gene hypoxanthine phosphoribosyltransferase (HPRT) were used as a control with expected product size of 135 base pairs. Products were visualized on an agarose gel.

#### **6.2.9 Image analysis of Lipo- $\beta$ Gal transduced vessels**

The luminal surface of all the stained arteries was photographed *en face* through a dissecting microscope. Quantification of positively stained tissue was done using Java Image processing software (Image J) from the

National Institute of Health. At days 3 and 7, neointimal formation could not be visualised or separated from the media, allowing only the vessel wall to be stained and quantified. However, at day 28 there was a significant neointimal formation observed which could be removed, stained and imaged separately to the vessel media.

#### **6.2.10 Endothelialisation Detection**

Fourteen days after stent deployment, a total of 8 animals were anaesthetised as described above (Lipo-Null (n=4) and Lipo-eNOS (n=4)). Five ml of 1% Evans blue (Sigma) was injected in to the left ear veins and the stents were retrieved 30 minutes after injection. The animals were euthanised prior to stent retrieval with an intravenous bolus of phenobarbitone. The stented blood vessels were fixed in 4% paraformaldehyde (PFA) and incised longitudinally. Photographs of the stented vessels were taken *en face* and areas of stent endothelialisation (white) and non-endothelialisation were analysed using Java image software.

#### **6.2.11 Tissue SEM**

The excised vessels were fixed in 2.5% glutaraldehyde solution for 2 hours and then rinsed with PBS solution. Dehydration was carried out by immersing the vessels in alcohol for 2 separate time periods at each concentration of 50%, 75%, 80%, 90% and 100% alcohol. Finally the vessels were immersed in hexamethyldisilazane (HMDS, Sigma-Aldrich, Ireland) for 30 minutes. Once the HMDS was removed, the vessels were allowed to air-dry for an hour. Samples were then placed in the gold-sputter coater (Emitech K550 Sputter Coater) and coated for 2 minutes at 25mA. Three separate images of each vessel were captured at a magnification of 3000 for image analysis (Hitachi S-4700 cold cathode field emission SEM).

### **6.2.12 Histological endothelial assessment**

In addition to the assessment of the stent endothelialisation at 14 days by Evans Blue, histological assessment of endothelialisation was also performed at day 28. Stents were retrieved at day 28 and embedded in resin following local perfusion fixation. Three serial sections were taken per stent and endothelialisation was assessed directly under the microscope. Independent groups of animals were analysed for Lipo-eNOS (n=12), Lipo-Null (n=10) and PC control stents (n=5) using this method.

### **6.2.13 Morphometric analysis**

Morphometric analysis was performed by Dr. Remu Virmani, CV Path Institute Inc (Gaithersburg MD, USA). The effects of Lipo-eNOS (n=12), Lipo-Null (n=10) and PC coated stents (n=5) on the vessel morphology, were assessed at 28 days in hypercholesterolemic animals. After anaesthesia the animals were locally perfusion fixed and the stented blood vessels were retrieved. The entire vessel segments were embedded in methylmethacrylate plastic. After polymerisation, each vessel was sectioned into 2-3mm portions, using a surgical micro-saw, and labelled proximal, mid and distal as appropriate. These stented vessel portions were then further sectioned on a rotary microtome to produce 4-5  $\mu\text{m}$  samples slices from each of the proximal-, mid- and distal sections of excised vessels. These sample slices were then subsequently mounted and stained with hematoxylin, eosin and elastic Van Giesson stains. All sections were examined by light microscopy for the presence of inflammation, thrombus and neointimal formation and vessel wall injury. The cross-sectional areas (EEL, IEL, and Lumen) were measured with digital morphometry. Neointimal thickness was measured as the distance from the inner surface of each stent strut to the luminal border.

#### **6.2.14 Statistical Analysis**

Data for all experiments were expressed and graphed either as the median value or as a mean $\pm$  standard deviation. Statistical analysis was performed using a one-way ANOVA with multiple paired comparisons to explore global differences; with group differences explored using student's t-test. A  $p < 0.05$  was considered significant.

### **6.3 Results**

#### **6.3.1 Lipo- $\beta$ gal stents *in vivo* time course**

Both PC coated and bare metal (CoCr) stents with lipoplex formulations carrying a LacZ ( $\beta$ gal) plasmid expressing beta-galactosidase were generated using the previously described pipetting technique with subsequent air drying. As described above, these were used to investigate transgene expression at 3, 7, 28 and 42 days. Reporter transgene expression was assessed by measuring the area, using Image J, of tissue expressing the transgene as a percentage of the total stented area. The medial value of expression was used for comparison purposes and this gives an index for relative transgene expression between the stent platforms. Figure 6.2 shows transgene expression following Lipofectin™-mediated delivery from PC stents (at 3, 7, 28 and 42 days) and from CoCr stents (at 28 and 42 days) only.

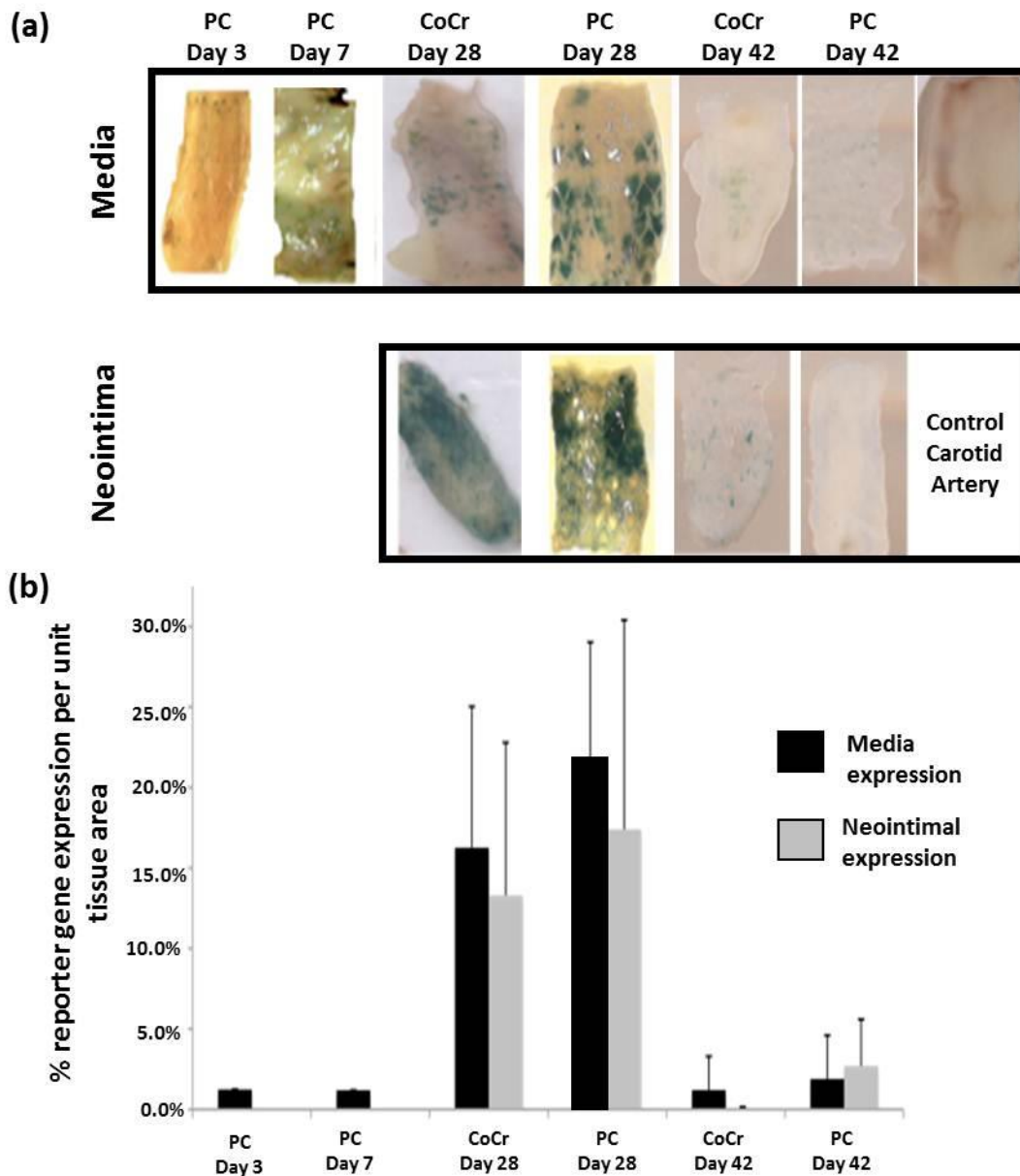


**Figure 6.2:** LacZ expression at 28 days post-deployment for both bare metal (CoCr) and PC coated stents measured at 3, 7, 28 and 42 days (n=2 for 3 and 7 day time-points, n=6-7 at 28 and 42 days). (a) Representative sections of the media and neointima at all time-points and (b) mean results with error bars demonstrating standard deviation are shown. Results are based on the percentage of the vessel's media or neointima covered by transgene-expressing tissue.

In Figure 6.2, part (a) shows representative images of whole vessel mounts retrieved from the excised vessels at each time-point. Part (b) compares the reporter gene expression per unit of tissue area (Black = Media, Grey = Neointima) found in the excised stents at 3, 7, 28 and 42 days. The images and graph clearly show that gene expression peaks at day

28, irrespective of stent platform (bare metal or PC-coated), with no significant difference between expression in the newly formed neointimal tissue (grey bars) or the underlying medial layer (black bars). Gene expression is at negligible levels when excised vessels, from both bare metal and PC-coated stent platforms, are examined at day 42. This experimental result revealed that expression was significantly higher at 28 days, for both stent platforms, in both the media (PC stent = 22.42%; CoCr = 16.26%) and neointima (PC stent = 16.88%; CoCr = 13.78%). Neointimal formation was found at 28 and 42 days and expression was assessed separately in both neointima and media of vessels at these time-points. However, at 42 days this expression had significantly decreased in both the medial (PC stent = 2.04%; CoCr = 1.71%) and the neointimal tissue (PC stent = 3.07%; CoCr = negligible) of stented vessels. Relative measurements showed that the media and neointima were equally targeted at both the later time points. However, it was noted that at 42 days the PC stents had more expression, but the difference between the different platforms was not found to be statistically significant.

### 6.3.2 Target cell population

Figure 6.3 illustrates that the delivery of Lipo- $\beta$ gal from a PC stent platform resulted in expression in both the neointima and media layers at 28 days post-stent deployment in normocholesterolemic animals.

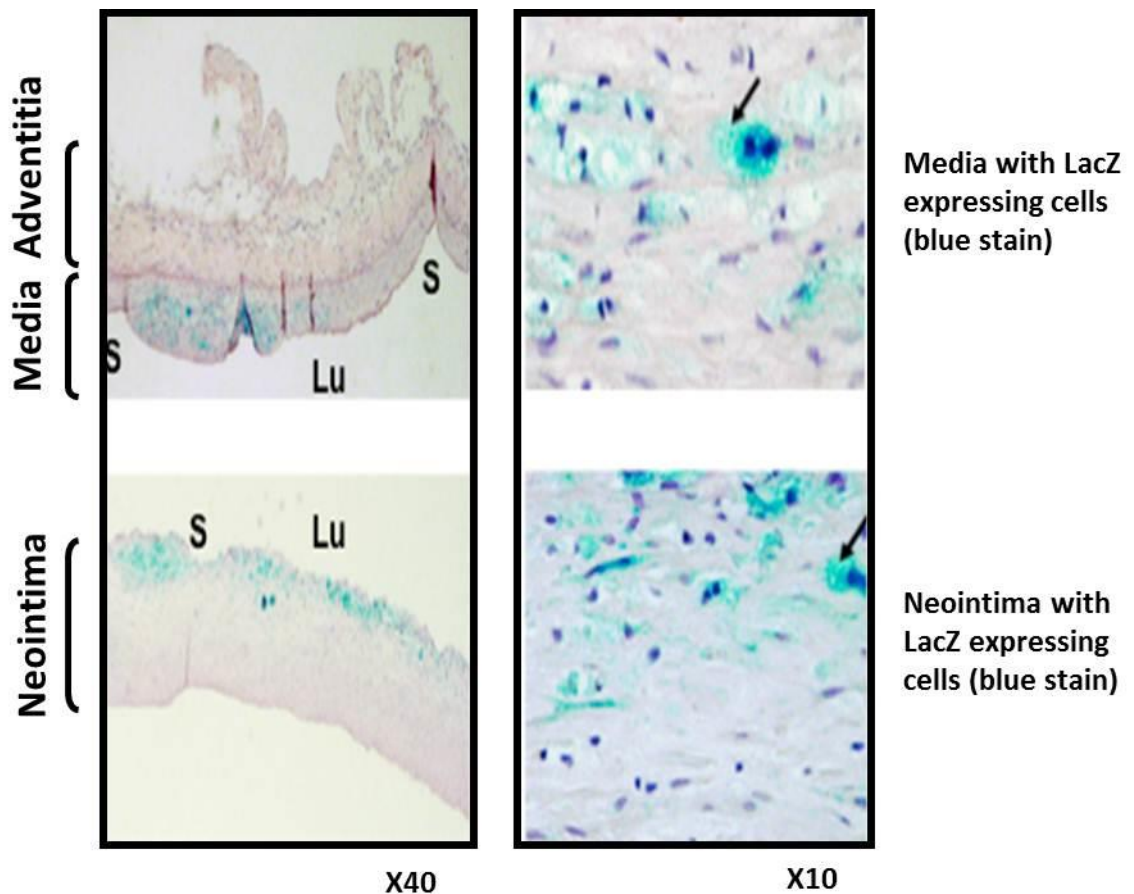


**Figure 6.3:** Expression of nuclear and cytoplasmic-targeted LacZ between stent struts at day 28 post-deployment in the common iliac of normocholesterolemic rabbits. Sections are stained using Xgal (Light blue), and counter-stained with hematoxylin-eosin (Nuclei are deep blue). Original magnification x40 and x10 respectively. Lu=Lumen, NI= Neointima, S= Site of Stent Strut.

When examined under light microscopy (first column), expression was observed in the media between the indentations of the struts. Moreover, as the delivery of cytoplasmic targeted LacZ may over-estimate the level of reporter transgene expression if allowed to diffuse, representative sections of nuclear targeted LacZ were subjected to histological comparison. The levels of reporter gene expression were determined using either cytoplasmic or nuclear-targeted LacZ, to ensure

that all successfully transduced cells, irrespective of where in the cell the expression occurs (nucleus or cytoplasm).

Figure 6.4 illustrates an attempt to better define the cell population targeted by the liposomal formulation in the neointimal tissue only. LacZ expression in the neointima stained with Xgal is shown in panels (a) and (b) of figure 6.4. The next section panels are fluorescently stained using (c)  $\alpha$ -actin antibodies and (d) RAM-11 antibodies, specific to macrophage identification, respectively. Panel (e) is an overlap of the Xgal stained cells in the neointimal (a) with SMCs identified with  $\alpha$ -actin antibodies (c) whereas panel (f) shows an overlap of Xgal stained cells from image (b) and RAM-11 antibodies from image (d). Interestingly, minimal overlap is noted for the smooth muscle cell phenotypes stained using  $\alpha$ -actin antibodies, whereas in contrast there is a significant overlap demonstrated in panel (f) when the  $\beta$ -galactosidase expression (b) is coincided with immune-fluorescent stained areas for the macrophage marker RAM-11 (d). Surprisingly, little expression could be seen in cells stained for smooth muscle phenotype with fluorescent labelled antibodies.

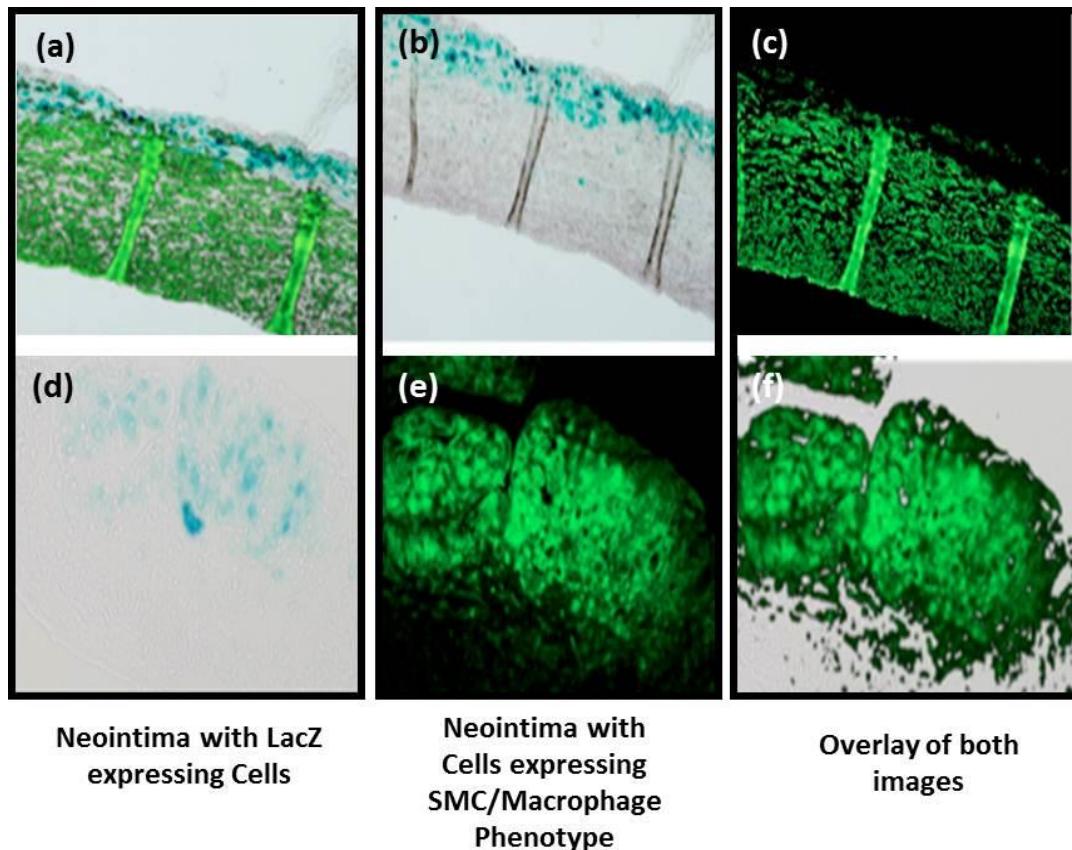


**Figure 6.4:** LacZ expression in the neointima stained with Xgal (a) and (b). Consecutive sections are fluorescently stained for smooth muscle cell phenotype stained using  $\alpha$ -actin antibodies (c) and macrophage phenotype using RAM-11 antibodies (d). A lack of co-localisation is noted for the smooth muscle cell phenotype staining using  $\alpha$ -actin antibodies (e) whereas in contrast a significant co-localization is observed when macrophage phenotype is examined using RAM-11 antibodies. (f) demonstrates an overlay of images. Sections were taken from vessels which had been treated with LipoLacZ-PC Stent deployed for 28 days in normocholesterolemic rabbits. LacZ expressions is denoted by blue stain and anti-body based phenotype is denoted by green fluorescence. Original magnification, x 10. Staining performed by Dr. Karl McCullagh.

### 6.3.3 Detection of eNOS expression

Confirmation of eNOS protein expression was demonstrated by RT-PCR and is shown in Figure 6.5. Iliac arteries co-transfected with LipoStents (as they were transduced with both the eNOS and  $\beta$ Gal plasmids in a ratio of 2:1), were harvested at 21 days post-stent placement.

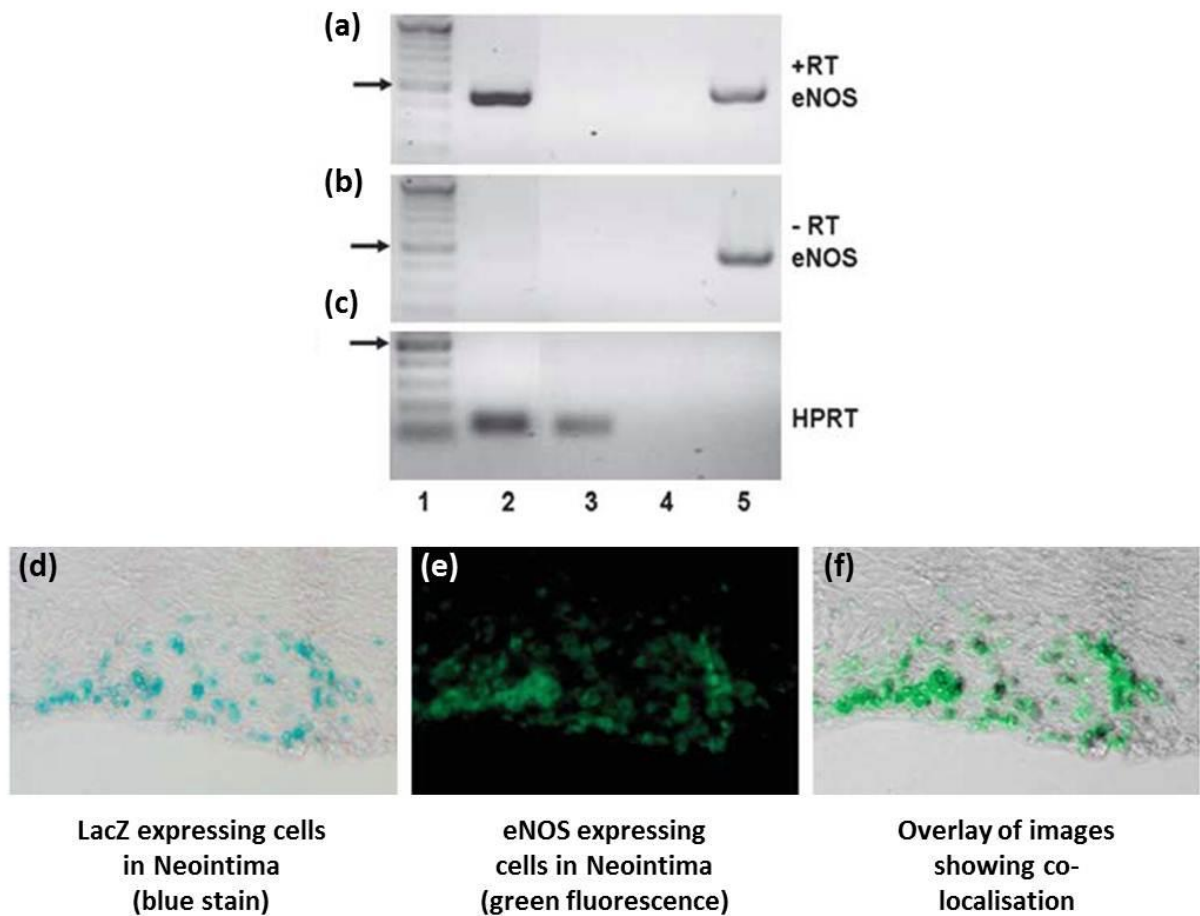


**Figure 6.5:** Detection of eNOS transgene expression in stented vessels harvested after 21 days. Expression of the eNOS transgene in rabbit vessels at 21 days post-deployment detected using RT-PCR: (Lane 1): 100 bp ladder (arrows indicate 500bp size), (Lane 2): RNA from Lipo-eNOS-stented rabbit common iliac artery, (Lane 3): RNA from a control lipoLacZ-stented artery without eNOS, (Lane 4): negative control without cDNA and (Lane 5): positive control with eNOS plasmid. (a) PCR reaction with reverse transcriptase (+RT), (b) PCR reaction without reverse transcriptase (-RT), (c) PCR reaction using primers for the endogenous rabbit housekeeping gene hypoxanthine phosphoribosyltransferase. Histological section of a combined Lipo-eNOS/LacZ-stented artery demonstrating (d) LacZ expression in blue, and (e) immunofluorescent detection of eNOS in green with (f) overlap seen when graphic overlay for both stains is used.

Panels (a), (b) and (c) in Figure 6.5 illustrate reverse transcriptase PCR to demonstrate eNOS cDNA expression in the aforementioned stented iliac arteries: (a) PCR reaction with reverse transcriptase (+RT), (b) without reverse transcriptase (-RT) and (c) PCR using endogenous rabbit house-keeping gene *hypoxanthine phosphoribosyltransferase* (HPRT). Lanes 1-5 are run across all RT-PCR samples: (Lane 1) 100 bp ladder (arrows indicate

500bp size), (Lane 2) RNA from Lipo-eNOS stented rabbit common iliac artery, (Lane 3) RNA from a control Lipo- $\beta$ gal stented artery (without eNOS), (Lane 4) negative control without cDNA and (Lane 5) positive control with eNOS plasmid. RNA obtained from these tissue samples demonstrated the presence of the appropriate sized-band for eNOS in arteries tested following RT-PCR as shown in Figure 6.5. Detection of the eNOS transgene was found in stented vessels harvested after 21 days compared with the null vector and the negative controls.

Figure 6.5 also illustrates neointimal tissues co-transfected with Lipo-eNOS and Lipo- $\beta$ gal stained for (d) LacZ (blue stained cells) to mark the transduced cells. These LacZ positive sections were also subjected to immunofluorescence (green stained cells) (e) and with an antibody raised against human eNOS. Histological sections showed that robust eNOS expression was detected in all regions where LacZ was expressed, indicating the co-expression (or co-localisation) of the two plasmids in panel (f), confirming eNOS delivery and expression from a Lipo-eNOS PC stent. Secondary antibody controls did not show any background fluorescence (data not shown).

#### **6.3.4 Endothelium regeneration**

Two weeks post-intervention, blood vessels were stained prior to sacrifice using Evans Blue. This stain allows areas of de-endothelialisation, viewed as areas of blue stain, whereas areas of intact endothelium remain white. Previous research groups illustrated that the angioplasty model utilised in this study results in complete denudation of the endothelial layer (Sharif *et al.*, 2006) and (Cooney *et al.*, 2007).

Figure 6.6 shows both Evans Blue at 14 days and histological analysis at 28 days post-stent deployment. For Evans Blue analysis, Lipo-eNOS (n=4) and Lipo-Null (n=4) controls were compared. Figure 6.6

contains representative images (n =1) of Evans Blue stained luminal surfaces of excised vessels.

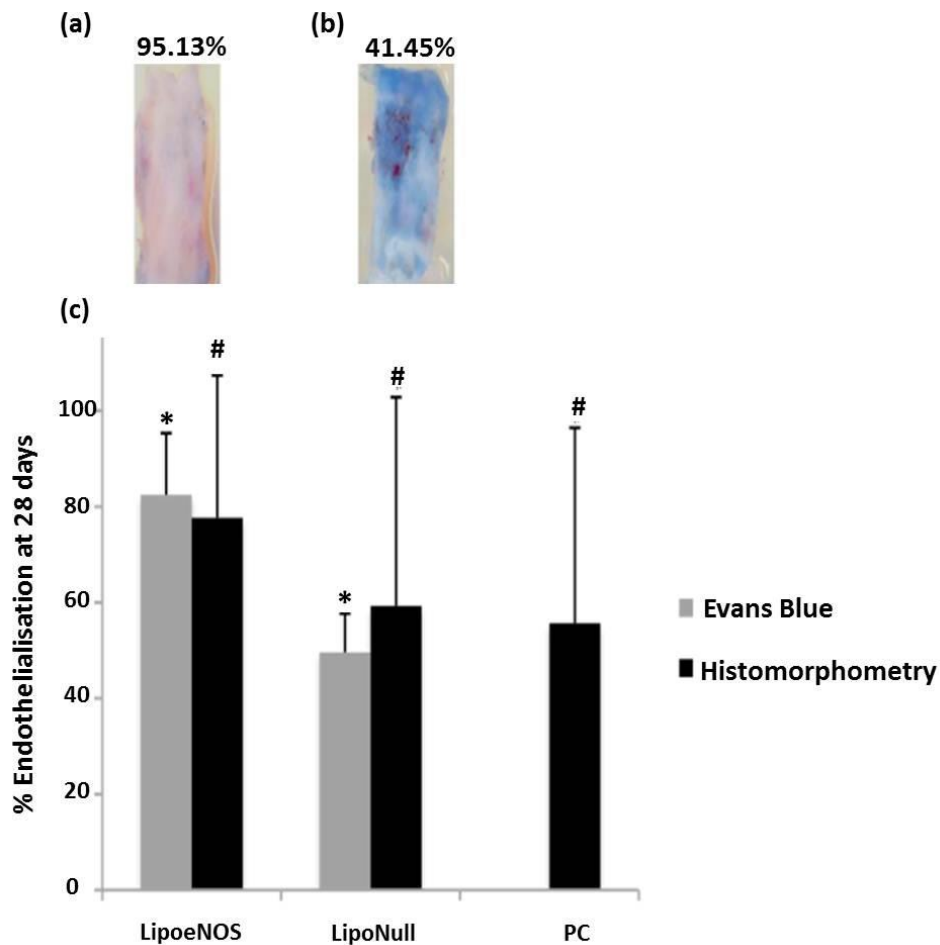


**Figure 6.6:** Quantified Endothelialisation as determined using Evans Blue at 14 days, and histological analysis at 28 days, post-stent deployment in the common iliac arteries of hypercholesterolemic rabbits. For Evans Blue, Lipo-eNOS and Lipo-Null controls are compared (n=4 each). For histological analysis, Lipo-eNOS (n=12), Lipo-Null (n=10) and PC stents without vector (n=5) are compared. Representative sections of the Evans Blue stained arteries are shown for each treatment group (A&B). In the graph (C) a significantly increased level of endothelialisation is noted for Lipo-eNOS stented group compared with controls for Evans Blue analysis (\*) and for histological analysis (#) using a Student's t-test ( $p < 0.05$ ).

Figure 6.6 (a) shows the luminal surface of a Lipo-eNOS stent vessel where 95.13% of the surface area has been re-endothelialised, this is a direct contrast to the of the Lipo-Null stented vessel (b) where the Evans Blue can be clearly visualised on non-endothelialised areas and the white areas of endothelialisation account for 41.45% of the surface area. For histological analysis, Lipo-eNOS (n=12), Lipo-Null (n=10) and PC stents

without vector (n=5) were compared. Representative whole vessel mounts of the Evans Blue-stained arteries are shown for each treatment group (a and b). In the graph, (c) a significantly increased level of endothelialisation is noted for Lipo-eNOS stented group compared with controls for Evans Blue analysis (\*) and for histological analysis (#) using the Student's t-test ( $p < 0.05$ ). At 2 weeks post-stenting, luminal Evans blue stain revealed that endothelial regeneration was significantly enhanced ( $p < 0.05$ , ANOVA) in vessels (n=4) which had stents coated with Lipo-eNOS, compared to those that had stents coated with Lipo-Null ( $82.48 \pm 12.86\%$  vs.  $49.58 \pm 8.16\%$ , Figure 6.6 (c)). This indicates that the delivery of the therapeutic gene has a significant impact on re-endothelialisation. The use of SEM allows the visualisation of endothelium regeneration at a microscopic level. SEM images shown in Figure 6.7 illustrate the difference in the inner lumen morphology for Lipo-eNOS versus control Lipo-Null stented cases.

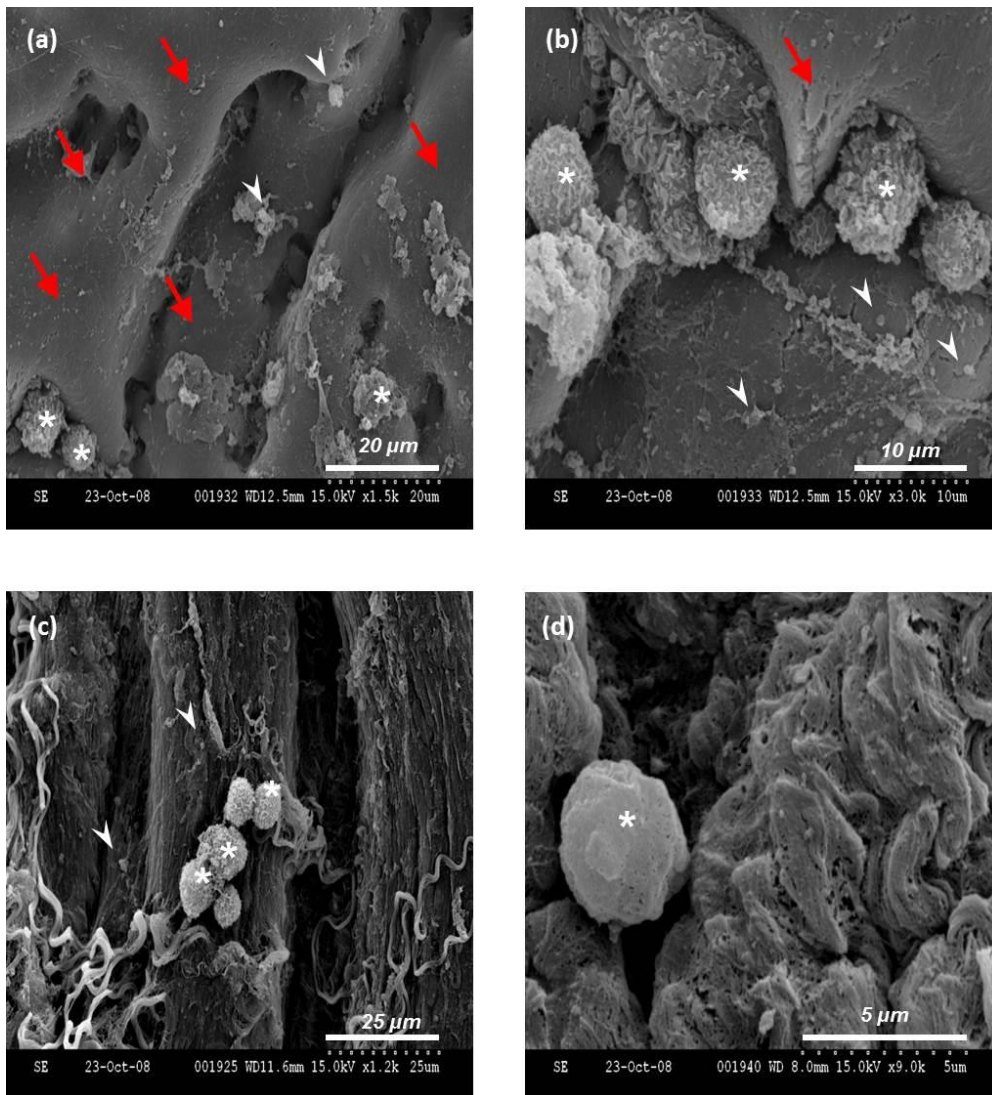


**Figure 6.7:** SEM images of excised vessels at 28 day post-deployment: (a) and (b): Lipo-eNOS/PC stent; (d) and (e) : Control Lipo-Null stent. (a) Clear presence of characteristic endothelial, cobblestone effect. (b) Magnified image of macrophages in close proximity to an endothelialised area. (c) Absence of endothelium recovery, stent removal exacerbates exposure of IEL. (d) High presence of inflammatory cells (neutrophils and macrophages) and no evidence of endothelium regeneration. All images are annotated with symbols: Endothelialisation (Red arrows), Leucocytes (white arrowheads) and Macrophages (\*).

Images (a) and (b) confirms the regeneration of the endothelium by the detection of its characteristic cobblestone appearance (indicated by red arrows). In contrast, images (c) and (d) do not illustrate the characteristic smooth, cobblestone appearance of endothelium. Instead the underlying exposed collagen of the internal elastic lamina (IEL), lying

perpendicular to the image, can be clearly seen. Interestingly, despite increased endothelial coverage, both the Lipo-eNOS stent and the control Lipo-Null stent were associated with the presence of inflammatory cells, macrophages (\*) and leucocytes (white arrowheads). This result is consistent with the analysis that liposomal delivery targets these inflammatory cells and the non-viral vector is inflammatory-cell mediated.

### **6.3.5 Histomorphometry**

Histomorphometrical analysis of the excised tissue was performed independently (by Dr. Renu Virmani, CV Path Inc.) and confirmed similar levels of re-endothelialisation for both the Lipo-eNOS (n = 12) and Lipo-Null (n = 10) controls, compared with the Evans Blue technique. PC stents (n = 5), without any vector, were used as the control. The majority of histomorphometric data generated when compared showed no real significant differences between stent groups across EEL, IEL, Lumen diameter, media or neointimal formation. However, the individual groups were then compared using a t-test, confirming that there was significantly better endothelialisation for Lipo-eNOS versus Lipo-Null and PC stents (p <0.05, Table 6.2). Using one-way ANOVA, to detect global differences, a significant effect was seen on endothelialisation when eNOS was delivered from a stent versus its controls (Lipo-Null and Lipo-βgal) at four weelution kinetics post-deployment. The inflammation score was also increased in the Lipo-eNOS group compared with the Lipo-Null and PC control stents, although not statistically so. The data also suggest that the majority of endothelialisation occurs within the first two weelution kinetics after deployment. Although the number of total occlusions (TO) that occurred across the stent groups was similar when compared against the % total occlusions (%TO), there is a notable reduction for the Lipo-eNOS group (2/12) compared to Lipo-Null (4/10) and PC stents (2/5), however this did not reach statistical significance (Table 6.2).

Stent (n)	EEL (mm <sup>3</sup> )	IEL (mm <sup>3</sup> )	Lumen $\emptyset$ (mm)	Media (mm)	NI (mm)	% Stenosis	Inflammation	% Endo	TO (%TO)
LipoeNOS (12)	5.54 ± 0.69	5.14 ± 0.64	1.27 ± 1.16	0.40 ± 0.23	3.80 ± 1.19	75.61 ± 2.37	0.40 ± 0.23	* 77.76 ± 9.70	2 (16.7)
LipoNull (10)	5.41 ± 0.87	5.05 ± 0.89	1.22 ± 1.44	0.42 ± 0.43	3.77 ± 1.06	77.85 ± 2.49	0.42 ± 0.43	* 59.30 ± 3.53	4 (40)
PC (5)	5.10 ± 0.75	4.58 ± 0.70	1.43 ± 1.24	0.53 ± 0.52	3.15 ± 0.88	71.00 ± 4.99	0.53 ± 0.52	* 55.69 ± 0.78	2 (40)

**Table 6.2:** Histomorphometric data from Lipo-eNOS, Lipo-Null and PC only stents at 28 days. EEL = External Elastic Lamina; IEL = Internal Elastic Lamina, Endo= Endothelialisation, TO = Total Occlusions. \* p < 0.05.

## 6.4 Discussion

This study succeeded in the objective of reporting efficient gene delivery with subsequent therapeutic gene delivery from stents using liposomes with or without a biocompatible coating. Moreover, this study identified the cell populations targeted by lipoplexes in the context of stent-based gene delivery to the vasculature *in vivo*.

It was demonstrated in Chapter 4 that pipette coating of liposomes onto stents was superior to aerosolisation. It was the aim of the present study to evaluate eNOS expression in the hypercholesterolemic NZW rabbit model 3, 7, 28 and 42 days after gene delivery. In this study, successful homogeneous liposome application enabled gene delivery from both PC coated as well as bare metal stents. This is in agreement with the findings of Fishbein and colleagues who showed that stable linkage to a stent allowed more focused delivery of a vector (Fishbein *et al.*, 2008; Fishbein *et al.*, 2006).

PC stents were used in further expression/therapeutic experiments for comparison purposes with previous viral based studies. Sharif *et al* previously investigated the use of viral vectors from PC stents, and specifically adenovirus and AAV serotype 2, for delivery of a transgene to the injured vasculature (Sharif *et al.*, 2006). This study shows increased

expression using a non-viral vector when a PC stent was used. Similarly, in the present study transgene expression was found to be maximal at 28 days post-stenting. Table 6.3 below compares the median values across the vectors and validates the suggestion that liposomal efficiency is enhanced when associated with local cellular proliferation in the form of neointimal formation.

Vector (PC Stent)	Site	Median Level of Expression
<b>Lipostent (Lipo-eNOS) †</b>	Media	22.42 %
	Neointima	16.88 %
<b>Adenovirus *</b>	Media	8.87 %
	Neointima	1.01 %
<b>Adeno-associated virus **</b>	Media	0.35 %
	Neointima	1.38 %

**Table 6.3:** Head-to-head comparison of median levels of expression between Adenoviral\*, Adeno-associated\*\* virus and Liposomal-based† gene delivery of LacZ (this present study) as a reporter gene at 28 days post-stent deployment.\* Data on viral expression derived from Sharif *et al*, 2006, † median level of expression from study presented in this thesis.

No significant difference was observed between the level of expression in the neointima or media, presented here, suggesting that the entire lipoplex or the plasmid DNA was released from the stent over a prolonged period. In contrast, adenoviral vectors (the most efficient viral vector tested) have relatively higher levels of expression in the media versus the neointima, at later time points. This observation supports the experimental profiles of elution kinetics of both adenovirus and liposomes examined in Chapter 3. One significant implication of this is that a non-viral vector delivered from a stent-based platform would be more beneficial for prolonged delivery of therapeutic genes to an area of increased cellular proliferation. Whether or not the observed differences in sustained gene release are due to different uptake mechanisms of lipoplexes (e.g. passive,

diffusion) and viruses (e.g. active, endocytosis) or due to varying release and gene expression profiles of these gene delivery systems based on their ability to adhere to PC coated or bare metal stents, remains to be investigated.

Furthermore, the results in this chapter indicate that the predominant cell type with lipoplex uptake were RAM11 positive, consistent with a macrophage phenotype, with little uptake in smooth muscle cells. This occurred despite the demonstration of smooth muscle transfection using lipoplex mediated gene delivery *in vitro* (Chapter 4). This suggests that lipoplexes are the vector of choice for carrying anti-inflammatory genes in future experiments aimed at the modulation of the inflammatory response to stenting caused by macrophages. The observed preferred uptake of lipoplexes by macrophages is also in contrast to adenoviral uptake from stents which resulted in transgene expression predominantly in smooth muscle cells (Sharif *et al.*, 2006). A prevalence of cells (with a macrophage phenotype) was noted in sections surrounding the stent struts when histologically analysed. This is consistent with the results of Rogers *et al* who showed a significant increase in macrophage accumulation at stent struts following stent deployment in rabbit iliac arteries which underwent a balloon injury prior to deployment (Rogers, Welt, Karnovsky, & Edelman, 1996). Similarly, the study presented in this chapter used prior balloon inflation to mimic an atherosclerotic lesion which enhances neointimal formation involving foamy macrophages.

Previous studies, such as performed by Lee and colleagues, have shown that *in vitro* liposome mediated gene delivery does not correlate with *in vivo* efficacy of liposome complexes when studied in the lung (E. R. Lee *et al.*, 1996). In addition, there are reports in the literature suggesting that optimal *in vivo* gene delivery with liposomes can be achieved systemically when the molecular ratio of cationic liposome to nucleic acid

in the lipoplex mixture (positive/negative charge ratio) is closer to 1 or greater (B. Schwartz *et al.*, 1995), (F. Liu *et al.*, 1997) and (J. P. Yang & Huang, 1997). This higher charge of the lipoplex complex also helps in reducing the host immune response (J. P. Yang & Huang, 1997). These previous studies have dealt with gene expression/drug release following systemic delivery of liposomes and do not relate to stent-based release of liposomes. The results in this study suggest that prolonged and efficient gene expression observed is possibly due to the intrinsic ability of the liposomes to bind efficiently with the stent surface, enabling sustained release *in vivo*. In addition, the sustained luminal wall contact could also play a significant part in this successful transduction. As pointed out by Fishbein and colleagues, direct gene delivery from a stent platform is advantageous as it decreases the risk of distal spread and encourages more efficient local delivery (Fishbein *et al.*, 2008). Scanning electron microscopy imaging demonstrated that liposomal application to a PC coated stent resulted in complete and smooth coating of the stent which may be a contributory factor in sustained luminal contact post-deployment.

With respect to the therapeutic gene of choice for this study, eNOS, several investigators have demonstrated suppressed intimal hyperplasia in animal vascular injury models with the local administration of exogenous NO in the form of NO donors (Rolland *et al.*, 2002) in porcine SFA, Maffia (Maffia *et al.*, 2002) in rat carotid or NO synthase genes (Varenne *et al.*, 1998) in porcine carotid. Sharif and colleagues have already demonstrated the ability of adenoviral gene delivery of eNOS to decrease smooth muscle cell proliferation both *in vitro* and *in vivo* in stent and injury based-models (Cooney *et al.*, 2007). However, in the present study there is a disconnect between re-endothelialisation, which is enhanced, and neointimal formation, which is not affected. Similar results were also noted when anti-CD34 stents were assessed (Nakazawa *et al.*, 2010).

Interestingly, Muhs *et al.*, using an infiltration catheter for intramural administration of lipoplex solution into the arterial wall, demonstrated significant reduced NI formation by the over-expression of iNOS (Muhs *et al.*, 2003). Replicating this protocol, Pfeiffer and colleagues also exhibited successful inhibition of intimal hyperplasia in an ePTFE bypass graft (Pfeiffer, Wallich, Sandmann, Schrader, & Godecke, 2006). Enhanced re-endothelialisation due to increased bioavailability of NO has been suggested to result in enhanced endothelial cell migration and/or mobilisation of endothelial progenitor cells. In this study, it can be speculated that this may be due to the cell type targeted, i.e. macrophages. Macrophages, unlike smooth muscle cells, have their own endogenous NOS in the form of iNOS. The expression of eNOS in cells carrying iNOS may deplete the co-factors required to produce NO and thereby contribute to the recognised uncoupling of iNOS. This uncoupling can lead to increased formation of super oxide which may enhance the inflammatory response as seen for Lipo-eNOS versus Lipo-Null (Table 6.1). An enhanced inflammatory response may prevent the manifestation of potential beneficial effects on neointimal formation by liposomal-delivered eNOS.

As mentioned in the introduction to this chapter, a recent report by Brito and colleagues has demonstrated the potential for liposomal gene delivery of eNOS when used in conjunction with PLGA and gelatin-based coatings (Brito *et al.*, 2010a). This showed promise in enhanced re-endothelialisation and reduced restenosis, however, in contrast to the study results presented here, the model used by Brito and co-workers used was a gentle denudation of the vessel rather than an inflation/deflation injury and was performed in a non-disease model, not in a hypercholesterolemic model as described in the present study. Moreover, this study used a neointima/media ratio as a clinical end-point rather than an evaluation of all histomorphometric data, as illustrated in Table 6.2 of this study. Another important element of the study included comparing

liposomal delivery from both a bare metal stent and a PC-coated stent which is of practical benefit when translating this research.

Although, this present study illustrates that eNOS can be successfully delivered to the vessel wall, irrespective of the stent platform used, the findings in this study clearly show that there is a disconnect between the re-endothelialisation, which is enhanced with the Lipo-eNOS stent ( $77.76 \pm 29.7 \%$ ) versus the Lipo-Null control ( $59.30 \pm 43.53 \%$ ), and the neointimal formation, which is not affected ( $3.8 \pm 1.19 \text{ mm}$  vs.  $3.77 \pm 1.06 \text{ mm}$ ). It could be argued that the non-viral liposome used in this present study targets macrophages which do not have their own endogenous NOS (unlike smooth muscle cells) in the form of iNOS. Therefore the expression of eNOS in cells carrying iNOS may deplete co-factors required to produce NO and thereby contribute to the recognised uncoupling of iNOS. This uncoupling can lead to an increased formation of superoxide, which may be responsible for the increased inflammatory response as observed in the Lipo-eNOS versus Lipo-Null stents ( $13.61 \pm 40.52$  vs.  $7.85 \pm 20$ ). This enhanced inflammatory response may inadvertently prevent re-endothelialisation by obscuring the quiescent process that the delivery of eNOS attempts to augment.

## 6.5 Conclusion

The purpose of the study described in this chapter was to evaluate if Lipo-eNOS could be delivered safely and efficaciously from a stent platform to the vasculature of an appropriate *in vivo* model.

Specifically, the study set out to: evaluate eNOS expression in the hypercholesterolemic NZW rabbit model 3, 7, 28 and 42 days after vessel wall gene delivery from both bare metal and PC-coated stents; measure key histomorphometric parameters (not just the neointima/media ratio);

and establish a correlation (if any) between the extent of re-endothelialisation and percentage neointimal area.

The results of this study clearly illustrate that Lipo-eNOS delivery (irrespective of the stent platform) to the blood vessel wall results in accelerated re-endothelialisation when compared to both controls (Lipo-Null or PC-stent only). However, the findings also establish that Lipo-eNOS does not reduce neointimal formation. Transgene expression is detected at early time-points in the media and later equally in the neointima.

The results presented here support the hypothesis that liposome-mediated gene delivery is capable of efficiently transducing the blood vessel wall *in vivo* for a prolonged duration when delivered on a stent platform with or without a biocompatible coating. The potential of therapeutic gene (eNOS) delivery using this system has also been illustrated. As already stated, the use of non-viral based delivery system reduces the bio-safety concerns associated with viral-based delivery systems. To this end, it may be beneficial to use this method as an adjunct to current drug eluting stents to enhancing re-endothelialisation with prevention of neointimal proliferation achieved through the cytotoxic/static actions of the drug-eluting portion. Enhanced re-endothelialisation may decrease the need for prolonged dual anti-platelet therapy an important consideration in patients who cannot tolerate this regimen (Tsai *et al.*, 2010). A rapid re-endothelialisation may also decrease the risk of late stent thrombosis following cessation of anti-platelet therapy.

## 7. Conclusions and Future Direction

### 7.1 Study Conclusions

The purpose of this concluding section is to critically appraise if the experimental plan performed produced results that supported the predictions originally outlined in the thesis hypothesis of this thesis.

The principal objective of the research contained within this thesis was to determine a polymer coating/non-viral vector combination that could successfully deliver a therapeutic gene, eNOS, to the site of vascular injury, produce NO and induce re-endothelialisation as quickly as possible thus arresting the proliferative nature of an exposed SMC medial layer.

The thesis had two main hypotheses:

- Stent-based non-viral vector delivery can safely target the vector to the site of vascular injury resulting in comparable gene expression to viral gene delivery from a stent.
- Non-viral mediated Lipo-eNOS delivery to the vasculature of a hypercholesterolemic rabbit model can reduce the incidence of ISR, through enhanced NO production and re-establishment of a functional endothelium.

The removal of endothelium during an angioplasty procedure causes the underlying medial layer to change phenotype, thus inducing the formation of neointimal hyperplasia in certain patient populations. It is envisioned that promoting re-endothelialisation at a very early stage will stimulate the exposed SMC medial layer to return to a quiescent, non-proliferative state, thus preventing the formation of a hyperplastic SMC mass in the neointima. Specifically, it is proposed that the delivery of a gene vector, encoding a therapeutic gene could achieve this. It is proposed that the delivery of a gene vector, namely a plasmid-lipoplex formulation

from a stent platform, encoding endothelial nitric oxide synthase (eNOS), to cells at the site of vascular injury will enable nitric oxide production at the site. Presentation of a GES containing eNOS should result in transfection of the cells at the site of injury but it will also have the potential to target circulatory cells that infiltrate the injury site during the inflammatory response. This localised methodology of cell transfection ought to initiate the production of nitric oxide (NO), capable of diffusing through the medial layers and also into the bloodstream. In theory, the production of NO should recruit endogenous progenitor endothelial cells to the site of vessel injury, thus inducing the formation of endothelium. In addition, by re-establishing the endothelial layer post-injury, it returns the non-thrombogenic properties of the intimal layer. This would be a significant event as it is the thrombogenicity of an exposed medial layer that warrants the long-term administration of anti-platelet therapy to prevent late stent thrombotic events.

## **7.2 Future Direction**

In summary, this section will briefly discuss the full implications of the emergence of results that either support or oppose the hypotheses, elucidate the limitations of the study and to provide recommendations for future work.

In Chapter 2, Pluronic was investigated as a potential dual gene vector, its major shortcoming was that the polymer's viscosity rendered it unsuitable as a stent coating. However the polymer could be an excellent candidate for a different type of stent structure, like a honey-combed or perforated stent that could hold a semi-liquid based vector. This would be a very attractive stent platform structure for controlled release of drugs and/or biologics into the vessel wall. The study presented in Chapter 2 also provided the impetus to continue to evaluate and screen the vector

candidates in appropriate 3D *in vitro* systems in Chapter 3 and into Phase 2 of the thesis. Overall, the initial studies in Chapters 2 and 3 demonstrated that an improved methodology of *in vitro* assessment has a significant impact on the interpretation of the results.

Chapter 3 began to explore the potential of correlating empirical data generated by the transfection and elution kinetic studies with the possibility of developing computational modelling techniques. This could emerge as a major area of research to help identify and predict the performance of a candidate genes (and vector combinations) at the initial screening stage. Tools like computational modelling are being increasingly used by R&D team during the product develop of convergent medical devices and regulatory agencies, such as the FDA, are very supportive of the use of such validated tools in the development of future medical devices.

Chapter 4 succeeded in demonstrating that the selection of a non-viral vector can be an efficient delivery vehicle in the vasculature when delivered from a stent scaffold. However, a major limitation that emerged was the negligible difference between the delivery vectors in this study. It was anticipated that a “lead” liposome would emerge however the liposomes used were too similar in their constitutive make-up to render any competitive edge when tested *in vitro*. The selection of a lead vector/stent platform candidate still relied on transition to a normocholesterolemic *in vivo* model to determine the most optimal formulation from both a polymer coated (PC) and non-coated stent platform.

The final study (Chapter 6) successfully examined the lead formulation for its therapeutic effect in a clinically relevant animal model-hypercholesterolemic NZW rabbit model. The primary limitation in this

study was in relation to the controls used. It was difficult to ascertain where competitive advantage of using a particular stent platform versus the liposomes selected conferred a more significant therapeutic effect. There is scope to expand out the controls to include balloon delivery of the selected liposomes to the vessel wall as a positive control.

In the context of the development of a GES, the properties of some polymer coatings used on DES could potentially afford the same control to a biologically active agent, such as a therapeutic gene. DES have primarily focused almost entirely on the anti-proliferative, anti-migratory and anti-inflammatory channels to prevent ISR. In the present work, what is of interest is to explore the GES from a pro-healing approach using a non-viral system.

The results presented here support the hypothesis that liposome-mediated gene delivery is capable of efficiently transducing the blood vessel wall *in vivo* for a prolonged duration when delivered on a stent platform with or without a biocompatible coating. The potential of therapeutic gene (eNOS) delivery using this system has also been illustrated. As already stated, the use of non-viral based delivery systems reduces the bio-safety concerns associated with viral-based delivery systems. To this end, it may be beneficial to use this method as an adjunct to current drug eluting stents to enhancing re-endothelialisation with prevention of neointimal proliferation achieved through the cytotoxic/static actions of the drug-eluting portion. Enhanced re-endothelialisation may decrease the need for prolonged dual anti-platelet therapy an important consideration in patients who cannot tolerate this regimen (Tsai *et al.*, 2010). A rapid re-endothelialisation may also decrease the risk of late stent thrombosis following cessation of anti-platelet therapy.

## BIBLIOGRAPHY

- Abe, T., Takahashi, S., & Fukuuchi, Y. (2002). Reduction of Alamar Blue, a novel redox indicator, is dependent on both the glycolytic and oxidative metabolism of glucose in rat cultured neurons. *Neurosci Lett*, 326(3), 179-182.
- Abid, M. R., Yano, K., Guo, S., Patel, V. I., Shrikhande, G., Spokes, K. C., . . . Aird, W. C. (2005). Forkhead transcription factors inhibit vascular smooth muscle cell proliferation and neointimal hyperplasia. *J Biol Chem*, 280(33), 29864-29873. doi: 10.1074/jbc.M502149200
- Abizaid, A., Costa, M. A., Centemero, M., Abizaid, A. S., Legrand, V. M., Limet, R. V., . . . Arterial Revascularization Therapy Study, G. (2001). Clinical and economic impact of diabetes mellitus on percutaneous and surgical treatment of multivessel coronary disease patients: insights from the Arterial Revascularization Therapy Study (ARTS) trial. *Circulation*, 104(5), 533-538.
- Abizaid, A., Kornowski, R., Mintz, G. S., Hong, M. K., Abizaid, A. S., Mehran, R., . . . Leon, M. B. (1998). The influence of diabetes mellitus on acute and late clinical outcomes following coronary stent implantation. *J Am Coll Cardiol*, 32(3), 584-589.
- Abraham, J., Abreu, P., Aglietta, M., Ahn, E. J., Allard, D., Allekotte, I., . . . Pierre Auger, C. (2010). Measurement of the depth of maximum of extensive air showers above  $10^{18}$  eV. *Phys Rev Lett*, 104(9), 091101.
- Addison, T., Cayre, O. J., Biggs, S., Armes, S. P., & York, D. (2010). Multi-layer films of block copolymer micelles adsorbed to colloidal templates. *Philos Trans A Math Phys Eng Sci*, 368(1927), 4293-4311. doi: 10.1098/rsta.2010.0151
- Agrawal, S. K., Macander, P. J., Cannon, A. D., & Roubin, G. S. (1991). The Gianturco-Roubin flexible intracoronary stent: clinical application and initial results. *Indian Heart J*, 43(6), 403-413.
- Ahmed, I. S., & Ayres, J. W. (2011). Comparison of in vitro and in vivo performance of a colonic delivery system. *Int J Pharm*, 409(1-2), 169-177. doi: 10.1016/j.ijpharm.2011.02.061
- Albiero, R., Silber, S., Di Mario, C., Cernigliaro, C., Battaglia, S., Reimers, B., . . . Investigators, R. (2004). Cutting balloon versus conventional balloon angioplasty for the treatment of in-stent restenosis: results

of the restenosis cutting balloon evaluation trial (RESCUT). *J Am Coll Cardiol*, 43(6), 943-949. doi: 10.1016/j.jacc.2003.09.054

- Alenius, M., Hammarlund-Udenaes, M., Hartvig, P., & Lindstrom, L. (2010). Knowledge and insight in relation to functional remission in patients with long-term psychotic disorders. *Soc Psychiatry Psychiatr Epidemiol*, 45(5), 523-529. doi: 10.1007/s00127-009-0096-3
- Alfonso, F., Perez-Vizcayno, M. J., Hernandez, R., Goicolea, J., Fernandez-Ortiz, A., Escaned, J., . . . Macaya, C. (1999). Long-term outcome and determinants of event-free survival in patients treated with balloon angioplasty for in-stent restenosis. *Am J Cardiol*, 83(8), 1268-1270, A1269.
- Alino, S. F., Benet, M., Dasi, F., & Crespo, J. (2003). Asialofetuin liposomes for receptor-mediated gene transfer into hepatic cells. *Methods Enzymol*, 373, 399-421. doi: 10.1016/S0076-6879(03)73026-2
- Allen, M., Law, F., & Rushton, N. (1994). The effects of diamond-like carbon coatings on macrophages, fibroblasts and osteoblast-like cells in vitro. *Clin Mater*, 17(1), 1-10.
- Allen, M., Myer, B., & Rushton, N. (2001). In vitro and in vivo investigations into the biocompatibility of diamond-like carbon (DLC) coatings for orthopedic applications. *J Biomed Mater Res*, 58(3), 319-328.
- Alt, E., Haehnel, I., Beilharz, C., Prietzel, K., Preter, D., Stemberger, A., . . . Schomig, A. (2000). Inhibition of neointima formation after experimental coronary artery stenting: a new biodegradable stent coating releasing hirudin and the prostacyclin analogue iloprost. *Circulation*, 101(12), 1453-1458.
- Ander, S., MacLennan, M., Bentil, S., Leavitt, B., & Chesler, N. (2005). Pressure-induced vector transport in human saphenous vein. *Ann Biomed Eng*, 33(2), 202-208.
- Andrianaivo, F., Lecocq, M., Wattiaux-De Coninck, S., Wattiaux, R., & Jadot, M. (2004). Hydrodynamics-based transfection of the liver: entrance into hepatocytes of DNA that causes expression takes place very early after injection. *J Gene Med*, 6(8), 877-883. doi: 10.1002/jgm.574
- Antimisiaris, S. G., Siablis, D., Liatsikos, E., Kalogeropoulou, C., Tsota, I., Tsotas, V., . . . Barbalias, G. A. (2000). Liposome-coated metal

stents: an in vitro evaluation of controlled-release modality in the ureter. *J Endourol*, 14(9), 743-747.

Aoki, J., Abizaid, A. C., Ong, A. T., Tsuchida, K., & Serruys, P. W. (2005). Serial assessment of tissue growth inside and outside the stent after implantation of drug-eluting stent in clinical trials. - Does delayed neointimal growth exist? *EuroIntervention*, 1(3), 235-255.

Aoki, J., Ong, A. T., Abizaid, A., den Heijer, P., Bonnier, H., McClean, D. R., . . . Serruys, P. W. (2005). One-year clinical outcome of various doses and pharmacokinetic release formulations of paclitaxel eluted from an erodible polymer - Insight in the Paclitaxel In-Stent Controlled Elution Study (PISCES). *EuroIntervention*, 1(2), 165-172.

Arap, M. A., Lahdenranta, J., Hajitou, A., Marini, F. C., 3rd, Wood, C. G., Wright, K. C., . . . Pasqualini, R. (2004). Model of unidirectional transluminal gene transfer. *Mol Ther*, 9(2), 305-310. doi: 10.1016/j.ymthe.2003.11.016

Arigita, C., Zuidam, N. J., Crommelin, D. J., & Hennink, W. E. (1999). Association and dissociation characteristics of polymer/DNA complexes used for gene delivery. *Pharm Res*, 16(10), 1534-1541.

Armbruster, V., Sauter, M., Krautkraemer, E., Meese, E., Kleiman, A., Best, B., . . . Mueller-Lantzsch, N. (2002). A novel gene from the human endogenous retrovirus K expressed in transformed cells. *Clin Cancer Res*, 8(6), 1800-1807.

Asahara, T., Bauters, C., Pastore, C., Kearney, M., Rossow, S., Bunting, S., . . . Isner, J. M. (1995). Local delivery of vascular endothelial growth factor accelerates reendothelialization and attenuates intimal hyperplasia in balloon-injured rat carotid artery. *Circulation*, 91(11), 2793-2801.

Babapulle, M. N., & Eisenberg, M. J. (2002). Coated stents for the prevention of restenosis: Part II. *Circulation*, 106(22), 2859-2866.

Babapulle, M. N., Joseph, L., Belisle, P., Brophy, J. M., & Eisenberg, M. J. (2004). A hierarchical Bayesian meta-analysis of randomised clinical trials of drug-eluting stents. *Lancet*, 364(9434), 583-591. doi: 10.1016/S0140-6736(04)16850-5

Bandak, S., Goren, D., Horowitz, A., Tzemach, D., & Gabizon, A. (1999). Pharmacological studies of cisplatin encapsulated in long-circulating

- liposomes in mouse tumor models. *Anticancer Drugs*, 10(10), 911-920.
- Banyay, M., Sarkar, M., & Graslund, A. (2003). A library of IR bands of nucleic acids in solution. *Biophys Chem*, 104(2), 477-488.
- Bar, F. W., van der Veen, F. H., Benzina, A., Habets, J., & Koole, L. H. (2000). New biocompatible polymer surface coating for stents results in a low neointimal response. *J Biomed Mater Res*, 52(1), 193-198.
- Barron, V., Lyons, E., Stenson-Cox, C., McHugh, P. E., & Pandit, A. (2003). Bioreactors for cardiovascular cell and tissue growth: a review. *Ann Biomed Eng*, 31(9), 1017-1030.
- Barthel, F., Remy, J. S., Loeffler, J. P., & Behr, J. P. (1993). Gene transfer optimization with lipospermine-coated DNA. *DNA Cell Biol*, 12(6), 553-560.
- Batrakova, E. V., Miller, D. W., Li, S., Alakhov, V. Y., Kabanov, A. V., & Elmquist, W. F. (2001). Pluronic P85 enhances the delivery of digoxin to the brain: in vitro and in vivo studies. *J Pharmacol Exp Ther*, 296(2), 551-557.
- Behr, J. P., Demeneix, B., Loeffler, J. P., & Perez-Mutul, J. (1989). Efficient gene transfer into mammalian primary endocrine cells with lipopolyamine-coated DNA. *Proc Natl Acad Sci U S A*, 86(18), 6982-6986.
- Belke, D. D., Gloss, B., Hollander, J. M., Swanson, E. A., Duplain, H., & Dillmann, W. H. (2006). In vivo gene delivery of HSP70i by adenovirus and adeno-associated virus preserves contractile function in mouse heart following ischemia-reperfusion. *Am J Physiol Heart Circ Physiol*, 291(6), H2905-2910. doi: 10.1152/ajpheart.00323.2006
- Bello-Roufai, M., Lambert, O., & Pitard, B. (2007). Relationships between the physicochemical properties of an amphiphilic triblock copolymers/DNA complexes and their intramuscular transfection efficiency. *Nucleic Acids Res*, 35(3), 728-739. doi: 10.1093/nar/gkl860
- Bennett, S. A. (2001). The potential role of the Australian Institute of Health and Welfare in a National Cardiac Surgery Database. *Heart Lung Circ*, 10(1 Suppl), S18-21. doi: 10.1046/j.1444-2892.2001.00070.x

- Berger, P. B., Kleiman, N. S., Pencina, M. J., Hsieh, W. H., Steinhubl, S. R., Jeremias, A., . . . Investigators, E. (2010). Frequency of major noncardiac surgery and subsequent adverse events in the year after drug-eluting stent placement results from the EVENT (Evaluation of Drug-Eluting Stents and Ischemic Events) Registry. *JACC Cardiovasc Interv*, 3(9), 920-927. doi: 10.1016/j.jcin.2010.03.021
- Bertrand, O. F., Sipehia, R., Mongrain, R., Rodes, J., Tardif, J. C., Bilodeau, L., . . . Bourassa, M. G. (1998). Biocompatibility aspects of new stent technology. *J Am Coll Cardiol*, 32(3), 562-571.
- Bettmann, M. A., Katzen, B. T., Whisnant, J., Brant-Zawadzki, M., Broderick, J. P., Furlan, A. J., . . . Roubin, G. (1998). Carotid stenting and angioplasty: a statement for healthcare professionals from the Councils on Cardiovascular Radiology, Stroke, Cardio-Thoracic and Vascular Surgery, Epidemiology and Prevention, and Clinical Cardiology, American Heart Association. *Stroke*, 29(1), 336-338.
- Bhatt, D. L. (2004). Inflammation and restenosis: is there a link? *Am Heart J*, 147(6), 945-947. doi: 10.1016/j.ahj.2003.12.027
- Bornfeldt, K. E. (2003). The cyclin-dependent kinase pathway moves forward. *Circ Res*, 92(4), 345-347. doi: 10.1161/01.RES.0000061765.06145.10
- Boussif, O., Lezoualc'h, F., Zanta, M. A., Mergny, M. D., Scherman, D., Demeneix, B., & Behr, J. P. (1995). A versatile vector for gene and oligonucleotide transfer into cells in culture and in vivo: polyethylenimine. *Proc Natl Acad Sci U S A*, 92(16), 7297-7301.
- Brazel, C. S., & Peppas, N. A. (1999). Dimensionless analysis of swelling of hydrophilic glassy polymers with subsequent drug release from relaxing structures. *Biomaterials*, 20(8), 721-732.
- Breen, A., O'Brien, T., & Pandit, A. (2009). Fibrin as a delivery system for therapeutic drugs and biomolecules. *Tissue Eng Part B Rev*, 15(2), 201-214. doi: 10.1089/ten.TEB.2008.0527
- Brilakis, E. S., Lasala, J. M., Cox, D. A., Berger, P. B., Bowman, T. S., Starzyk, R. M., & Dawkins, K. D. (2010). Outcomes after implantation of the TAXUS paclitaxel-eluting stent in saphenous vein graft lesions: results from the ARRIVE (TAXUS Peri-Approval Registry: A Multicenter Safety Surveillance) program. *JACC Cardiovasc Interv*, 3(7), 742-750. doi: 10.1016/j.jcin.2010.04.012

- Brito, L. A., Chandrasekhar, S., Little, S. R., & Amiji, M. M. (2010a). In vitro and in vivo studies of local arterial gene delivery and transfection using lipopolyplexes-embedded stents. *J Biomed Mater Res A*, *93*(1), 325-336. doi: 10.1002/jbm.a.32488
- Brito, L. A., Chandrasekhar, S., Little, S. R., & Amiji, M. M. (2010b). Non-viral eNOS gene delivery and transfection with stents for the treatment of restenosis. *Biomed Eng Online*, *9*, 56. doi: 10.1186/1475-925X-9-56
- Brown, B. G., Zhao, X. Q., Sacco, D. E., & Albers, J. J. (1993). Atherosclerosis regression, plaque disruption, and cardiovascular events: a rationale for lipid lowering in coronary artery disease. *Annu Rev Med*, *44*, 365-376. doi: 10.1146/annurev.me.44.020193.002053
- Brown, D. J., Rzucidlo, E. M., Merenick, B. L., Wagner, R. J., Martin, K. A., & Powell, R. J. (2005). Endothelial cell activation of the smooth muscle cell phosphoinositide 3-kinase/Akt pathway promotes differentiation. *J Vasc Surg*, *41*(3), 509-516. doi: 10.1016/j.jvs.2004.12.024
- Brown, M. A., Iyer, R. K., & Radisic, M. (2008). Pulsatile perfusion bioreactor for cardiac tissue engineering. *Biotechnol Prog*, *24*(4), 907-920. doi: 10.1002/btpr.11
- Brown, M. D., Schatzlein, A. G., & Uchegbu, I. F. (2001). Gene delivery with synthetic (non viral) carriers. *Int J Pharm*, *229*(1-2), 1-21.
- Brunt, K. R., Hall, S. R., Ward, C. A., & Melo, L. G. (2007). Endothelial progenitor cell and mesenchymal stem cell isolation, characterization, viral transduction. *Methods Mol Med*, *139*, 197-210.
- Budker, V. G., Subbotin, V. M., Budker, T., Sebestyen, M. G., Zhang, G., & Wolff, J. A. (2006). Mechanism of plasmid delivery by hydrodynamic tail vein injection. II. Morphological studies. *J Gene Med*, *8*(7), 874-888. doi: 10.1002/jgm.920
- Bureau, M. F., Wasungu, L., Juge, L., Scherman, D., Rols, M. P., & Mignet, N. (2012). Investigating relationship between transfection and permeabilization by the electric field and/or the Pluronic(R) L64 in vitro and in vivo. *J Gene Med*, *14*(3), 204-215. doi: 10.1002/jgm.2610

- Burke, S. E., Lubbers, N. L., Chen, Y. W., Hsieh, G. C., Mollison, K. W., Luly, J. R., & Wegner, C. D. (1999). Neointimal formation after balloon-induced vascular injury in Yucatan minipigs is reduced by oral rapamycin. *J Cardiovasc Pharmacol*, *33*(6), 829-835.
- Burton, P. B., Yacoub, M. H., & Barton, P. J. (1998). Rapamycin (sirolimus) inhibits heart cell growth in vitro. *Pediatr Cardiol*, *19*(6), 468-470. doi: 10.1007/s002469900359
- Carter, A. J. (2002). Drug-eluting stents for the prevention of restenosis: Standing the test of time. *Catheter Cardiovasc Interv*, *57*(1), 69-71. doi: 10.1002/ccd.10306
- Chan, E. S., Fernandez, P., Merchant, A. A., Montesinos, M. C., Trzaska, S., Desai, A., . . . Cronstein, B. N. (2006). Adenosine A2A receptors in diffuse dermal fibrosis: pathogenic role in human dermal fibroblasts and in a murine model of scleroderma. *Arthritis Rheum*, *54*(8), 2632-2642. doi: 10.1002/art.21974
- Chan, J. S., Wang, T. T., Zhang, S. L., Chen, X., & Carriere, S. (2000). Catecholamines and angiotensinogen gene expression in kidney proximal tubular cells. *Mol Cell Biochem*, *212*(1-2), 73-79.
- Chang, M. W., Barr, E., Seltzer, J., Jiang, Y. Q., Nabel, G. J., Nabel, E. G., . . . Leiden, J. M. (1995). Cytostatic gene therapy for vascular proliferative disorders with a constitutively active form of the retinoblastoma gene product. *Science*, *267*(5197), 518-522.
- Chatrchyan, S., Khachatryan, V., Sirunyan, A. M., Tumasyan, A., Adam, W., Bergauer, T., . . . Collaboration, C. M. S. (2014). Search for invisible decays of Higgs bosons in the vector boson fusion and associated ZH production modes. *Eur Phys J C Part Fields*, *74*(8), 2980. doi: 10.1140/epjc/s10052-014-2980-6
- Chen, M. S., John, J. M., Chew, D. P., Lee, D. S., Ellis, S. G., & Bhatt, D. L. (2006). Bare metal stent restenosis is not a benign clinical entity. *Am Heart J*, *151*(6), 1260-1264. doi: 10.1016/j.ahj.2005.08.011
- Chen, R. Y., Westfall, A. O., Mugavero, M. J., Cloud, G. A., Raper, J. L., Chatham, A. G., . . . Saag, M. S. (2003). Duration of highly active antiretroviral therapy regimens. *Clin Infect Dis*, *37*(5), 714-722. doi: 10.1086/377271
- Chieffo, A., Park, S. J., Meliga, E., Sheiban, I., Lee, M. S., Latib, A., . . . Colombo, A. (2008). Late and very late stent thrombosis following

drug-eluting stent implantation in unprotected left main coronary artery: a multicentre registry. *Eur Heart J*, 29(17), 2108-2115. doi: 10.1093/eurheartj/ehn270

Cini, N., Tulun, T., Decher, G., & Ball, V. (2010). Step-by-step assembly of self-patterning polyelectrolyte films violating (almost) all rules of layer-by-layer deposition. *J Am Chem Soc*, 132(24), 8264-8265. doi: 10.1021/ja102611q

Cirulli, E. T., & Goldstein, D. B. (2007). In vitro assays fail to predict in vivo effects of regulatory polymorphisms. *Hum Mol Genet*, 16(16), 1931-1939. doi: 10.1093/hmg/ddm140

Clarke, M. C., Littlewood, T. D., Figg, N., Maguire, J. J., Davenport, A. P., Goddard, M., & Bennett, M. R. (2008). Chronic apoptosis of vascular smooth muscle cells accelerates atherosclerosis and promotes calcification and medial degeneration. *Circ Res*, 102(12), 1529-1538. doi: 10.1161/CIRCRESAHA.108.175976

Committee for Advanced, T., Secretariat, C. A. T. S., Schneider, C. K., Salmikangas, P., Jilma, B., Flamion, B., . . . Celis, P. (2010). Challenges with advanced therapy medicinal products and how to meet them. *Nat Rev Drug Discov*, 9(3), 195-201. doi: 10.1038/nrd3052

Cook, S. L., Eigler, N. L., Shefer, A., Goldenberg, T., Forrester, J. S., & Litvack, F. (1991). Percutaneous excimer laser coronary angioplasty of lesions not ideal for balloon angioplasty. *Circulation*, 84(2), 632-643.

Cooney, R., Hynes, S. O., Sharif, F., Howard, L., & O'Brien, T. (2007). Effect of gene delivery of NOS isoforms on intimal hyperplasia and endothelial regeneration after balloon injury. *Gene Ther*, 14(5), 396-404.

Costa, R. A., & Moussa, I. D. (2006). Percutaneous treatment of coronary bifurcation lesions in the era of drug-eluting stents. *Minerva Cardioangiol*, 54(5), 577-589.

Couvreur, P., Barratt, G., Fattal, E., Legrand, P., & Vauthier, C. (2002). Nanocapsule technology: a review. *Crit Rev Ther Drug Carrier Syst*, 19(2), 99-134.

Crowther, M. A. (2005). Pathogenesis of atherosclerosis. *Hematology Am Soc Hematol Educ Program*, 436-441. doi: 10.1182/asheducation-2005.1.436

- D'Souza, B. N., Edelstein, L. C., Pegman, P. M., Smith, S. M., Loughran, S. T., Clarke, A., . . . Walls, D. (2004). Nuclear factor kappa B-dependent activation of the antiapoptotic bfl-1 gene by the Epstein-Barr virus latent membrane protein 1 and activated CD40 receptor. *J Virol*, *78*(4), 1800-1816.
- Daemen, J., Wenaweser, P., Tsuchida, K., Abrecht, L., Vaina, S., Morger, C., . . . Serruys, P. W. (2007). Early and late coronary stent thrombosis of sirolimus-eluting and paclitaxel-eluting stents in routine clinical practice: data from a large two-institutional cohort study. *Lancet*, *369*(9562), 667-678. doi: 10.1016/S0140-6736(07)60314-6
- Dalby, B., Cates, S., Harris, A., Ohki, E. C., Tilkins, M. L., Price, P. J., & Ciccarone, V. C. (2004). Advanced transfection with Lipofectamine 2000 reagent: primary neurons, siRNA, and high-throughput applications. *Methods*, *33*(2), 95-103. doi: 10.1016/j.ymeth.2003.11.023
- Das, S. K., Chung, S., Zervantonakis, I., Atnafu, J., & Kamm, R. D. (2008). A microfluidic platform for studying the effects of small temperature gradients in an incubator environment. *Biomicrofluidics*, *2*(3), 34106. doi: 10.1063/1.2988313
- Das, T., Ghosh, D., Bhattacharyya, T. K., & Maiti, T. K. (2007). Biocompatibility of diamond-like nanocomposite thin films. *J Mater Sci Mater Med*, *18*(3), 493-500. doi: 10.1007/s10856-007-2009-x
- Dauerman, H. L., Baim, D. S., Cutlip, D. E., Sparano, A. M., Gibson, C. M., Kuntz, R. E., . . . Cohen, D. J. (1998). Mechanical debulking versus balloon angioplasty for the treatment of diffuse in-stent restenosis. *Am J Cardiol*, *82*(3), 277-284.
- De Angel, R. E., Smith, S. M., Glickman, R. D., Perkins, S. N., & Hursting, S. D. (2010). Antitumor effects of ursolic acid in a mouse model of postmenopausal breast cancer. *Nutr Cancer*, *62*(8), 1074-1086. doi: 10.1080/01635581.2010.492092
- Delgado, D., Gascon, A. R., Del Pozo-Rodriguez, A., Echevarria, E., Ruiz de Garibay, A. P., Rodriguez, J. M., & Solinis, M. A. (2012). Dextran-protamine-solid lipid nanoparticles as a non-viral vector for gene therapy: in vitro characterization and in vivo transfection after intravenous administration to mice. *Int J Pharm*, *425*(1-2), 35-43. doi: 10.1016/j.ijpharm.2011.12.052

- Demaneche, S., Jocteur-Monrozier, L., Quiquampoix, H., & Simonet, P. (2001). Evaluation of biological and physical protection against nuclease degradation of clay-bound plasmid DNA. *Appl Environ Microbiol*, *67*(1), 293-299. doi: 10.1128/AEM.67.1.293-299.2001
- Desai, M. P., Labhasetwar, V., Walter, E., Levy, R. J., & Amidon, G. L. (1997). The mechanism of uptake of biodegradable microparticles in Caco-2 cells is size dependent. *Pharm Res*, *14*(11), 1568-1573.
- Dhanoya, A., Chain, B. M., & Keshavarz-Moore, E. (2011). The impact of DNA topology on polyplex uptake and transfection efficiency in mammalian cells. *J Biotechnol*, *155*(4), 377-386. doi: 10.1016/j.jbiotec.2011.07.023
- Dibra, A., Mehilli, J., Braun, S., Hadamitzky, M., Baum, H., Dirschinger, J., . . . Kastrati, A. (2005). Inflammatory response after intervention assessed by serial C-reactive protein measurements correlates with restenosis in patients treated with coronary stenting. *Am Heart J*, *150*(2), 344-350. doi: 10.1016/j.ahj.2004.09.030
- Dobesh, P. P., Stacy, Z. A., Ansara, A. J., & Enders, J. M. (2004). Drug-eluting stents: a mechanical and pharmacologic approach to coronary artery disease. *Pharmacotherapy*, *24*(11), 1554-1577. doi: 10.1592/phco.24.16.1554.50955
- Donawa, M. E. (2008). The evolving process of European combination product review, Part I. *Med Device Technol*, *19*(6), 32, 34-35.
- Doornekamp, F. N., Borst, C., Haudenschild, C. C., & Post, M. J. (1996). Fogarty and percutaneous transluminal coronary angioplasty balloon injury induce comparable damage to the arterial wall but lead to different healing responses. *J Vasc Surg*, *24*(5), 843-850.
- Dotter, C. T., & Judkins, M. P. (1964). Transluminal Treatment of Arteriosclerotic Obstruction. Description of a New Technic and a Preliminary Report of Its Application. *Circulation*, *30*, 654-670.
- Drachman, D. E., & Simon, D. I. (2005). Inflammation as a mechanism and therapeutic target for in-stent restenosis. *Curr Atheroscler Rep*, *7*(1), 44-49.
- Dvir, T., Benishti, N., Shachar, M., & Cohen, S. (2006). A novel perfusion bioreactor providing a homogenous milieu for tissue regeneration. *Tissue Eng*, *12*(10), 2843-2852. doi: 10.1089/ten.2006.12.2843

- Dwarakanath, R. S., Sahar, S., Lanting, L., Wang, N., Stemerman, M. B., Natarajan, R., & Reddy, M. A. (2008). Viral vector-mediated 12/15-lipoxygenase overexpression in vascular smooth muscle cells enhances inflammatory gene expression and migration. *J Vasc Res*, *45*(2), 132-142. doi: 10.1159/000109966
- El-Kamel, A. H. (2002). In vitro and in vivo evaluation of Pluronic F127-based ocular delivery system for timolol maleate. *Int J Pharm*, *241*(1), 47-55.
- Erbacher, P., Zou, S., Bettinger, T., Steffan, A. M., & Remy, J. S. (1998). Chitosan-based vector/DNA complexes for gene delivery: biophysical characteristics and transfection ability. *Pharm Res*, *15*(9), 1332-1339.
- Erbel, R., Haude, M., Hopp, H. W., Franzen, D., Rupprecht, H. J., Heublein, B., . . . Probst, P. (1998). Coronary-artery stenting compared with balloon angioplasty for restenosis after initial balloon angioplasty. Restenosis Stent Study Group. *N Engl J Med*, *339*(23), 1672-1678. doi: 10.1056/NEJM199812033392304
- Falcetti, E., Hall, S. M., Phillips, P. G., Patel, J., Morrell, N. W., Haworth, S. G., & Clapp, L. H. (2010). Smooth muscle proliferation and role of the prostacyclin (IP) receptor in idiopathic pulmonary arterial hypertension. *Am J Respir Crit Care Med*, *182*(9), 1161-1170. doi: 10.1164/rccm.201001-0011OC
- Falk, E., & Fernandez-Ortiz, A. (1995). Role of thrombosis in atherosclerosis and its complications. *Am J Cardiol*, *75*(6), 3B-11B.
- Faneca, H., Simoes, S., & de Lima, M. C. (2002). Evaluation of lipid-based reagents to mediate intracellular gene delivery. *Biochim Biophys Acta*, *1567*(1-2), 23-33.
- Farb, A., Burke, A. P., Kolodgie, F. D., & Virmani, R. (2003). Pathological mechanisms of fatal late coronary stent thrombosis in humans. *Circulation*, *108*(14), 1701-1706. doi: 10.1161/01.CIR.0000091115.05480.B0
- Farb, A., Weber, D. K., Kolodgie, F. D., Burke, A. P., & Virmani, R. (2002). Morphological predictors of restenosis after coronary stenting in humans. *Circulation*, *105*(25), 2974-2980.

- Feigenblum, D., Walker, R., & Schneider, R. J. (1998). Adenovirus induction of an interferon-regulatory factor during entry into the late phase of infection. *J Virol*, *72*(11), 9257-9266.
- Felgner, P. L. (1997). Nonviral strategies for gene therapy. *Sci Am*, *276*(6), 102-106.
- Felgner, P. L., Gadek, T. R., Holm, M., Roman, R., Chan, H. W., Wenz, M., . . . Danielsen, M. (1987). Lipofection: a highly efficient, lipid-mediated DNA-transfection procedure. *Proc Natl Acad Sci U S A*, *84*(21), 7413-7417.
- Ferrari, S., Geddes, D. M., & Alton, E. W. (2002). Barriers to and new approaches for gene therapy and gene delivery in cystic fibrosis. *Adv Drug Deliv Rev*, *54*(11), 1373-1393.
- Fesinmeyer, M. D., North, K. E., Ritchie, M. D., Lim, U., Franceschini, N., Wilkens, L. R., . . . Peters, U. (2013). Genetic risk factors for BMI and obesity in an ethnically diverse population: results from the population architecture using genomics and epidemiology (PAGE) study. *Obesity (Silver Spring)*, *21*(4), 835-846. doi: 10.1002/oby.20268
- Fischer, L., Preis, M., Weisz, A., Koren, B., Lewis, B. S., & Flugelman, M. Y. (2002). Viral vectors for vascular gene therapy. *Exp Clin Cardiol*, *7*(2-3), 106-112.
- Fishbein, I., Alferiev, I., Bakay, M., Stachelek, S. J., Sobolewski, P., Lai, M., . . . Levy, R. J. (2008). Local delivery of gene vectors from bare-metal stents by use of a biodegradable synthetic complex inhibits in-stent restenosis in rat carotid arteries. *Circulation*, *117*(16), 2096-2103.
- Fishbein, I., Alferiev, I. S., Nyanguile, O., Gaster, R., Vohs, J. M., Wong, G. S., . . . Levy, R. J. (2006). Bisphosphonate-mediated gene vector delivery from the metal surfaces of stents. *Proc Natl Acad Sci U S A*, *103*(1), 159-164. doi: 10.1073/pnas.0502945102
- Fishbein, I., Chorny, M., Adamo, R. F., Forbes, S. P., Corrales, R. A., Alferiev, I. S., & Levy, R. J. (2013). Endovascular Gene Delivery from a Stent Platform: Gene- Eluting Stents. *Angiol Open Access*, *1*(2). doi: 10.4172/2329-9495.1000109
- Fishbein, I., Chorny, M., & Levy, R. J. (2010). Site-specific gene therapy for cardiovascular disease. *Curr Opin Drug Discov Devel*, *13*(2), 203-213.

- Flanagan, T. C., Wilkins, B., Black, A., Jockenhoevel, S., Smith, T. J., & Pandit, A. S. (2006). A collagen-glycosaminoglycan co-culture model for heart valve tissue engineering applications. *Biomaterials*, 27(10), 2233-2246. doi: 10.1016/j.biomaterials.2005.10.031
- Frank, S., Kolb, N., Werner, E. R., & Pfeilschifter, J. (1998). Coordinated induction of inducible nitric oxide synthase and GTP-cyclohydrolase I is dependent on inflammatory cytokines and interferon-gamma in HaCaT keratinocytes: implications for the model of cutaneous wound repair. *J Invest Dermatol*, 111(6), 1065-1071. doi: 10.1046/j.1523-1747.1998.00433.x
- Frerix, A., Geilenkirchen, P., Muller, M., Kula, M. R., & Hubbuch, J. (2007). Separation of genomic DNA, RNA, and open circular plasmid DNA from supercoiled plasmid DNA by combining denaturation, selective renaturation and aqueous two-phase extraction. *Biotechnol Bioeng*, 96(1), 57-66. doi: 10.1002/bit.21166
- Frid, M. G., Shekhonin, B. V., Koteliansky, V. E., & Glukhova, M. A. (1992). Phenotypic changes of human smooth muscle cells during development: late expression of heavy caldesmon and calponin. *Dev Biol*, 153(2), 185-193.
- Froeschl, M., Olsen, S., Ma, X., & O'Brien, E. R. (2004). Current understanding of in-stent restenosis and the potential benefit of drug eluting stents. *Curr Drug Targets Cardiovasc Haematol Disord*, 4(1), 103-117.
- Fu, Y., & Kao, W. J. (2010). Drug release kinetics and transport mechanisms of non-degradable and degradable polymeric delivery systems. *Expert Opin Drug Deliv*, 7(4), 429-444. doi: 10.1517/17425241003602259
- Fuchs, J. R., Nasser, B. A., & Vacanti, J. P. (2001). Tissue engineering: a 21st century solution to surgical reconstruction. *Ann Thorac Surg*, 72(2), 577-591.
- Fujii, K., Masutani, M., Kobayashi, Y., Tateishi, J., Kawasaki, D., Ohyanagi, M., . . . Leon, M. B. (2004). Contribution of early lumen loss after balloon angioplasty for in-stent restenosis to lumen loss at follow-up. *Catheter Cardiovasc Interv*, 63(1), 52-56. doi: 10.1002/ccd.20097
- Fujii, K., Masutani, M., & Ohyanagi, M. (2008). Contribution of organized thrombus to in-stent restenosis after sirolimus-eluting stent

implantation: optical coherence tomography findings. *Eur Heart J*, 29(11), 1385. doi: 10.1093/eurheartj/ehm570

Funakoshi, K., & Egashira, K. (2007). [Molecular mechanism of in-stent restenosis and novel treatment strategy of gene-eluting stent developed with bioabsorbable nanoparticle electrodeposition]. *Nihon Yakurigaku Zasshi*, 129(3), 171-176.

Funamoto, K., Zervantonakis, I. K., Liu, Y., Ochs, C. J., Kim, C., & Kamm, R. D. (2012). A novel microfluidic platform for high-resolution imaging of a three-dimensional cell culture under a controlled hypoxic environment. *Lab Chip*, 12(22), 4855-4863. doi: 10.1039/c2lc40306d

Fuster, V., Badimon, L., Badimon, J. J., & Chesebro, J. H. (1992). The pathogenesis of coronary artery disease and the acute coronary syndromes (2). *N Engl J Med*, 326(5), 310-318.

Gallo, R., Padurean, A., Jayaraman, T., Marx, S., Roque, M., Adelman, S., . . . Badimon, J. J. (1999). Inhibition of intimal thickening after balloon angioplasty in porcine coronary arteries by targeting regulators of the cell cycle. *Circulation*, 99(16), 2164-2170.

Gao, X., & Huang, L. (1991). A novel cationic liposome reagent for efficient transfection of mammalian cells. *Biochem Biophys Res Commun*, 179(1), 280-285.

Gao, X., & Huang, L. (1995). Cationic liposome-mediated gene transfer. *Gene Ther*, 2(10), 710-722.

Garratt, K. N., Holmes, D. R., Jr., & Roubin, G. S. (1991). Early outcome after placement of a metallic intracoronary stent: initial Mayo Clinic experience. *Mayo Clin Proc*, 66(3), 268-275.

Gaymalov, Z. Z., Yang, Z., Pisarev, V. M., Alakhov, V. Y., & Kabanov, A. V. (2009). The effect of the nonionic block copolymer pluronic P85 on gene expression in mouse muscle and antigen-presenting cells. *Biomaterials*, 30(6), 1232-1245. doi: 10.1016/j.biomaterials.2008.10.064

Ge, L., Iakovou, I., Cosgrave, J., Chieffo, A., Montorfano, M., Michev, I., . . . Colombo, A. (2005). Immediate and mid-term outcomes of sirolimus-eluting stent implantation for chronic total occlusions. *Eur Heart J*, 26(11), 1056-1062. doi: 10.1093/eurheartj/ehi191

- Gebhart, C. L., Sriadibhatla, S., Vinogradov, S., Lemieux, P., Alakhov, V., & Kabanov, A. V. (2002). Design and formulation of polyplexes based on pluronic-polyethyleneimine conjugates for gene transfer. *Bioconjug Chem*, 13(5), 937-944.
- Germing, A., von Dryander, S., Bojara, W., Lawo, T., Grewe, P., Machraoui, A., & Lemke, B. (2002). Coronary artery stenting in diabetes mellitus--unfavourable clinical outcome due to increased rate of myocardial ischemia and percutaneous interventions. *Eur J Med Res*, 7(6), 265-270.
- Gibbons, A., Padilla-Carlin, D., Kelly, C., Hickey, A. J., Taggart, C., McElvaney, N. G., & Cryan, S. A. (2011). The effect of liposome encapsulation on the pharmacokinetics of recombinant secretory leukocyte protease inhibitor (rSLPI) therapy after local delivery to a guinea pig asthma model. *Pharm Res*, 28(9), 2233-2245. doi: 10.1007/s11095-011-0454-1
- Gilmore, T. D. (2006). Introduction to NF-kappaB: players, pathways, perspectives. *Oncogene*, 25(51), 6680-6684. doi: 10.1038/sj.onc.1209954
- Ginn, S. L., Alexander, I. E., Edelstein, M. L., Abedi, M. R., & Wixon, J. (2013). Gene therapy clinical trials worldwide to 2012 - an update. *J Gene Med*, 15(2), 65-77. doi: 10.1002/jgm.2698
- Giral, P., Kahn, J. F., Andre, J. M., Carreau, V., Dourmap, C., Bruckert, E., & Chapman, M. J. (2007). Carotid atherosclerosis is not related to past tuberculosis in hypercholesterolemic patients. *Atherosclerosis*, 190(1), 150-155. doi: 10.1016/j.atherosclerosis.2006.01.008
- Goh, D., Tan, A., Farhatnia, Y., Rajadas, J., Alavijeh, M. S., & Seifalian, A. M. (2013). Nanotechnology-based gene-eluting stents. *Mol Pharm*, 10(4), 1279-1298. doi: 10.1021/mp3006616
- Gomella, L. G., Mastrangelo, M. J., McCue, P. A., Maguire, H. J., Mulholland, S. G., & Lattime, E. C. (2001). Phase i study of intravesical vaccinia virus as a vector for gene therapy of bladder cancer. *J Urol*, 166(4), 1291-1295.
- Gordon, E. M., Skotzko, M., Kundu, R. K., Han, B., Andrades, J., Nimni, M., . . . Hall, F. L. (1997). Capture and expansion of bone marrow-derived mesenchymal progenitor cells with a transforming growth factor-beta1-von Willebrand's factor fusion protein for retrovirus-

mediated delivery of coagulation factor IX. *Hum Gene Ther*, 8(11), 1385-1394. doi: 10.1089/hum.1997.8.11-1385

- Govender, S., Jacobs, E. P., Bredenkamp, M. W., & Swart, P. (2005). A robust approach to studying the adsorption of Pluronic F108 on nonporous membranes. *J Colloid Interface Sci*, 282(2), 306-313. doi: 10.1016/j.jcis.2004.08.138
- Grassi, G., Noro, E., Farra, R., Guarnieri, G., Lapasin, R., Grassi, M., . . . Alhaique, F. (2006). Rheological and mechanical properties of Pluronic-alginate gels for drug-eluting stent coating. *J Control Release*, 116(2), e85-87. doi: 10.1016/j.jconrel.2006.09.063
- Grayson, W. L., Martens, T. P., Eng, G. M., Radisic, M., & Vunjak-Novakovic, G. (2009). Biomimetic approach to tissue engineering. *Semin Cell Dev Biol*, 20(6), 665-673. doi: 10.1016/j.semcdb.2008.12.008
- Grigsby, C. L., & Leong, K. W. (2010). Balancing protection and release of DNA: tools to address a bottleneck of non-viral gene delivery. *J R Soc Interface*, 7 Suppl 1, S67-82. doi: 10.1098/rsif.2009.0260
- Gruntzig, A. (1979). [Clinical experience with coronary intra-arterial dilatation using catheters. Results (author's transl)]. *Ann Cardiol Angeiol (Paris)*, 28(7), 487-489.
- Gunn, J., Holt, C. M., Francis, S. E., Shepherd, L., Grohmann, M., Newman, C. M., . . . Cumberland, D. C. (1997). The effect of oligonucleotides to c-myb on vascular smooth muscle cell proliferation and neointima formation after porcine coronary angioplasty. *Circ Res*, 80(4), 520-531.
- Gunzburg, W. H., & Salmons, B. (1995). Virus vector design in gene therapy. *Mol Med Today*, 1(9), 410-417.
- Gutensohn, K., Beythien, C., Bau, J., Fenner, T., Grewe, P., Koester, R., . . . Kuehn, P. (2000). In vitro analyses of diamond-like carbon coated stents. Reduction of metal ion release, platelet activation, and thrombogenicity. *Thromb Res*, 99(6), 577-585.
- Guzman, R. J., Hirschowitz, E. A., Brody, S. L., Crystal, R. G., Epstein, S. E., & Finkel, T. (1994). In vivo suppression of injury-induced vascular smooth muscle cell accumulation using adenovirus-mediated transfer of the herpes simplex virus thymidine kinase gene. *Proc Natl Acad Sci U S A*, 91(22), 10732-10736.

- Habara, S., Mitsudo, K., Goto, T., Kadota, K., Fujii, S., Yamamoto, H., . . . Inoue, K. (2008). The impact of lesion length and vessel size on outcomes after sirolimus-eluting stent implantation for in-stent restenosis. *Heart*, *94*(9), 1162-1165. doi: 10.1136/hrt.2007.128595
- Hacein-Bey-Abina, S., de Saint Basile, G., & Cavazzana-Calvo, M. (2003). Gene therapy of X-linked severe combined immunodeficiency. *Methods Mol Biol*, *215*, 247-259.
- Hacein-Bey-Abina, S., von Kalle, C., Schmidt, M., Le Deist, F., Wulffraat, N., McIntyre, E., . . . Fischer, A. (2003). A serious adverse event after successful gene therapy for X-linked severe combined immunodeficiency. *N Engl J Med*, *348*(3), 255-256. doi: 10.1056/NEJM200301163480314
- Haensler, J., & Szoka, F. C., Jr. (1993). Polyamidoamine cascade polymers mediate efficient transfection of cells in culture. *Bioconjug Chem*, *4*(5), 372-379.
- Hamblin, K. A., Armstrong, S. J., Barnes, K. B., Davies, C., Wong, J. P., Blanchard, J. D., . . . Atkins, H. S. (2014). Liposome encapsulation of ciprofloxacin improves protection against highly virulent *Francisella tularensis* strain Schu S4. *Antimicrob Agents Chemother*, *58*(6), 3053-3059. doi: 10.1128/AAC.02555-13
- Hamm, C. W., Hugenholtz, P. G., & Investigators, T. (2003). Silicon carbide-coated stents in patients with acute coronary syndrome. *Catheter Cardiovasc Interv*, *60*(3), 375-381. doi: 10.1002/ccd.10656
- Harrington, R. A., Califf, R. M., Holmes, D. R., Jr., Pieper, K. S., Lincoff, A. M., Berdan, L. G., . . . Topol, E. J. (1999). Is all unstable angina the same? insights from the Coronary Angioplasty Versus Excisional Atherectomy Trial (CAVEAT-I). The CAVEAT-Investigators. *Am Heart J*, *137*(2), 227-233.
- Hassan, A. K., Bergheanu, S. C., Stijnen, T., van der Hoeven, B. L., Snoep, J. D., Plevier, J. W., . . . Wouter Jukema, J. (2010). Late stent malapposition risk is higher after drug-eluting stent compared with bare-metal stent implantation and associates with late stent thrombosis. *Eur Heart J*, *31*(10), 1172-1180. doi: 10.1093/eurheartj/ehn553
- Hayase, M., Del Monte, F., Kawase, Y., Macneill, B. D., McGregor, J., Yoneyama, R., . . . Hajjar, R. J. (2005). Catheter-based antegrade intracoronary viral gene delivery with coronary venous blockade.

*Am J Physiol Heart Circ Physiol*, 288(6), H2995-3000. doi: 10.1152/ajpheart.00703.2004

Hendriks, B. S., Reynolds, J. G., Klinz, S. G., Geretti, E., Lee, H., Leonard, S. C., . . . Wickham, T. J. (2012). Multiscale kinetic modeling of liposomal Doxorubicin delivery quantifies the role of tumor and drug-specific parameters in local delivery to tumors. *CPT Pharmacometrics Syst Pharmacol*, 1, e15. doi: 10.1038/psp.2012.16

Herman, I. M., Newcomb, P. M., Coughlin, J. E., & Jacobson, S. (1987). Characterization of microvascular cell cultures from normotensive and hypertensive rat brains: pericyte-endothelial cell interactions in vitro. *Tissue Cell*, 19(2), 197-206.

Heublein, B., Ozbek, C., & Pethig, K. (1998). Silicon carbide-coated stents: clinical experience in coronary lesions with increased thrombotic risk. *J Endovasc Surg*, 5(1), 32-36. doi: 10.1583/1074-6218(1998)005<0032:SCCSCE>2.0.CO;2

Heye, S., Vanbeckevoort, D., Blockmans, D., Nevelsteen, A., & Maleux, G. (2005). Iatrogenic main renal artery injury: treatment by endovascular stent-graft placement. *Cardiovasc Intervent Radiol*, 28(1), 93-94. doi: 10.1007/s00270-004-0050-4

Hiatt, B. L., Ikeno, F., Yeung, A. C., & Carter, A. J. (2002). Drug-eluting stents for the prevention of restenosis: in quest for the Holy Grail. *Catheter Cardiovasc Interv*, 55(3), 409-417.

Hill, R. A., Dundar, Y., Bakhai, A., Dickson, R., & Walley, T. (2004). Drug-eluting stents: an early systematic review to inform policy. *Eur Heart J*, 25(11), 902-919. doi: 10.1016/j.ehj.2004.03.023

Hilts, P. J. (2000). F.D.A. says researcher failed to report a second death linked to gene therapy. *N Y Times Web*, A20.

Hinuber, C., Kleemann, C., Friederichs, R. J., Haubold, L., Scheibe, H. J., Schuelke, T., . . . Baumann, M. J. (2010). Biocompatibility and mechanical properties of diamond-like coatings on cobalt-chromium-molybdenum steel and titanium-aluminum-vanadium biomedical alloys. *J Biomed Mater Res A*, 95(2), 388-400. doi: 10.1002/jbm.a.32851

Hishikawa, T., Iihara, K., Yamada, N., Ishibashi-Ueda, H., & Miyamoto, S. (2010). Assessment of necrotic core with intraplaque hemorrhage in atherosclerotic carotid artery plaque by MR imaging with 3D

gradient-echo sequence in patients with high-grade stenosis. Clinical article. *J Neurosurg*, 113(4), 890-896. doi: 10.3171/2010.3.JNS091057

Hoerstrup, S. P., Zund, G., Sodian, R., Schnell, A. M., Grunenfelder, J., & Turina, M. I. (2001). Tissue engineering of small caliber vascular grafts. *Eur J Cardiothorac Surg*, 20(1), 164-169.

Hofma, S. H., van Beusekom, H. M., Serruys, P. W., & van Der Giessen, W. J. (2001). Recent Developments in Coated Stents. *Curr Interv Cardiol Rep*, 3(1), 28-36.

Hojo, S., Shimizu, K., Yositate, H., Muraji, M., Tsujimoto, H., & Tatebe, W. (2003). The relationship between electropermeabilization and cell cycle and cell size of *Saccharomyces cerevisiae*. *IEEE Trans Nanobioscience*, 2(1), 35-39.

Hojo, Y., Ikeda, U., Takahashi, M., & Shimada, K. (2002). Increased levels of monocyte-related cytokines in patients with unstable angina. *Atherosclerosis*, 161(2), 403-408.

Hojo, Y., & Shimada, K. (1998). [Role of cytokines in acute coronary syndrome]. *Nihon Rinsho*, 56(10), 2500-2503.

Holladay, C., Keeney, M., Newland, B., Mathew, A., Wang, W., & Pandit, A. (2010). A reliable method for detecting complexed DNA in vitro. *Nanoscale*, 2(12), 2718-2723. doi: 10.1039/c0nr00456a

Hollweck, T., Akra, B., Haussler, S., Uberfuhr, P., Schmitz, C., Pfeifer, S., . . . Eissner, G. (2011). A novel pulsatile bioreactor for mechanical stimulation of tissue engineered cardiac constructs. *J Funct Biomater*, 2(3), 107-118. doi: 10.3390/jfb2030107

Honda, H., Meguro, T., Takizawa, K., & Isoyama, S. (2005). Use of everolimus-eluting stent with a bioresorbable polymer coating for treatment of recurrent in-stent restenosis. *J Invasive Cardiol*, 17(2), 112-115.

Hong, M. K., Mehran, R., Mintz, G. S., & Leon, M. B. (1997). Restenosis after coronary angioplasty. *Curr Probl Cardiol*, 22(1), 1-36.

Hong, R. L., Huang, C. J., Tseng, Y. L., Pang, V. F., Chen, S. T., Liu, J. J., & Chang, F. H. (1999). Direct comparison of liposomal doxorubicin with or without polyethylene glycol coating in C-26 tumor-bearing

mice: is surface coating with polyethylene glycol beneficial? *Clin Cancer Res*, 5(11), 3645-3652.

- Hong, R. L., Sheen, T. S., Ko, J. Y., Hsu, M. M., Wang, C. C., & Ting, L. L. (1999). Induction with mitomycin C, doxorubicin, cisplatin and maintenance with weekly 5-fluorouracil, leucovorin for treatment of metastatic nasopharyngeal carcinoma: a phase II study. *Br J Cancer*, 80(12), 1962-1967. doi: 10.1038/sj.bjc.6690627
- Hong, S. J., Kim, M. H., Ahn, T. H., Ahn, Y. K., Bae, J. H., Shim, W. J., . . . Lim, D. S. (2006). Multiple predictors of coronary restenosis after drug-eluting stent implantation in patients with diabetes. *Heart*, 92(8), 1119-1124. doi: 10.1136/hrt.2005.075960
- Horcas, I., Fernandez, R., Gomez-Rodriguez, J. M., Colchero, J., Gomez-Herrero, J., & Baro, A. M. (2007). WSXM: a software for scanning probe microscopy and a tool for nanotechnology. *Rev Sci Instrum*, 78(1), 013705. doi: 10.1063/1.2432410
- Horobin, R. W. (2001). The problem of proprietary dyes, with special reference to alamar blue, a proprietary dye revealed. *Biotech Histochem*, 76(4), 163-164.
- Hossfeld, S., Nolte, A., Hartmann, H., Recke, M., Schaller, M., Walker, T., . . . Krastev, R. (2013). Bioactive coronary stent coating based on layer-by-layer technology for siRNA release. *Acta Biomater*, 9(5), 6741-6752. doi: 10.1016/j.actbio.2013.01.013
- Htay, T., & Liu, M. W. (2005). Drug-eluting stent: a review and update. *Vasc Health Risk Manag*, 1(4), 263-276.
- Hu, Y., Krishan, A., Nie, W., Sridhar, K. S., Mayer, L. D., & Bally, M. (2004). Synergistic cytotoxicity of pyrazoloacridine with doxorubicin, etoposide, and topotecan in drug-resistant tumor cells. *Clin Cancer Res*, 10(3), 1160-1169.
- Huang, G. M., Li, G. S., Zhu, G. Y., Lai, Y. M., Zhang, H. X., Wang, J., & Wang, H. R. (2002). Safety and bioactivity of intracoronary delivery of naked plasmid DNA encoding human atrial natriuretic factor. *Acta Pharmacol Sin*, 23(7), 609-611.
- Huang, Q., Hong, B., Xu, Y., & Liu, J. (2009). Very late thrombosis in a patient with a drug-eluting stent for intracranial atherosclerotic stenosis. *J Clin Neurosci*, 16(12), 1631-1633. doi: 10.1016/j.jocn.2009.01.025

- Iakovou, I., Sangiorgi, G. M., Stankovic, G., Corvaja, N., Vitrella, G., Ferraro, M., & Colombo, A. (2005). Results and follow-up after implantation of four or more sirolimus-eluting stents in the same patient. *Catheter Cardiovasc Interv*, *64*(4), 436-439; discussion 440-431. doi: 10.1002/ccd.20305
- Indolfi, C., Coppola, C., Torella, D., Arcucci, O., & Chiariello, M. (1999). Gene therapy for restenosis after balloon angioplasty and stenting. *Cardiol Rev*, *7*(6), 324-331.
- Inoue, T., Croce, K., Morooka, T., Sakuma, M., Node, K., & Simon, D. I. (2011). Vascular inflammation and repair: implications for re-endothelialization, restenosis, and stent thrombosis. *JACC Cardiovasc Interv*, *4*(10), 1057-1066. doi: 10.1016/j.jcin.2011.05.025
- Irving, R. J., & Walker, B. R. (1999). Blood vessel structure in hypertension. *Saudi J Kidney Dis Transpl*, *10*(3), 257-266.
- Izumrudov, V. A., Kharlampieva, E., & Sukhishvili, S. A. (2005). Multilayers of a globular protein and a weak polyacid: role of polyacid ionization in growth and decomposition in salt solutions. *Biomacromolecules*, *6*(3), 1782-1788. doi: 10.1021/bm050096v
- Jabara, R., Pendyala, L., Geva, S., Chen, J., Chronos, N., & Robinson, K. (2009). Novel fully bioabsorbable salicylate-based sirolimus-eluting stent. *EuroIntervention*, *5 Suppl F*, F58-64. doi: 10.4244/EIJV5IFA10
- Jain, R. A. (2000). The manufacturing techniques of various drug loaded biodegradable poly(lactide-co-glycolide) (PLGA) devices. *Biomaterials*, *21*(23), 2475-2490.
- Janero, D. R., & Ewing, J. F. (2000). Nitric oxide and postangioplasty restenosis: pathological correlates and therapeutic potential. *Free Radic Biol Med*, *29*(12), 1199-1221.
- Javier, A. F., Bata-Csorgo, Z., Ellis, C. N., Kang, S., Voorhees, J. J., & Cooper, K. D. (1997). Rapamycin (sirolimus) inhibits proliferating cell nuclear antigen expression and blocks cell cycle in the G1 phase in human keratinocyte stem cells. *J Clin Invest*, *99*(9), 2094-2099. doi: 10.1172/JCI119382
- Jeon, E., Kim, H. D., & Kim, J. S. (2003). Pluronic-grafted poly-(L)-lysine as a new synthetic gene carrier. *J Biomed Mater Res A*, *66*(4), 854-859. doi: 10.1002/jbm.a.10012

- Jeremias, A., Haude, M., Ge, J., Gorge, G., Liu, F., Konorza, T., & Erbel, R. (1997). [Emergency stent implantation in the area of extensive muscle bridging of the anterior interventricular ramus after post-interventional dissection]. *Z Kardiol*, *86*(5), 367-372.
- Jewell, C. M., Zhang, J., Fredin, N. J., Wolff, M. R., Hacker, T. A., & Lynn, D. M. (2006). Release of plasmid DNA from intravascular stents coated with ultrathin multilayered polyelectrolyte films. *Biomacromolecules*, *7*(9), 2483-2491. doi: 10.1021/bm0604808
- Jockenhoevel, S., Zund, G., Hoerstrup, S. P., Chalabi, K., Sachweh, J. S., Demircan, L., . . . Turina, M. (2001). Fibrin gel -- advantages of a new scaffold in cardiovascular tissue engineering. *Eur J Cardiothorac Surg*, *19*(4), 424-430.
- Jockenhoevel, S., Zund, G., Hoerstrup, S. P., Schnell, A., & Turina, M. (2002). Cardiovascular tissue engineering: a new laminar flow chamber for in vitro improvement of mechanical tissue properties. *ASAIO J*, *48*(1), 8-11.
- Joner, M., Finn, A. V., Farb, A., Mont, E. K., Kolodgie, F. D., Ladich, E., . . . Virmani, R. (2006). Pathology of drug-eluting stents in humans: delayed healing and late thrombotic risk. *J Am Coll Cardiol*, *48*(1), 193-202.
- Jones, E. A., le Noble, F., & Eichmann, A. (2006). What determines blood vessel structure? Genetic prespecification vs. hemodynamics. *Physiology (Bethesda)*, *21*, 388-395. doi: 10.1152/physiol.00020.2006
- Kalnins, U., Erglis, A., Dinne, I., Kumsars, I., & Jegere, S. (2002). Clinical outcomes of silicon carbide coated stents in patients with coronary artery disease. *Med Sci Monit*, *8*(2), P116-20.
- Kaplan, A. V., Baim, D. S., Smith, J. J., Feigal, D. A., Simons, M., Jefferys, D., . . . Leon, M. B. (2004). Medical device development: from prototype to regulatory approval. *Circulation*, *109*(25), 3068-3072. doi: 10.1161/01.CIR.0000134695.65733.64
- Karra, D., & Dahm, R. (2010). Transfection techniques for neuronal cells. *J Neurosci*, *30*(18), 6171-6177. doi: 10.1523/JNEUROSCI.0183-10.2010

- Kastrati, A., Mehilli, J., Dirschinger, J., Pache, J., Ulm, K., Schuhlen, H., . . . Schomig, A. (2001). Restenosis after coronary placement of various stent types. *Am J Cardiol*, *87*(1), 34-39.
- Kastrati, A., Schomig, A., Dirschinger, J., Mehilli, J., von Welser, N., Pache, J., . . . Neumann, F. J. (2000). Increased risk of restenosis after placement of gold-coated stents: results of a randomized trial comparing gold-coated with uncoated steel stents in patients with coronary artery disease. *Circulation*, *101*(21), 2478-2483.
- Kataoka, T., Grube, E., Honda, Y., Morino, Y., Hur, S. H., Bonneau, H. N., . . . Fitzgerald, P. J. (2002). 7-hexanoyltaxol-eluting stent for prevention of neointimal growth: an intravascular ultrasound analysis from the Study to COmpare REstenosis rate between QueST and QuaDS-QP2 (SCORE). *Circulation*, *106*(14), 1788-1793.
- Kawano, H., Koide, Y., Baba, T., Nakamizo, R., Toda, G., Takenaka, M., & Yano, K. (2004). Granulation tissue with eosinophil infiltration in the restenotic lesion after coronary stent implantation. *Circ J*, *68*(7), 722-723.
- Kawaura, C., Noguchi, A., Furuno, T., & Nakanishi, M. (1998). Atomic force microscopy for studying gene transfection mediated by cationic liposomes with a cationic cholesterol derivative. *FEBS Lett*, *421*(1), 69-72.
- Kekicheff, P., Schneider, G. F., & Decher, G. (2013). Size-controlled polyelectrolyte complexes: direct measurement of the balance of forces involved in the triggered collapse of layer-by-layer assembled nanocapsules. *Langmuir*, *29*(34), 10713-10726. doi: 10.1021/la402003b
- Kerr, D. (2003). Clinical development of gene therapy for colorectal cancer. *Nat Rev Cancer*, *3*(8), 615-622. doi: 10.1038/nrc1147
- Khademhosseini, A., Suh, K. Y., Yang, J. M., Eng, G., Yeh, J., Levenberg, S., & Langer, R. (2004). Layer-by-layer deposition of hyaluronic acid and poly-L-lysine for patterned cell co-cultures. *Biomaterials*, *25*(17), 3583-3592. doi: 10.1016/j.biomaterials.2003.10.033
- Khnouf, R., Beebe, D. J., & Fan, Z. H. (2009). Cell-free protein expression in a microchannel array with passive pumping. *Lab Chip*, *9*(1), 56-61. doi: 10.1039/b808034h

- Kholova, I., Koota, S., Kaskenpaa, N., Leppanen, P., Narvainen, J., Kavac, M., . . . Yla-Herttuala, S. (2007). Adenovirus-mediated gene transfer of human vascular endothelial growth factor-d induces transient angiogenic effects in mouse hind limb muscle. *Hum Gene Ther*, *18*(3), 232-244. doi: 10.1089/hum.2006.100
- Kibbe, M. R., Li, J., Nie, S., Watkins, S. C., Lizonova, A., Kovesdi, I., . . . Tzeng, E. (2000). Inducible nitric oxide synthase (iNOS) expression upregulates p21 and inhibits vascular smooth muscle cell proliferation through p42/44 mitogen-activated protein kinase activation and independent of p53 and cyclic guanosine monophosphate. *J Vasc Surg*, *31*(6), 1214-1228.
- Kibos, A., Campeanu, A., & Tintoiu, I. (2007). Pathophysiology of coronary artery in-stent restenosis. *Acute Card Care*, *9*(2), 111-119. doi: 10.1080/17482940701263285
- Kiefer, K., Clement, J., Garidel, P., & Peschka-Suss, R. (2004). Transfection efficiency and cytotoxicity of nonviral gene transfer reagents in human smooth muscle and endothelial cells. *Pharm Res*, *21*(6), 1009-1017.
- Kim, H. J., Bae, I. S., Cho, S. J., Boo, J. H., Lee, B. C., Heo, J., . . . Hong, B. (2012). Synthesis and characteristics of NH<sub>2</sub>-functionalized polymer films to align and immobilize DNA molecules. *Nanoscale Res Lett*, *7*, 30. doi: 10.1186/1556-276X-7-30
- Kimura, T., Isshiki, T., Hayashi, Y., Oshima, S., Namura, M., Nakashima, H., . . . Mitsudo, K. (2010). Incidence and outcome of surgical procedures after sirolimus-eluting stent implantation: a report from the j-Cypher registry. *Cardiovasc Interv Ther*, *25*(1), 29-39. doi: 10.1007/s12928-009-0005-4
- Kipshidze, N., Moses, J. W., Serruys, P. W., Colombo, A., Kipshidze, N. N., & Leon, M. B. (2003). [Recent trend in interventional cardiology--drug-containing stents]. *Ter Arkh*, *75*(9), 89-94.
- Kirkpatrick, C. J., Kampe, M., Rixen, H., Fischer, E. G., Ruchatz, D., & Mittermayer, C. (1990). In vitro studies on the expansion of endothelial cell monolayers on components of the basement membrane. *Virchows Arch B Cell Pathol Incl Mol Pathol*, *58*(3), 207-213.
- Kirkpatrick, K., Ogunkolade, W., Elkak, A., Bustin, S., Jenkins, P., Ghilchik, M., & Mokbel, K. (2002). The mRNA expression of cyclo-oxygenase-

2 (COX-2) and vascular endothelial growth factor (VEGF) in human breast cancer. *Curr Med Res Opin*, 18(4), 237-241. doi: 10.1185/030079902125000633

Klingel, K., Selinka, H. C., Huber, M., Sauter, M., Leube, M., & Kandolf, R. (2000). Molecular pathology and structural features of enteroviral replication. Toward understanding the pathogenesis of viral heart disease. *Herz*, 25(3), 216-220.

Klionsky, D. J., Abdalla, F. C., Abeliovich, H., Abraham, R. T., Acevedo-Arozena, A., Adeli, K., . . . Zuckerbraun, B. (2012). Guidelines for the use and interpretation of assays for monitoring autophagy. *Autophagy*, 8(4), 445-544.

Klugherz, B. D., Song, C., DeFelice, S., Cui, X., Lu, Z., Connolly, J., . . . Levy, R. J. (2002). Gene delivery to pig coronary arteries from stents carrying antibody-tethered adenovirus. *Hum Gene Ther*, 13(3), 443-454. doi: 10.1089/10430340252792576

Kobayashi, N., Hirata, K., Chen, S., Kawase, A., Nishikawa, M., & Takakura, Y. (2004). Hepatic delivery of particulates in the submicron range by a hydrodynamics-based procedure: implications for particulate gene delivery systems. *J Gene Med*, 6(4), 455-463. doi: 10.1002/jgm.531

Koping-Hoggard, M., Mel'nikova, Y. S., Varum, K. M., Lindman, B., & Artursson, P. (2003). Relationship between the physical shape and the efficiency of oligomeric chitosan as a gene delivery system in vitro and in vivo. *J Gene Med*, 5(2), 130-141. doi: 10.1002/jgm.327

Kornowski, R., Hong, M. K., Tio, F. O., Bramwell, O., Wu, H., & Leon, M. B. (1998). In-stent restenosis: contributions of inflammatory responses and arterial injury to neointimal hyperplasia. *J Am Coll Cardiol*, 31(1), 224-230.

Koynova, R., Wang, L., & Macdonald, R. C. (2008). Cationic phospholipids forming cubic phases: lipoplex structure and transfection efficiency. *Mol Pharm*, 5(5), 739-744. doi: 10.1021/mp800011e

Kozinski, M., Sukiennik, A., Rychter, M., Kubica, J., & Sinkiewicz, W. (2007). [Restenosis after coronary angioplasty: pathomechanism and potential targets for therapeutic intervention. Focus on inflammation]. *Postepy Hig Med Dosw (Online)*, 61, 58-73.

- Kraynov, E., Martin, S. W., Hurst, S., Fahmi, O. A., Dowty, M., Cronenberger, C., . . . Wang, D. (2011). How current understanding of clearance mechanisms and pharmacodynamics of therapeutic proteins can be applied for evaluation of their drug-drug interaction potential. *Drug Metab Dispos*, *39*(10), 1779-1783. doi: 10.1124/dmd.111.040808
- Kremastinos, D. (2007). Stents wars. *Hellenic J Cardiol*, *48*(6), 387.
- Kremneva, L. V., Semukhin, M. V., & Kuznetsov, V. A. (2006). [Inflammation as a risk factor for restenosis and cardiovascular complications after transcatheter intracoronary interventions]. *Ter Arkh*, *78*(3), 89-95.
- Krishnan, J., Kirkin, V., Steffen, A., Hegen, M., Weih, D., Tomarev, S., . . . Sleeman, J. P. (2003). Differential in vivo and in vitro expression of vascular endothelial growth factor (VEGF)-C and VEGF-D in tumors and its relationship to lymphatic metastasis in immunocompetent rats. *Cancer Res*, *63*(3), 713-722.
- Kuhel, D. G., Zhu, B., Witte, D. P., & Hui, D. Y. (2002). Distinction in genetic determinants for injury-induced neointimal hyperplasia and diet-induced atherosclerosis in inbred mice. *Arterioscler Thromb Vasc Biol*, *22*(6), 955-960.
- Kulldorff, M., McShane, L. M., Schatzkin, A., Freedman, L. S., Wargovich, M. J., Woods, C., . . . Moler, J. (2000). Measuring cell proliferation in the rectal mucosa. comparing bromodeoxyuridine (BrdU) and proliferating cell nuclear antigen (PCNA) assays. *J Clin Epidemiol*, *53*(8), 875-883.
- Kullo, I. J., & Cooper, L. T. (2010). Early identification of cardiovascular risk using genomics and proteomics. *Nat Rev Cardiol*, *7*(6), 309-317. doi: 10.1038/nrcardio.2010.53
- Kullo, I. J., Mozes, G., Schwartz, R. S., Gloviczki, P., Crotty, T. B., Barber, D. A., . . . O'Brien, T. (1997). Adventitial gene transfer of recombinant endothelial nitric oxide synthase to rabbit carotid arteries alters vascular reactivity. *Circulation*, *96*(7), 2254-2261.
- Kumaraswamy, P., Sethuraman, S., & Krishnan, U. M. (2014). Designing in vitro strategies and in vivo models for Alzheimer's disease - promises & challenges. *Curr Alzheimer Res*, *11*(6), 588-607.
- Kuntz, R. E., Piana, R., Pomerantz, R. M., Carrozza, J., Fishman, R., Mansour, M., . . . Baim, D. S. (1992). Changing incidence and management of

abrupt closure following coronary intervention in the new device era. *Cathet Cardiovasc Diagn*, 27(3), 183-190.

Kustikova, O. S., Schiedlmeier, B., Brugman, M. H., Stahlhut, M., Bartels, S., Li, Z., & Baum, C. (2009). Cell-intrinsic and vector-related properties cooperate to determine the incidence and consequences of insertional mutagenesis. *Mol Ther*, 17(9), 1537-1547. doi: 10.1038/mt.2009.134

Laeremans, H., Rensen, S. S., Ottenheijm, H. C., Smits, J. F., & Blankesteyn, W. M. (2010). Wnt/frizzled signalling modulates the migration and differentiation of immortalized cardiac fibroblasts. *Cardiovasc Res*, 87(3), 514-523. doi: 10.1093/cvr/cvq067

Lake-Bruse, K. D., Faraci, F. M., Shesely, E. G., Maeda, N., Sigmund, C. D., & Heistad, D. D. (1999). Gene transfer of endothelial nitric oxide synthase (eNOS) in eNOS-deficient mice. *Am J Physiol*, 277(2 Pt 2), H770-776.

Lasic, D. D., & Papahadjopoulos, D. (1995). Liposomes revisited. *Science*, 267(5202), 1275-1276.

Latchman, D. S. (2001). Gene therapy with herpes simplex virus vectors: progress and prospects for clinical neuroscience. *Neuroscientist*, 7(6), 528-537.

Lattime, E. C., Lee, S. S., Eisenlohr, L. C., & Mastrangelo, M. J. (1996). In situ cytokine gene transfection using vaccinia virus vectors. *Semin Oncol*, 23(1), 88-100.

Laube, N., Kleinen, L., Bradenahl, J., & Meissner, A. (2007). Diamond-like carbon coatings on ureteral stents--a new strategy for decreasing the formation of crystalline bacterial biofilms? *J Urol*, 177(5), 1923-1927. doi: 10.1016/j.juro.2007.01.016

Lavasanifar, A., Samuel, J., & Kwon, G. S. (2002). Poly(ethylene oxide)-block-poly(L-amino acid) micelles for drug delivery. *Adv Drug Deliv Rev*, 54(2), 169-190.

Lee, E. R., Marshall, J., Siegel, C. S., Jiang, C., Yew, N. S., Nichols, M. R., . . . Cheng, S. H. (1996). Detailed analysis of structures and formulations of cationic lipids for efficient gene transfer to the lung. *Hum Gene Ther*, 7(14), 1701-1717.

- Lee, E. T., Lu, M., Bennett, P. H., & Keen, H. (2001). Vascular disease in younger-onset diabetes: comparison of European, Asian and American Indian cohorts of the WHO Multinational Study of Vascular Disease in Diabetes. *Diabetologia*, *44 Suppl 2*, S78-81.
- Lee, K. B., Song, S. Y., Paik, S. H., & Shin, W. H. (2011). Delayed intra-articular migration of the IntraFix outer sheath after anterior cruciate ligament reconstruction: a case report. *Knee*, *18*(5), 347-349. doi: 10.1016/j.knee.2010.05.013
- Lee, S. W., Tam, F. C., & Chan, K. K. (2011). Very late stent thrombosis due to DES fracture: description of a case and review of potential causes. *Catheter Cardiovasc Interv*, *78*(7), 1101-1105. doi: 10.1002/ccd.23101
- Leon, M. B., Bakhai, A., & Cardiovascular Research Foundation, L. H. H. N. Y. N. Y. U. S. A. M. L. N. (2003). Drug-eluting stents and glycoprotein IIb/IIIa inhibitors: combination therapy for the future. *Am Heart J*, *146*(4 Suppl), S13-17. doi: 10.1016/j.ahj.2003.09.004
- Li, J., Liu, W. L., Yi, X., Feng, G. K., Lu, Z., Jiang, X. J., & Li, X. Y. (2015). Paclitaxel-coated balloons for the treatment of patients with in-stent restenosis: A meta-analysis of angiographic and clinical data. *Exp Ther Med*, *9*(6), 2285-2292. doi: 10.3892/etm.2015.2431
- Li, J. J. (2009). [Inflammation may play a key role in in-stent restenosis.]. *Zhonghua Xin Xue Guan Bing Za Zhi*, *37*(3), 210-212.
- Li, Q., Xia, Y. Y., Tang, J. C., Wang, R. Y., Bei, C. Y., & Zeng, Y. (2011). In vitro and in vivo biocompatibility investigation of diamond-like carbon coated nickel-titanium shape memory alloy. *Artif Cells Blood Substit Immobil Biotechnol*, *39*(3), 137-142. doi: 10.3109/10731199.2010.502880
- Libby, P. (2002). Inflammation in atherosclerosis. *Nature*, *420*(6917), 868-874. doi: 10.1038/nature01323
- Libby, P. (2008a). The molecular mechanisms of the thrombotic complications of atherosclerosis. *J Intern Med*, *263*(5), 517-527. doi: 10.1111/j.1365-2796.2008.01965.x
- Libby, P. (2008b). Role of inflammation in atherosclerosis associated with rheumatoid arthritis. *Am J Med*, *121*(10 Suppl 1), S21-31. doi: 10.1016/j.amjmed.2008.06.014

- Lim, S. Y., Lee, D. G., Sivakumaran, P., Crombie, D., Slavin, J., Dottori, M., . . . Dilley, R. J. (2012). In vivo tissue engineering chamber supports human induced pluripotent stem cell survival and rapid differentiation. *Biochem Biophys Res Commun*, *422*(1), 75-79. doi: 10.1016/j.bbrc.2012.04.108
- Lindstrom, S., & Andersson-Svahn, H. (2010). Overview of single-cell analyses: microdevices and applications. *Lab Chip*, *10*(24), 3363-3372. doi: 10.1039/c0lc00150c
- Lipton, B. H., Bensch, K. G., & Karasek, M. A. (1991). Microvessel endothelial cell transdifferentiation: phenotypic characterization. *Differentiation*, *46*(2), 117-133.
- Liu, F., Qi, H., Huang, L., & Liu, D. (1997). Factors controlling the efficiency of cationic lipid-mediated transfection in vivo via intravenous administration. *Gene Ther*, *4*(6), 517-523.
- Liu, F., Song, Y., & Liu, D. (1999). Hydrodynamics-based transfection in animals by systemic administration of plasmid DNA. *Gene Ther*, *6*(7), 1258-1266. doi: 10.1038/sj.gt.3300947
- Liu, X., De Scheerder, I., & Desmet, W. (2004). Dexamethasone-eluting stent: an anti-inflammatory approach to inhibit coronary restenosis. *Expert Rev Cardiovasc Ther*, *2*(5), 653-660. doi: 10.1586/14779072.2.5.653
- Lloyd-Jones, D., Adams, R. J., Brown, T. M., Carnethon, M., Dai, S., De Simone, G., . . . Stroke Statistics, S. (2010). Executive summary: heart disease and stroke statistics--2010 update: a report from the American Heart Association. *Circulation*, *121*(7), 948-954. doi: 10.1161/CIRCULATIONAHA.109.192666
- Loeffler, J. P., & Behr, J. P. (1993). Gene transfer into primary and established mammalian cell lines with lipopolyamine-coated DNA. *Methods Enzymol*, *217*, 599-618.
- Lompre, A. M., Hadri, L., Merlet, E., Keuylian, Z., Mougnot, N., Karakikes, I., . . . Lipskaia, L. (2013). Efficient transduction of vascular smooth muscle cells with a translational AAV2.5 vector: a new perspective for in-stent restenosis gene therapy. *Gene Ther*, *20*(9), 901-912. doi: 10.1038/gt.2013.13
- Luscher, T. F., Steffel, J., Eberli, F. R., Joner, M., Nakazawa, G., Tanner, F. C., & Virmani, R. (2007). Drug-eluting stent and coronary thrombosis:

biological mechanisms and clinical implications. *Circulation*, 115(8), 1051-1058. doi: 10.1161/CIRCULATIONAHA.106.675934

Mach, F. (2000). Toward new therapeutic strategies against neointimal formation in restenosis. *Arterioscler Thromb Vasc Biol*, 20(7), 1699-1700.

Maffia, P., Ianaro, A., Sorrentino, R., Lippolis, L., Maiello, F. M., del Soldato, P., . . . Cirino, G. (2002). Beneficial effects of NO-releasing derivative of flurbiprofen (HCT-1026) in rat model of vascular injury and restenosis. *Arterioscler Thromb Vasc Biol*, 22(2), 263-267.

Maiellaro, K., & Taylor, W. R. (2007). The role of the adventitia in vascular inflammation. *Cardiovasc Res*, 75(4), 640-648. doi: 10.1016/j.cardiores.2007.06.023

Maillard, L., Van Belle, E., Smith, R. C., Le Roux, A., Deneffe, P., Steg, G., . . . Walsh, K. (1997). Percutaneous delivery of the gax gene inhibits vessel stenosis in a rabbit model of balloon angioplasty. *Cardiovasc Res*, 35(3), 536-546.

Majno, G. (1998). Chronic inflammation: links with angiogenesis and wound healing. *Am J Pathol*, 153(4), 1035-1039. doi: 10.1016/S0002-9440(10)65648-9

Mancia, G., Facchetti, R., Parati, G., & Zanchetti, A. (2012). Visit-to-visit blood pressure variability, carotid atherosclerosis, and cardiovascular events in the European Lacidipine Study on Atherosclerosis. *Circulation*, 126(5), 569-578. doi: 10.1161/CIRCULATIONAHA.112.107565

Mani, G., Feldman, M. D., Patel, D., & Agrawal, C. M. (2007). Coronary stents: a materials perspective. *Biomaterials*, 28(9), 1689-1710. doi: 10.1016/j.biomaterials.2006.11.042

Maniatis, T. (2012). On the road from classical to modern molecular biology. *Nat Med*, 18(10), 1499-1502. doi: 10.1038/nm.2931

Mann, B. K., & West, J. L. (2001). Tissue engineering in the cardiovascular system: progress toward a tissue engineered heart. *Anat Rec*, 263(4), 367-371.

Mann, M. J., Gibbons, G. H., Hutchinson, H., Poston, R. S., Hoyt, E. G., Robbins, R. C., & Dzau, V. J. (1999). Pressure-mediated

oligonucleotide transfection of rat and human cardiovascular tissues. *Proc Natl Acad Sci U S A*, 96(11), 6411-6416.

- Marso, S. P., Mak, K. H., & Topol, E. J. (1999). Diabetes mellitus: biological determinants of atherosclerosis and restenosis. *Semin Interv Cardiol*, 4(3), 129-143. doi: 10.1053/siic.1999.0086
- Martin, R. S., Root, P. D., & Spence, D. M. (2006). Microfluidic technologies as platforms for performing quantitative cellular analyses in an in vitro environment. *Analyst*, 131(11), 1197-1206. doi: 10.1039/b611041j
- Marx, S. O., Jayaraman, T., Go, L. O., & Marks, A. R. (1995). Rapamycin-FKBP inhibits cell cycle regulators of proliferation in vascular smooth muscle cells. *Circ Res*, 76(3), 412-417.
- Masai, H., Kaziro, Y., & Arai, K. (1983). Definition of oriR, the minimum DNA segment essential for initiation of R1 plasmid replication in vitro. *Proc Natl Acad Sci U S A*, 80(22), 6814-6818.
- Mastrangelo, M. J., Maguire, H. C., & Lattime, E. C. (2000). Intralesional vaccinia/GM-CSF recombinant virus in the treatment of metastatic melanoma. *Adv Exp Med Biol*, 465, 391-400. doi: 10.1007/0-306-46817-4\_34
- Masuda, S., Nakano, K., Funakoshi, K., Zhao, G., Meng, W., Kimura, S., . . . Egashira, K. (2011). Imatinib mesylate-incorporated nanoparticle-eluting stent attenuates in-stent neointimal formation in porcine coronary arteries. *J Atheroscler Thromb*, 18(12), 1043-1053.
- Mathiowitz, E., Jacob, J. S., Jong, Y. S., Carino, G. P., Chickering, D. E., Chaturvedi, P., . . . Morrell, C. (1997). Biologically erodable microspheres as potential oral drug delivery systems. *Nature*, 386(6623), 410-414. doi: 10.1038/386410a0
- Matsumoto, I., Wilce, P. A., Buckley, T., Dodd, P., Puzke, J., Spanagel, R., . . . Schmidt, L. G. (2001). Ethanol and gene expression in brain. *Alcohol Clin Exp Res*, 25(5 Suppl ISBRA), 82S-86S.
- Matsumoto, T., & Nagayama, K. (2012). Tensile properties of vascular smooth muscle cells: bridging vascular and cellular biomechanics. *J Biomech*, 45(5), 745-755. doi: 10.1016/j.jbiomech.2011.11.014

- Mauri, L., Bonan, R., Weiner, B. H., Legrand, V., Bassand, J. P., Popma, J. J., . . . Kuntz, R. E. (2002). Cutting balloon angioplasty for the prevention of restenosis: results of the Cutting Balloon Global Randomized Trial. *Am J Cardiol*, *90*(10), 1079-1083.
- McFadden, E. P., Stabile, E., Regar, E., Cheneau, E., Ong, A. T., Kinnaird, T., . . . Serruys, P. W. (2004). Late thrombosis in drug-eluting coronary stents after discontinuation of antiplatelet therapy. *Lancet*, *364*(9444), 1519-1521. doi: 10.1016/S0140-6736(04)17275-9
- McGill, H. C., Jr., McMahan, C. A., Herderick, E. E., Malcom, G. T., Tracy, R. E., & Strong, J. P. (2000). Origin of atherosclerosis in childhood and adolescence. *Am J Clin Nutr*, *72*(5 Suppl), 1307S-1315S.
- McKenna, C. J., Wilson, S. H., Camrud, A. R., Berger, P. B., Holmes, D. R., Jr., & Schwartz, R. S. (1998). Neointimal response following rotational atherectomy compared to balloon angioplasty in a porcine model of coronary in-stent restenosis. *Cathet Cardiovasc Diagn*, *45*(3), 332-336.
- McMahon, A. C., Zreiqat, H., & Lowe, H. C. (2008). Carotid artery stenting in the Zucker rat: a novel, potentially 'diabetes-specific' model of in-stent restenosis. *Diab Vasc Dis Res*, *5*(2), 145-146. doi: 10.3132/dvdr.2008.024
- Mehling, M., & Tay, S. (2014). Microfluidic cell culture. *Curr Opin Biotechnol*, *25*, 95-102. doi: 10.1016/j.copbio.2013.10.005
- Mehran, R., Dangas, G., Abizaid, A., Lansky, A. J., Mintz, G. S., Pichard, A. D., . . . Leon, M. B. (2001). Treatment of focal in-stent restenosis with balloon angioplasty alone versus stenting: Short- and long-term results. *Am Heart J*, *141*(4), 610-614. doi: 10.1067/mhj.2001.113998
- Mehran, R., Mintz, G. S., Satler, L. F., Pichard, A. D., Kent, K. M., Bucher, T. A., . . . Leon, M. B. (1997). Treatment of in-stent restenosis with excimer laser coronary angioplasty: mechanisms and results compared with PTCA alone. *Circulation*, *96*(7), 2183-2189.
- Mei, L., Sun, H., & Song, C. (2009). Local delivery of modified paclitaxel-loaded poly(epsilon-caprolactone)/pluronic F68 nanoparticles for long-term inhibition of hyperplasia. *J Pharm Sci*, *98*(6), 2040-2050. doi: 10.1002/jps.21581
- Mendes, J. B., Campos, P. P., Ferreira, M. A., Bakhle, Y. S., & Andrade, S. P. (2007). Host response to sponge implants differs between

subcutaneous and intraperitoneal sites in mice. *J Biomed Mater Res B Appl Biomater*, 83(2), 408-415. doi: 10.1002/jbm.b.30810

Menown, I., Lowe, R., & Penn, I. (2005). Passive stent coatings in the drug-eluting era. *J Invasive Cardiol*, 17(4), 222-228.

Mertsching, H., Walles, T., Hofmann, M., Schanz, J., & Knapp, W. H. (2005). Engineering of a vascularized scaffold for artificial tissue and organ generation. *Biomaterials*, 26(33), 6610-6617. doi: 10.1016/j.biomaterials.2005.04.048

Meuwissen, M., Siebes, M., Chamuleau, S. A., van Eck-Smit, B. L., Koch, K. T., de Winter, R. J., . . . Piek, J. J. (2002). Hyperemic stenosis resistance index for evaluation of functional coronary lesion severity. *Circulation*, 106(4), 441-446.

Meyer, G., Merval, R., & Tedgui, A. (1996). Effects of pressure-induced stretch and convection on low-density lipoprotein and albumin uptake in the rabbit aortic wall. *Circ Res*, 79(3), 532-540.

Michel, M., Izquierdo, A., Decher, G., Voegel, J. C., Schaaf, P., & Ball, V. (2005). Layer by layer self-assembled polyelectrolyte multilayers with embedded phospholipid vesicles obtained by spraying: integrity of the vesicles. *Langmuir*, 21(17), 7854-7859. doi: 10.1021/la050497w

Miles, C. A. (1994). Differential scanning calorimetry (DSC): protein structure probe useful for the study of damaged tendons. *Equine Vet J*, 26(4), 255-256.

Miller, A. D. (1990). Progress toward human gene therapy. *Blood*, 76(2), 271-278.

Milliat, F., Francois, A., Isoir, M., Deutsch, E., Tamarat, R., Tarlet, G., . . . Benderitter, M. (2006). Influence of endothelial cells on vascular smooth muscle cells phenotype after irradiation: implication in radiation-induced vascular damages. *Am J Pathol*, 169(4), 1484-1495. doi: 10.2353/ajpath.2006.060116

Minuth, W. W., Schumacher, K., Strehl, R., & Kloth, S. (2000). Physiological and cell biological aspects of perfusion culture technique employed to generate differentiated tissues for long term biomaterial testing and tissue engineering. *J Biomater Sci Polym Ed*, 11(5), 495-522.

- Mironov, V., Kasyanov, V. A., Yost, M. J., Visconti, R., Twal, W., Trusk, T., . . . Markwald, R. R. (2006). Cardiovascular tissue engineering I. Perfusion bioreactors: a review. *J Long Term Eff Med Implants*, *16*(2), 111-130.
- Mitchell, S. B., Sanders, J. E., Garbini, J. L., & Schuessler, P. K. (2001). A device to apply user-specified strains to biomaterials in culture. *IEEE Trans Biomed Eng*, *48*(2), 268-273. doi: 10.1109/10.909648
- Moghimi, S. M., & Hunter, A. C. (2001). Capture of stealth nanoparticles by the body's defences. *Crit Rev Ther Drug Carrier Syst*, *18*(6), 527-550.
- Monnink, S. H., van Boven, A. J., Peels, H. O., Tigchelaar, I., de Kam, P. J., Crijns, H. J., & van Oeveren, W. (1999). Silicon-carbide coated coronary stents have low platelet and leukocyte adhesion during platelet activation. *J Investig Med*, *47*(6), 304-310.
- Moreno, P. R., Fallon, J. T., Murcia, A. M., Leon, M. N., Simosa, H., Fuster, V., & Palacios, I. F. (1999). Tissue characteristics of restenosis after percutaneous transluminal coronary angioplasty in diabetic patients. *J Am Coll Cardiol*, *34*(4), 1045-1049.
- Morgan, R. A., & Anderson, W. F. (1993). Human gene therapy. *Annu Rev Biochem*, *62*, 191-217. doi: 10.1146/annurev.bi.62.070193.001203
- Moussa, I., Di Mario, C., Reimers, B., Akiyama, T., Tobis, J., & Colombo, A. (1997). Subacute stent thrombosis in the era of intravascular ultrasound-guided coronary stenting without anticoagulation: frequency, predictors and clinical outcome. *J Am Coll Cardiol*, *29*(1), 6-12.
- Muhs, A., Heublein, B., Schletter, J., Herrmann, A., Rudiger, M., Sturm, M., . . . von der Leyen, H. E. (2003). Preclinical evaluation of inducible nitric oxide synthase lipoplex gene therapy for inhibition of stent-induced vascular neointimal lesion formation. *Hum Gene Ther*, *14*(4), 375-383. doi: 10.1089/104303403321208970
- Muntner, P., He, J., Astor, B. C., Folsom, A. R., & Coresh, J. (2005). Traditional and nontraditional risk factors predict coronary heart disease in chronic kidney disease: results from the atherosclerosis risk in communities study. *J Am Soc Nephrol*, *16*(2), 529-538. doi: 10.1681/ASN.2004080656
- Myckatyn, T. M., Ellis, R. A., Grand, A. G., Sen, S. K., Lowe, J. B., 3rd, Hunter, D. A., & Mackinnon, S. E. (2002). The effects of rapamycin in murine

peripheral nerve isografts and allografts. *Plast Reconstr Surg*, 109(7), 2405-2417.

- Nabel, E. G., Plautz, G., & Nabel, G. J. (1990). Site-specific gene expression in vivo by direct gene transfer into the arterial wall. *Science*, 249(4974), 1285-1288.
- Nabel, G. J., Nabel, E. G., Yang, Z. Y., Fox, B. A., Plautz, G. E., Gao, X., . . . Chang, A. E. (1993). Direct gene transfer with DNA-liposome complexes in melanoma: expression, biologic activity, and lack of toxicity in humans. *Proc Natl Acad Sci U S A*, 90(23), 11307-11311.
- Nagaoka, T., Kaburagi, Y., Hamaguchi, Y., Hasegawa, M., Takehara, K., Steeber, D. A., . . . Sato, S. (2000). Delayed wound healing in the absence of intercellular adhesion molecule-1 or L-selectin expression. *Am J Pathol*, 157(1), 237-247. doi: 10.1016/S0002-9440(10)64534-8
- Nageh, T., Duncan, E., & Thomas, M. R. (2004). Regression of coronary in-stent restenosis. *Catheter Cardiovasc Interv*, 62(2), 201-202. doi: 10.1002/ccd.20093
- Nageh, T., & Meier, B. (2005). Treatment of in-stent restenosis. *Int J Cardiol*, 104(3), 245-250. doi: 10.1016/j.ijcard.2004.10.040
- Nakano, K., Egashira, K., Masuda, S., Funakoshi, K., Zhao, G., Kimura, S., . . . Sunagawa, K. (2009). Formulation of nanoparticle-eluting stents by a cationic electrodeposition coating technology: efficient nano-drug delivery via bioabsorbable polymeric nanoparticle-eluting stents in porcine coronary arteries. *JACC Cardiovasc Interv*, 2(4), 277-283. doi: 10.1016/j.jcin.2008.08.023
- Nakatani, M., Takeyama, Y., Shibata, M., Yorozuya, M., Suzuki, H., Koba, S., & Katagiri, T. (2003). Mechanisms of restenosis after coronary intervention: difference between plain old balloon angioplasty and stenting. *Cardiovasc Pathol*, 12(1), 40-48.
- Nakazawa, G., Granada, J. F., Alviar, C. L., Tellez, A., Kaluza, G. L., Guilhemier, M. Y., . . . Virmani, R. (2010). Anti-CD34 antibodies immobilized on the surface of sirolimus-eluting stents enhance stent endothelialization. *JACC Cardiovasc Interv*, 3(1), 68-75. doi: 10.1016/j.jcin.2009.09.015

- Naldini, L., Blomer, U., Gallay, P., Ory, D., Mulligan, R., Gage, F. H., . . . Trono, D. (1996). In vivo gene delivery and stable transduction of nondividing cells by a lentiviral vector. *Science*, 272(5259), 263-267.
- Narayanan, N. K., Nargi, D., Randolph, C., & Narayanan, B. A. (2009). Liposome encapsulation of curcumin and resveratrol in combination reduces prostate cancer incidence in PTEN knockout mice. *Int J Cancer*, 125(1), 1-8. doi: 10.1002/ijc.24336
- New, G., Moses, J. W., Roubin, G. S., Leon, M. B., Colombo, A., Iyer, S. S., . . . Kipshidze, N. (2002). Estrogen-eluting, phosphorylcholine-coated stent implantation is associated with reduced neointimal formation but no delay in vascular repair in a porcine coronary model. *Catheter Cardiovasc Interv*, 57(2), 266-271. doi: 10.1002/ccd.10339
- Newman, K. D., Dunn, P. F., Owens, J. W., Schulick, A. H., Virmani, R., Sukhova, G., . . . Dichek, D. A. (1995). Adenovirus-mediated gene transfer into normal rabbit arteries results in prolonged vascular cell activation, inflammation, and neointimal hyperplasia. *J Clin Invest*, 96(6), 2955-2965.
- Nguyen, C. M., & Levy, A. J. (2010). The mechanics of atherosclerotic plaque rupture by inclusion/matrix interfacial decohesion. *J Biomech*, 43(14), 2702-2708. doi: 10.1016/j.jbiomech.2010.06.012
- Nicolau, C., & Sene, C. (1982). Liposome-mediated DNA transfer in eukaryotic cells. Dependence of the transfer efficiency upon the type of liposomes used and the host cell cycle stage. *Biochim Biophys Acta*, 721(2), 185-190.
- Niculescu, F., & Rus, H. G. (1990). [The role of endothelial cells in inflammation and immunity]. *Bacteriol Virusol Parazitol Epidemiol*, 35(2), 97-112.
- Niklason, L. E., Gao, J., Abbott, W. M., Hirschi, K. K., Houser, S., Marini, R., & Langer, R. (1999). Functional arteries grown in vitro. *Science*, 284(5413), 489-493.
- Nimesh, S., Kumar, R., & Chandra, R. (2006). Novel polyallylamine-dextran sulfate-DNA nanoplexes: highly efficient non-viral vector for gene delivery. *Int J Pharm*, 320(1-2), 143-149. doi: 10.1016/j.ijpharm.2006.03.050
- Nishiyama, K., Shizuta, S., Doi, T., Morimoto, T., & Kimura, T. (2010). Sudden cardiac death after PCI and CABG in the bare-metal stent

era: Incidence, prevalence, and predictors. *Int J Cardiol*, 144(2), 263-266. doi: 10.1016/j.ijcard.2009.01.040

Novelli, G., Borgiani, P., Giardina, E., Mango, R., Contino, G., Romeo, F., & Mehta, J. L. (2003). Role of genetics in prevention of coronary atherosclerosis. *Curr Opin Cardiol*, 18(5), 368-371.

O'Brien, J., Wilson, I., Orton, T., & Pognan, F. (2000). Investigation of the Alamar Blue (resazurin) fluorescent dye for the assessment of mammalian cell cytotoxicity. *Eur J Biochem*, 267(17), 5421-5426.

O'Brien, M. E., Wigler, N., Inbar, M., Rosso, R., Grischke, E., Santoro, A., . . . Group, C. B. C. S. (2004). Reduced cardiotoxicity and comparable efficacy in a phase III trial of pegylated liposomal doxorubicin HCl (CAELYX/Doxil) versus conventional doxorubicin for first-line treatment of metastatic breast cancer. *Ann Oncol*, 15(3), 440-449.

Obata, J. E., Nakamura, T., Kitta, Y., Saito, Y., Sano, K., Fujioka, D., . . . Kugiyama, K. (2013). In-stent restenosis is inhibited in a bare metal stent implanted distal to a sirolimus-eluting stent to treat a long de novo coronary lesion with small distal vessel diameter. *Catheter Cardiovasc Interv*, 82(6), E777-787. doi: 10.1002/ccd.24841

Obergfell, A., Strotmann, J., Bonz, A., Bauersachs, J., Ertl, G., Walter, U., & Grossmann, R. (2004). Impaired platelet responses to clopidogrel and ticlopidine in a patient with recurrent coronary stent stenosis. *Thromb Haemost*, 92(6), 1446-1447.

Ochiya, T., Takahama, Y., Baba-Toriyama, H., Tsukamoto, M., Yasuda, Y., Kikuchi, H., & Terada, M. (1999). Evaluation of cationic liposome suitable for gene transfer into pregnant animals. *Biochem Biophys Res Commun*, 258(2), 358-365. doi: 10.1006/bbrc.1999.0590

Oh, B., & Lee, C. H. (2013). Nanofiber for cardiovascular tissue engineering. *Expert Opin Drug Deliv*, 10(11), 1565-1582. doi: 10.1517/17425247.2013.830608

Oku, N., Yamazaki, Y., Matsuura, M., Sugiyama, M., Hasegawa, M., & Nango, M. (2001). A novel non-viral gene transfer system, polycation liposomes. *Adv Drug Deliv Rev*, 52(3), 209-218.

Ong, A. T., Hoye, A., Aoki, J., van Mieghem, C. A., Rodriguez Granillo, G. A., Sonnenschein, K., . . . Serruys, P. W. (2005). Thirty-day incidence and six-month clinical outcome of thrombotic stent occlusion after

bare-metal, sirolimus, or paclitaxel stent implantation. *J Am Coll Cardiol*, 45(6), 947-953. doi: 10.1016/j.jacc.2004.09.079

Ouyang, L. Z., Wang, H., Zhu, M., Zou, J., & Chung, C. Y. (2004). Microstructure of MmM(5)/Mg multi-layer hydrogen storage films prepared by magnetron sputtering. *Microsc Res Tech*, 64(4), 323-329. doi: 10.1002/jemt.20089

Ozawa, M., Okamura, A., Date, M., Higuchi, Y., Nagai, H., Shibuya, M., . . . Fujii, K. (2012). Third in-stent restenosis in sirolimus eluting stents: predictors of the next restenosis. *Catheter Cardiovasc Interv*, 79(1), 91-96. doi: 10.1002/ccd.22916

Pagliari, L. C., Keyhani, A., Williams, D., Woods, D., Liu, B., Perrotte, P., . . . Dinney, C. P. (2003). Repeated intravesical instillations of an adenoviral vector in patients with locally advanced bladder cancer: a phase I study of p53 gene therapy. *J Clin Oncol*, 21(12), 2247-2253. doi: 10.1200/JCO.2003.09.138

Palmer, D. H., Chen, M. J., & Kerr, D. J. (2003). Taking Gene Therapy into the Clinic. *J Biomed Biotechnol*, 2003(1), 71-77. doi: 10.1155/S111072430320913X

Pannier, A. K., & Shea, L. D. (2004). Controlled release systems for DNA delivery. *Mol Ther*, 10(1), 19-26. doi: 10.1016/j.ymthe.2004.03.020

Panyam, J., Williams, D., Dash, A., Leslie-Pelecky, D., & Labhasetwar, V. (2004). Solid-state solubility influences encapsulation and release of hydrophobic drugs from PLGA/PLA nanoparticles. *J Pharm Sci*, 93(7), 1804-1814. doi: 10.1002/jps.20094

Park, S. J., Shim, W. H., Ho, D. S., Raizner, A. E., Park, S. W., Hong, M. K., . . . Mintz, G. S. (2003). A paclitaxel-eluting stent for the prevention of coronary restenosis. *N Engl J Med*, 348(16), 1537-1545. doi: 10.1056/NEJMoa021007

Partridge, K. A., & Oreffo, R. O. (2004). Gene delivery in bone tissue engineering: progress and prospects using viral and nonviral strategies. *Tissue Eng*, 10(1-2), 295-307. doi: 10.1089/107632704322791934

Pecora, A., Aguirreburualde, M. S., Aguirreburualde, A., Leunda, M. R., Odeon, A., Chiavenna, S., . . . Wigdorovitz, A. (2012). Safety and efficacy of an E2 glycoprotein subunit vaccine produced in mammalian cells to prevent experimental infection with bovine

viral diarrhoea virus in cattle. *Vet Res Commun*, 36(3), 157-164. doi: 10.1007/s11259-012-9526-x

Peetla, C., & Labhasetwar, V. (2008). Biophysical characterization of nanoparticle-endothelial model cell membrane interactions. *Mol Pharm*, 5(3), 418-429. doi: 10.1021/mp700140a

Perkins, N. D., & Gilmore, T. D. (2006). Good cop, bad cop: the different faces of NF-kappaB. *Cell Death Differ*, 13(5), 759-772. doi: 10.1038/sj.cdd.4401838

Perlman, H., Sata, M., Krasinski, K., Dorai, T., Buttyan, R., & Walsh, K. (2000). Adenovirus-encoded hammerhead ribozyme to Bcl-2 inhibits neointimal hyperplasia and induces vascular smooth muscle cell apoptosis. *Cardiovasc Res*, 45(3), 570-578.

Perlstein, I., Connolly, J. M., Cui, X., Song, C., Li, Q., Jones, P. L., . . . Levy, R. J. (2003). DNA delivery from an intravascular stent with a denatured collagen-poly(lactide-co-glycolide) acid-controlled release coating: mechanisms of enhanced transfection. *Gene Ther*, 10(17), 1420-1428. doi: 10.1038/sj.gt.3302043

Perry, T. E., & Roth, S. J. (2003). Cardiovascular tissue engineering: constructing living tissue cardiac valves and blood vessels using bone marrow, umbilical cord blood, and peripheral blood cells. *J Cardiovasc Nurs*, 18(1), 30-37.

Pfeiffer, T., Wallich, M., Sandmann, W., Schrader, J., & Godecke, A. (2006). Lipoplex gene transfer of inducible nitric oxide synthase inhibits the reactive intimal hyperplasia after expanded polytetrafluoroethylene bypass grafting. *J Vasc Surg*, 43(5), 1021-1027. doi: 10.1016/j.jvs.2006.01.014

Pfister, S. L., & Campbell, W. B. (1996). Role of endothelium-derived metabolites of arachidonic acid in enhanced pulmonary artery contractions in female rabbits. *Hypertension*, 27(1), 43-48.

Pitard, B., Bello-Roufai, M., Lambert, O., Richard, P., Desigaux, L., Fernandes, S., . . . Escande, D. (2004). Negatively charged self-assembling DNA/poloxamine nanospheres for in vivo gene transfer. *Nucleic Acids Res*, 32(20), e159. doi: 10.1093/nar/gnh153

Pober, J. S., & Cotran, R. S. (1990). The role of endothelial cells in inflammation. *Transplantation*, 50(4), 537-544.

- Poon, M., Marx, S. O., Gallo, R., Badimon, J. J., Taubman, M. B., & Marks, A. R. (1996). Rapamycin inhibits vascular smooth muscle cell migration. *J Clin Invest*, *98*(10), 2277-2283. doi: 10.1172/JCI119038
- Powell, R. J., Goodney, P., Mendelsohn, F. O., Moen, E. K., Annex, B. H., & Investigators, H. G. F. T. (2010). Safety and efficacy of patient specific intramuscular injection of HGF plasmid gene therapy on limb perfusion and wound healing in patients with ischemic lower extremity ulceration: results of the HGF-0205 trial. *J Vasc Surg*, *52*(6), 1525-1530. doi: 10.1016/j.jvs.2010.07.044
- Prince, H. M. (1998). Gene transfer: a review of methods and applications. *Pathology*, *30*(4), 335-347.
- Prpic, R., Teirstein, P. S., Reilly, J. P., Moses, J. W., Tripuraneni, P., Lansky, A. J., . . . Leon, M. B. (2002). Long-term outcome of patients treated with repeat percutaneous coronary intervention after failure of gamma-brachytherapy for the treatment of in-stent restenosis. *Circulation*, *106*(18), 2340-2345.
- Prud'homme, G. J., Draghia-Akli, R., & Wang, Q. (2007). Plasmid-based gene therapy of diabetes mellitus. *Gene Ther*, *14*(7), 553-564. doi: 10.1038/sj.gt.3302907
- Puel, J., Joffre, F., Rousseau, H., Guermonprez, J. L., Lancelin, B., Morice, M. C., . . . Bounhoure, J. P. (1987). [Self-expanding coronary endoprosthesis in the prevention of restenosis following transluminal angioplasty. Preliminary clinical study]. *Arch Mal Coeur Vaiss*, *80*(8), 1311-1312.
- Punchard, M. A., Stenson-Cox, C., O'Cearbhaill E, D., Lyons, E., Gundy, S., Murphy, L., . . . Barron, V. (2007). Endothelial cell response to biomechanical forces under simulated vascular loading conditions. *J Biomech*, *40*(14), 3146-3154. doi: 10.1016/j.jbiomech.2007.03.029
- Qiao, J. H., Tripathi, J., Mishra, N. K., Cai, Y., Tripathi, S., Wang, X. P., . . . Rajavashisth, T. B. (1997). Role of macrophage colony-stimulating factor in atherosclerosis: studies of osteopetrotic mice. *Am J Pathol*, *150*(5), 1687-1699.
- Radke, P. W., Friese, K., Buhr, A., Nagel, B., Harland, L. C., Kaiser, A., . . . Hoffmann, R. (2006). Comparison of coronary restenosis rates in matched patients with versus without diabetes mellitus. *Am J Cardiol*, *98*(9), 1218-1222. doi: 10.1016/j.amjcard.2006.06.015

- Radke, P. W., Kaiser, A., Frost, C., & Sigwart, U. (2003). Outcome after treatment of coronary in-stent restenosis; results from a systematic review using meta-analysis techniques. *Eur Heart J*, *24*(3), 266-273.
- Rahman, P. K., Pasirayi, G., Auger, V., & Ali, Z. (2009). Development of a simple and low cost microbioreactor for high-throughput bioprocessing. *Biotechnol Lett*, *31*(2), 209-214. doi: 10.1007/s10529-008-9853-8
- Raje, S., Cao, J., Newman, A. H., Gao, H., & Eddington, N. D. (2003). Evaluation of the blood-brain barrier transport, population pharmacokinetics, and brain distribution of benzotropine analogs and cocaine using in vitro and in vivo techniques. *J Pharmacol Exp Ther*, *307*(2), 801-808. doi: 10.1124/jpet.103.053504
- Ramgopal, Y., Mondal, D., Venkatraman, S. S., & Godbey, W. T. (2008). Sustained release of complexed and naked DNA from polymer films. *J Biomed Mater Res B Appl Biomater*, *85*(2), 496-503. doi: 10.1002/jbm.b.30971
- Raper, S. E., Chirmule, N., Lee, F. S., Wivel, N. A., Bagg, A., Gao, G. P., . . . Batshaw, M. L. (2003). Fatal systemic inflammatory response syndrome in a ornithine transcarbamylase deficient patient following adenoviral gene transfer. *Mol Genet Metab*, *80*(1-2), 148-158.
- Rauchhaus, M., Gross, M., Schulz, S., Francis, D. P., Greiser, P., Norwig, A., . . . Glaser, C. (2002). The E-selectin SER128ARG gene polymorphism and restenosis after successful coronary angioplasty. *Int J Cardiol*, *83*(3), 249-257.
- Resina, S., Prevot, P., & Thierry, A. R. (2009). Physico-chemical characteristics of lipoplexes influence cell uptake mechanisms and transfection efficacy. *PLoS One*, *4*(6), e6058. doi: 10.1371/journal.pone.0006058
- Rex, J. H., Walsh, T. J., Nettleman, M., Anaissie, E. J., Bennett, J. E., Bow, E. J., . . . Wu, T. (2001). Need for alternative trial designs and evaluation strategies for therapeutic studies of invasive mycoses. *Clin Infect Dis*, *33*(1), 95-106. doi: 10.1086/320876
- Richard, P., Bossard, F., Desigaux, L., Lanctin, C., Bello-Roufai, M., & Pitard, B. (2005). Amphiphilic block copolymers promote gene delivery in vivo to pathological skeletal muscles. *Hum Gene Ther*, *16*(11), 1318-1324. doi: 10.1089/hum.2005.16.1318

- Riessen, R., Axel, D. I., Fenchel, M., Herzog, U. U., Rossmann, H., & Karsch, K. R. (1999). Effect of HMG-CoA reductase inhibitors on extracellular matrix expression in human vascular smooth muscle cells. *Basic Res Cardiol*, *94*(5), 322-332.
- Riessen, R., Isner, J. M., Blessing, E., Loushin, C., Nikol, S., & Wight, T. N. (1994). Regional differences in the distribution of the proteoglycans biglycan and decorin in the extracellular matrix of atherosclerotic and restenotic human coronary arteries. *Am J Pathol*, *144*(5), 962-974.
- Riessen, R., Rahimizadeh, H., Blessing, E., Takeshita, S., Barry, J. J., & Isner, J. M. (1993). Arterial gene transfer using pure DNA applied directly to a hydrogel-coated angioplasty balloon. *Hum Gene Ther*, *4*(6), 749-758. doi: 10.1089/hum.1993.4.6-749
- Rinfret, S., Cutlip, D. E., Katsiyannis, P. T., Ho, K. K., Cohen, D. J., Carrozza, J. P., Jr., & Laham, R. J. (2002). Rheolytic thrombectomy and platelet glycoprotein IIb/IIIa blockade for stent thrombosis. *Catheter Cardiovasc Interv*, *57*(1), 24-30. doi: 10.1002/ccd.10275
- Robertson, K. E., McDonald, R. A., Oldroyd, K. G., Nicklin, S. A., & Baker, A. H. (2012). Prevention of coronary in-stent restenosis and vein graft failure: does vascular gene therapy have a role? *Pharmacol Ther*, *136*(1), 23-34. doi: 10.1016/j.pharmthera.2012.07.002
- Roger, V. L., Go, A. S., Lloyd-Jones, D. M., Adams, R. J., Berry, J. D., Brown, T. M., . . . Stroke Statistics, S. (2011). Heart disease and stroke statistics--2011 update: a report from the American Heart Association. *Circulation*, *123*(4), e18-e209. doi: 10.1161/CIR.0b013e3182009701
- Rogers, C., Welt, F. G., Karnovsky, M. J., & Edelman, E. R. (1996). Monocyte recruitment and neointimal hyperplasia in rabbits. Coupled inhibitory effects of heparin. *Arterioscler Thromb Vasc Biol*, *16*(10), 1312-1318.
- Rolland, P. H., Bartoli, J. M., Piquet, P., Mekkaoui, C., Nott, S. H., Moulin, G., . . . Mesana, T. (2002). Local delivery of NO-donor molsidomine post-PTA improves haemodynamics, wall mechanics and histomorphometry in atherosclerotic porcine SFA. *Eur J Vasc Endovasc Surg*, *23*(3), 226-233. doi: 10.1053/ejvs.2001.1556
- Romano, G. (2012). Development of safer gene delivery systems to minimize the risk of insertional mutagenesis-related malignancies: a

critical issue for the field of gene therapy. *ISRN Oncol*, 2012, 616310. doi: 10.5402/2012/616310

- Romano, G., Marino, I. R., Pentimalli, F., Adamo, V., & Giordano, A. (2009). Insertional mutagenesis and development of malignancies induced by integrating gene delivery systems: implications for the design of safer gene-based interventions in patients. *Drug News Perspect*, 22(4), 185-196. doi: 10.1358/dnp.2009.22.4.1367704
- Rosanio, S., Tocchi, M., Patterson, C., & Runge, M. S. (1999). Prevention of restenosis after percutaneous coronary interventions: the medical approach. *Thromb Haemost*, 82 Suppl 1, 164-170.
- Rosenthal, N., Kornhauser, J. M., Donoghue, M., Rosen, K. M., & Merlie, J. P. (1989). Myosin light chain enhancer activates muscle-specific, developmentally regulated gene expression in transgenic mice. *Proc Natl Acad Sci U S A*, 86(20), 7780-7784.
- Rowinsky, E. K., & Donehower, R. C. (1995). Paclitaxel (taxol). *N Engl J Med*, 332(15), 1004-1014. doi: 10.1056/NEJM199504133321507
- Sadelain, M. (2004). Insertional oncogenesis in gene therapy: how much of a risk? *Gene Ther*, 11(7), 569-573. doi: 10.1038/sj.gt.3302243
- Salu, K. J., Bosmans, J. M., Bult, H., & Vrints, C. J. (2004). Drug-eluting stents: a new treatment in the prevention of restenosis. Part I: Experimental studies. *Acta Cardiol*, 59(1), 51-61.
- Saurer, E. M., Jewell, C. M., Kuchenreuther, J. M., & Lynn, D. M. (2009). Assembly of erodible, DNA-containing thin films on the surfaces of polymer microparticles: toward a layer-by-layer approach to the delivery of DNA to antigen-presenting cells. *Acta Biomater*, 5(3), 913-924. doi: 10.1016/j.actbio.2008.08.022
- Schechter, A. N., & Gladwin, M. T. (2003). Hemoglobin and the paracrine and endocrine functions of nitric oxide. *N Engl J Med*, 348(15), 1483-1485. doi: 10.1056/NEJMcibr023045
- Scheinman, M., Ascher, E., Levi, G. S., Hingorani, A., Shirazian, D., & Seth, P. (1999). p53 gene transfer to the injured rat carotid artery decreases neointimal formation. *J Vasc Surg*, 29(2), 360-369.
- Schiele, F., Vuilleminot, A., Meneveau, N., Pales-Espinosa, D., Gupta, S., & Bassand, J. P. (1999). Effects of increasing balloon pressure on

mechanism and results of balloon angioplasty for treatment of restenosis after Palmaz-Schatz stent implantation: an angiographic and intravascular ultrasound study. *Catheter Cardiovasc Interv*, 46(3), 314-321. doi: 10.1002/(SICI)1522-726X(199903)46:3<314::AID-CCD11>3.0.CO;2-I

Schillinger, M., Exner, M., Mlekusch, W., Rumpold, H., Ahmadi, R., Sabeti, S., . . . Minar, E. (2002). Vascular inflammation and percutaneous transluminal angioplasty of the femoropopliteal artery: association with restenosis. *Radiology*, 225(1), 21-26. doi: 10.1148/radiol.2251011809

Schmolka, I. R. (1994). Physical basis for poloxamer interactions. *Ann N Y Acad Sci*, 720, 92-97.

Schroeder, J. S., & Gao, S. Z. (1995). Calcium blockers and atherosclerosis: lessons from the Stanford Transplant Coronary Artery Disease/Diltiazem Trial. *Can J Cardiol*, 11(8), 710-715.

Schwartz, B., Benoist, C., Abdallah, B., Scherman, D., Behr, J. P., & Demeneix, B. A. (1995). Lipospermine-based gene transfer into the newborn mouse brain is optimized by a low lipospermine/DNA charge ratio. *Hum Gene Ther*, 6(12), 1515-1524.

Schwartz, R. S., Edelman, E. R., Carter, A., Chronos, N., Rogers, C., Robinson, K. A., . . . Consensus, C. (2002). Drug-eluting stents in preclinical studies: recommended evaluation from a consensus group. *Circulation*, 106(14), 1867-1873.

Schwartz, R. S., Edelman, E. R., Carter, A., Chronos, N. A., Rogers, C., Robinson, K. A., . . . Virmani, R. (2004). Preclinical evaluation of drug-eluting stents for peripheral applications: recommendations from an expert consensus group. *Circulation*, 110(16), 2498-2505. doi: 10.1161/01.CIR.0000145164.85178.2E

Schwartz, R. S., & Henry, T. D. (2002). Pathophysiology of coronary artery restenosis. *Rev Cardiovasc Med*, 3 Suppl 5, S4-9.

Schwartz, S. M. (1983). Cellular proliferation in atherosclerosis and hypertension. *Proc Soc Exp Biol Med*, 173(1), 1-13.

Schwartz, S. M., & Reidy, M. A. (1987). Common mechanisms of proliferation of smooth muscle in atherosclerosis and hypertension. *Hum Pathol*, 18(3), 240-247.

- Schwartz, S. M., Virmani, R., & Rosenfeld, M. E. (2000). The good smooth muscle cells in atherosclerosis. *Curr Atheroscler Rep*, 2(5), 422-429.
- Scott, N. A. (2006). Restenosis following implantation of bare metal coronary stents: pathophysiology and pathways involved in the vascular response to injury. *Adv Drug Deliv Rev*, 58(3), 358-376. doi: 10.1016/j.addr.2006.01.015
- Sehgal, S. N. (1998). Rapamune (RAPA, rapamycin, sirolimus): mechanism of action immunosuppressive effect results from blockade of signal transduction and inhibition of cell cycle progression. *Clin Biochem*, 31(5), 335-340.
- Seliktar, D., Black, R. A., Vito, R. P., & Nerem, R. M. (2000). Dynamic mechanical conditioning of collagen-gel blood vessel constructs induces remodeling in vitro. *Ann Biomed Eng*, 28(4), 351-362.
- Serruys, P. W., de Jaegere, P., Kiemeneij, F., Macaya, C., Rutsch, W., Heyndrickx, G., . . . et al. (1994). A comparison of balloon-expandable-stent implantation with balloon angioplasty in patients with coronary artery disease. Benestent Study Group. *N Engl J Med*, 331(8), 489-495. doi: 10.1056/NEJM199408253310801
- Serruys, P. W., Ruygrok, P., Neuzner, J., Piek, J. J., Seth, A., Schofer, J. J., . . . Daemen, J. (2006). A randomised comparison of an everolimus-eluting coronary stent with a paclitaxel-eluting coronary stent: the SPIRIT II trial. *EuroIntervention*, 2(3), 286-294.
- Serruys, P. W., Strauss, B. H., Beatt, K. J., Bertrand, M. E., Puel, J., Rickards, A. F., . . . et al. (1991). Angiographic follow-up after placement of a self-expanding coronary-artery stent. *N Engl J Med*, 324(1), 13-17. doi: 10.1056/NEJM199101033240103
- Sharif, F., Daly, K., Crowley, J., & O'Brien, T. (2004). Current status of catheter- and stent-based gene therapy. *Cardiovasc Res*, 64(2), 208-216. doi: 10.1016/j.cardiores.2004.07.003
- Sharif, F., Hynes, S. O., Cooney, R., Howard, L., McMahon, J., Daly, K., . . . O'Brien, T. (2008). Gene-eluting stents: adenovirus-mediated delivery of eNOS to the blood vessel wall accelerates re-endothelialization and inhibits restenosis. *Mol Ther*, 16(10), 1674-1680.
- Sharif, F., Hynes, S. O., McMahon, J., Cooney, R., Conroy, S., Dockery, P., . . . O'Brien, T. (2006). Gene-eluting stents: comparison of adenoviral

and adeno- associated viral gene delivery to the blood vessel wall in vivo. *Hum Gene Ther*, 17(7), 741-750. doi: 10.1089/hum.2006.17.741

Sharma, S. K., Kini, A., Mehran, R., Lansky, A., Kobayashi, Y., & Marmur, J. D. (2004). Randomized trial of Rotational Atherectomy Versus Balloon Angioplasty for Diffuse In-stent Restenosis (ROSTER). *Am Heart J*, 147(1), 16-22.

Shin, E. S., Garcia-Garcia, H. M., & Serruys, P. W. (2010). A new method to measure necrotic core and calcium content in coronary plaques using intravascular ultrasound radiofrequency-based analysis. *Int J Cardiovasc Imaging*, 26(4), 387-396. doi: 10.1007/s10554-009-9567-6

Sibbing, D., Laugwitz, K. L., Bott-Flugel, L., & Pache, J. (2009). Very late stent thrombosis 42 months after implantation of sirolimus-eluting stent and discontinuation of antiplatelet therapy. *Case Rep Med*, 2009, 713292. doi: 10.1155/2009/713292

Sick, P. B., Gelbrich, G., Kalnins, U., Erglis, A., Bonan, R., Aengevaeren, W., . . . Schuler, G. (2004). Comparison of early and late results of a Carbofilm-coated stent versus a pure high-grade stainless steel stent (the Carbostent-Trial). *Am J Cardiol*, 93(11), 1351-1356, A1355. doi: 10.1016/j.amjcard.2004.02.029

Sidney, S., Rosamond, W. D., Howard, V. J., Luepker, R. V., National Forum for Heart, D., & Stroke, P. (2013). The "heart disease and stroke statistics--2013 update" and the need for a national cardiovascular surveillance system. *Circulation*, 127(1), 21-23. doi: 10.1161/CIRCULATIONAHA.112.155911

Siepmann, F., Herrmann, S., Winter, G., & Siepmann, J. (2008). A novel mathematical model quantifying drug release from lipid implants. *J Control Release*, 128(3), 233-240. doi: 10.1016/j.jconrel.2008.03.009

Sigwart, U., Puel, J., Mirkovitch, V., Joffre, F., & Kappenberger, L. (1987). Intravascular stents to prevent occlusion and restenosis after transluminal angioplasty. *N Engl J Med*, 316(12), 701-706. doi: 10.1056/NEJM198703193161201

Silva, G. V., Fernandes, M. R., Madonna, R., Clubb, F., Oliveira, E., Jimenez-Quevedo, P., . . . Perin, E. C. (2009). Comparative healing response after sirolimus- and paclitaxel-eluting stent implantation in a pig

model of restenosis. *Catheter Cardiovasc Interv*, 73(6), 801-808. doi: 10.1002/ccd.21879

Simpson, J. B., Selmon, M. R., Robertson, G. C., Cipriano, P. R., Hayden, W. G., Johnson, D. E., & Fogarty, T. J. (1988). Transluminal atherectomy for occlusive peripheral vascular disease. *Am J Cardiol*, 61(14), 96G-101G.

Sims-Williams, F. (1988). A review of British Standard 6871: 1987. *J Sterile Serv Manage*, 5(5), 19.

Sinnaeve, P., Varenne, O., Collen, D., & Janssens, S. (1999). Gene therapy in the cardiovascular system: an update. *Cardiovasc Res*, 44(3), 498-506.

Skyttberg, N., Linder, R., & Carlsson, J. (2006). [Drug-eluting stents can increase the risk of late stent thrombosis]. *Lakartidningen*, 103(39), 2845-2847.

Smit, F. E., & Dohmen, P. M. (2015). Cardiovascular tissue engineering: where we come from and where are we now? *Med Sci Monit Basic Res*, 21, 1-3. doi: 10.12659/MSMBR.893546

Song, H., Liu, S., Li, C., Geng, Y., Wang, G., & Gu, Z. (2014). Pluronic L64-mediated stable HIF-1 $\alpha$  expression in muscle for therapeutic angiogenesis in mouse hindlimb ischemia. *Int J Nanomedicine*, 9, 3439-3452. doi: 10.2147/IJN.S65353

Sriadibhatla, S., Yang, Z., Gebhart, C., Alakhov, V. Y., & Kabanov, A. (2006). Transcriptional activation of gene expression by pluronic block copolymers in stably and transiently transfected cells. *Mol Ther*, 13(4), 804-813. doi: 10.1016/j.ymthe.2005.07.701

Srivastava, S., Gorham, S. D., & Courtney, J. M. (1990). The attachment and growth of an established cell line on collagen, chemically modified collagen, and collagen composite surfaces. *Biomaterials*, 11(3), 162-168.

Stassen, F. R., Vainas, T., & Bruggeman, C. A. (2008). Infection and atherosclerosis. An alternative view on an outdated hypothesis. *Pharmacol Rep*, 60(1), 85-92.

Steinberg, D. (2006). The pathogenesis of atherosclerosis. An interpretive history of the cholesterol controversy, part IV: the 1984 coronary

primary prevention trial ends it--almost. *J Lipid Res*, 47(1), 1-14. doi: 10.1194/jlr.R500014-JLR200

- Steinhubl, S. R., Tan, W. A., Foody, J. M., & Topol, E. J. (1999). Incidence and clinical course of thrombotic thrombocytopenic purpura due to ticlopidine following coronary stenting. EPISTENT Investigators. Evaluation of Platelet IIb/IIIa Inhibitor for Stenting. *JAMA*, 281(9), 806-810.
- Stephan, D. J., Yang, Z. Y., San, H., Simari, R. D., Wheeler, C. J., Felgner, P. L., . . . Nabel, E. G. (1996). A new cationic liposome DNA complex enhances the efficiency of arterial gene transfer in vivo. *Hum Gene Ther*, 7(15), 1803-1812. doi: 10.1089/hum.1996.7.15-1803
- Su, H. S., & Wang, Y. F. (2006). [Progress in research of chitosan as a non-viral gene delivery vector]. *Yi Chuan*, 28(10), 1321-1324.
- Swerlick, R. A., & Lawley, T. J. (1993). Role of microvascular endothelial cells in inflammation. *J Invest Dermatol*, 100(1), 111S-115S.
- Tahir, H., Hoekstra, A. G., Lorenz, E., Lawford, P. V., Hose, D. R., Gunn, J., & Evans, D. J. (2011). Multi-scale simulations of the dynamics of in-stent restenosis: impact of stent deployment and design. *Interface Focus*, 1(3), 365-373. doi: 10.1098/rsfs.2010.0024
- Takahashi, H., Letourneur, D., & Grainger, D. W. (2007). Delivery of large biopharmaceuticals from cardiovascular stents: a review. *Biomacromolecules*, 8(11), 3281-3293. doi: 10.1021/bm700540p
- Tang, R., Ji, W., & Wang, C. (2011). Synthesis and characterization of new poly(ortho ester amidine) copolymers for nonviral gene delivery. *Polymer (Guildf)*, 52(4), 921-932. doi: 10.1016/j.polymer.2010.12.057
- Tanigawa, N., Sawada, S., & Kobayashi, M. (1995). Reaction of the aortic wall to six metallic stent materials. *Acad Radiol*, 2(5), 379-384.
- Teirstein, P. S. (2010). Drug-eluting stent restenosis: an uncommon yet pervasive problem. *Circulation*, 122(1), 5-7. doi: 10.1161/CIRCULATIONAHA.110.962423
- Tepliakov, A. T., & Rybal'chenko, E. V. (2008). [The role of cytokines in restenosing coronary stents and the efficiency of its secondary prophylaxis with statins]. *Klin Med (Mosk)*, 86(8), 32-39.

- Teramoto, T., Sasaki, J., Ishibashi, S., Birou, S., Daida, H., Dohi, S., . . . Yokote, K. (2013). Cardiovascular disease risk factors other than dyslipidemia. Executive summary of the Japan Atherosclerosis Society (JAS) guidelines for the diagnosis and prevention of atherosclerotic cardiovascular diseases in Japan - 2012 version. *J Atheroscler Thromb*, *20*(10), 733-742.
- They, M., Racine, V., Pepin, A., Piel, M., Chen, Y., Sibarita, J. B., & Bornens, M. (2005). The extracellular matrix guides the orientation of the cell division axis. *Nat Cell Biol*, *7*(10), 947-953. doi: 10.1038/ncb1307
- Thierry, B., Winnik, F. M., Merhi, Y., Silver, J., & Tabrizian, M. (2003). Bioactive coatings of endovascular stents based on polyelectrolyte multilayers. *Biomacromolecules*, *4*(6), 1564-1571. doi: 10.1021/bm0341834
- Thomson, L. A., Law, F. C., Rushton, N., & Franks, J. (1991). Biocompatibility of diamond-like carbon coating. *Biomaterials*, *12*(1), 37-40.
- Tian, B., & Brasier, A. R. (2003). Identification of a nuclear factor kappa B-dependent gene network. *Recent Prog Horm Res*, *58*, 95-130.
- Toda, M. (2005). [Gene therapy for brain tumors using herpes simplex virus vector]. *Nihon Rinsho*, *63 Suppl 9*, 510-514.
- Towae, F., Zahn, R., & Zeymer, U. (2009). Repeat late instent-stenosis after an interval of four years in the same lesion after bare-metal and drug-eluting stent: a case report. *Cases J*, *2*, 9407. doi: 10.1186/1757-1626-2-9407
- Trion, A., & van der Laarse, A. (2004). Vascular smooth muscle cells and calcification in atherosclerosis. *Am Heart J*, *147*(5), 808-814. doi: 10.1016/j.ahj.2003.10.047
- Trisal, V., Paulson, T., Hans, S. S., & Mittal, V. (2002). Carotid artery restenosis: an ongoing disease process. *Am Surg*, *68*(3), 275-279; discussion 279-280.
- Tsai, T. T., Ho, P. M., Xu, S., Powers, J. D., Carroll, N. M., Shetterly, S. M., . . . Magid, D. J. (2010). Increased risk of bleeding in patients on clopidogrel therapy after drug-eluting stents implantation: insights from the HMO Research Network-Stent Registry (HMORN-stent). *Circ Cardiovasc Interv*, *3*(3), 230-235. doi: 10.1161/CIRCINTERVENTIONS.109.919001

- Uchio, E., Hatano, H., Mitsui, K., Sugita, M., Okada, K., Goto, K., . . . Ohno, S. (1994). A retrospective study of herpes simplex keratitis over the last 30 years. *Jpn J Ophthalmol*, *38*(2), 196-201.
- Ueno, H., Kanellakis, P., Agrotis, A., & Bobik, A. (2000). Blood flow regulates the development of vascular hypertrophy, smooth muscle cell proliferation, and endothelial cell nitric oxide synthase in hypertension. *Hypertension*, *36*(1), 89-96.
- Uno, K., & Nicholls, S. J. (2010). Biomarkers of inflammation and oxidative stress in atherosclerosis. *Biomark Med*, *4*(3), 361-373. doi: 10.2217/bmm.10.57
- Van Belle, E., Abolmaali, K., Bauters, C., McFadden, E. P., Lablanche, J. M., & Bertrand, M. E. (1999). Restenosis, late vessel occlusion and left ventricular function six months after balloon angioplasty in diabetic patients. *J Am Coll Cardiol*, *34*(2), 476-485.
- van der Hoeven, B. L., Schaliij, M. J., & van der Wall, E. E. (2005). [Percutaneous coronary intervention with stent placement versus bypass operation in symptomatic multiple-vessel disease; lessons from an observational study]. *Ned Tijdschr Geneesk*, *149*(51), 2837-2840.
- Varenne, O., Pislaru, S., Gillijns, H., Van Pelt, N., Gerard, R. D., Zoldhelyi, P., . . . Janssens, S. P. (1998). Local adenovirus-mediated transfer of human endothelial nitric oxide synthase reduces luminal narrowing after coronary angioplasty in pigs. *Circulation*, *98*(9), 919-926.
- Varenne, O., & Sinnaeve, P. (2000). Gene Therapy for Coronary Restenosis: A Promising Strategy for the New Millennium? *Curr Interv Cardiol Rep*, *2*(4), 309-315.
- Velasco, J., Menendez, C. L., Alonso de la Campa, J., Pinto, J., & Crespo, M. (2005). Cyanoacrylate hepatic pseudotumor: role of fine needle aspiration. *Acta Cytol*, *49*(5), 585-586.
- Venne, A., Li, S., Mandeville, R., Kabanov, A., & Alakhov, V. (1996). Hypersensitizing effect of pluronic L61 on cytotoxic activity, transport, and subcellular distribution of doxorubicin in multiple drug-resistant cells. *Cancer Res*, *56*(16), 3626-3629.
- Verma, I. M., & Somia, N. (1997). Gene therapy -- promises, problems and prospects. *Nature*, *389*(6648), 239-242. doi: 10.1038/38410

- Virmani, R., Farb, A., Guagliumi, G., & Kolodgie, F. D. (2004). Drug-eluting stents: caution and concerns for long-term outcome. *Coron Artery Dis*, *15*(6), 313-318.
- Virmani, R., Liistro, F., Stankovic, G., Di Mario, C., Montorfano, M., Farb, A., . . . Colombo, A. (2002). Mechanism of late in-stent restenosis after implantation of a paclitaxel derivate-eluting polymer stent system in humans. *Circulation*, *106*(21), 2649-2651.
- vom Dahl, J., Dietz, U., Haager, P. K., Silber, S., Niccoli, L., Buettner, H. J., . . . Klues, H. G. (2002). Rotational atherectomy does not reduce recurrent in-stent restenosis: results of the angioplasty versus rotational atherectomy for treatment of diffuse in-stent restenosis trial (ARTIST). *Circulation*, *105*(5), 583-588.
- Wagner, E. (2008). Converging paths of viral and non-viral vector engineering. *Mol Ther*, *16*(1), 1-2. doi: 10.1038/sj.mt.6300378
- Waksman, R. (2002). Drug-eluting stents: from bench to bed. *Cardiovasc Radiat Med*, *3*(3-4), 226-241.
- Waksman, R., Ajani, A. E., Pinnow, E., Cheneau, E., Leborgne, L., Dieble, R., . . . Lindsay, J. (2002). Twelve versus six months of clopidogrel to reduce major cardiac events in patients undergoing gamma-radiation therapy for in-stent restenosis: Washington Radiation for In-Stent restenosis Trial (WRIST) 12 versus WRIST PLUS. *Circulation*, *106*(7), 776-778.
- Waksman, R., Ajani, A. E., White, R. L., Pinnow, E., Mehran, R., Bui, A. B., . . . Lindsay, J. (2001). Two-year follow-up after beta and gamma intracoronary radiation therapy for patients with diffuse in-stent restenosis. *Am J Cardiol*, *88*(4), 425-428.
- Walther, W., Stein, U., Voss, C., Schmidt, T., Schleef, M., & Schlag, P. M. (2003). Stability analysis for long-term storage of naked DNA: impact on nonviral in vivo gene transfer. *Anal Biochem*, *318*(2), 230-235.
- Wang, D., & Sadee, W. (2006). Searching for polymorphisms that affect gene expression and mRNA processing: example ABCB1 (MDR1). *AAPS J*, *8*(3), E515-520. doi: 10.1208/aapsj080361
- Wang, M., Yang, H., Zheng, L. Y., Zhang, Z., Tang, Y. B., Wang, G. L., . . . Guan, Y. Y. (2012). Downregulation of TMEM16A calcium-activated chloride channel contributes to cerebrovascular remodeling during

hypertension by promoting basilar smooth muscle cell proliferation. *Circulation*, 125(5), 697-707. doi: 10.1161/CIRCULATIONAHA.111.041806

Wang, R., Hughes, T., Beck, S., Vakil, S., Li, S., Pantano, P., & Draper, R. K. (2013). Generation of toxic degradation products by sonication of Pluronic(R) dispersants: implications for nanotoxicity testing. *Nanotoxicology*, 7(7), 1272-1281. doi: 10.3109/17435390.2012.736547

Wani, M. C., Taylor, H. L., Wall, M. E., Coggon, P., & McPhail, A. T. (1971). Plant antitumor agents. VI. The isolation and structure of taxol, a novel antileukemic and antitumor agent from *Taxus brevifolia*. *J Am Chem Soc*, 93(9), 2325-2327.

Warrenburg, S., Schwartz, G. E., Henderson, R., Crits-Christoph, P., & Nuzzo, P. (1986). Calcium, race, and hypertension. *Ann Intern Med*, 104(6), 892-893.

Weber, C., & Noels, H. (2011). Atherosclerosis: current pathogenesis and therapeutic options. *Nat Med*, 17(11), 1410-1422. doi: 10.1038/nm.2538

Wei, Q., Liu, Z., Fei, Y., Peng, D., Zuo, H., Huang, X., . . . Zhang, X. (2011). Adeno-associated viral vector mediated and cardiac-specific delivery of CD151 gene in ischemic rat hearts. *J Huazhong Univ Sci Technolog Med Sci*, 31(1), 46-51. doi: 10.1007/s11596-011-0148-2

Westby, M., Nakayama, G. R., Butler, S. L., & Blair, W. S. (2005). Cell-based and biochemical screening approaches for the discovery of novel HIV-1 inhibitors. *Antiviral Res*, 67(3), 121-140. doi: 10.1016/j.antiviral.2005.06.006

Whelan, D. M., van Beusekom, H. M., & van der Giessen, W. J. (1997). Foreign body contamination during stent implantation. *Cathet Cardiovasc Diagn*, 40(3), 328-332.

Whelan, D. M., van der Giessen, W. J., Krabbendam, S. C., van Vliet, E. A., Verdouw, P. D., Serruys, P. W., & van Beusekom, H. M. (2000). Biocompatibility of phosphorylcholine coated stents in normal porcine coronary arteries. *Heart*, 83(3), 338-345.

White, G. C., 2nd. (2001). Gene therapy in hemophilia: clinical trials update. *Thromb Haemost*, 86(1), 172-177.

- Williams, D. F. (1989). A model for biocompatibility and its evaluation. *J Biomed Eng*, 11(3), 185-191.
- Wilson, P. W. (2012). Insulin resistance and ischemic myocardial injury post-percutaneous coronary interventions. *JACC Cardiovasc Interv*, 5(11), 1168-1169. doi: 10.1016/j.jcin.2012.09.001
- Wong, M. K., & Gotlieb, A. I. (1986). Endothelial cell monolayer integrity. I. Characterization of dense peripheral band of microfilaments. *Arteriosclerosis*, 6(2), 212-219.
- Wong, P. B., Wiley, E. O., Johnson, W. E., Ryder, O. A., O'Brien, S. J., Haussler, D., . . . G10Kcos. (2012). Tissue sampling methods and standards for vertebrate genomics. *Gigascience*, 1(1), 8. doi: 10.1186/2047-217X-1-8
- Yamauchi, F., Koyamatsu, Y., Kato, K., & Iwata, H. (2006). Layer-by-layer assembly of cationic lipid and plasmid DNA onto gold surface for stent-assisted gene transfer. *Biomaterials*, 27(18), 3497-3504. doi: 10.1016/j.biomaterials.2006.02.004
- Yang, J., Wang, N., Zhang, X., Xu, J., Ling, F., Zhou, L., & Ye, X. (2006). Late angiographic stent thrombosis in a drug-eluting stent that occurred 20 months after premature discontinuation of clopidogrel administration. *Int Heart J*, 47(5), 707-713.
- Yang, J. P., & Huang, L. (1997). Overcoming the inhibitory effect of serum on lipofection by increasing the charge ratio of cationic liposome to DNA. *Gene Ther*, 4(9), 950-960.
- Yang, N. S., Sun, W. H., & McCabe, D. (1996). Developing particle-mediated gene-transfer technology for research into gene therapy of cancer. *Mol Med Today*, 2(11), 476-481.
- Yeh, E. T., Anderson, H. V., Pasceri, V., & Willerson, J. T. (2001). C-reactive protein: linking inflammation to cardiovascular complications. *Circulation*, 104(9), 974-975.
- Yin, H. F., Wang, Q. J., & Li, N. (2002). [The research progress in the disease model of knock-out mouse]. *Yi Chuan*, 24(4), 463-469.
- Yoneda, M., Hirofujii, T., Anan, H., Matsumoto, A., Hamachi, T., Nakayama, K., & Maeda, K. (2001). Mixed infection of *Porphyromonas gingivalis* and *Bacteroides forsythus* in a murine abscess model: involvement

of gingipains in a synergistic effect. *J Periodontal Res*, 36(4), 237-243.

- Zakrzewska, K. E., Samluk, A., Wierzbicki, M., Jaworski, S., Kutwin, M., Sawosz, E., . . . Pluta, K. D. (2015). Analysis of the cytotoxicity of carbon-based nanoparticles, diamond and graphite, in human glioblastoma and hepatoma cell lines. *PLoS One*, 10(3), e0122579. doi: 10.1371/journal.pone.0122579
- Zeng, J. H., Yang, Z., & Xu, J. (2004). [The study on correlation of c-myc gene expression with vascular smooth muscle cell proliferation in patients with portal hypertension]. *Zhonghua Wai Ke Za Zhi*, 42(9), 543-545.
- Zhang, G., Budker, V., & Wolff, J. A. (1999). High levels of foreign gene expression in hepatocytes after tail vein injections of naked plasmid DNA. *Hum Gene Ther*, 10(10), 1735-1737. doi: 10.1089/10430349950017734
- Zhang, G., Budker, V. G., Ludtke, J. J., & Wolff, J. A. (2004). Naked DNA gene transfer in mammalian cells. *Methods Mol Biol*, 245, 251-264.
- Zhang, J., & Zhu, K. Y. (2006). Characterization of a chitin synthase cDNA and its increased mRNA level associated with decreased chitin synthesis in *Anopheles quadrimaculatus* exposed to diflubenzuron. *Insect Biochem Mol Biol*, 36(9), 712-725. doi: 10.1016/j.ibmb.2006.06.002
- Zhang, N., Chittasupho, C., Duangrat, C., Siahaan, T. J., & Berkland, C. (2008). PLGA nanoparticle-peptide conjugate effectively targets intercellular cell-adhesion molecule-1. *Bioconjug Chem*, 19(1), 145-152. doi: 10.1021/bc700227z
- Zhang, S., Chan, K. H., Prud'homme, R. K., & Link, A. J. (2012). Synthesis and evaluation of clickable block copolymers for targeted nanoparticle drug delivery. *Mol Pharm*, 9(8), 2228-2236. doi: 10.1021/mp3000748
- Zhang, S., Prud'homme, R. K., & Link, A. J. (2011). Block copolymer nanoparticles as nanobeads for the polymerase chain reaction. *Nano Lett*, 11(4), 1723-1726. doi: 10.1021/nl200271d
- Zhang, W., Cao, X., Huang, X., Wang, J., Tao, Q., & Ye, T. (1997). In vivo distribution and gene expression of genetically modified

hepatocytes after intrasplenic transplantation. *Sci China C Life Sci*, 40(5), 554-560. doi: 10.1007/BF03183596

Zhen, H., Fang, F., Zhou, Y. F., Li, G., & Dong, Y. S. (2006). [T cell-mediated protective effect in cytomegalovirus infected murine astrocytes]. *Xi Bao Yu Fen Zi Mian Yi Xue Za Zhi*, 22(5), 571-574.

Zilla, P., Fasol, R., Deutsch, M., Fischlein, T., Minar, E., Hammerle, A., . . . Kadletz, M. (1987). Endothelial cell seeding of polytetrafluoroethylene vascular grafts in humans: a preliminary report. *J Vasc Surg*, 6(6), 535-541.

Zimmermann, W. H., Schneiderbanger, K., Schubert, P., Didie, M., Munzel, F., Heubach, J. F., . . . Eschenhagen, T. (2002). Tissue engineering of a differentiated cardiac muscle construct. *Circ Res*, 90(2), 223-230.

Zohlhofer, D., Klein, C. A., Richter, T., Brandl, R., Murr, A., Nuhrenberg, T., . . . Neumann, F. J. (2001). Gene expression profiling of human stent-induced neointima by cDNA array analysis of microscopic specimens retrieved by helix cutter atherectomy: Detection of FK506-binding protein 12 upregulation. *Circulation*, 103(10), 1396-1402.

Zwaal, R. F., & Hemker, H. C. (1982). Blood cell membranes and haemostasis. *Haemostasis*, 11(1), 12-39.